December 2020

Crustal Evolution of the New England Appalachians: The Rise and Fall of a Long-Lived Orogenic Plateau

Ian Hillenbrand

CRUSTAL EVOLUTION OF THE NEW ENGLAND APPALACHIANS: THE RISE AND FALL OF A LONG-LIVED OROGENIC PLATEAU

A Thesis Presented

by

IAN W. HILLENBRAND

Submitted to the Graduate School of the
University of Massachusetts Amherst in partial fulfillment
of the requirements for the degree of

MASTER OF SCIENCE

September 2020

Geosciences

CRUSTAL EVOLUTION OF THE NEW ENGLAND APPALACHIANS: THE RISE AND FALL OF A LONG-LIVED OROGENIC PLATEAU

A Thesis Presented

by

IAN W. HILLENBRAND

Approved as to style and content by:

____
Michael L. Williams

____
Paul M. Karabinos, Member

____
Michael J. Jercinovic, Member

____
R. Mark Leckie, Member

____
Stephen Burns, Department Head
Geosciences

ACKNOWLEDGMENTS

I deeply appreciate the support that so many people have provided throughout the course of this research. I cannot express how much I appreciate the support and guidance Michael L. Williams who has expressed constant interest in this research. To Paul Karabinos of Williams College, I express gratitude for strengthening and challenging my understanding of Appalachian tectonics. Thanks also go to Michael J. Jercinovic has been exceeding helpful in all realms of microanalysis and his attention to detail is second to none.

Almost too many to name but I appreciate conversations, assistance, and collegiately of Haiying Gao, Steve Turner, Craig Dietsch, Mark Leckie, Dyk Eusden, Dwight Bradley, Will Amidon, Dave West, Don Wise, and the members of the New England Geology/Geophysics Group. This work would not have been possible with the support and input of fellow graduate students Dan Tjapkes, Justin Mistikaway, Cong Li, Alex Hammerstrom, and Kaitlyn Suarez.

I recognize and appreciate financial support for various aspects of this research from the National Science Foundation grant EAR 1736/167 (to H. Gao, M. Williams, and V. Levin), the Marland Pratt and Katherine Fowler Billings Research Award, Leo M. Hall Award from the Department of Geosciences, University of Massachusetts Amherst, and the Geological Society of Connecticut Student Research Fund.

ABSTRACT

CRUSTAL EVOLUTION OF THE NEW ENGLAND APPALACHIANS: THE RISE AND FALL OF A LONG-LIVED OROGENIC PLATEAU

SEPTEMBER 2020

IAN W. HILLENBRAND, B.A., BATES COLLEGE

M.S., UNIVERSITY OF MASSACHUSETTS, AMHERST

Directed by: Professor Michael L. Williams

The rise and demise of mountain belts, caused by growth, modification, or removal of the continental lithosphere are fundamental processes that influence almost all Earth systems. Understanding the nature, timing, and significance of active processes in the creation and evolution of modern mountain belts is challenged by a lack of middle crustal and lower crustal exposures. Analogues can be found in ancient orogens, whose deeply eroded roots offer a window into deeper processes, yet this record is complicated by overprinting events and complex deformational histories. Research presented herein constrains the tectonic history of multistage Appalachian Orogen, type locality of the Wilson cycle. Data-driven analysis of newly assembled geochronologic, geochemical, and geothermobarometric databases are synthesized with structural fabrics and geophysical imaging to constrain the timing and nature of crustal thickening and thinning events. Results identify a two-stage crustal thickening history in the dominant Acadian Orogeny and suggest the existence of a high elevation, low relief orogenic plateau. This plateau, the Acadian altiplano, formed in central and southern New England by ca. 380 Ma and exited for at least 50 m.y. until underwent orogen parallel collapse ca. 330-310

Ma. Collapse of the plateau likely formed the geophysically observed 12-15 km offset in Moho depth in western New England, and implies that the step has existed for ca. 300 m.y. These data constrain a four-dimensional record of crustal evolution over a period exceeding 100 m.y. Recognition of the Acadian altiplano may have important implications for the genesis of critical Li deposits, paleoclimate, and evolution of the Appalachian basin. Further, present a region that may provide an analogue for studying mid-crustal processes such as partial melting, ductile flow, and plutonism underneath modern plateaus.

TABLE OF CONTENTS

Page

LIST OF TABLES

Table Page

LIST OF FIGURES

CHAPTER 1

INTRODUCTION

1.1 Introduction

Mountain belts are earth's loftiest landscapes and their formation is a complex interplay between Earth's deep and surface processes (Harrison et al., 1992; DeCelles, 2004; Molnar et al., 2015). The uplift of mountains affects global climate (Raymo and Ruddiman, 1992; France-Lanord and Derry, 1997; Miao et al., 2012; Armijo et al., 2015), atmospheric and oceanic circulation patterns (Molnar et al., 1993; Zhisheng et al., 2001; Schmittner et al., 2011), and the motion of tectonic plates (Iaffaldano et al., 2006) while their denudation supplies nutrients critical to life in the oceans and terrestrial systems (Porder et al., 2007; Meert and Lieberman, 2008; Campbell and Squire, 2010). Orogenesis is also linked to the formation and concentration of critical mineral deposits and natural resources (Sun et al., 2011; Richards, 2015; Bradley et al., 2017). In spite of the profound importance of understanding the rise and fall of mountain belts, many critical aspects are poorly constrained. First order questions regarding orogenic evolution such the tempo and timing of orogenic uplift and collapse, the nature of these processes, and their implications for broader Earth process are actively debated (e.g. Dalziel and Dewey, 2019; Kapp and DeCelles, 2019; Macdonald et al., 2019; Ryan and Dewey, 2019; Yasunari, 2020). One of the primary goals for geologists and geophysicists is building models of how mountain belts evolve in space and time.

Recent advances in analytical techniques (Harrison et al., 2009; Gehrels, 2014; Williams et al., 2017; Yakymchuk et al., 2017; Bosse and Villa, 2019) have led to increases in the precision and accuracy of geochronological and geochemical analyses, the rate at which the data can be collected, and better understandings of the significance of chronologic data. Increases in both data and data availability have facilitated global and regional compilations lending new insights into Earth processes and evolution (Keller and Schoene, 2012, 2018; Profeta et al., 2015; Roberts and Spencer, 2015; Turner and Langmuir, 2015; Farner and Lee, 2017; Kellett et al., 2020). Geophysical imaging, in particular the EARTHSCOPE geophysics-geology collaboration (www.earthscope.org) has significantly advanced understanding of the crustal, lithospheric, and mantle processes (Zandt et al., 2004; Schmandt and Lin, 2014; Li et al., 2018; Yang and Gao, 2018; Long et al., 2019).

In the light of these recent studies, critical re-examination of the tectonic history of both modern and ancient mountain belts is required. The Appalachian orogen preserves a full Wilson cycle and has served as an inspiration, testbed, and model of plate tectonics for decades (Wilson, 1966; Thompson et al., 1968; Bird and Dewey, 1970; Naylor, 1971; McKerrow and Ziegler, 1972; Robinson and Hall, 1980; Bradley, 1983; van Staal et al., 1998; Dalziel and Dewey, 2019). At least five phases of Paleozoic orogenesis are recognized which were followed by Mesozoic extension (Wise, 1992; Robinson et al., 1998; van Staal et al., 2009). This history is preserved in the form of accreted terranes, poly-deformed and metamorphosed rocks, abundant magmatism, and sedimentary basins. The multistage nature of the orogen has also challenged geologists and geophysicists in ascribing particular characteristics to specific events, challenging researchers' ability to build a comprehensive model of crustal evolution for the composite history (Zartman, 1977; Robinson and Hall, 1980; Robinson et al., 1998; van Staal et al., 2009; Li et al., 2018).

Integration of a wide range of quantitative geochronologic, geochemical, and geothermobarometric analyses with geophysical imaging and structural analyses may provide new insight into the tectonic history. The New England Appalachians are particularly well suited to this type of data-driven, multidisciplinary tectonic analysis. The literature of quantitative geologic data spans over 60 years (Hurley et al., 1959, 1960; Long and Kulp, 1962; Faul et al., 1963; Clark and Kulp, 1968; Harper, 1968; Zartman et al., 1970; Naylor, 1971; Tracy et al., 1976; Ashwal et al., 1979; Zartman, 1988) and the region continues to be the subject of active study and debate (Macdonald et al., 2017, 2014; Amidon et al., 2016; Bradley and O'Sullivan, 2017; Waldron et al., 2017; Karabinos et al., 2017; Wolfe and Spear, 2018; Levin et al., 2018; Li et al., 2018, 2020; Valley et al., 2019; Hollocher et al., 2019; Kim et al., 2019; Long et al., 2019; Perrot et al., 2020). However, harnessing this expansive and potentially powerful dataset has been limited due to the scatter of data across peer reviewed articles, conference guidebooks, and student theses.

The aim of this thesis is to place new, data-driven constraints on the four-dimensional crustal and tectonic evolution of the New England Appalachians through the lens of a comprehensive geologic database. Quantitative geologic data including geochronological, geochemical, and geothermobarometric analyses are integrated with new geophysical imaging of the crust and mantle. Synthesis of these datasets with geophysical imaging are used to characterize and constrain the timing and nature of the crustal evolution. Collectively, these datasets contribute to global geologic compilations whereas the results of geospatial analysis and interpretations provide a clearer picture of

Appalachian tectonics and how orogens evolve through time. Moreover, they offer insights into the processes involving the uplift and collapse of orogenic plateaus.

1.2 Purpose and General Approach

The research undertaken in this project focuses on the terrane scale tectonic analysis of the New England Appalachians. Data compiled herein include whole rock and mineral geochemistry, geothermobarometry, and geochronology which were integrated with existing structural and petrologic studies. Geospatial and quantitative analyses were designed to test hypotheses and constrain the overall tectonic and structural evolution of the Appalachian orogen.

1.3 Thesis Organization

This thesis is organized into three main chapters (2-4), which each address a different portion of the tectonic and crustal evolution of the New England Appalachians. Each chapter is organized as an independent contribution which have, or are in preparation to be, submitted to peer-reviewed journals. Given this consideration, there will be some overlap in background.

Chapter 2 focuses on the compilation of new geochemical, geothermobarometric, and geochronologic databases for the New England Appalachians. This newly compiled dataset, the New England Geologic Database (NED), are available online as interactive maps and tables (https://sites.google.com/umass.edu/ned) and can be downloaded as .csv files. The chapter then explores applications of this dataset to the igneous record of crustal evolution and detrital mineral studies. Compilations of the ages of igneous rocks are compared and contrasted with the model ages of the timing of mantle extraction. The crustal and mantle contributions to the petrogenesis of New England igneous rocks are further explored with time series of isotopic data. Isotopic data and trace element data show paired shifts in the Taconic, Acadian, and Neoacadian orogenies. These cyclical trends suggest increased amounts of crustal recycling during peak orogenesis, perhaps as a function of crustal thickening. Then, the functionality of the database in regard to detrital minerals studies is explored. Detrital zircon, monazite, and rutile at the mouth of the Merrimack River closely match in-situ zircon, monazite, and hornblende dates from the Merrimack River watershed. This integrated source and sink analysis provides refined constraints on the provenance of Merrimack River sediments and may offer new constraints on the regional cooling history.

Chapter 3 examines the crustal thickness evolution of northern New England during the Acadian-Neoacadian orogeny from the perspective of igneous geochemistry. Trace element and isotopic methods were applied to a set of carefully filtered set of samples. The results suggest a two-stage crustal thickening history. Initial crustal thickening occurred progressively from to southeast to northwest resulting in a consistent thickness of ~ 40 km across New England by ~400 Ma. Subsequently, the crustal thickness of central New England doubled by 380 Ma, yielding estimates on the order of those of the modern Andean Altiplano and Tibetan plateau. Further, these results imply a 30-40 km variation in crustal thickness along 300 km of orogenic strike. Comparison of Acadian and modern crustal thickness estimates show that, to a first order, the distribution of metamorphic facies at the modern erosional can be explained by variable Acadian collapse, quantifying the inferences of earlier petrologic studies. This suggests that a) the distribution is related to initial crustal thickness which in turn b) influenced the nature of orogenic collapse, exhuming deeper levels of the crust where it was previously thickened.

Chapter 4 builds upon the results of Chapter 3 and tests the hypothesis of an orogenic plateau in the Acadian orogeny. This chapter presents geospatial analysis of thermochronologic and thermobarometric data which are then integrated with geochronologic analyses, geochemical data presented in Chapter 3, and geophysical imaging. Thermobarometric and $^{40}Ar/^{39}Ar$ hornblende, muscovite, and biotite dates show distinct trends and discontinuities near the trace of a 12-15 km offset in Moho depth imaged by P-S teleseismic receiver functions (Li et al., 2018). East of this offset calculated metamorphic pressures are consistent across a 20,000 km^2 region, suggestive of a low relief (plateau-like) surface. This same region shows evidence for very slow cooling and block-like exhumation, also suggestive of a plateau. Together, petrologic, thermochronologic, and geochemical crustal thickness estimates suggest that central New England represents the exhumed mid-crust of a 50-70 km thick orogenic plateau which existed for ≥50 m.y. Protracted dates of anatectic rocks indicate a partially molten mid-crust, favoring the development of a low relief plateau. Integration of monazite geochronology and chemistry with structural fabrics constrain the timing and nature of crustal thickening and thinning and are consistent with the results of Chapter 3. This chapter demonstrates that the geophysically imaged Moho step offset must be Paleozoic in age and that it formed during plateau collapse. The uplift of an orogenic plateau may have played a role in facilitating climatic and biotic instability during the late Devonian and in the generation of a belt of Li-rich pegmatites. The identification of the Acadian altiplano provides a new constraint on the evolution of orogenic plateaus and offers a window in the mid-crust beneath modern plateaus.

1.4 Summary

Analysis presented in this thesis integrates a new database of quantitative geologic data with existing field observations and geophysical measurements to constrain the crustal evolution of the New England Appalachians from the Paleozoic to present. This thesis places new constraints on the timing and nature of Paleozoic magmatic events, the degree and nature of crustal thickening in the Acadian-Neoacadian orogeny, and the age and tectonic significance of a 12-15 km offset in Moho depth in western New England. The primary broader implication of this research is providing a mid-crustal perspective on the rise and fall of orogenic plateaus. Further, the research approach applied in this thesis provides an example of how orogen scale geologic databases can yield important new insights to the tectonic and crustal evolution of mountain belts and continental lithosphere.

1.5 References

Amidon, W.H., Roden-Tice, M., Anderson, A.J., McKeon, R.E., and Shuster, D.L., 2016, Late cretaceous unroofing of the White Mountains, New Hampshire, USA: An episode of passive margin rejuvenation? Geology, v. 44, p. 415–418, doi:10.1130/G37429.1.

Armijo, R., Lacassin, R., Coudurier-Curveur, A., and Carrizo, D., 2015, Coupled tectonic evolution of Andean orogeny and global climate: Earth-Science Reviews, doi:10.1016/j.earscirev.2015.01.005.

Ashwal, L.D., Leo, G.W., Robinson, P., Zartman, R.E., and Hall, D.J., 1979, The Belchertown quartz monzodiorite pluton, West-central Massachusetts; a syntectonic Acadian intrusion: American Journal of Science, v. 279, p. 936–969.

Bird, J.M., and Dewey, J.F., 1970, Lithosphere plate-continental margin tectonics and the evolution of the appalachian orogen: Geological Society of America Bulletin, v. 81, p. 1031–1060, doi:10.1130/0016-7606(1970)81[1031:LPMTAT]2.0.CO;2.

Bosse, V., and Villa, I.M., 2019, Petrochronology and hygrochronology of tectono-metamorphic events: Gondwana Research, v. 71, p. 76–90, doi:10.1016/j.gr.2018.12.014.

Bradley, D.C., 1983, Tectonics of the Acadian Orogeny in New England and adjacent Canada (USA): Journal of Geology, v. 91, p. 381–400, doi:10.1086/628785.

Bradley, D.C., McCauley, A.D., and Stillings, L.L., 2017, Mineral-deposit model for lithium-cesium-tantalum pegmatites: Scientific Investigations Report, doi:10.3133/sir20105070O.

Bradley, D.C., and O'Sullivan, P., 2017, Detrital zircon geochronology of pre- and syncollisional strata, Acadian orogen, Maine Appalachians: Basin Research, v. 29, p. 571–590, doi:10.1111/bre.12188.

Campbell, I.H., and Squire, R.J., 2010, The mountains that triggered the Late Neoproterozoic increase in oxygen: The Second Great Oxidation Event: Geochimica et Cosmochimica Acta, v. 74, p. 4187–4206, doi:10.1016/j.gca.2010.04.064.

Clark, G.S., and Kulp, J.L., 1968, Isotopic age study of metamorphism and intrusion in western Connecticut and southeastern New York: American Journal of Science, v. 266, p. 865–894.

Dalziel, I.W.D., and Dewey, J.F., 2019, The classic wilson cycle revisited: Geological Society Special Publication, v. 470, p. 19–38, doi:10.1144/SP470.1.

DeCelles, P.G., 2004, Late Jurassic to Eocene evolution of the Cordilleran thrust belt and foreland basin system, western U.S.A: American Journal of Science, v. 304, p. 105–168, doi:10.2475/ajs.304.2.105.

Farner, M.J., and Lee, C.T.A., 2017, Effects of crustal thickness on magmatic differentiation in subduction zone volcanism: A global study: Earth and Planetary Science Letters, doi:10.1016/j.epsl.2017.04.025.

Faul, H., Stern, T.W., Thomas, H.H., and Elmore, P.L.D., 1963, Ages of intrusion and metamorphism in the northern Appalachians: American Journal of Science, v. 261, p. 1–19.

France-Lanord, C., and Derry, L.A., 1997, Organic carbon burial forcing of the carbon cycle from himalayan erosion: Nature, doi:10.1038/36324.

Gehrels, G., 2014, Detrital Zircon U-Pb Geochronology Applied to Tectonics: Annual Review of Earth and Planetary Sciences, v. 42, p. 127–149, doi:10.1146/annurev-earth-050212-124012.

Harper, C.T., 1968, Isotopic ages from the Appalachians and their tectonic significance: Canadian Journal of Earth Sciences, v. 5, p. 49–59.

Harrison, T.M., Célérier, J., Aikman, A.B., Hermann, J., and Heizler, M.T., 2009, Diffusion of 40Ar in muscovite: Geochimica et Cosmochimica Acta, v. 73, p. 1039–1051, doi:10.1016/j.gca.2008.09.038.

Harrison, T.M., Copeland, P., Kidd, W.S.F., and Yin, A., 1992, Raising Tibet: Science, v. 255, p. 1663–1670, doi:10.1126/science.255.5052.1663.

Hollocher, K., Robinson, P., Lucas, B., and Mabee, S., 2019, Geochemistry of intrusive rocks on the Prescott Peninsula, central Massachusetts, USA: Implications for late detachment faulting within the Ordovician Taconian volcanic arc: American Journal of Science, v. 319, p. 658–693, doi:10.2475/08.2019.02.

Hurley, P.M., Boucot, A.J., Albee, A.L., Faul, H., Pinson, W.H., and Fairbairn, H.W., 1959, Minimum age of the Lower Devonian slate near Jackman, Maine: Geological Society of America Bulletin, v. 70, p. 947–950.

Hurley, P.M., Fairbairn, H.W., Pinson, W.H., and Faure, G., 1960, KA and Rb-Sr minimum ages for the Pennsylvanian section in the Narragansett Basin: Geochimica et Cosmochimica Acta, v. 18, p. 247–258.

Iaffaldano, G., Bunge, H.P., and Dixon, T.H., 2006, Feedback between mountain belt growth and plate convergence: Geology, v. 34, p. 893–896, doi:10.1130/G22661.1.

Kapp, P., and DeCelles, P.G., 2019, Mesozoic–Cenozoic geological evolution of the Himalayan-Tibetan orogen and working tectonic hypotheses: American Journal of Science, v. 319, p. 159–254, doi:10.2475/03.2019.01.

Karabinos, P., Macdonald, F.A., and Crowley, J.L., 2017, Bridging the gap between the foreland and hinterland I: Geochronology and plate tectonic geometry of Ordovician magmatism and terrane accretion on the Laurentian margin of New England: American Journal of Science, v. 317, p. 515–554, doi:10.2475/05.2017.01.

Keller, B., and Schoene, B., 2018, Plate tectonics and continental basaltic geochemistry throughout Earth history: Earth and Planetary Science Letters, v. 481, p. 290–304, doi:10.1016/j.epsl.2017.10.031.

Keller, C.B., and Schoene, B., 2012, Statistical geochemistry reveals disruption in secular lithospheric evolution about 2.5 Gyr ago: Nature, v. 485, p. 490–493, doi:10.1038/nature11024.

Kellett, D.A., Pehrsson, S., Skipton, D.R., Regis, D., Camacho, A., Schneider, D.A., and Berman, R., 2020, Thermochronological history of the Northern Canadian Shield: Precambrian Research, v. 342, p. 105703, doi:10.1016/j.precamres.2020.105703.

Kim, J., Klepeis, K., Webb, L., and Amidon, W., 2019, New Insights on the Ordovician-Neogene Tectonic History of the Champlain Valley Belt from Drone Surveys, Photogammetry, and Geochronology, West-Central Vermont: New England Intercollegiate Geological Conference, v. B1, p. 90.

Levin, V., Long, M.D., Skryzalin, P., Li, Y., and López, I., 2018, Seismic evidence for a recently formed mantle upwelling beneath New England: Geology, v. 46, p. 87–90, doi:10.1130/G39641.1.

Li, C., Gao, H., and Williams, M.L., 2020, Seismic characteristics of the eastern North American crust with Ps converted waves: terrane accretion and modification of continental crust: Journal of Geophysical Research: Solid Earth, doi:10.1029/2019jb018727.

Li, C., Gao, H., Williams, M.L., and Levin, V., 2018, Crustal Thickness Variation in the Northern Appalachian Mountains: Implications for the Geometry of 3-D Tectonic Boundaries Within the Crust: Geophysical Research Letters, v. 45, p. 6061–6070, doi:10.1029/2018GL078777.

Long, M.D., Aragon, J.C., Yang, X., Gao, H., Goldhagen, G., Ford, H., and Kuiper, Y.D., 2019, Modification of Lithospheric Structure beneath Connecticut via Subduction, Terrane Accretion, and Rifting: Insights from the SEISCONN Experiment, *in* Geological Society of America Abstracts with Programs, doi:10.1130/abs/2019NE-327980.

Long, L.E., and Kulp, J.L., 1962, Isotopic age study of the metamorphic history of the Manhattan and Reading Prongs: Geological Society of America Bulletin, v. 73, p. 969–996.

Macdonald, F.A., Karabinos, P.M., Crowley, J.L., Hodgin, E.B., Crockford, P.W., and Delano, J.W., 2017, Bridging the gap between the foreland and hinterland II: Geochronology and tectonic setting of Ordovician magmatism and basin formation on the Laurentian margin of New England and Newfoundland: American Journal of Science, v. 317, p. 555.

Macdonald, F.A., Ryan-Davis, J., Coish, R.A., Crowley, J.L., and Karabinos, P.M., 2014, A newly identified Gondwanan terrane in the northern Appalachian Mountains: Implications for the Taconic orogeny and closure of the Iapetus Ocean: Geology, v. 43, p. 539–542, doi:10.1130/G36575Y.1.

Macdonald, F.A., Swanson-Hysell, N. l, Park, Y., Lisiecki, L., and Jagoutz, O., 2019, Arc-continent collisions in the tropics set Earth's climate state: Science, v. 364, p. 181–184.

McKerrow, W.S., and Ziegler, A.M., 1972, Palaeozoic Oceans: Nature Physical Science, doi:10.1038/physci240092b0.

Meert, J.G., and Lieberman, B.S., 2008, The Neoproterozoic assembly of Gondwana and its relationship to the Ediacaran-Cambrian radiation: Gondwana Research, v. 14, p. 5–21, doi:10.1016/j.gr.2007.06.007.

Miao, Y., Herrmann, M., Wu, F., Yan, X., and Yang, S., 2012, What controlled Mid-Late Miocene long-term aridification in Central Asia? - Global cooling or Tibetan Plateau uplift: A review: Earth-Science Reviews, v. 112, p. 155–172, doi:10.1016/j.earscirev.2012.02.003.

Molnar, P., England, P.C., and Jones, C.H., 2015, Mantle dynamics, isostasy, and the support of high terrain: Journal of Geophysical Research: Solid Earth, v. 120, p. 1932–1957, doi:10.1002/2014JB011724.

Molnar, P., England, P., and Martinod, J., 1993, Mantle dynamics, uplift of the Tibetan Plateau, and the Indian Monsoon: Reviews of Geophysics, v. 31, p. 357–396, doi:10.1029/93RG02030.

Naylor, R.S., 1971, Acadian orogeny: An abrupt and brief event: Science, v. 172, p. 558–560, doi:10.1126/science.172.3983.558.

Perrot, M., Tremblay, A., Ruffet, G., Labrousse, L., Gervais, F., and Caroir, F., 2020, Diachronic metamorphic and structural evolution of the Connecticut Valley–Gaspé trough, Northern Appalachians: Journal of Metamorphic Geology, v. 38, p. 3–27, doi:10.1111/jmg.12510.

Porder, S., Vitousek, P.M., Chadwick, O.A., Chamberlain, C.P., and Hilley, G.E., 2007, Uplift, erosion, and phosphorus limitation in terrestrial ecosystems: Ecosystems, v. 10, p. 159–171, doi:10.1007/s10021-006-9011-x.

Profeta, L., Ducea, M.N., Chapman, J.B., Paterson, S.R., Gonzales, S.M.H., Kirsch, M., Petrescu, L., and DeCelles, P.G., 2015, Quantifying crustal thickness over time in magmatic arcs: Scientific Reports, doi:10.1038/srep17786.

Raymo, M.E., and Ruddiman, W.F., 1992, Tectonic forcing of late Cenozoic climate: Nature, v. 359, p. 117–122, doi:10.1038/359117a0.

Richards, J.P., 2015, Tectonic, magmatic, and metallogenic evolution of the Tethyan orogen: From subduction to collision: Ore Geology Reviews, v. 70, p. 323–345, doi:10.1016/j.oregeorev.2014.11.009.

Roberts, N.M.W., and Spencer, C.J., 2015, The zircon archive of continent formation through time: Geological Society Special Publication, doi:10.1144/SP389.14.

Robinson, P., and Hall, L.M., 1980, Tectonic synthesis of southern New England, *in* International Geological Correlation Project, Proceedings, Project, v. 27, p. 73–82.

Robinson, P., Tucker, R.D., Bradley, D., Berry IV, H.N., and Osberg, P.H., 1998, Paleozoic orogens in New England, USA: GFF, v. 120, p. 119–148, doi:10.1080/11035899801202119.

Ryan, P.D., and Dewey, J.F., 2019, The sources of metamorphic heat during collisional orogeny: The Barrovian Enigma: Canadian Journal of Earth Sciences, v. 56, p. 1309–1317, doi:10.1139/cjes-2018-0182.

Schmandt, B., and Lin, F.C., 2014, P and S wave tomography of the mantle beneath the United States: Geophysical Research Letters, doi:10.1002/2014GL061231.

Schmittner, A., Silva, T.A.M., Fraedrich, K., Kirk, E., and Lunkeit, F., 2011, Effects of mountains and ice sheets on global ocean circulation: Journal of Climate, v. 24, p. 2814–2829, doi:10.1175/2010JCLI3982.1.

van Staal, C.R., Dewey, J.F., Niocaill, C. Mac, and Mckerrow, W.S., 1998, The Cambrian-Silurian tectonic evolution of the northern Appalachians and British Caledonides: history of a complex, west and southwest Pacific- type segment of Iapetus: Geological Society Special Publication, v. 143, p. 197–242, doi:10.1144/GSL.SP.1998.143.01.17.

van Staal, C.R., Whalen, J.B., Valverde-Vaquero, P., Zagorevski, A., and Rogers, N., 2009, Pre-Carboniferous, episodic accretion-related, orogenesis along the Laurentian margin of the northern Appalachians: Geological Society, London, Special Publications, v. 327, p. 271–316, doi:10.1144/SP327.13.

Sun, W., Zhang, H., Ling, M.X., Ding, X., Chung, S.L., Zhou, J., Yang, X.Y., and Fan, W., 2011, The genetic association of adakites and Cu-Au ore deposits: International Geology Review, v. 53, p. 691–703, doi:10.1080/00206814.2010.507362.

Thompson, J.B.J., Robinson, P., and Trask, N.J., 1968, Nappes and gneiss domes in west-central New England, *in* Zen, E.-A., White, W.S., Hadley, J., and Thompson, J.J. eds., Studies of Appalachian geology: Northern and Maritime, New York, Interscience, p. 203–218.

Tracy, R.J., Robinson, P., and Thompson, A.B., 1976, Garnet composition and zoning in the determination of temperature and pressure of metamorphism, central Massachusetts: American Mineralogist, v. 61, p. 762–775.

Turner, S.J., and Langmuir, C.H., 2015, The global chemical systematics of arc front stratovolcanoes: Evaluating the role of crustal processes: Earth and Planetary Science Letters, doi:10.1016/j.epsl.2015.03.056.

Valley, P.M., Walsh, G.J., Merschat, A.J., and McAleer, R.J., 2019, Geochronology of the Oliverian Plutonic Suite and the Ammonoosuc Volcanics in the Bronson Hill arc: Western New Hampshire, USA: Geosphere, v. 16, doi:10.1130 /GES02170.1.

Waldron, J.W.F., Schofield, D.I., and Murphy, J.B., 2017, Diachronous Palaeozoic accretion of peri-Gondwanan terranes at the Laurentianmargin: Geological Society of London Special Publication,.

Williams, M.L., Jercinovic, M.J., Mahan, K.H., and Dumond, G., 2017, Electron Microprobe Petrochronology: Reviews in Mineralogy and Geochemistry, v. 83, p. 153–182, doi:10.2138/rmg.2017.83.5.

Wilson, J.T., 1966, Did the Atlantic Close and then Re-Open? Nature, doi:10.1038/211676a0.

Wise, D.U., 1992, Dip domain method applied to the Mesozoic Connecticut Valley Rift Basins: Tectonics, v. 11, p. 1357–1368, doi:10.1029/92TC01103.

Wolfe, O.M., and Spear, F.S., 2018, Determining the amount of overstepping required to nucleate garnet during Barrovian regional metamorphism, Connecticut Valley Synclinorium: Journal of Metamorphic Geology, v. 36, p. 79–94, doi:10.1111/jmg.12284.

Yakymchuk, C., Clark, C., and White, R.W., 2017, Phase Relations, Reaction Sequences and Petrochronology: Reviews in Mineralogy and Geochemistry, v. 83, p. 13–53, doi:10.2138/rmg.2017.83.2.

Yang, X., and Gao, H., 2018, Full-Wave Seismic Tomography in the Northeastern United States: New Insights Into the Uplift Mechanism of the Adirondack Mountains: Geophysical Research Letters, v. 45, p. 5992–6000, doi:10.1029/2018GL078438.

Yasunari, T., 2020, The Uplift of the Himalaya-Tibetan Plateau and Human Evolution: An Overview on the Connection Among the Tectonics, Eco-Climate System and Human Evolution During the Neogene Through the Quaternary Period, *in* Himalayan Weather and Climate and their Impact on the Environment, p. 281–305, doi:10.1007/978-3-030-29684-1_15.

Zandt, G., Gilbert, H., Owens, T.J., Ducea, M., Saleeby, J., and Jones, C.H., 2004, Active foundering of a continental arc root beneath the southern Sierra Nevada in California: Nature, doi:10.1038/nature02847.

Zartman, R.E., 1977, Geochronology of some alkalic rock provinces in eastern and central United States: Annual Review of Earth and Planetary Sciences, v. 5, p. 257–286.

Zartman, R.E., 1988, Three decades of geochronologic studies in the New England Appalachians: Geological Society of America Bulletin, v. 100, p. 1168–1180, doi:10.1130/0016-7606(1988)100<1168:TDOGSI>2.3.CO;2.

Zartman, R.E., Hurley, P.M., Krueger, H.W., and Giletti, B.J., 1970, A Permian disturbance of K-Ar radiometric ages in New England: Its occurrence and cause: Geological Society of America Bulletin, v. 81, p. 3359–3374.

Zhisheng, A., Kutzbach, J.E., Prell, W.L., and Porter, S.C., 2001, Evolution of Asian monsoons and phased uplift of the Himalaya - Tibetan plateau since Late Miocene times: Nature, doi:10.1038/35075035.

CHAPTER 2

A NEW GEOLOGIC DATABASE FOR THE NEW ENGLAND APPALACHIANS

2.1 Abstract

Regional geologic databases are increasingly important for interpreting geologic data, creating and testing new hypotheses, and serving as data repositories. A new database of previously published geochronologic, geochemical, and geothermobarometric data is presented for the Appalachian Orogen, New England, USA. Over 22,000 individual data points been compiled, digitized, and georeferenced. Each dataset is accessible via interactive web-based maps and data tables. Filtered datasets are downloadable as comma separated values (.csv). Then, the database is used to interrogate the crustal evolution, as recorded by isotopic systems in igneous records and test its utility for detrital mineral studies. A compilation of igneous crystallization dates reveals major peaks in magmatism are identified at ca. 470, 450, 415, and 374 Ma with minor peaks at 600, 268, 194 and 124 Ma. Depleted mantle Sm-Nd model ages show a large double peak at 1240 and 1380 Ma with subordinate peaks at 870 and 1710 Ma. Time series of Nd and O isotopes and Sr/Y ratios show isotopic shifts associated with major orogenic events and peaks in igneous crystallization ages. Shifts towards more evolved isotopic values suggest an increased component of re-worked continental crust during these episodes, perhaps related to crustal thickening as suggested by Sr/Y. Comparisons between detrital minerals and compiled data show strong correlations and provide more rigorous provenance constraints, and, possibly, regional post-orogenic cooling rates.

2.2 Introduction

Quantitative data are a cornerstone of geologic research, informing studies on the scale of a single mineral grain to global processes. Quantitative data are becoming increasingly accessible, with tools such as LA-ICPMS, EPMA, and MC-ICP-MS leading to rapid expansion of compositional and geochronologic datasets (Gehrels, 2014). The increasing quantity and quality of analytical data along with increases in computing power has led to the development of regional and global compilations which have provided new insights on regional tectonics (Chapman and Kapp, 2017; Chapman et al., 2017; Thigpen and Hatcher Jr., 2017; Kellett et al., 2020), global secular evolution (Condie and Kröner, 2008; Bradley, 2011; Keller and Schoene, 2012, 2018), and new understandings of modern geologic processes at a global scale (Gale et al., 2013; Chiaradia, 2015; Profeta et al., 2015; Turner and Langmuir, 2015b, 2015a; Farner and Lee, 2017; Hu et al., 2017). These databases also serve as repositories for published data which are easily accessible for testing or developing hypotheses. However, significant gaps in compilations exist between global and regional datasets. The former focus primarily on recently published data and may be biased to modern tectonic settings, excluding a large portion of the published literature while the latter are more comprehensive but are spatially, and often temporally, restricted. Further compounding access to geologic data is its scatter across journal articles, field guidebooks, geologic survey publications, student theses and, in some cases, only available in conference abstracts.

The northern Appalachian orogen has inspired plate tectonic models for decades (Wilson, 1966; Thompson et al., 1968; Bird and Dewey, 1970; McKerrow and Ziegler,

1972) and continues to be a region of active study, yielding new insights and discoveries (Macdonald et al., 2014; Karabinos et al., 2017; Kuiper et al., 2017; Levin et al., 2018; Li et al., 2018, 2020; Cartwright et al., 2019; Long et al., 2019; Perrot et al., 2020). The rocks preserve evidence for a full Wilson cycle, from the breakup of Rodinia through the the assembly of Pangea to the formation of the Atlantic Ocean and may provide exposures of analogues for active tectonic processes (Kuiper, 2016; Hillenbrand et al., 2019). However, no unified database of geologic data exists for the northern Appalachians despite scientific interest, its potential utility, and the expansive literature.

This chapter presents a newly assembled, centralized database for geochronologic, geochemical, and geothermobarometric data for the northern Appalachian orogen. This dataset is accessible through an interactive, web-based interface. The chapter then explores the implications for crustal evolution using geochemical data and its application to detrital mineral studies.

2.3 Geologic Background

The northern Appalachian Mountains were constructed in the Paleozoic in a series of orogenic events, each of which have been interpreted to represent terrane accretion, which ultimately culminated in the closure of the Iapetus Ocean and formation of Pangea (Wilson, 1966; Hatcher, 2010; Waldron et al., 2014). Five phases of Paleozoic orogenesis are presently recognized (Robinson et al., 1998; van Staal et al., 2009; Karabinos et al., 2017) which were followed by Mesozoic extension (Wise, 1992; Olsen, 1997; Roden-Tice and Wintsch, 2002). The present complex distribution of lithotectonic elements are shown on Figure 1.

The Middle-Late Ordovician (475-440 Ma) Taconic orogeny is interpreted to record the collision between island arc(s) and the Laurentian margin (Stanley and Ratcliffe, 1985; van Staal et al., 2009; Karabinos et al., 2017). Collision between the Shelburne Falls arc, constructed on the Gondwanan-derived Moretown terrane, and rocks of the Laurentian margin is interpreted to have occurred by 475 Ma (Karabinos et al., 1998, 2017; Macdonald et al., 2014, 2017) and resulted in the emplacement of allochthons, Barrovian metamorphism, and development of a foreland basin (Stanley and Ratcliffe, 1985; Ettensohn, 1994; Macdonald et al., 2017). Continued convergence has been interpreted to have been accommodated by a reversal in subduction polarity thought to have occurred between 466 and 455 Ma (Karabinos et al., 2017). Karabinos et al. (1998, 2017) suggested this event initiated a west-dipping subduction zone under Laurentia and the newly accreted Moretown terrane. Magmatic arc rocks of the Bronson Hill arc are interpreted to have formed above this subduction zone between 455 and 440 Ma (Karabinos et al., 1998, 2017). Alternatively to a switch in subduction polarity, termination of the Taconic Orogeny has been attributed to docking of the peri-Gondwanan Gander terrane (van Staal et al., 2008, 2009)

Accretion of the Gander terrane to the Taconic-modified Laurentian margin is interpreted to have occurred in the Late Ordovician-Early Silurian (440-423 Ma) Salinic orogeny (van Staal et al., 2008, 2009; Kellett et al., 2017). The Salinic Orogeny is interpreted to have an early (445-430 Ma) accretionary phase followed by 430-422 Ma collision-related orogenesis (van Staal et al., 2008, 2009). These phases are well characterized in Maritime Canada but the nature of the Salinic Orogeny is poorly understood in New England (Wathen et al., 2015; Eusden et al., 2017; Kim et al., 2019).

The time of interpreted accretion in New England also was a period of basin formation and extension (for example, Rankin et al., 2007; McWilliams et al., 2010; Perrot et al., 2018; Karabinos et al., 2019), prompting the suggestion that the accretion of the Gander terrane was a "soft" orogeny (Perrot et al., 2018). Evidence of Salinic orogenesis may also have been overprinted by the subsequent Acadian orogeny.

The Late Silurian to Middle Devonian (425-380 Ma) Acadian orogeny, deemed the dominant mountain building event in New England (Hatcher, 2010), is generally attributed to the collision and subsequent accretion of the Gondwanan-derived Avalon terrane to Laurentia. The Acadian orogeny produced polyphase deformation, widespread high-grade metamorphism, and a thick wedge of sediments shed westward from the orogen (Robinson et al., 1998; Eusden et al., 2000; van Staal et al., 2009; Ettensohn et al., 2019). The deformation front has been interpreted to have migrated progressively westward into the Laurentian hinterland during the Devonian (Bradley et al., 2000) and reached its final structural limit by the Middle Devonian (Bradley et al., 2000; van Staal et al., 2009). High precision geochronology over the past few decades have led to reinterpretation and subdivision of the Acadian Orogeny into the 420-380 Ma Acadian and the 380-350 Ma Neoacadian orogenies, respectively (Eusden and Barreiro, 1988; Robinson et al., 1998; van Staal et al., 2009) and a recently recognized period of 350-300 Ma lateral transpression and escape (Massey et al., 2017b). The period of 330-310 Ma may represent orogenic collapse in central New England (Hillenbrand et al., 2019).

Carboniferous to Permian deformation in coastal Maine was characterized by dextral strike-slip faulting on the Norumbega Fault zone (West Jr and Lux, 1993; Robinson et al., 1998; Swanson, 1999). Strain was progressively localized, from a diffuse

>25 km wide heterogeneously distributed ductile shear structures to a 1 km high strain mylonite zone (Hubbard, 1999). This transition is thought to have occurred during cooling and exhumation (West Jr. et al., 1988; West Jr and Roden-Tice, 2003).

The Permian Alleghenian orogeny (300-260 Ma) is final major orogenic event in the New England Appalachians (Robinson et al., 1998; Hatcher, 2010). It has been interpreted to represent continent-continent collision between Gondwana and Laurentia during the final assembly of Pangea (Hatcher, 2010). Deformation and metamorphism attributed to the Alleghanian orogeny are restricted to southeasternmost New England (Wintsch et al., 1992, 2014).

Subsequent tectonism in the New England Appalachians has been dominated by extension, characterized by basin formation, mafic magmatism, and faulting in the Mesozoic (Wise, 1992; Olsen, 1997; Roden-Tice and Wintsch, 2002; Roden-Tice et al., 2009). Cretaceous (ca. 130 Ma) magmatism has been noted across New England and been linked by some to passage of the Great Meteor hotspot (Crough, 1981). However, this interpretation has been challenged by recent geochronologic work (Kinney et al., 2019). Periods of high erosion and increased strain have been linked to passive margin re-activation (Amidon et al., 2016; Kim et al., 2019), potentially related to mantle dynamics (Menke et al., 2018; Yang and Gao, 2018).

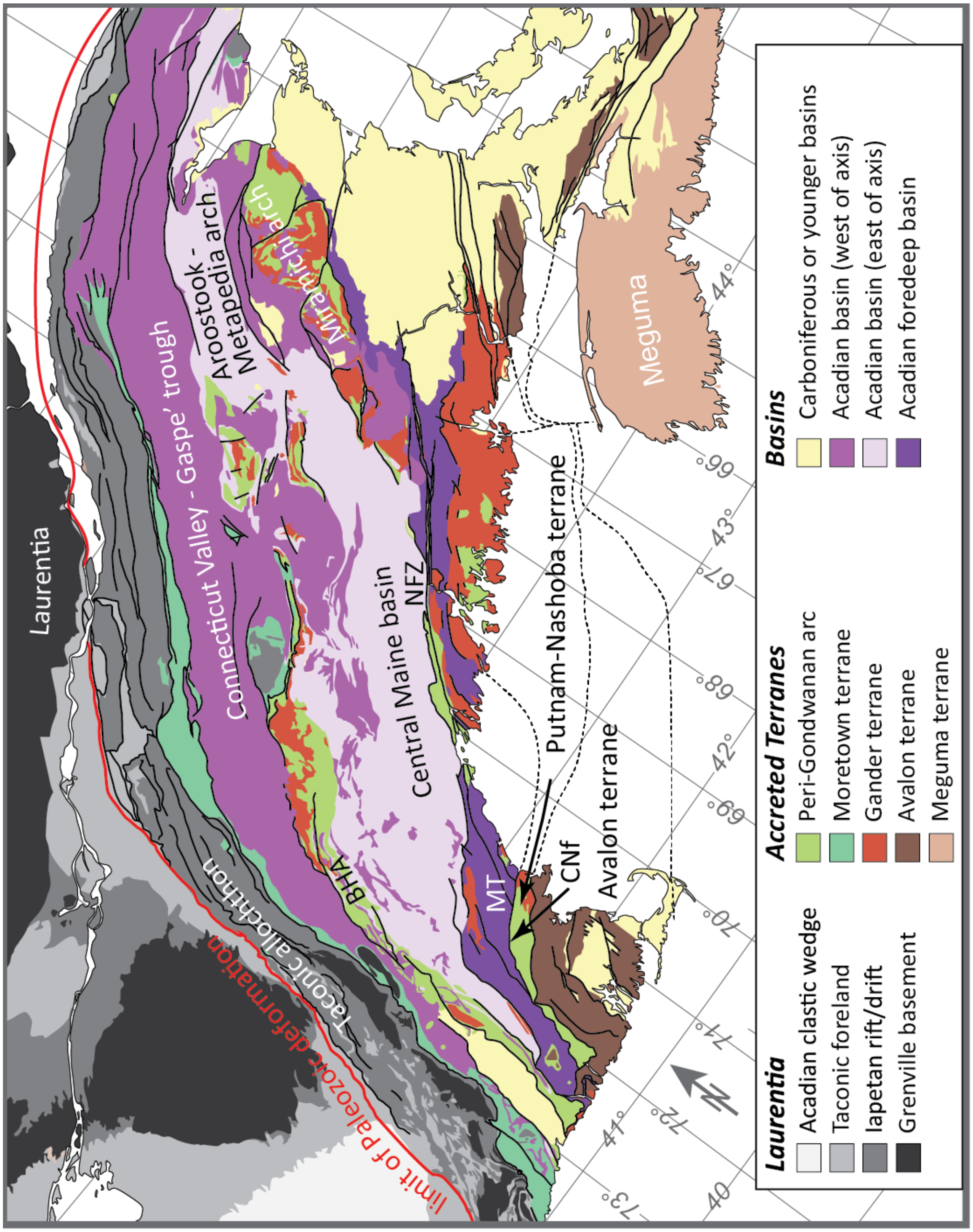

Figure 1: Simplified lithotectonic map of the northern Appalachians modified from Hibbard et al. (2006) after Massey et al. (2017) and Karabinos et al. (2017). BHA: Bronson Hill composite arc, MT: Merrimack trough, NFZ: Norumbega Fault zone.

2.4 Database

A new database of geochemical, geochronologic, and geothermobarometric analyses, called the New England Geologic Database, or NED, was compiled for the northern Appalachians. Data were digitized primarily from peer-reviewed papers, geologic survey publications, field guides, and student theses. In certain cases, abstracts were included as necessary for completeness. The scope of the compilation covers the region north of the New Jersey Highlands and New Brunswick, south of the Bay of St. Lawrence along the strike of the Appalachian orogen. The adjacent Appalachian basin in New York State and Pennsylvania are included as are the offshore New England seamount chain.

Sample locations are recorded in decimal degree format (°N latitude and °E longitude) using the NAD 1984 (2011) reference coordinate system. Individual analyses were assigned sample locations using, in order of preferred method, provided coordinates, descriptions of the sample location, or georeferencing a map of the sample locality. Error involved in georeferencing was estimated by measuring the radius of the map marker. This provides a minimum error as it cannot account for errors involved in drafting the map or limitations in georeferencing. Samples which did not have a specific sample locality were placed in the approximate center of the study area, or in the case of igneous plutonic rocks, at the center of the pluton following the database of Bradley et al. (2015). For these samples, location error was assigned as the radius of the igneous body. Geochemical analyses of metasedimentary rocks lacking sample localities were not georeferenced out of consideration for their significant heterogeneity.

Geochemical, geochronologic, and geothermobarometric datasets have been compiled into separates databases with a unique set of attributes. Datasets were originally compiled in Microsoft Excel and converted to web-based Google Sheets spreadsheets. These spreadsheets are reformatted by the Awesome Table service and embedded into a host website, https://sites.google.com/umass.edu/ned (Fig. 2). The databases can be accessed from the sidebar to the left or links on the homepage (Fig. 2). Each page has an interactive map viewer, a set of filters, and data table. Basemaps for the interactive map viewer are hosted by Google Maps with access to street, terrain, and satellite maps. Clicking on an individual sample will bring up information about the sample in the map window and highlight the data point in the data table. Filters can be used to selectively view certain portions of the data set or search for individual samples, authors, or formations. The entire dataset, or a selected portion, can be downloaded as a comma separated values file (.csv).

Figure 2: New England Geologic Database (NED) homepage.

2.4.1 Geochronology

More than 6,000 geochronologic analyses of igneous, metamorphic, and sedimentary rocks were compiled (Figure 3). Dates are reported in million years (Ma) and errors are reported the 2-sigma level. Date refers of the measured parent and daughter values calculated by the original investigators. The associated age interpretation column refers to the interpretation of a date, such as the age of a particular rock or process (i.e. magmatic crystallization, metamorphism, cooling).

The decay system, material analyzed, description of analytical results, and analytical method are reported for each sample. Where reported, the analysis location and description of sample locality are also included, following methods outlined above. Older geochronologic methods which have been shown to be unreliable (e.g. Pb-alpha) were excluded. In most cases these have been superseded by more recent analyses using more reliable chronometers with more precise methods. Rb/Sr dates post-1980 with well-defined isochrons were included. Analyses from publications pre-1977 were recalculated to the decay constants of Steiger and Jager (1977) using the ArAR program of Mercer and Hodges (2016).

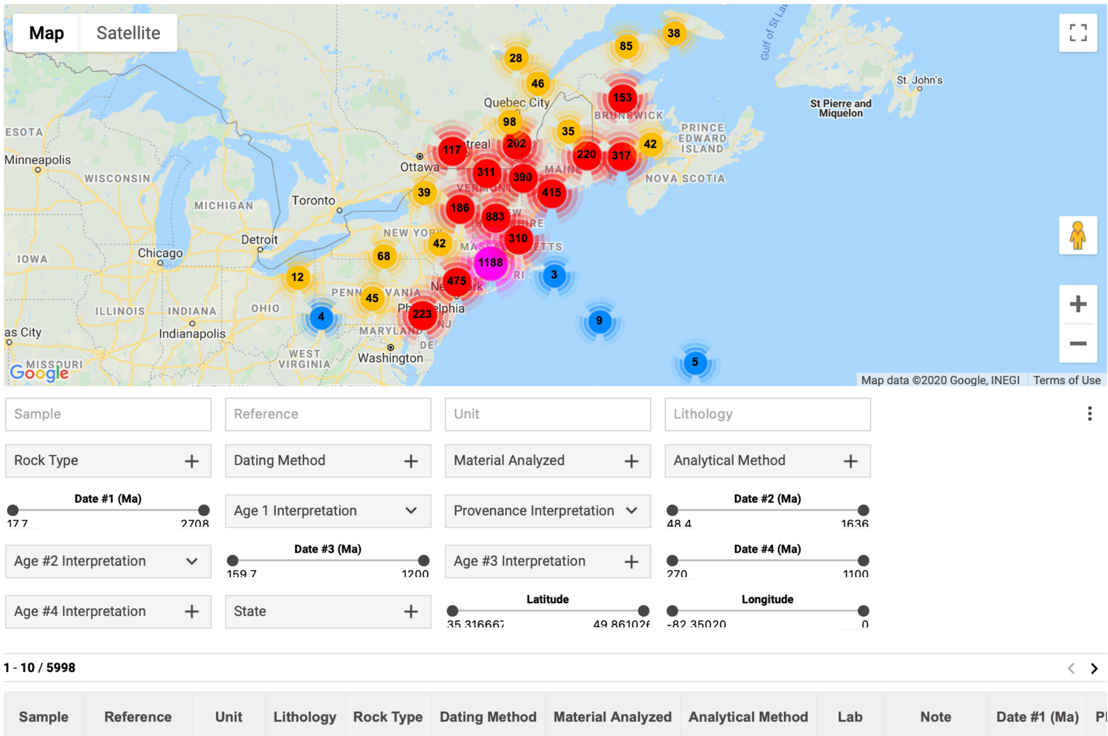

Figure 3: Screenshot of the online interface for the NED geochronology database.

2.4.2 Geochemistry

More than 15,000 whole rock geochemical analyses of either major or trace element or isotopic data have been compiled (Figure 4). Igneous, sedimentary, and metamorphic rocks are included in this database. However, the database is heavily biased towards (meta)igneous rocks due to sampling bias(es). The vast majority of analyses of are whole-rock samples. Major elements are reported in weight percent (wt%) and trace elements are reported in parts per million (ppm). We have compiled present and original Rb/Sr, Sm/Nd, Lu/Hf, and Pb radiogenic isotopes and C, O, S, and H stable isotope ratios. All data are reported as presented in the data source. Lu-Hf and Sm-Nd are reported in ratio and epsilon notation form. C, O, S, and H reported in permil relative to commonly accepted and used standards.

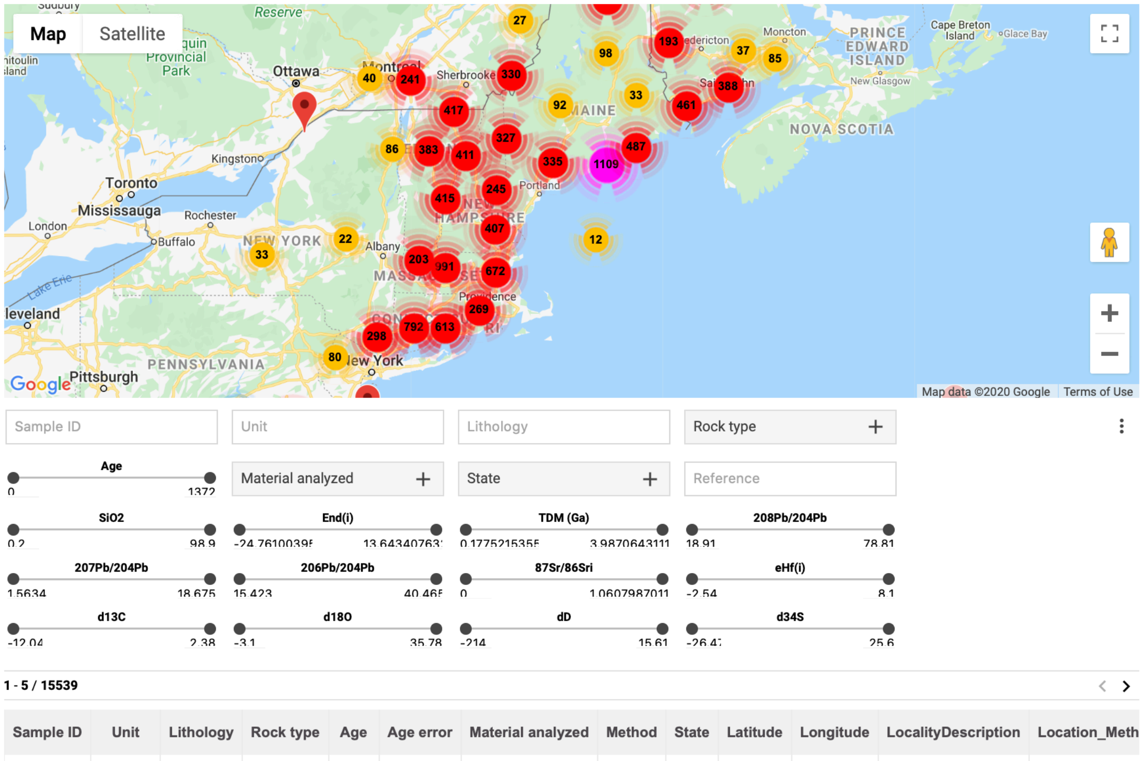

Figure 4: Screenshot of the online interface for the NED geochemistry database.

2.4.3 Geothermobarometry

Greater than 1,000 quantitative thermobarometric estimates of temperatures and/or pressures have been compiled from metamorphic and igneous rocks (Fig. 5). Temperatures are reported in degrees Celsius and pressures are reported in kilobars. In adjacent columns the event these conditions are interpreted to record (e.g. Taconic, Acadian, Alleghanian) and the stage in the P-T history (prograde, peak, or retrograde) are reported as interpreted by the original author. Where reported, the technique, phases, and equilibria/reactions used to interpret pressure and temperature are included. Sample locality, rock unit or formation, and diagnostic mineral assemblage(s) are also included, when reported by the author.

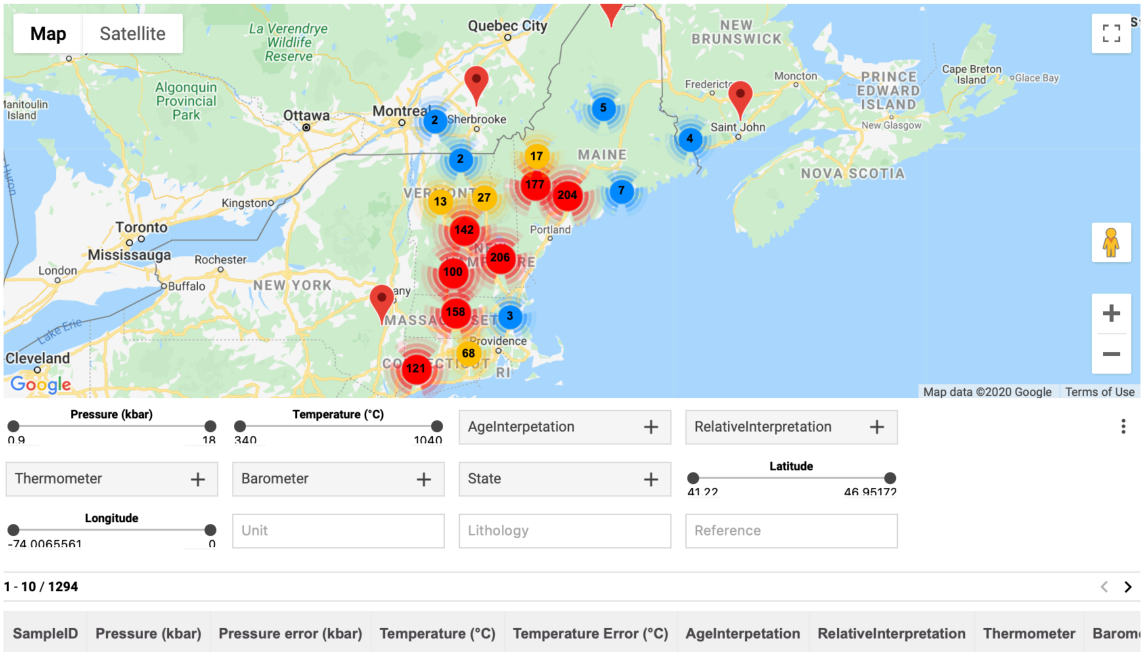

Figure 5: Screenshot of the online interface for the NED geothermobarometry database.

2.5 Applications

In addition to serving as a data repository, the database should be applicable to investigating geologic and tectonic questions. Next, this chapter explores applications of the database to the timing of regional magmatism and crust formation, the identification and significance of trends in isotopic and trace element geochemical data, and to sedimentary provenance.

First, the igneous rock record is investigated along with its implications for the tectonic and crustal evolution. The apparent peaks of igneous activity are identified, using the largest dataset of igneous ages compiled to date from New England. Then, these are compared to Nd depleted mantle model ages to constrain the timing of crustal growth.

Then, the geochemical record of collisional orogenesis is examined. Peaks and troughs in igneous activity during Paleozoic orogenesis are compared with key isotopic and trace element ratios. Periodic shifts from depleted to enriched isotopic values and increases in Sr/Y ratios are observed during the Taconic, Acadian, and Neoacadian orogenic events, which may, in part, be linked to crustal thickening during collisional orogenesis.

Thirdly, the utility of this database for detrital mineral studies is examined. Compiled data from the Merrimack watershed are qualitatively and quantitively compared to published analyses of detrital minerals from the river mouth. Generally strong correlations are observed between detrital minerals ages and previously published dates from the same watershed.

2.5.1 Geochemical Insights into New England crustal evolution

The ages and chemistry of igneous rocks can act as important tracers of the timescales and nature of tectonic activity (van Staal et al., 2009; Chapman and Kapp, 2017; Chapman et al., 2017) and as a record of crustal evolution (DePaolo et al., 1992; Keller and Schoene, 2012). The integration of geochronologic, major and trace element, and isotopic data can identify peaks and lulls in magmatism, the sources of igneous rocks, and changes in the nature of magmatism over time. Here, the timing of igneous rocks and potential protolith ages are examined, followed by an examination of geochemical trends during Paleozoic collisional orogenesis.

To constrain the temporal distribution of igneous rocks, ages interpreted to represent igneous crystallization were extracted from the NED geochronology database. When multiple ages were available for an igneous rock or plutonic body, U-Pb dates on zircon or monazite were preferred due to the analytical precision and refractory nature. Age data are visualized in Figure 6 as histograms and kernel density functions (Vermeesch, 2012). Histograms permit visual inspection of the number of samples comprising each peak but are limited by a standard bin size. A uniform bin width may not be the most accurate representative of unimodal age distributions and does not consider uncertainties. In contrast, kernel density estimates provide a continuous visualization and as a means to identify relative peaks and troughs of ages. Kernel density functions were used to visualize this dataset rather than probability density plots because they are considered more statistically robust, to facilitate comparison between different analytical methods with differing levels of precision, and the adaptive nature of the estimates (e.g. Vermeesch, 2012). Kernel density functions were calculated using an open-source Java application developed by Pieter Vermeesch (Density Plotter, http://www.ucl.ac.uk/~ucfbpve/densityplotter/).

A total of 968 dates are plotted in Figure 6. Relative peaks are observed at ca. 470, 450, 415, 375, 195, and 120 Ma with subordinate peaks at ca. 600, 550, and 280 Ma. A continuum of dates is observed between 950 and 1400 Ma. Minima are observed at 130 to 160, 240, 340 to 300, 510 to 570, and 670 to 800 Ma. These observations are similar to those made by Bradley et al. (2015) using a smaller compilation of the ages of igneous rocks and the U-Pb ages of detrital zircon of river and beach modern sands from New England.

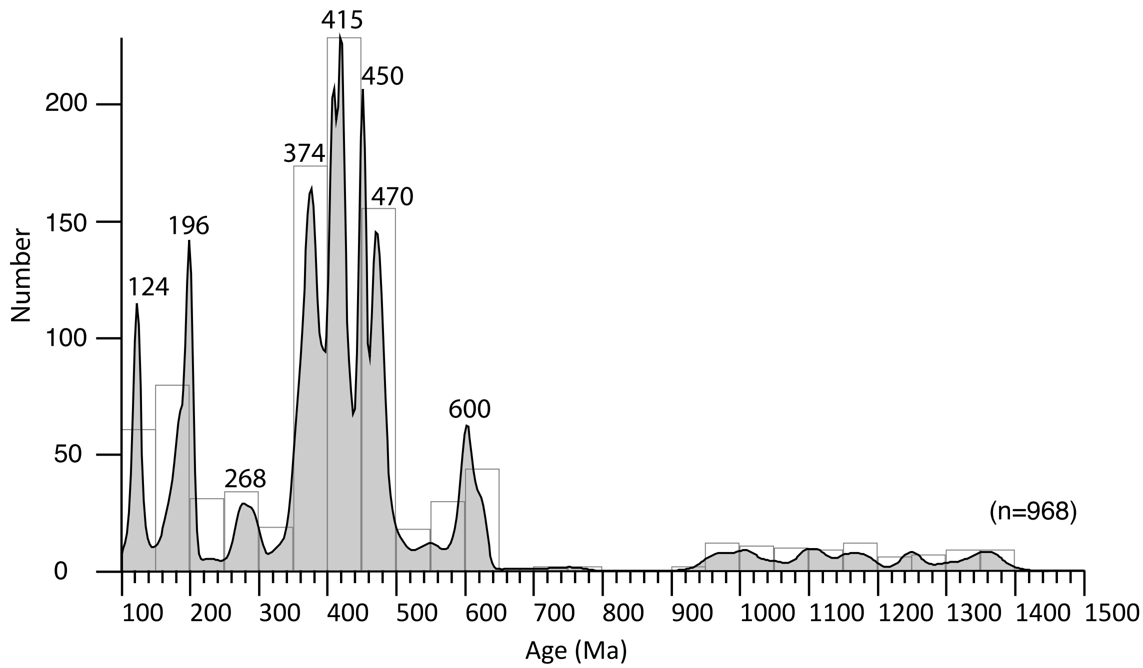

Figure 6: Kernel density function of radiometric dates interpreted to record the age of igneous rocks in New England.

.

The distribution of dates in Figure 5 correlates with known geologic events in the northern Appalachians, as expected from this compiled dataset. The continuum of Mesoproterozoic dates is from inliers of Grenville-aged basement in western New England (Walsh et al., 2004; Karabinos et al., 2008). The Neoproterozoic dates are predominantly from inliers of Gondwanan-derived basement such as the Moretown, Gander, and Avalon terranes (Tucker and Robinson, 1990; Thompson et al., 2007; Walsh et al., 2011; Dorais et al., 2012; Macdonald et al., 2014) while a smaller proportion are from magmatism related to the rifting of Rodinia and opening of the Iapetus ocean (Kumarapeli et al., 1989; Walsh and Aleinikoff, 1999; Tollo et al., 2004).

Ordovician peaks at ~470 and ~450 are predominantly from tonalites and granites of the Shelburne Falls and Bronson Hill arcs of the Taconic orogeny (Karabinos et al., 1998, 2017; Moench and Aleinikoff, 2002). Fig. 6 shows two distinct age maxima, though recently Valley et al. (2019) showed a continuum of dates in Ordovician arc rocks of western New England. Further high precision geochronology, accompanied by geochemical analyses, are required to assess this continuum and whether it represents a single arc, multiple arcs involving a reversal in subduction polarity, or involve other geodynamic processes such as slab-breakoff or delamination.

A late Silurian to Early Devonian peak relates to igneous activity across New England, from Connecticut to Maine. Active magmatism in this time interval occurred in the New Hampshire Plutonic Series and Piscataquis arc of northern Maine during the early Acadian orogeny (Robinson et al., 1998; Bradley et al., 2000; Tucker et al., 2001). “Acadian” peaks are observed ca. 415 and 374 Ma, with compositions ranging from tonalitic to granodiorites and leucogranites (Harrison et al., 1987; Robinson et al., 1998; Dorais, 2003). The subordinate peak at ca. 268 correlates to the Alleghanian orogeny with igneous rocks of this event predominantly exposed in southeastern New England, southern Maine, and southern New Hampshire (Zartman and Hermes, 1987; Tomascak et al., 1996; Walsh et al., 2007). This peak is proportionally smaller than the Acadian and Taconic peaks.

Mesozoic peaks at ca. 124 and 196 Ma are narrow and sharp. They are likely related to ca. 200 Ma magmatism of the Central Atlantic Magmatic Province (Jourdan et al., 2009; Blackburn et al., 2013; McHone et al., 2014), the ca. 168-190 Ma White Mountain batholith (Doherty and Lyons, 1980; Eby et al., 1992; Kinney et al., 2019), and Cretaceous magmatism hypothesized to be related to the Great Meteor Hotspot (Crough, 1981; Foland et al., 1985; Eby, 1989). The relatively sharp, narrow peaks suggest that these may represent more episodic events than the wide range of Paleozoic dates which are related to protracted orogenesis.

While crystallization ages record the time of formation of igneous rocks, they alone do not constrain their petrogenesis or source. Fox example it is challenging to determine whether igneous rocks represent the time of crust formation derived from melting of the mantle or if they are the product of re-melting older crust solely on geochronologic dates. Geochemical data in the form of radiogenic isotopes may discriminate between these predominantly crust and mantle derived rocks and place constraints on the timing of crust formation.

The samarium-neodymium (Sm-Nd) system is often used to discriminate between crustal reworking and crust formation due to the differential partitioning of Sm and Nd during mantle melting. Further, "crust formation" model ages can be calculated if the isotopic evolution of the mantle is assumed to be known over time (DePaolo et al., 1992). While these ages are highly dependent on the type of model chosen (e.g. depleted mantle vs. chondritic uniform mantle) and can be affected by mixing of crustal and mantle components, they offer a potentially useful tool to examine the timing of crust formation.

Sm-Nd model ages were calculated using a single-stage depleted mantle model (DePaolo, 1981). Samples with an apparent high degree of Sm/Nd fractionation ($^{147}Sm/^{144}Nd > 0.17$) were removed. A total of 361 analyses passed this filter and were illustrated on Figure 7 using both a histogram (100 m.y. bins) and an adaptive kernel density estimate. The data exhibit a somewhat gaussian-like distribution with a large Mesoproterozoic double peak at ca. 1250 and 1375 Ma, subordinate "shoulder" peaks at 880 and 1725 Ma, and a smaller peak at ca. 2050 Ma. These main peaks have tails extending to as young as 300 Ma and to as old as 2800 Ma. Overall, the model ages suggest that these igneous rocks are predominantly derived from the recycling crust of that was apparently extracted from the mantle in the Proterozoic. This inference is generally consistent with models involving the derivation of basement blocks from Gondwana or potentially Laurentia inferred from isotopic and geochronologic evidence (Thompson et al., 2007, 2012; Dorais et al., 2012; Miller et al., 2018).

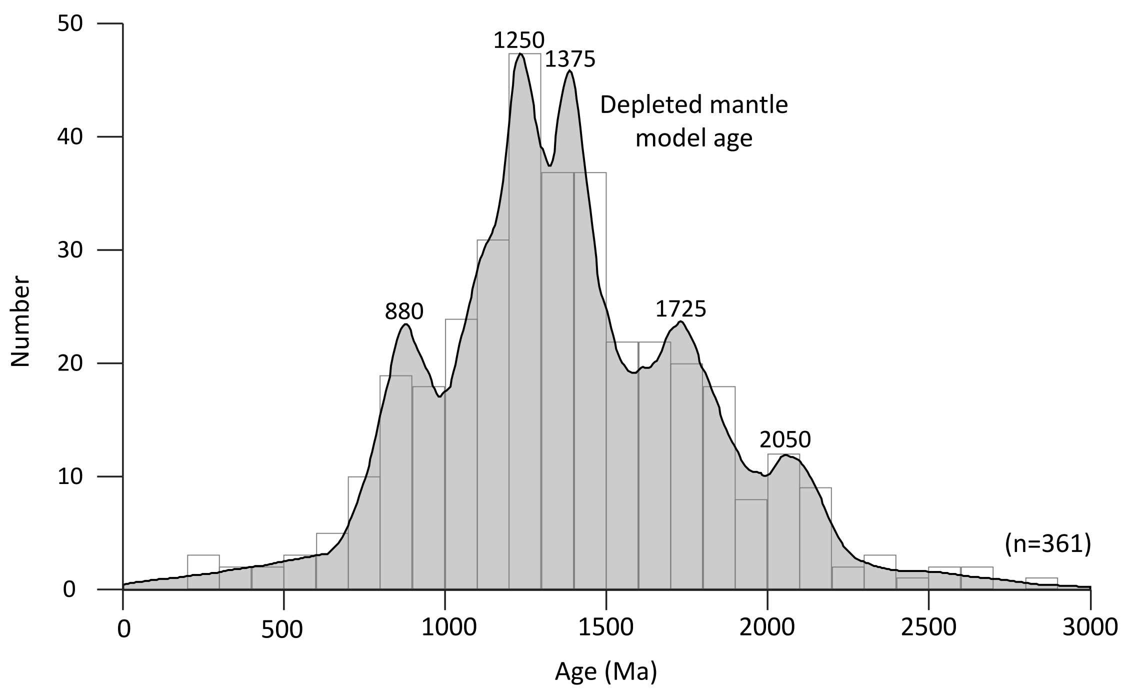

Figure 7: Histogram and kernel density function of depleted mantle model ages.

More insight may be gained into the nature and significance of the prolonged period of Paleozoic magmatism and tectonism by integrating the ages of igneous crystallization with geochemical data. Next, the apparent peaks in magmatic activity are compared with the Nd and O isotope geochemistry, and Sr/Y ratios. Together, these geochemical signatures may decipher between times of

Examining the period of accretionary collisional tectonics (ca. 500 to 350 Ma; van Staal et al., 2009; Karabinos et al., 2017; Robinson et al., 1998), peaks of magmatic crystallization dates occur at ca. 470, 450, 408, and 376 Ma (Figure 7A). Relative minima are observed ca. 430 and 390 Ma but there are no magmatic gaps.

Figure 7B shows initial Neodymium (Nd) isotopes, in epsilon notation, from igneous rocks. ^{143}Nd is produced by decay of ^{147}Sm with a 106-Gy half-life. Samarium is more compatible in the mantle than Neodymium and thus the mantle will evolve over time towards a more radiogenic Nd isotopic composition while the crust will have less radiogenic values. The Nd isotope record shows most positive (juvenile or mantle-like) εNd_i values ca. 480-475 Ma. However, εNd_i values become progressively more negative (evolved) to 450-440 Ma. By ca. 425 εNd_i values are more positive, with some approaching values of the depleted mantle. However, there are a number of plutons with more depleted values, which increase in proportion to ca. 400 Ma. Between 400 and 380 Ma εNd_i values occupy a narrow range between -2 and -4 $\varepsilon Nd_.$ Values between 380 and 350 Ma show a wide range between strongly negative values of -8 to positive values of ~3. These latter values vary geographically, with positive values from Coastal Maine (Oak Hill and Deer Isle plutons), and negative values from Neoacadian plutons of central and southern New England. These results suggest an apparently higher mantle component in magmas ca. 500-470 and ~425 Ma while magmas 470-450 Ma and 420-350 Ma are more consistent with a larger degree of crustal components.

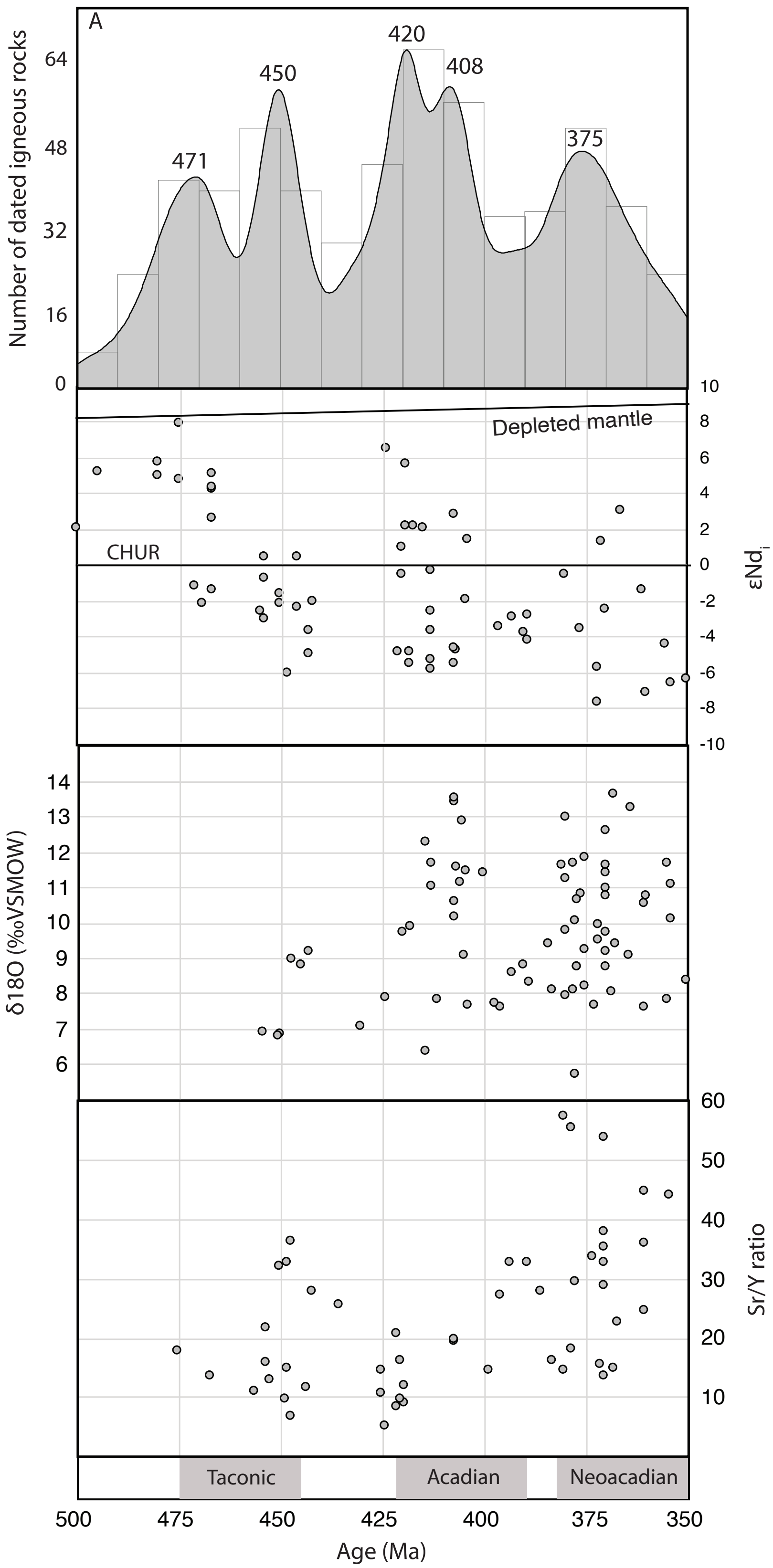
A
Number of dated igneous rocks
64
48
32
16
0
471
450
420
408
375
Depleted mantle
CHUR
10
8
6
4
2
0
-2
-4
-6
-8
-10
εNdi
δ18O (‰VSMOW)
14
13
12
11
10
9
8
7
6
60
50
40
30
20
10
Sr/Y ratio
Taconic
Acadian
Neoacadian
500
475
450
425
400
375
350
Age (Ma)

Figure 8: Compilation of geochronologic and geochemical data during the Taconic-Acadian-Neoacadian interval, 500 to 350 Ma. A) Kernel density function of radiometric dates interpreted to record the age of igneous crystallization. B) Initial Nd isotopic composition. Depleted mantle and CHUR (chondritic uniform reservoir) evolution lines are overlain for reference. C)) Oxygen stable isotope composition of igneous rocks normalized to Vienna standard mean ocean water (VSMOW), and D) ratio of Sr to Y filtered using the parameters of Hu et al. (2017).

Oxygen stable isotopes are another isotopic proxy to discriminate between crustal recycling and mantle-derived additions. Mantle-derived rocks will generally have values of ~5.5 (normalized to SMOW) while rocks incorporating a significant sedimentary or upper crustal component will exhibit more positive values due to interactions with surface water (Dorais and Paige, 2000; Fu et al., 2014).

Limited oxygen isotope analyses are available for rocks older than 415 Ma. They mostly show values between 5.5 and 8‰ which are suggestive of a mantle or island arc-like source (Fu et al., 2014). Between 450 and 425 Ma O isotopes shift from these lighter to heavier values of 10-15‰ by ca. 400 Ma. Intriguingly few heavy values are recorded ca. 400-380 Ma. Subsequently, isotopic values show more heavier O isotope, albeit with a large degree of scatter.

Crustal melting is likely to occur in the thickened crust of orogens (England and Thompson, 1984). The ratio of Sr to Y in intermediate igneous rocks in collisional margins serves a proxy for crustal thickness (Chapman et al., 2015; Chiaradia, 2015; Profeta et al., 2015; Farner and Lee, 2017; Hu et al., 2017). It is thought that as crustal thickness increases garnet becomes stabilized in the lower crust while plagioclase breaks down. Garnet strongly partitions Y and heavy rare earth elements, while the breakdown of plagioclase releases Sr and, to some extent, light rare earths (Profeta et al., 2015; Hu et al., 2017). Hence, resulting igneous rocks in a thickened crust will have greater Sr/Y ratios than those in a relatively thinner crust. To compare Sr/Y ratios with the isotopic data, the geochemical dataset was filtered following the parameters given by Hu et al. (2017): SiO_2 = 55–72 wt%, MgO = 0.5–6.0 wt.%, Rb/Sr <0.35, Sr/Y = <60, and La= <60 ppm and then averaged by pluton. Given the potential differences in tectonic setting across this time period, Sr/Y ratios were not converted to absolute crustal thicknesses and the ratios are compared instead. As Sr/Y shows a linear relationship with crustal thickness in continental arcs (Chapman et al., 2015) and syn-collisional rocks (Hu et al., 2017), the relative changes in the Sr/Y ratio are indicative of changes in crustal thickness.

Low values are observed ca. 475 Ma and increase to 450 Ma. Subsequently they show a small decrease by ~425 Ma (Fig. 8). Values increase after 420, peaking ca. 380 Ma. These peaks in Sr/Y ratios at ~450 Ma, 420-400 Ma, and 380-350 Ma correlate with the Taconic, Acadian, and Neoacadian orogenies and with the positive to negative shifts observed in Nd isotopes.

Highly positive (approaching depleted mantle values) ca 475-480 Ma are compatible with a model of volcanism on an island arc prior to ca. 475 Ma collision with Laurentia. The decrease in $_{Ndi}$ values may be the result of a number of processes including: to increased subduction of increasing amounts of highly Laurentian-derived sediment (Keller et al., 2019), increased crustal thickness post-collision increased degree of assimilation of evolved crust (DePaolo et al., 2019), or subcontinental lithospheric mantle (Whalen and Hildebrand, 2019), a shift of magmatism onto Laurentia following subduction polarity reversal (Karabinos et al., 1998, 2017), landward migration of arc magmatism (Chapman et al., 2017), or mantle wedge heterogeneity (Turner et al., 2017)Another possibility is a shift in the tectonic regime for magma generation from a within-plate setting to arc or syn-collisional setting (van Staal et al., 2009).

Acadian-age (425-380 Ma) Nd isotopes show a shift from positive to negative values. This shift is also accompanied by a shift towards positive values in O isotopes. This indicates a relative increase crustal component involved in the generation of magma and relative decrease in the proportion of the mantle derived contribution.

A shift towards negative ε_{Ndi} and heavier $\delta^{18}O$ is seen again from ca. 380 to 355 Ma (Fig. 2.5). This corresponds with the age range of the Neoacadian Orogeny (Robinson et al., 1998; van Staal et al., 2009)The trends in Nd and O proceed to relatively more unradiogenic Nd isotopic values and to heavier $\delta^{18}O$ values than the shifts in the Acadian Orogeny.

Each orogen (Taconic, Acadian, Neoacadian) exhibits a generally negative trend in εNd_i and a positive trend in O isotopes. Generally, this suggests a greater contribution of reworked crustal or (meta)sedimentary material compared to mantle-derived material. This can be produced by a variety of process (Chapman et al., 2017; DePaolo et al., 2019), one of which is crustal thickening. The connection between crustal thickness and isotopic ratios may be tested by comparison with Sr/Y ratios. Sr/Y values and, by inference, crustal thickness values increase between 470 and 450 Ma, whereas Nd isotopes trend from very positive to negative values. Sr/Y values are low ca. 425 Ma, where strongly positive isotopic values are observed. Ca. 420 to 400 Ma, Sr/Y values increase slightly, and the Nd and O isotopes display more evolved values. The highest Sr/Y ratios are observed in the timespan of the Neoacadian orogeny, where high O isotopes and Nd isotopes are observed. From these data, there is a similarity between increased Sr/Y ratios and more evolved or crustal Nd and O isotopic values. While there may be several processes at play, such as increased juvenile input to the pre-470 Ma Taconic island arcs, increased degrees of crustal melting or assimilation are inferred here during periods crustal thickening and terrane collision, consistent with other regional studies (Dorais and Paige, 2000; Alexander et al., 2019; DePaolo et al., 2019). The crustal and mantle contributions of Nd isotopes are analyzed in further detail in Chapter 3 and the Acadian to Neoacadian crustal thickness evolution is quantified.

Notably, Nd and O isotope isotopes are anti-correlated in the Acadian (420-380 Ma) and Neoacadian (380-350 Ma) intervals. This trend argues for increased reworking of felsic continental crust and re-melting of sedimentary rocks. Indeed, leucogranites are widespread in the New England Appalachians, especially in the 370-350 Ma age range (Dorais and Paige, 2000). In terms of the crustal evolution, this suggests that there may have been more crustal growth during the early, arc-like phase of orogenesis than the later phases, when magmatism involved more reworking of existing continental material.

Critically, the current sampling record, especially for O isotopes, is incomplete. The lack of O isotopic analyses available for pre-Silurian igneous rocks in New England shows that data coverage is not complete. Future $\delta^{18}O$ analyses would also benefit from analyzing individual minerals, especially zircon, rather than bulk whole-rock samples. Mineral analyses, especially zircon, are far less prone to post-intrusion alteration from fluids or meteoric water. The time series presented here would also benefit from more advanced statistical techniques such as bootstrap resampling to quantify these relationships (Keller and Schoene, 2012, 2018).

These results present a larger of number igneous crystallization dates of the New England Appalachians. There are peaks in ages at ca. 470, 450, 415, 375, 195, and 120Ma with subordinate peaks at ca. 600, 550, and 280 Ma. The period between 475 and 350 Ma has a large spread of dates. Comparison of this dates in this period with Nd isotopes show three shifts from positive to negative isotopic values. The shifts are correlate with the Taconic, Acadian, and Neoacadian orogenies, suggesting that a decrease in Nd isotopes may be a signature of orogenesis. Shifts from mantle-to arc like O isotopes to more typical crustal values occurs in the Acadian and Neoacadian orogenies. The combination of these isotopic signatures suggests an increase in the degree of re-worked crustal or sedimentary component in igneous rocks, potentially associated with crustal thickening. These results present an approach for identifying first order temporal geochemical trends during collisional orogenesis and may present an isotopic fingerprint to identifying the nature of comparatively less well constrained orogens.

2.5.2 Detrital Mineral Geochronology

Detrital mineral geochronology is rapidly developing as an important part of tectonic studies (Gehrels, 2014). The ages of detrital minerals can be used to constrain the depositional age, reconstruct provenance, characterize a sedimentary unit, and test paleogeographic reconstructions. However, an active question is how whole detrital mineral populations reproduce the age distribution of the source region.

Gaschnig (2019) published LA-ICPMS detrital zircon, monazite, rutile, and titanite dates from garnet-rich sand at the mouth of the Merrimack River, MA (Fig. 9). The Merrimack River drains southern New Hampshire and some of northeastern

Massachusetts transecting Neoproterozoic basement rocks, Ordovician arc rocks, Silurian to Devonian metasediments and igneous rocks, and Mesozoic A-type granites. Gaschnig (2019) qualitatively compared the results of their study with the published literature but did not directly compare their dates against published geochronology from the watershed. Here, I directly compare data detrital and in-place samples and more quantitatively evaluate their similarity.

All in-place (in-situ) samples from the database were selected from within the Merrimack River watershed. Samples that were collected outside of the strict boundary of the Merrimack River watershed but are parts of units that extend into the watershed were also included. The distribution of samples and values used in the compilations are shown in Figure 7.

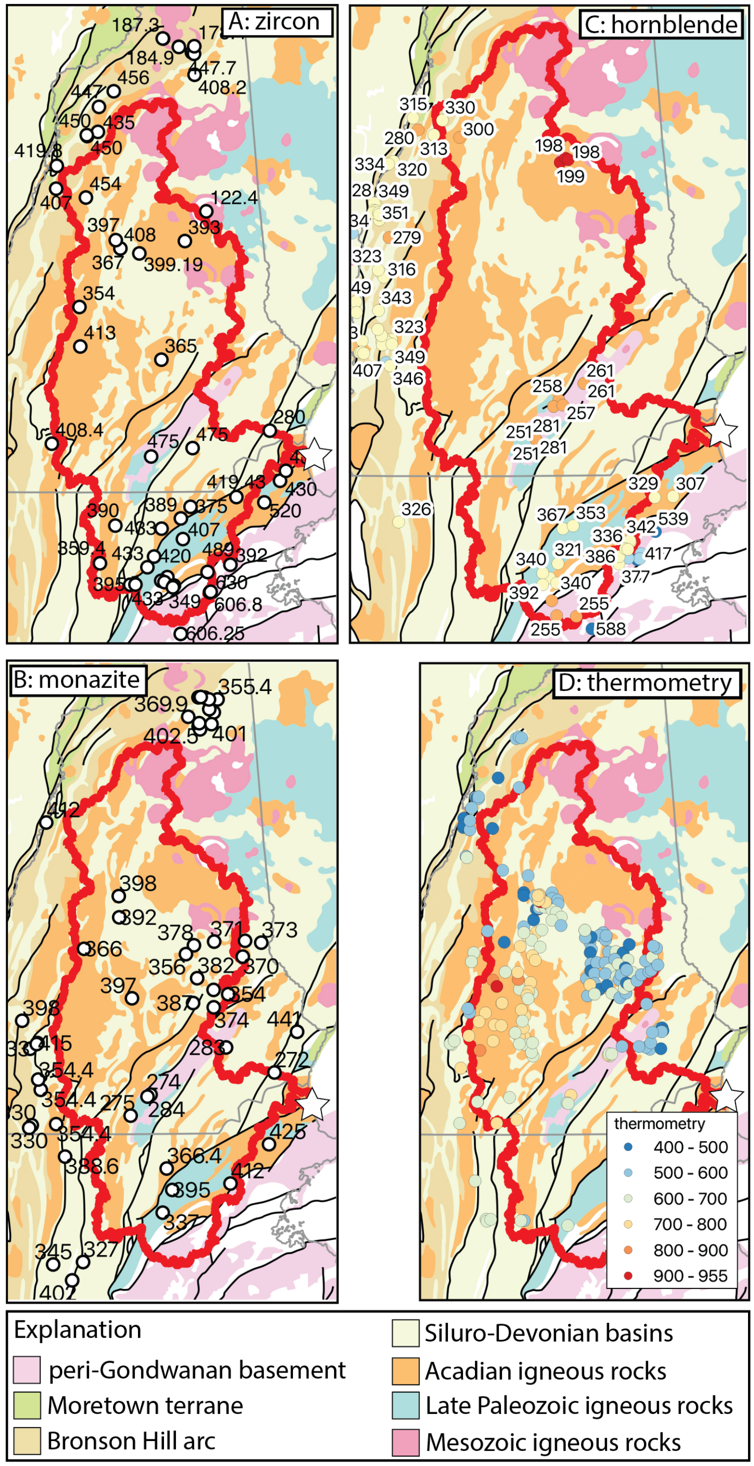

Figure 9: Distribution of zircon (A), monazite (B), hornblende (C) dates, and metamorphic temperatures (D) used to compare with detrital datasets of Gaschnig (2019). Star indicates location of Plum Island. Red outline is extent of the Merrimack River watershed.

Zircon shows similar peaks in both age spectra at ~396, 290, 190, 124 Ma (Fig. 2.7A). However, the in-situ sample shows greater proportion of Ordovician dates. However, these make up a relatively small proportion of the Merrimack watershed (Fig. 8A).

Monazite dates show first order similarities with a large peak centered in the Devonian and subordinate Permian peak. Whereas the detrital samples show single large peaks, the in-situ samples show a range of values between 390 and 350 Ma. This may reflect differences in analytical techniques used in the Gaschnig (2019) study and in-place analyses. Gaschnig (2019) dated grains using LA-ICPMS without conducting prior grain mapping to focus analyses on compositional domains. The relatively large spot size of the excimer laser beam used (15-µm) by Gaschnig (2019) may also have preferentially sampled the largest monazite domains. The younger (380-350 Ma) dates that are relatively less abundant may not have been analyzed if they formed thin rims around large domains. In contrast, many samples from the in-situ population were mapped prior to analysis and dated by EPMA techniques, targeting multiple compositional domains (Pyle et al., 2005; McCulla, 2016; Massey et al., 2017a)

No in-situ U-Pb analyses of rutile have been published for the Merrimack River watershed. However, the nominal closure temperature of rutile, while poorly constrained (Blackburn et al., 2011)is thought to be similar, or perhaps slightly higher (650°C; Vry and Baker, 2006), than that of Ar in hornblende (~500°C; Harrison, 1982). On a probability density plot of common Pb-corrected $^{238}U/^{206}Pb$ dates, three distributions were of rutile dates were identified, (1) a small Ordovician and Silurian population centered at ca. 430 Ma, (2) a continuum of dates between 330 and 390 Ma with a peak at

365 Ma, and (3) a sharp and narrow peak at 250 Ma. A probability density plot of hornblende dates from the Merrimack River watershed show a small peak at ~431 Ma, a wide, dominant peak at 340-330 Ma, and a narrow peak at 260 Ma. To a first order, the abundance and distribution of $^{40}Ar/^{39}Ar$ hornblende dates are remarkably similar to U-Pb rutile dates. This supports the hypothesis of Gaschnig (2019) that the rutile U-Pb dates likely record regional cooling. The distribution of $^{40}Ar/^{39}Ar$ hornblende dates is generally younger than that of the similar U-Pb rutile peak. If both of these age populations represent cooling, hornblende ages would be expected to be relatively younger given the somewhat lower closure temperature of Ar in hornblende. This seems a reasonable assumption given the known diffusivity rates and strong similarities in the age distributions. Assuming nominal closure temperatures of ~650°C for Pb in rutile and ~500°C for Ar in hornblende, estimates of regional cooling rates can be calculated. The ca. 7 Ma offset between the early Silurian peaks suggests a relatively fast cooling rate of 21°C/m.y. Differences between of 18 to 35 m.y. between the "Acadian" peaks suggests relatively slow cooling rates of 4 to 8°C/m.y. The nearly identical peaks ca. 260-250 Ma suggest very rapid exhumation. These cooling rates are all geologically reasonable and are in the range of other estimates for regional cooling from each of these events. Relatively rapid post-Taconic (late Ordovician-Early Silurian) cooling is suggested from coupled monazite-xenotime thermometry and geochronology (Hillenbrand, unpublished data) and from hornblende dates from western England (discussed in Karabinos et al., 2017). Relatively slow post-Acadian cooling rates of have been interpreted in a number of studies from central New England (Tracy and Dietsch, 1982; Harrison et al., 1989; Pyle et al., 2005). However, rapid cooling of the Massabesic gneiss in the Permian is

indicated by nearly concordant of hornblende, biotite and K-feldspar $^{40}Ar/^{39}Ar$ dates (Dorais et al., 2012)

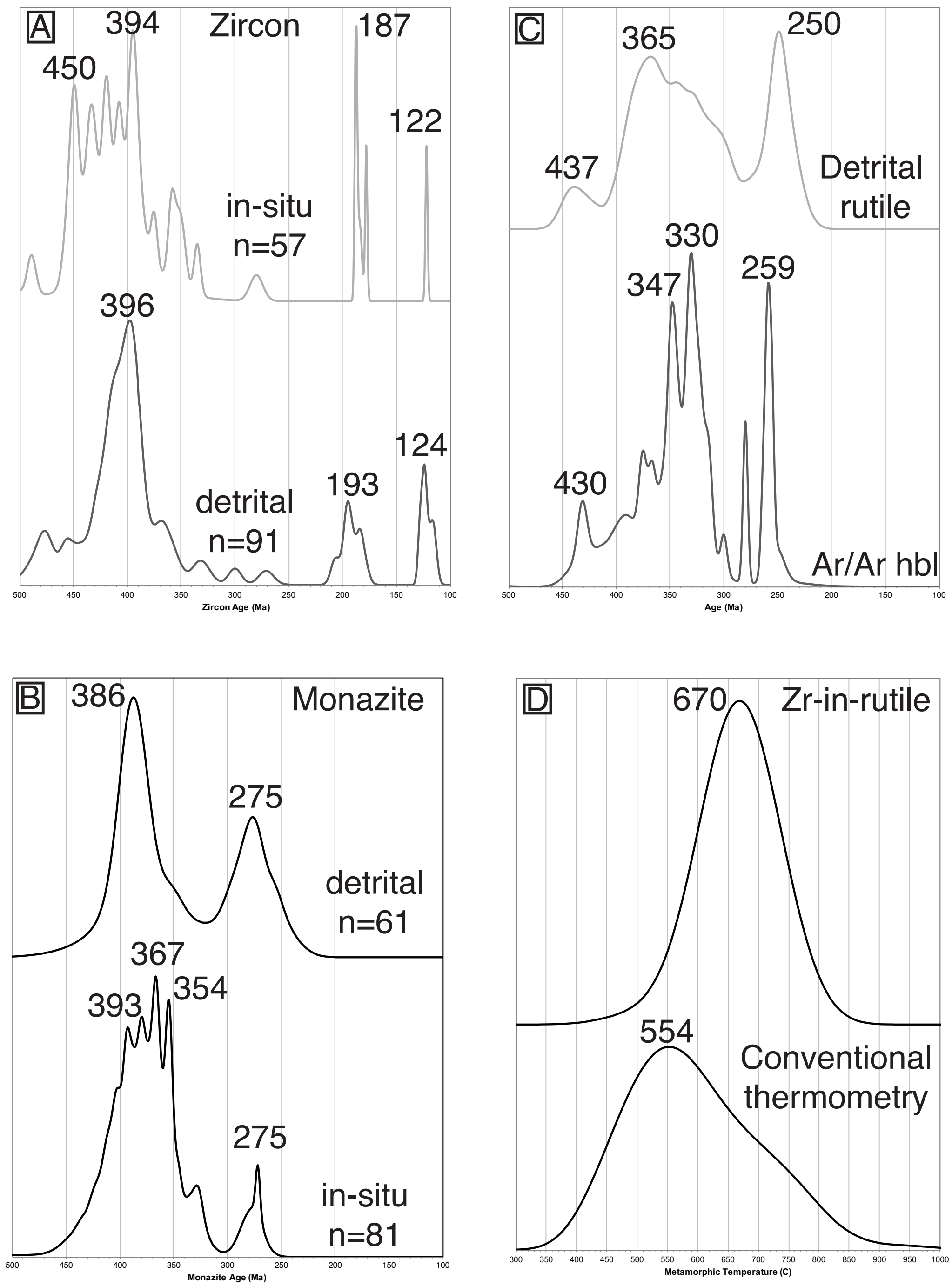

Figure 10: Normalized probability density functions of detrital and in-situ zircon (A), monazite (B), and rutile/hornblende (C) dates, and thermometry (D).

The correlation between $^{40}Ar/^{39}Ar$ hornblende and U-Pb rutile dates may allow for speculation on the sources of rutile. As suggested by Gaschnig (2019), the Permian peak almost certainly can be attributed to the Massabesic Gneiss complex and perhaps partially to rocks of the Avalon terrane (Fig. 10C). The range of Acadian dates likely comes from cooling of rocks of the Central Maine and Merrimack basins. However, the provenance of the late Silurian population is less well constrained. Gaschnig (2019) suggested that it may be from rocks of the Connecticut Valley Synclincorium or Bronson Hill anticlinorium, where pre-Acadian dates are locally preserved (Spear and Harrison, 1989). However, these generally lie outside of the Merrimack River watershed (Fig. 10C). Another possibility not considered by Gaschnig (2019) is the Nashoba terrane and Lexington Mafic Complex which preserves Silurian hornblende dates (Attenoukon, 2009). These hypotheses could be tested with a program of U-Pb rutile dating of in-place samples in the Merrimack River watershed.

In additional to geochronologic data, Gaschnig (2019) reported Zr-in-rutile temperatures for a subset of the dated rutile grains. These temperatures average ~670°C and trends towards higher temperatures with older dates (Gaschnig, 2019). Zr-in-rutile temperatures were compared with temperatures derived from thermometry from the watershed (primarily garnet-biotite Fe-Mg exchange thermometry). Results from Zr-in-rutile are approximately 100°C higher temperatures than temperatures compiled for the region (Fig. 10D). One factor may be that Gaschnig (2019) calculated temperatures at a model pressure of 8 kbar, which is much higher than pressures reported outside of the Massabesic Gneiss. However, this cannot be responsible for the entirety of the 100°C shift in temperatures. The lower rates of Zr diffusion in rutile may preserve higher temperatures than Fe-Mg exchange. However, this also may not apply to the entire dataset, as garnet-biotite temperatures up to 850°C are reported from the southern portion of the watershed (Fig. 8D). In contrast, temperatures from the northern portion of the watershed are generally below 600°C. If the temperatures reported from both systems are correct, it may suggest that the detrital rutile was predominantly derived from the southwestern part of the watershed, where higher temperatures are reported, and not from the northern portion. Thus, they may constrain the source of rutile to the southern portion of the watershed. This hypothesis could also be tested with Zr-in-rutile geothermometry of in-place samples from the Merrimack watershed.

To facilitate evaluation of detrital and in-place samples' similarity/dissimilarity, each population was plotted in the context of metric multidimensional scaling (MDS) statistical analyses (Vermeesch, 2013) (Vermeesch, 2013) to (Fig. 11). MDS utilizes the statistical effect size of the Kolmogorov-Smirnov test (i.e., dimensionless distances) as a measure of dissimilarity to produce a map of points where similar samples cluster together and dissimilar samples plot far apart (Vermeesch, 2013). Nearest neighbor tie lines place solid lines between the most statistically similar populations and dashed lines between the next most similar samples.

The detrital and in-situ zircon and monazite cluster closely to each other, with the zircon samples nearly overlapping. A solid tie lines between hornblende and detrital rutile indicates they are most similar to each other. This test provides some statistical evidence for the qualitative observation of the similarity of intra mineral detrital and in-situ age spectra and dissimilarity between minerals observed in Figure 10.

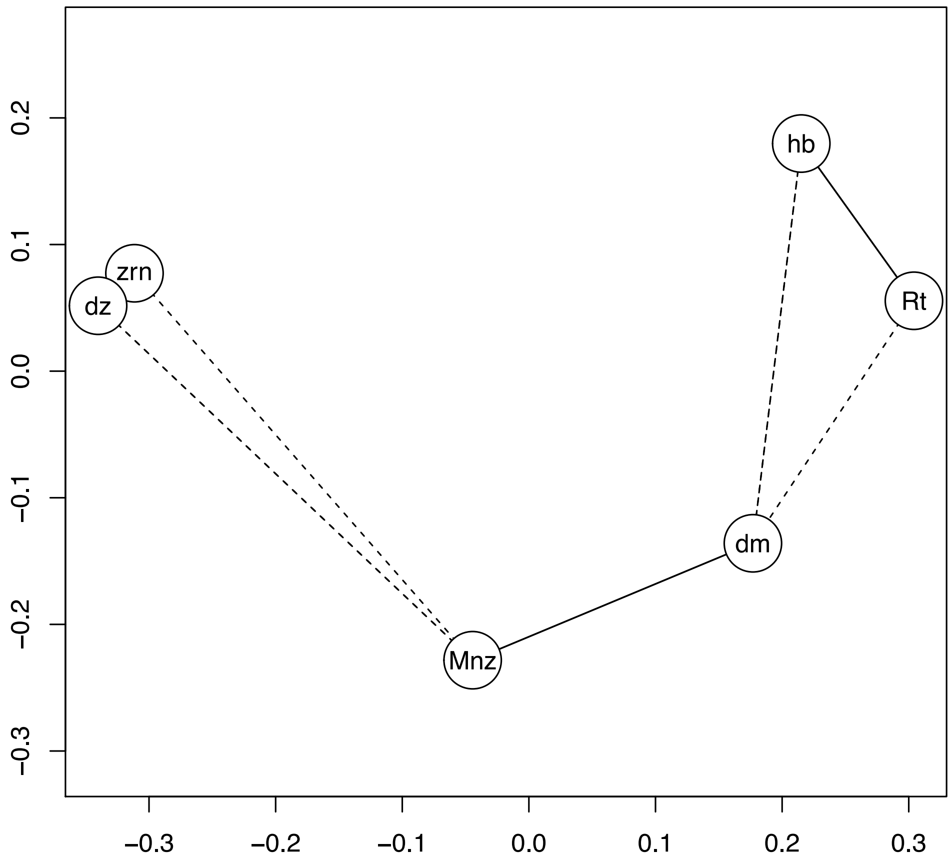

Figure 11: Metric multidimensional scaling (MDS) map (after Vermeesch, 2013) providing two-dimensional visualization of dimensionless Kolmogorov-Smirnov (K-S) distances between age spectra for all samples. Spatial proximity of points correlates with statistical similarity. Solid lines tie most similar neighbors, and dashed lines tie second most similar neighbors. DZ: detrital zircon; zrn: in-situ zircon; Mnz: in-situ monazite; dm: detrital monazite; hb: in-situ hornblende; Rt: detrital rutile.

2.5.3 Integration of geologic and geophysical data to build the "Acadian altiplano" hypothesis

A third example of this databases' utility is in constraining the timing of crustal structures and its role in building the hypothesis of an orogenic plateau during the Acadian Orogeny (Hillenbrand et al., 2019; 2020; Chapters 3 and 4 of this thesis). Details of the methodology and hypothesis are briefly summarized here in the context of the database. These findings are discussed further in Chapter 3 of this thesis.

Li et al. (2018) recently recognized a 12-15 km Moho step in western New England. The significance of the Moho step is a first order question in the crustal and tectonic evolution of New England. To constrain the timing of this feature, contour maps of thermochronologic data ($^{40}Ar/^{39}Ar$ in hornblende, muscovite, biotite and K-feldspar, and apatite fission tracks) showed an offset in $^{40}Ar/^{39}Ar$ hornblende, muscovite, biotite dates along the trend of the Moho step. Dates, interpreted as recording the age of regional cooling, are older than 420 Ma west of the step and generally younger than 380 Ma east of the step. The older dates are interpreted as recording cooling from the Grenvillian, Salinic, and Taconic orogenies while the younger dates are interpreted as recording cooling from the Acadian Orogeny. A 40 m.y. thermochronologic lag is observed between $^{40}Ar/^{39}Ar$ hornblende and muscovite dates, suggesting very slow cooling rates, consistent with petrologic data. This same region of slow cooling in central New England shows consistent 0.6 GPa metamorphic pressures, which imply low topographic relief, and 55-70 km elevations, that suggest high elevation.

Together, the consistent $^{40}Ar/^{39}Ar$ cooling ages, crustal thickness estimates, and metamorphic pressures suggest the existence of a low relief, high elevation plateau in the Devonian of central New England that was later exhumed as a block. A wide range of ages of anatectic rocks in central New England suggest the mid-crust of the Acadian Orogeny experienced protracted periods of partial melting, potentially analogous to zones underlying modern orogenic plateaus (Nelson et al., 1996). The presence of a hot, partial molten mid-crust creates a rheologically weak mid-crust that favors the formation of a low-relief plateau (Jamieson et al., 2004). The ages and geochemistry of monazite were integrated with structural fabrics to constrain the timing and kinematics of plateau growth and collapse. Early monazite, before 380 Ma, are enriched in Y suggesting they pre-date garnet growth and crustal thickening. Monazite dated between 380 and 330 Ma is depleted in Y, indicating growth in equilibrium with garnet which was stabilized by crustal thickening. 330 to 310 Ma monazite is enriched in Y, suggesting monazite growth during the breakdown of garnet due to exhumation. This youngest population is microstructurally associated with N-S stretching lineations, indicating exhumation and plateau collapse occurred parallel to the orogen.

A distinct break in $^{40}Ar/^{39}Ar$ hornblende, muscovite, and biotite dates is observed at the edge of the interpreted plateau and across Moho step imaged by Li et al. (2018). West of the step, cooling ages are >420 Ma while they are <380 Ma to the east. This indicates that rocks to the east must have been much hotter and juxtaposed against each other after 380 Ma and likely after 340 Ma. Low temperature thermochronometers such as $^{40}Ar/^{39}Ar$ in K-feldspar, fission tracks in apatite and zircon, and the (U-Th/He) system in apatite indicate that similar thermal histories after ~300 Ma. Thus, the Moho step must be Paleozoic in age and likely formed during 330 to 310 Ma plateau collapse.

The orogenic plateau hypothesis may explain the distribution of detrital zircon dates in foreland basin. Modern orogenic plateaus play large roles on regional and global climate, suggesting that effects of the Acadian altiplano paleoclimate should be considered going forward. Additionally, a belt of 380-330 Ma Li-bearing pegmatites occur along the trend of the Moho step. The spatial association with the edge of the proposed plateau and timing suggest that pegmatite genesis may be related to the paleo-plateau and may offer insights into deeper processes beneath the hyper-arid, Li-rich basins along the axis of the modern Andean.

2.7 Discussion

This chapter has presented a new database of geochronologic, geochemical, and geothermobarometric analyses from the northern Appalachians accessible via an easy to use online interface. It has also shown the utility of this dataset for examining regional geochemical trends, constraining the provenance of detrital minerals, and building hypotheses for crustal evolution.

This thesis has likely only scratched the surface of the possibilities of this database. Many other potential uses of this database exist. More advanced statistical methods, such as bootstrapping, may be able to see through geologic scatter to identify statistically significant changes in major, trace element, or isotope geochemistry.

The database should be further integrated with geophysical imaging to constrain the connections between surface geology and lithospheric structure. One example worthy of further investigation are tomographically identified low velocity zones in eastern North America (Yang and Gao, 2018) which has led to hypotheses involving lithospheric thinning and edge driven convection (Menke et al., 2018). It is possible that large scale geospatial analysis of thermochronologic and geochemical data may be able to test timing the emergence of these low velocity zones and test for evidence of lithospheric thinning. Raster calculations of regional cooling maps, such as those present in Chapter 3, can be used to calculate regional cooling rates. Changes in cooling rates or patterns may be associated with the low velocity zones causing surface uplift and bears further investigation. The hypothesis of lithospheric thinning may be testable with an examination of the geochemistry of Mesozoic to recent mafic dikes. Recent studies (e.g. Guo et al., 2020) have provided evidence that lithospheric thickness influences the composition of basalts in continental settings. Basalts erupted in thinner lithosphere may be expected to have characteristic features such as higher ratios of incompatible elements such as $[La/Sm]_N$, Ba/Zr, and Zr/Yb (Guo et al., 2020).This signature might be predicted if the hypothesis of Menke et al. (2018) is correct. Age constraints on basalts exhibiting this signature may place bounds on the timing of the Northern Appalachians Anomaly.

The utility of the database may also be increased by integrating additional data and data coverage. Presently, many geologic maps in the northern Appalachians are unpublished and inaccessible to most researchers (M.L. Williams, personal communication). Incorporating a database of these maps may be a rewarding direction. It may also be useful in future iterations to include primary datasets such as geochronologic isotope ratios and mineral compositions used to calculate pressure and temperature conditions. As the New England portion of the Appalachian database is populated, it may also be of interest to expand the database to coverage the southern Appalachians, especially as new geophysical datasets become available (Li et al., 2020)

2.7 References Cited

Alexander, E., Wielicki, M.M., Harrison, T.M., DePaolo, D.J., Zhao, Z.D., and Zhu, D.C., 2019, Hf and Nd Isotopic Constraints on Pre - and Syn - collisional Crustal Thickness of Southern Tibet Journal of Geophysical Research : Solid Earth: Journal of Geophysical Research: Solid Earth, v. 124, p. 1–17, doi:10.1029/2019JB017696.

Amidon, W.H., Roden-Tice, M., Anderson, A.J., McKeon, R.E., and Shuster, D.L., 2016, Late cretaceous unroofing of the White Mountains, New Hampshire, USA: An episode of passive margin rejuvenation? Geology, v. 44, p. 415–418, doi:10.1130/G37429.1.

Attenoukon, M.B., 2009, Age and Origins of Metamorphic Fabrics and the Tectonics of Southeastern New England: [PhD thesis] Indiana University, 295 p.

Bird, J.M., and Dewey, J.F., 1970, Lithosphere plate-continental margin tectonics and the evolution of the appalachian orogen: Geological Society of America Bulletin, v. 81, p. 1031–1060, doi:10.1130/0016-7606(1970)81[1031:LPMTAT]2.0.CO;2.

Blackburn, T., Bowring, S.A., Schoene, B., Mahan, K., and Dudas, F., 2011, U-Pb thermochronology: Creating a temporal record of lithosphere thermal evolution: Contributions to Mineralogy and Petrology, doi:10.1007/s00410-011-0607-6.

Blackburn, T.J., Olsen, P.E., Bowring, S.A., McLean, N.M., Kent, D. V., Puffer, J., McHone, G., Rasbury, E.T., and Et-Touhami, M., 2013, Zircon U-Pb geochronology links the end-triassic extinction with the central Atlantic magmatic province: Science, doi:10.1126/science.1234204.

Bradley, D.C., 2011, Secular trends in the geologic record and the supercontinent cycle: Earth-Science Reviews, v. 108, p. 16–33, doi:10.1016/j.earscirev.2011.05.003.

Bradley, D.C., O'Sullivan, P., and Bradley, L.M., 2015, Detrital zircons from modern sands in New England and the timing of Neoproterozoic to Mesozoic Magmatism: American Journal of Science, v. 315, p. 460.

Bradley, D.C., Tucker, R.D., Lux, D.R., Harris, A.G., and McGregor, D.C., 2000, Migration of the Acadian Orogen and Foreland Basin across the northern Appalachians of Maine and adjacent areas: U.S. Geological Survey Professional Paper, v. 1624, p. 1- 49.

Cartwright, S.F.A., West, Jr., D.P., and Amidon, W.H., 2019, Depositional constraints from detrital zircon geochronology of strata from multiple lithotectonic belts in south-central Maine, USA: Atlantic Geology, v. 136, p. 093–136, doi:10.4138/atlgeol.2019.003.

Chapman, J.B., Ducea, M.N., DeCelles, P.G., and Profeta, L., 2015, Tracking changes in crustal thickness during orogenic evolution with Sr/Y: An example from the North American Cordillera: Geology, v. 43, p. 919–922, doi:10.1130/G36996.1.

Chapman, J.B., Ducea, M.N., Kapp, P., Gehrels, G.E., and DeCelles, P.G., 2017, Spatial and temporal radiogenic isotopic trends of magmatism in Cordilleran orogens: Gondwana Research, v. 48, p. 189–204, doi:10.1016/j.gr.2017.04.019.

Chapman, J.B., and Kapp, P., 2017, Tibetan Magmatism Database: Geochemistry, Geophysics, Geosystems, v. 18, p. 4229–4234, doi:10.1002/2017GC007217.

Chiaradia, M., 2015, Crustal thickness control on Sr/Y signatures of recent arc magmas: an Earth scale perspective: Science Reports, v. 5, doi:10.1038/srep08115.

Condie, K.C., and Kröner, A., 2008, When did plate tectonics begin? Evidence from the geologic record: Special Paper of the Geological Society of America, v. 440, p. 281–294, doi:10.1130/2008.2440(14).

Crough, S.T., 1981, Mesozoic hotspot epeirogeny in eastern North America: Geology, v. 9, p. 2–6, doi:10.1130/0091-7613(1981)9<2:MHEIEN>2.0.CO;2.

DePaolo, D.J., 1981, Neodymium isotopes in the Colorado Front Range and crust-mantle evolution in the Proterozoic: Nature, v. 291, p. 193–196, doi:10.1038/291193a0.

DePaolo, D.J., Harrison, T.M., Wielicki, M., Zhao, Z., Zhu, D.C., Zhang, H., and Mo, X., 2019, Geochemical evidence for thin syn-collision crust and major crustal thickening between 45 and 32 Ma at the southern margin of Tibet: Gondwana Research, v. 73, p. 123–135, doi:10.1016/j.gr.2019.03.011.

DePaolo, D.J., Perry, F., and Baldrige, W., 1992, Crustal versus mantle sources of granitic magmas: a two-parameter model based on Nd isotopic studies: Earth Science Transactions of the Royal Society of Edinburgh, v. 83, p. 439–446.

Doherty, J.T., and Lyons, J.B., 1980, Mesozoic erosion rates in northern New England.: Geological Society of America Bulletin, v. 91, p. 16–20, doi:10.1130/0016-7606(1980)91<16:MERINN>2.0.CO;2.

Dorais, M.J., 2003, The petrogenesis and emplacement of the New Hamshire plutonic suite: American Journal of Science, v. 303, p. 447.

Dorais, M.J., and Paige, M.L., 2000, Regional geochemical and isotopic variations of Northern New England plutons: Implications for magma sources and for Grenville and Avalon basement-terrane boundaries: Bulletin of the Geological Society of America, v. 112, p. 900–914, doi:10.1130/0016-7606(2000)112<900:RGAIVO>2.0.CO;2.

Dorais, M.J., Wintsch, R.P., Kunk, M.J., Aleinikoff, J., Burton, W., Underdown, C., and Kerwin, C.M., 2012, P-T-t conditions, Nd and Pb isotopic compositions and detrital zircon geochronology of the Massabesic Gneiss Complex, New Hampshire: Isotopic and metamorphic evidence for the identification of Gander basement, central New England: American Journal of Science, v. 312, p. 1049, doi:10.2475/10.2012.01.

Eby, N., 1989, Petrology and geochemistry of Mount Yamaska, Quebec, Canada: a mafic representative of the Monteregian Hills igneous province, *in* p. 63–82, doi:10.13140/RG.2.1.2270.3760.

Eby, G.N., Krueger, H.W., and Creasy, J.W., 1992, Geology, geochronology, and geochemistry of the White Mountain batholith, New Hampshire: Special Paper of the Geological Society of America, doi:10.1130/SPE268-p379.

England, P.C., and Thompson, A.B., 1984, Pressure - temperature - time paths of regional metamorphism I. heat transfer during the evolution of regions of thickened continental crust: Journal of Petrology, doi:10.1093/petrology/25.4.894.

Ettensohn, F.R., 1994, Tectonic Control on Formation and Cyclicity of Major Appalachian Unconformities and Associated Stratigraphic Sequences, *in* Tectonic And Eustatic Controls on Sedimentary Cycles, doi:10.2110/csp.94.04.0217.

Ettensohn, F.R., Pashin, J.C., and Gilliam, W., 2019, The Appalachian and Black Warrior Basins: Foreland Basins in the Eastern United States, *in* Miall, A.D. ed., The Sedimentary Basins of the United States and Canada, p. 129–237, doi:10.1016/b978-0-444-63895-3.00004-8.

Eusden, J.D., Baker, S., Cargill, J., Divan, E., Hillenbrand, I., O'Sullivan, P., and Wheatcroft, A., 2017, C3: Transect From the Migmatized Central Maine Belt to the Bronson Hill Anticlinorium:

Eusden, J.D., and Barreiro, B., 1988, The timing of peak high-grade metamorphism in central-eastern New England: Atlantic Geology, v. 24, p. 241–255.

Eusden, J.D., Guzofski, C.A., Robinson, A.C., and Tucker, R.D., 2000, Timing of the Acadian Orogeny in Northern New Hampshire: The Journal of Geology, v. 108, p. 219–232, doi:10.1086/314396.

Farner, M.J., and Lee, C.T.A., 2017, Effects of crustal thickness on magmatic differentiation in subduction zone volcanism: A global study: Earth and Planetary Science Letters, doi:10.1016/j.epsl.2017.04.025.

Foland, K.A., Henderston, C.M.B., and Gleason, J., 1985, Petrogenesis of the magmatic complex at Mount Ascutney, Vermont, USA I: Assimilation of crust by mafic magmas based on Sr and O isotopic and major element relationships: Contributions to Mineralogy and Petrology, v. 90, p. 331–345.

Fu, B., Cliff, J., and Zartman, R.E., 2014, Zircon oxygen isotopic constraints from plutonic rocks on the magmatic and crustal evolution of the northern Appalachians in southern New England, USA: Canadian Journal of Earth Sciences, v. 51, p. 485–499.

Gale, A., Dalton, C.A., Langmuir, C.H., Su, Y., and Schilling, J.G., 2013, The mean composition of ocean ridge basalts: v. 14, 489–518 p., doi:10.1029/2012GC004334.

Gaschnig, R.M., 2019, Benefits of a Multiproxy Approach to Detrital Mineral Provenance Analysis: An Example from the Merrimack River, New England, USA: Geochemistry, Geophysics, Geosystems, v. 20, p. 1557–1573, doi:10.1029/2018GC008005.

Gehrels, G., 2014, Detrital Zircon U-Pb Geochronology Applied to Tectonics: Annual Review of Earth and Planetary Sciences, v. 42, p. 127–149, doi:10.1146/annurev-earth-050212-124012.

Guo, P., Niu, Y., Sun, P., Gong, H., and Wang, X., 2020, Lithosphere thickness controls continental basalt compositions: An illustration using Cenozoic basalts from eastern China: Geology, v. 48, p. 128–133, doi:10.1130/G46710.1.

Harrison, T.M., 1982, Diffusion of 40Ar in Hornblende: Contributions to Mineralogy and Petrology, v. 78, p. 324–331, doi:10.2475/ajs.303.5.410.

Harrison, T.M., Aleinikoff, J.N., and Compston, W., 1987, Observations and controls on the occurrence of inherited zircon in Concord-type granitoids, New Hampshire: Geochimica et Cosmochimica Acta, v. 51, p. 2549–2558, doi:10.1016/0016-7037(87)90305-X.

Harrison, T.M., Spear, F.S., and Heizler, M.T., 1989, Geochronologic studies in central New England II: post-Acadian hinged and differential uplift: Geology, v. 17, p. 185–189, doi:10.1130/0091-7613(1989)017<0185:GSICNE>2.3.CO;2.

Hatcher, R.D., 2010, The Appalachian orogen: A brief summary: From Rodinia to Pangea: The Lithotectonic Record of the Appalachian Region: Geological Society of America Memoir, v. 206, p. 1–19, doi:10.1130/2010.1206(01).

Hibbard, J.P., van Staal, C.R., Rankin, D.W., and Williams, H., 2006, Lithotectonic map of the Appalachian Orogen, Canada-United States of America:, doi:10.4095/221912.

Hillenbrand, I.W., 2020, Crustal evolution of the New England Appalachians: the rise and fall of a long-lived orogenic plateau: University of Massachusetts, 159 p.

Hillenbrand, I., Williams, M.L., Li, C., and Gao, H., 2019, Rise and Fall of the Acadian Altiplano: Geological Society of America Abstracts with Programs, v. 51, doi:10.1130/abs/2019AM-340957.

Hu, F., Ducea, M.N., Liu, S., and Chapman, J.B., 2017, Quantifying Crustal Thickness in Continental Collisional Belts : Global Perspective and a Geologic Application: Scientific Reports, v. 7, p. 1–10, doi:10.1038/s41598-017-07849-7.

Hubbard, M.S., 1999, Norumbega fault zone: Part of an orogen-parallel strike-slip system, northern Appalachians: Special Paper of the Geological Society of America, p. 155–166, doi:10.1130/0-8137-2331-0.155.

Jamieson, R.A., Beaumont, C., Medvedev, S., and Nguyen, M.H., 2004, Crustal channel flows: 2. Numerical models with implications for metamorphism in the Himalayan-Tibetan orogen: Journal of Geophysical Research: Solid Earth, v. 109, p. 1–24, doi:10.1029/2003JB002811.

Jourdan, F., Marzoli, A., Bertrand, H., Cirilli, S., Tanner, L.H., Kontak, D.J., McHone, G., Renne, P.R., and Bellieni, G., 2009, 40Ar/39Ar ages of CAMP in North America: implications for the Triassic–Jurassic boundary and the 40K decay constant bias: LITHOS, v. 110, p. 167–180.

Karabinos, P., Macdonald, F.A., and Crowley, J.L., 2017, Bridging the gap between the foreland and hinterland I: Geochronology and plate tectonic geometry of Ordovician magmatism and terrane accretion on the Laurentian margin of New England: American Journal of Science, v. 317, p. 515–554, doi:10.2475/05.2017.01.

Karabinos, P., Morris, D., Hamilton, M., and Rayner, N., 2008, Age, origin, and tectonic significance of Mesoproterozoic and Silurian felsic sills in the Berkshire massif, Massachusetts: American Journal of Science, v. 308, p. 787–812, doi:10.2475/06.2008.03.

Karabinos, P., Samson, S.D., Hepburn, J.C., and Stoll, H.M., 1998, Taconian orogeny in the New England Appalachians: Collision between Laurentia and the Shelburne Falls arc: Geology, v. 26, p. 215–218, doi:10.1130/0091-7613(1998)026<0215:TOITNE>2.3.CO;2.

Karabinos, P., Westerman, D.S., Crowley, J.L., and Macdonald, F.A., 2019, Stratigraphic and Structural Evidence for a Fault Contact Between Ordovician Arc Rocks and the Connecticut Valley-Gaspé Sequence in Vermont, *in* New England Intercollegiate Geological Conference, v. C1, p. 145–176.

Keller, C.B., Husson, J.M., Mitchell, R.N., Bottke, W.F., Gernon, T.M., Boehnke, P., Bell, E.A., Swanson-Hysell, N.L., and Peters, S.E., 2019, Neoproterozoic glacial origin of the Great Unconformity: Proceedings of the National Academy of Sciences, v. 116, p. 1136–1145, doi:10.1073/pnas.1804350116.

Keller, B., and Schoene, B., 2018, Plate tectonics and continental basaltic geochemistry throughout Earth history: Earth and Planetary Science Letters, v. 481, p. 290–304, doi:10.1016/j.epsl.2017.10.031.

Keller, C.B., and Schoene, B., 2012, Statistical geochemistry reveals disruption in secular lithospheric evolution about 2.5 Gyr ago: Nature, v. 485, p. 490–493, doi:10.1038/nature11024.

Kellett, D.A., Pehrsson, S., Skipton, D.R., Regis, D., Camacho, A., Schneider, D.A., and Berman, R., 2020, Thermochronological history of the Northern Canadian Shield: Precambrian Research, v. 342, p. 105703, doi:10.1016/j.precamres.2020.105703.

Kellett, D.A., van Staal, C., Wilson, R.A., and Rogers, N., 2017, The age of salinic deformation constrained by 40Ar/39Ar dating of multiple cleavage domains: Bathurst Supergroup, New Brunswick Appalachians: American Journal of Science, v. 317, p. 338–368.

Kim, J., Klepeis, K., Webb, L., and Amidon, W., 2019, New Insights on the Ordovician-Neogene Tectonic History of the Champlain Valley Belt from Drone Surveys, Photogammetry, and Geochronology, West-Central Vermont: New England Intercollegiate Geological Conference, v. B1, p. 90.

Kinney, S.T., Maclennan, S.A., Setera, J., Schoene, B., Vantongeren, J., Oksen, P.E., Strauss, J. V, Town, C.F., and Bradley, D., 2019, Causal Implications of a new zircon U-Pb frameowrk for Mesozoic magmatism in northern New England and Quebec: What are the Rift/Post-rift igneous rocks of the White Mountains? Geological Society of America Abstracts with Programs, v. 51, doi:10.1130/abs/2019NE-328495.

Kuiper, Y.D., 2016, Development of the Norumbega fault system in mid-Paleozoic New England, USA: An integrated subducted oceanic ridge model: Geology, v. 44, p. 455–458, doi:10.1130/G37599.1.

Kuiper, Y.D., Thompson, M.D., Barr, S.M., White, C.E., Hepburn, J.C., and Crowley, J.L., 2017, Detrital zircon evidence for Paleoproterozoic West African crust along the eastern North American continental margin, Georges Bank, offshore Massachusetts, USA: Geology, v. 45, p. 811–814.

Kumarapeli, P.S., Dunning, G.R., Pintson, H., and Shaver, J., 1989, Geochemistry and U–Pb zircon age of comenditic metafelsites of the Tibbit Hill Formation, Quebec Appalachians: Canadian Journal of Earth Sciences, v. 26, p. 1374–1383.

Levin, V., Long, M.D., Skryzalin, P., Li, Y., and López, I., 2018, Seismic evidence for a recently formed mantle upwelling beneath New England: Geology, v. 46, p. 87–90, doi:10.1130/G39641.1.

Li, C., Gao, H., and Williams, M.L., 2020, Seismic characteristics of the eastern North American crust with Ps converted waves: terrane accretion and modification of continental crust: Journal of Geophysical Research: Solid Earth, doi:10.1029/2019jb018727.

Li, C., Gao, H., Williams, M.L., and Levin, V., 2018, Crustal Thickness Variation in the Northern Appalachian Mountains: Implications for the Geometry of 3-D Tectonic Boundaries Within the Crust: Geophysical Research Letters, v. 45, p. 6061–6070, doi:10.1029/2018GL078777.

Long, M.D., Benoit, M.H., Aragon, J.C., and King, S.D., 2019, Seismic imaging of mid-crustal structure beneath central and eastern North America: Possibly the elusive Grenville deformation? Geology, v. 47, p. 371–374, doi:10.1130/G46077.1.

Macdonald, F.A., Karabinos, P.M., Crowley, J.L., Hodgin, E.B., Crockford, P.W., and Delano, J.W., 2017, Bridging the gap between the foreland and hinterland II: Geochronology and tectonic setting of Ordovician magmatism and basin formation on the Laurentian margin of New England and Newfoundland: American Journal of Science, v. 317, p. 555.

Macdonald, F.A., Ryan-Davis, J., Coish, R.A., Crowley, J.L., and Karabinos, P.M., 2014, A newly identified Gondwanan terrane in the northern Appalachian Mountains: Implications for the Taconic orogeny and closure of the Iapetus Ocean: Geology, v. 43, p. 539–542, doi:10.1130/G36575Y.1.

Massey, M.A., Berg, C.A., and Moecher, D.P., 2017a, Pre- and Syn-Kinematic P-T Constraints Acoss a Zone of Transpession, Vertical Extrusion, and Lateral Escape in the Southern New England Appalachians: Geological Society of America Abstracts with Programs, v. 49, doi:10.1130/abs/2017NE-291167.

Massey, M.A., Moecher, D.P., Walker, T.B., O'Brien, T.M., and Rohrer, L.P., 2017b, The role and extent of dextral transpression and lateral escape on the post-Acadian tectonic evolution of South-Central New England: American Journal of Science, v. 317, p. 34–94, doi:10.2475/01.2017.02.

McCulla, J.K., 2016, Dating Deformation in the Palmer Zone of Transpression, Central Massachusetts: Temporal Constraints on Models for Progressive Deformation in the Middle Crust [MS thesis]: University of Kentucky, 166 p.

McHone, J.G., Hussey II, A.M., West Jr., D.P., and Bailey, D.G., 2014, The Christmas Cove Dyke of coastal Maine, USA, and regional sources for Early Mesozoic flood basalts in northeastern North America: Atlantic Geology, v. 50, p. 66–90, doi:10.4138/atlgeol.2014.004.

McKerrow, W.S., and Ziegler, A.M., 1972, Palaeozoic Oceans: Nature Physical Science, doi:10.1038/physci240092b0.

McWilliams, C.K., Walsh, G.J., and Wintsch, R.P., 2010, Silurian-Devonian age and tectonic setting of the Connecticut Valley-Gaspé trough in Vermont based on U-Pb SHRIMP analyses of detrital zircons: American Journal of Science, v. 310, p. 325–363, doi:10.2475/05.2010.01.

Menke, W., Lamoureux, J., Abbott, D., Hopper, E., Hutson, D., and Marrero, A., 2018, Crustal Heating and Lithospheric Alteration and Erosion Associated With Asthenospheric Upwelling Beneath Southern New England (USA): Journal of Geophysical Research: Solid Earth, v. 123, p. 8995–9008, doi:10.1029/2018JB015921.

Mercer, C.M., and Hodges, K. V, 2016, ArAR — A software tool to promote the robust comparison of K–Ar and 40Ar/39Ar dates published using different decay, isotopic, and monitor-age parameters: Chemical Geology, v. 440, p. 148–163, doi:https://doi.org/10.1016/j.chemgeo.2016.06.020.

Miller, B. V, Barr, S.M., Tesfai, F., and White, C.E., 2018, Tonian Fe-Ti-P ferronorite and alkali anorthosite in the northern Appalachian orogen, southern New Brunswick, Canada: Amazonian basement in Ganderia? Precambrian Research, v. 317, p. 77–88.

Moench, R.H., and Aleinikoff, J.N., 2002, Stratigraphy, geochronology, and accretionary terrane settings of two Bronson Hill arc sequences, northern New England: Physics and Chemistry of the Earth, v. 27, p. 47–95, doi:10.1016/S1474-7065(01)00003-1.

Nelson, K.D. et al., 1996, Partially molten middle crust beneath southern Tibet: Synthesis of project INDEPTH results: Science, v. 274, p. 1684–1688, doi:10.1126/science.274.5293.1684.

Olsen, P.E., 1997, Stratigraphic Record of the Early Mesozoic Breakup of Pangea in the Laurasia-Gondwana Rift System: Annual Review of Earth and Planetary Sciences, v. 25, p. 337–401, doi:10.1146/annurev.earth.25.1.337.

Perrot, M., Tremblay, A., Ruffet, G., and David, J., 2018, Detrital U-Pb and 40Ar/39Ar geochronology of the Connecticut Valley-Gaspé trough, southern Quebec and northern Vermont – Transitional tectonism from Salinic to Acadian orogenic cycles: Tectonophysics, v. 745, p. 430–452, doi:10.1016/j.tecto.2018.08.006.

Perrot, M., Tremblay, A., Ruffet, G., Labrousse, L., Gervais, F., and Caroir, F., 2020, Diachronic metamorphic and structural evolution of the Connecticut Valley–Gaspé trough, Northern Appalachians: Journal of Metamorphic Geology, v. 38, p. 3–27, doi:10.1111/jmg.12510.

Profeta, L., Ducea, M.N., Chapman, J.B., Paterson, S.R., Gonzales, S.M.H., Kirsch, M., Petrescu, L., and DeCelles, P.G., 2015, Quantifying crustal thickness over time in magmatic arcs: Scientific Reports, doi:10.1038/srep17786.

Pyle, J.M., Spear, F.S., Cheney, J.T., and Layne, G., 2005, Monazite ages in the Chesham Pond Nappe, SW New Hampshire, U.S.A.: Implications for assembly of central New England thrust sheets: American Mineralogist, v. 90, p. 592–606, doi:10.2138/am.2005.1341.

Rankin, D.W., Coish, R.A., Tucker, R.D., Peng, Z.X., Wilson, S.A., and Rouff, A.A., 2007, Silurian extension in the Upper Connecticut Valley, United States and the origin of middle Paleozoic basins in the Quebec embayment: American Journal of Science, v. 307, p. 216–264.

Robinson, P., Tucker, R.D., Bradley, D., Berry IV, H.N., and Osberg, P.H., 1998, Paleozoic orogens in New England, USA: GFF, v. 120, p. 119–148, doi:10.1080/11035899801202119.

Roden-Tice, M.K., and Wintsch, R.P., 2002, Early Cretaceous normal faulting in southern New England: Evidence from apatite and zircon fission-track ages: The Journal of Geology, v. 110, p. 159–178, doi:10.1086/338281.

Roden-Tice, M.K., West Jr, D.P., Potter, J.K., Raymond, S.M., and Winch, J.L., 2009, Presence of a Long-Term Lithospheric Thermal Anomaly: Evidence from Apatite Fission-Track Analysis in Northern New England: The Journal of Geology, v. 117, p. 627–641, doi:10.1086/605995.

Spear, F.S., and Harrison, T.M., 1989, Geochronologic studies in central New England I: evidence for pre- Acadian metamorphism in eastern Vermont: Geology, v. 17, p. 181–184, doi:10.1130/0091-7613(1989)017<0181:GSICNE>2.3.CO;2.

van Staal, C.R., Currie, K.L., Rowbotham, G., Goodfellow, W., and Rogers, N., 2008, Pressure-temperature paths and exhumation of Late Ordovician-Early Silurian blueschists and associated metamorphic nappes of the Salinic Brunswick subduction complex, northern Appalachians: Bulletin of the Geological Society of America, doi:10.1130/B26324.1.

van Staal, C.R., Whalen, J.B., Valverde-Vaquero, P., Zagorevski, A., and Rogers, N., 2009, Pre-Carboniferous, episodic accretion-related, orogenesis along the Laurentian margin of the northern Appalachians: Geological Society, London, Special Publications, v. 327, p. 271–316, doi:10.1144/SP327.13.

Stanley, R.S., and Ratcliffe, N.M., 1985, Tectonic synthesis of the Taconian orogeny in western New England (USA).: Geological Society of America Bulletin, doi:10.1130/0016-7606(1985)96<1227:TSOTTO>2.0.CO;2.

Steiger, R.H., and Jäger, E., 1977, Subcommission on geochronology: Convention on the use of decay constants in geo- and cosmochronology: Earth and Planetary Science Letters, doi:10.1016/0012-821X(77)90060-7.

Swanson, M.T., 1999, Kinematic indicators for regional dextral shear along the Norumbega fault system in the Casco Bay area, coastal Maine: Geological Society of America Special Papers, v. 331, p. 1–23, doi:10.1130/0-8137-2331-0.1.

Thigpen, J.R., and Hatcher Jr., R.D., 2017, Paleozoic tectonic evolution of the western Blue Ridge, southern Appalachians: A critical examination of long-standing conflicts in a polydeformed system (R. D. Law, J. R. Thigpen, A. J. Merschat, & H. H. Stowell, Eds.): Linkages and Feedbacks in Orogenic Systems, v. 213, p. 0, doi:10.1130/2017.1213(04).

Thompson, M.D., Barr, S.M., and Grunow, A.M., 2012, Avalonian perspectives on Neoproterozoic paleogeography: Evidence from Sm-Nd isotope geochemistry and detrital zircon geochronology in SE New England, USA: Bulletin, v. 124, p. 517–531.

Thompson, M.D., Grunow, A.M., and Ramezani, J., 2007, Late Neoproterozoic paleogeography of the southeastern New England Avalon zone: Insights from U-Pb geochronology and paleomagnetism: Geological Society of America Bulletin, v. 119, p. 681–696.

Thompson, J.B.J., Robinson, P., and Trask, N.J., 1968, Nappes and gneiss domes in west-central New England, *in* Zen, E.-A., White, W.S., Hadley, J., and Thompson, J.J. eds., Studies of Appalachian geology: Northern and Maritime, New York, Interscience, p. 203–218.

Tollo, R.P., Aleinikoff, J.N., Bartholomew, M.J., and Rankin, D.W., 2004, Neoproterozoic A-type granitoids of the central and southern Appalachians: intraplate magmatism associated with episodic rifting of the Rodinian supercontinent: Precambrian Research, v. 128, p. 3–38.

Tomascak, P.B., Krogstad, E.J., and Walker, R.J., 1996, U-Pb Monazite Geochronology of Granitic Rocks from Maine : Implications for Late Paleozoic Tectonics in the Northern Appalachians Author (s): Paul B . Tomascak , Eirik J . Krogstad and Richard J . Walker Published by : The University of Chicago Press St: The Journal of Geology, v. 104, p. 185–195.

Tracy, R.J., and Dietsch, C.W., 1982, High-temperature retrograde reactions in pelitic gneiss, central Massachusetts.: Canadian Mineralogist, v. 20, p. 425–437.

Tucker, R.D., Osberg, P.H., and Iv, H.N.B., 2001, The Geology of a Part of Acadia and the Nature of the Acadian Orogeny Across Central and Eastern Maine: American Journal of Science, v. 301, p. 205–260, doi:10.2475/ajs.301.3.205.

Tucker, R.D., and Robinson, P., 1990, Geological Society of America Bulletin Age and setting of the Bronson Hill magmatic arc : A re-evaluation based on U-Pb zircon ages in southern New England: Geological Society of America Bulletin, v. 102, p. 1404–1419, doi:10.1130/0016-7606(1990)102<1404.

Turner, S.J., and Langmuir, C.H., 2015a, The global chemical systematics of arc front stratovolcanoes: Evaluating the role of crustal processes: Earth and Planetary Science Letters, doi:10.1016/j.epsl.2015.03.056.

Turner, S.J., and Langmuir, C.H., 2015b, What processes control the chemical compositions of arc front stratovolcanoes? Geochemistry, Geophysics, Geosystems, doi:10.1002/2014GC005633.

Turner, S.J., Langmuir, C.H., Dungan, M.A., and Escrig, S., 2017, The importance of mantle wedge heterogeneity to subduction zone magmatism and the origin of EM1: Earth and Planetary Science Letters, v. 472, p. 216–228, doi:10.1016/j.epsl.2017.04.051.

Valley, P.M., Walsh, G.J., Merschat, A.J., and McAleer, R.J., 2019, Geochronology of the Oliverian Plutonic Suite and the Ammonoosuc Volcanics in the Bronson Hill arc: Western New Hampshire, USA: Geosphere, v. 16, doi:10.1130 /GES02170.1.

Vermeesch, P., 2013, Multi-sample comparison of detrital age distributions: Chemical Geology, v. 341, p. 140–146, doi:10.1016/j.chemgeo.2013.01.010.

Vermeesch, P., 2012, On the visualisation of detrital age distributions: Chemical Geology, v. 312–313, p. 190–194, doi:10.1016/j.chemgeo.2012.04.021.

Vry, J.K., and Baker, J.A., 2006, LA-MC-ICPMS Pb-Pb dating of rutile from slowly cooled granulites: Confirmation of the high closure temperature for Pb diffusion in rutile: Geochimica et Cosmochimica Acta, v. 70, p. 1807–1820, doi:10.1016/j.gca.2005.12.006.

Waldron, J.W.F., Schofield, D.I., Murphy, J.B., and Thomas, C.W., 2014, How was the Iapetus Ocean infected with subduction? Geology, v. 42, p. 1095–1098, doi:10.1130/G36194.1.

Walsh, G.J., and Aleinikoff, J.N., 1999, U-Pb zircon age of metafelsite from the Pinney Hollow Formation; implications for the development of the Vermont Appalachians: American Journal of Science, v. 299, p. 157–170.

Walsh, G.J., Aleinikoff, J.N., and Dorais, M.J., 2011, Bedrock geologic map of the Grafton quadrangle, Worcester County, Massachusetts: US Department of the Interior, US Geological Survey.

Walsh, G.J., Aleinikoff, J.N., and Fanning, C., 2004, U-Pb geochronology and evolution of Mesoproterozoic basement rocks, western Connecticut, *in* Proterozoic tectonic evolution of the Grenville orogen in North America, Geological Society of America Inc.

Walsh, G.J., Aleinikoff, J.N., and Wintsch, R.P., 2007, Origin of the Lyme Dome and implications for the timing of multiple Alleghanian deformational and intrusive events in southern Connecticut: American Journal of Science, v. 307, p. 168–215, doi:10.2475/06.2007.06.

Wathen, B., Helou, C., Wintsch, R.P., Deasy, R.T., Yi, K., and McAleer, R., 2015, Deformation spanning 200 Million Years Along the peri-Laurentian (Pumpkin Ground Orthogneiss) Buttress and the East Derby Shear Zone, South-Central Connecticut, *in* Gilmore, M.S. and Resor, P.G. eds., Guidebook to field trips in Connecticut and Massachusetts: Middletown, Connecticut, Middletown, Connecticut, Wesleyan University, p. 153–173.

West Jr., D.P., Lux, D.R., and Hussey II, A.M., 1988, 40 Ar/ 39 Ar hornblende ages from southwestern Maine: evidence for Late Paleozoic metamorphism: 1988, doi:10.4138/1653.

West Jr, D.P., and Lux, D.R., 1993, Dating mylonitic deformation by the 40Ar-39Ar method: An example from the Norumbega fault zone, Maine: Earth and Planetary Science Letters, v. 120, p. 221–237.

West Jr, D.P., and Roden-Tice, M.K., 2003, Late Cretaceous reactivation of the Norumbega fault zone, Maine: Evidence from apatite fission-track ages: Geology, v. 31, p. 649–652.

Whalen, J.B., and Hildebrand, R.S., 2019, Trace element discrimination of arc, slab failure, and A-type granitic rocks: Lithos, v. 348, doi:10.1016/j.lithos.2019.105179.

Wilson, J.T., 1966, Did the Atlantic Close and then Re-Open? Nature, doi:10.1038/211676a0.

Wintsch, R.P., Sutter, J.F., Kunk, M.J., Aleinikoff, J.N., and Dorais, M.J., 1992, Contrasting P-T-t paths: Thermochronologic evidence for a Late Paleozoic final assembly of the Avalon Composite Terrane in the New England Appalachians: Tectonics, v. 11, p. 672–689.

Wintsch, R.P., Yi, K., and Dorais, M.J., 2014, Crustal thickening by tectonic wedging of the Ganderian rocks, southern New England, USA: Evidence from cataclastic zircon microstructures and U–Pb ages: Journal of Structural Geology, v. 69, p. 428–448, doi:https://doi.org/10.1016/j.jsg.2014.07.019.

Wise, D.U., 1992, Dip domain method applied to the Mesozoic Connecticut Valley Rift Basins: Tectonics, v. 11, p. 1357–1368, doi:10.1029/92TC01103.

Yang, X., and Gao, H., 2018, Full-Wave Seismic Tomography in the Northeastern United States: New Insights Into the Uplift Mechanism of the Adirondack Mountains: Geophysical Research Letters, v. 45, p. 5992–6000, doi:10.1029/2018GL078438.

Zartman, R.E., and Hermes, O.D., 1987, Archean inheritance in zircon from late Paleozoic granites from the Avalon zone of southeastern New England: an African connection: Earth and Planetary Science Letters, v. 82, p. 305–315.

CHAPTER 3

ACADIAN CRUSTAL EVOLUTION OF NEW ENGLAND: GEOCHEMICAL CONSTRAINTS ON THE TIMING AND MAGNITUDE OF CRUSTAL THICKENING, ITS IMPLICATIONS FOR THE METAMORPHIC FIELD GRADIENT, AND EVIDENCE FOR AN OROGENIC PLATEAU

3.1 Abstract

Thick continental crust is an intrinsic property of mountain belts and determining the timing and magnitude of crustal thickening as well as assessing to what degree there are regional differences are critical concerns in understanding the evolution of Earth's lithosphere. However, in multiphase and ancient orogens, this history is difficult to constrain. Here, geochemical and isotopic data from widely distributed igneous rocks were used to reconstruct paleo-crustal thickness in the New England Appalachians. Two phases of crustal thickening are identified each with a distinct spatial character. An early phase, ca. 420-400 Ma, involved progressive thickening from the southeast to the northwest and resulted in a relatively constant ca. 40 km crustal thickness. A subsequent crustal thickening event 400-480 Ma produced a large north-south crustal thickness gradient, from 55-70 km in southern and New England to ~40 km in northern Maine. Crustal thickness values and inferred paleo-elevations of 2.5-4.5 km from central and southern New England are suggestive of an orogenic plateau. Mid to late Devonian crustal thicknesses show a strong correlation with mapped metamorphic isograds, with higher metamorphic grade corresponding to greater paleocrustal thickness. This suggests that regions of greater thickness underwent greater degrees of orogenic collapse in

contrast to regions of thinner, perhaps more stable, crust. Thus, in this manner, primary crustal thickness is related to the exposure of the present metamorphic field gradient.

3.2 Introduction

Many convergent orogens, such the Alps, the Himalaya, and the Grenville, are characterized by multiple phases of the closure of ocean basins, terrane accretion, and orogenesis. Characterization of the timing and significance of each stage is fundamental for building tectonic models, constraining the formation and modification of continental lithosphere, and understanding the broader impacts of orogenesis on processes such as climate and atmospheric circulation (Molnar et al., 1993; Armijo et al., 2015). However, interpreting the multistage nature of these events is challenged by the overprinting effects of polyphase metamorphism and deformation and limits of geochronologic methods. Thus, one of the great challenges for geologists and geophysicists is to ascribe particular characteristics to specific events in order to build comprehensive models of crustal evolution through the composite history

The Acadian orogeny has long been recognized as the dominant tectono-thermal event in the New England Appalachians, but recent studies have shown that it involved multiple tectonic stages that took places over tens of m.y. (Robinson et al., 1998; Bradley et al., 2000; Tucker et al., 2001; Robinson, 2003; van Staal et al., 2009). However, the significance of the Acadian (425-400 Ma; Robinson et al., 1998) and Neocadian (380-350 Ma) events in New England remains unclear despite evidence in the form of accreted terranes, poly-deformed and metamorphosed rocks, and a thick wedge of sediments shed westward from the orogen because of overprinting events.

The sensitivity of igneous rock chemistry to crustal thickness provides a potential means to see through this overprint. The trace element and isotopic composition of recent convergent margin rocks show coherent trends with crustal thickness (Mantle and Collins, 2008; Chapman et al., 2015; Chiaradia, 2015; Profeta et al., 2015; Hu et al., 2017; DePaolo et al., 2019). This relationship can be extended to older rocks to constrain crustal thickness at the time of their intrusion. This represents an alternative to traditional geothermobarometric methods, which provide information on the depth of burial of rocks as a proxy for crustal thickening, but this method requires an assumption of thermodynamic equilibrium, is prone to disruption by overprinting events, and are challenging to directly date.

Here, trace element and isotopic geochemical proxies are used to quantify and constrain the crustal thickness evolution of New England. Two major crustal thickening events are identified, each with a distinct character. An initial event swept from the southeast to northwest from 420 to 400 Ma. A second event nearly doubled the crustal thickness in southern and central New England. The crustal thickness, high paleo-elevation estimates and the long-lived nature of this event suggest the creation of an orogenic plateau. Then, a correlation between paleo-crustal thickness and presently exposed metamorphic isograds is shown. Differing degrees of orogenic collapse, related to primary degrees of Acadian-Neoacadian crustal thickening, provide and explanation for the distribution of the exposure of this metamorphic field gradient.

3.3 Geologic Background

The tectonic elements of the Appalachian orogen record multiple phases of Paleozoic to Mesozoic tectonism (Fig 12). Orogenesis began with the Ordovician

Taconic orogeny, interpreted to be representate closure of the Iapetus ocean due collision between the Laurentian margin and Ordovician island arc(s) built on the Gondwanan-derived Moretown terrane (Karabinos et al., 2017). The subsequent Silurian Salinic orogeny involved accretion of the peri-Gondwanan Gander terrane to Taconic-modified composite Laurentia but did not produce significant deformation in New England (van Staal et al., 2009). The late Silurian to Devonian (ca. 420-380 Ma) Acadian orogeny, is marked by nappe emplacement, magmatism, and the development of a large sedimentary wedge in (Robinson et al., 1998; van Staal et al., 2009). This event is generally attributed to collision between composite Laurentia and the peri-Gondwanan Avalon terrane (Robinson et al., 1998; van Staal et al., 2009). The main phase of Acadian orogenesis was followed by the enigmatic late Devonian to early Carboniferous Neo-Acadian orogeny (380-350 Ma; Robinson et al., 1998). Neo-Acadian orogenesis has been characterized on the basis of high-grade metamorphism reaching granulite facies in central Massachusetts, plutonism, and the overprinting of earlier Acadian fabrics and structures (Robinson et al., 1998). Neoacadian plutons were deformed by ~350 to 300 Ma dextral transpression and associated high strain zones (Massey et al., 2017). Both Neoacadian orogenesis and subsequent transpression have been suggested to be linked to the docking of the Meguma terrane to the Laurentian margin (van Staal et al., 2009; Massey et al., 2017). The 300-260 Ma Alleghanian orogeny is interpreted to record collision of Gondwana with Laurentia and the final assembly of Pangea, although its effects are restricted primarily to southeastern New England (Robinson et al., 1998). Early Mesozoic rifting associated with the breakup of Pangea led to magmatism and development of thin-skinned normal faults and associated sedimentary basins with additional faulting or fault reactivation occurring in the late Mesozoic.

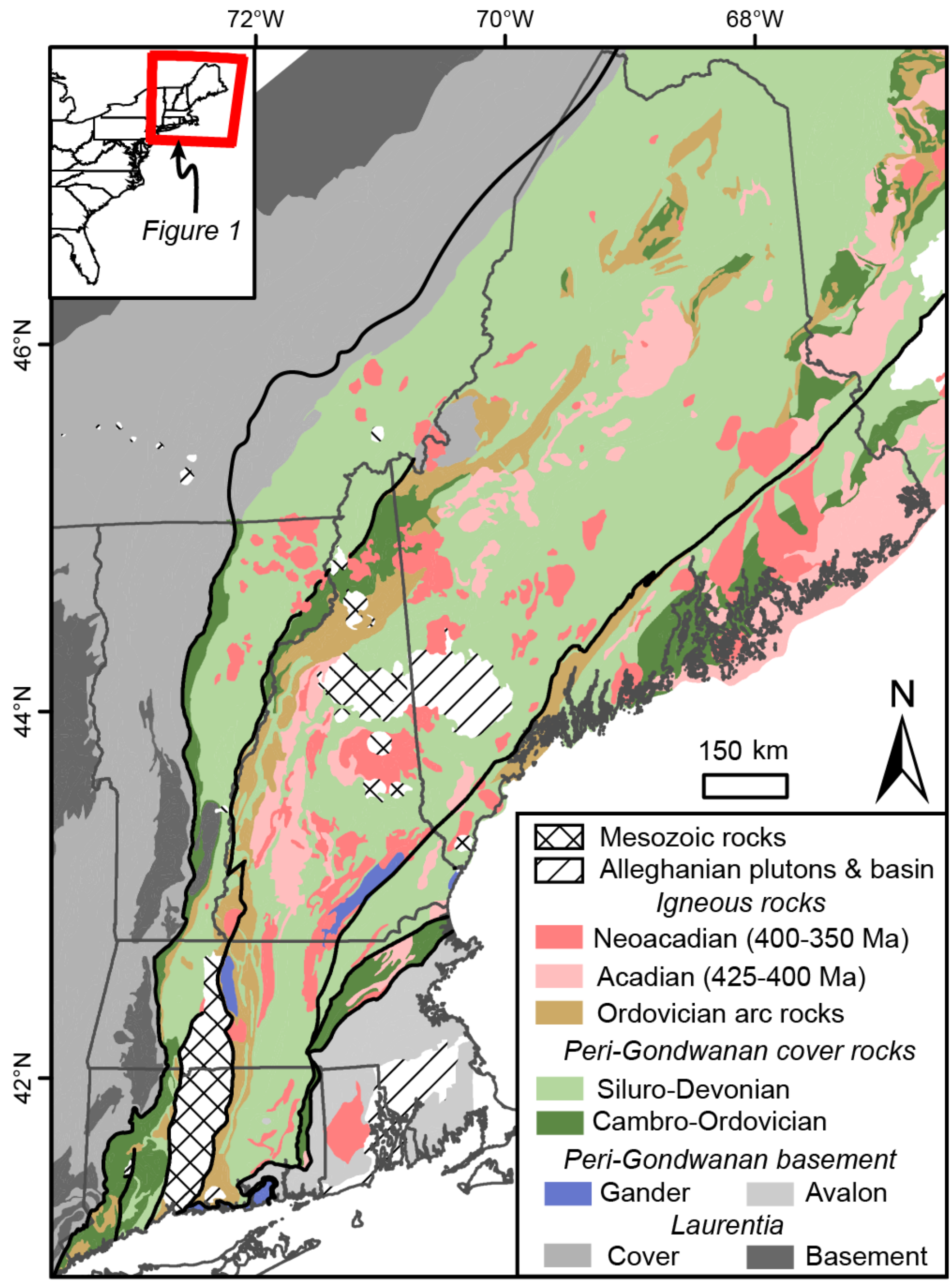

Figure 12: Simplified tectonic map of the northern Appalachians modified from Hibbard et al. (2006) after Karabinos et al. (2017).

3.4 Methods

Paleo-crustal thicknesses were constrained using recently proposed calibrations based on correlations between the chemistry of modern convergent margin magmas and Moho depth (Hu et al., 2017; DePaolo et al., 2019). Trace element ratios (e.g. Sr/Y, La/Yb) in syn-collisional magmas are governed by element partitioning controlled by the residual phases during melting, primarily plagioclase and garnet, and to some extent, amphibole (Chapman et al., 2015; Hu et al., 2017). Plagioclase is stable at pressures <1 GPa and strongly partitions Sr and, to a lesser extent, the light rare earth elements (e.g. La). As crustal thickness increases, plagioclase becomes unstable (at pressures >1.2 GPa) and Sr will likely enter the melt phase. On the other hand, Y and Yb are incompatible at low pressures, but readily partition into garnet at high-pressure (greater crustal thickness). Amphibole, if present, may also elevate the Sr/Y and La/Yb ratios. Thus, greater Sr/Y and La/Yb ratios are indicative of a greater depth or pressure at which magmatic differentiation occurred.

Sr/Y and La/Yb crustal thickness estimates were utilized the calibration of Hu et al. (2017) for syn-collisional magmas. A new geochemical database for the northern Appalachians was compiled and filtered for intermediate-composition rocks with SiO_2 = 55–72 wt%, MgO = 0.5–6.0 wt.%, Rb/Sr <0.35, Sr/Y = <60, and La= <60 ppm following Hu et al. (2017). The Rb/Sr filter was applied to remove samples that have experienced high degrees of fractionation within the crust whereas Sr/Y and La samples were removed due to their poorly defined petrogenesis with adakitic features (Hu et al., 2017). Samples that passed these filters but exhibited extensional or cumulate characteristics (e.g. lack of Th/Nb or Th/Ta anomaly, positive Eu/Eu*, enrichment in Al, and generally depleted characteristics) were excluded. Mineralized or highly altered samples were removed on the basis of reported field observations, high LOI (>2.5 wt%), a lack of linear relationships among the major elements, and/or anomalous trace element systematics. A total of 245 geochemical analyses from forty igneous complexes passed these filters. Subsequently, the median Sr/Y and chondrite-normalized La/Yb (La/Yb_n) ratio of each igneous complex were calculated. A summary of trace element samples are provided in Appendix A and a complete set of compiled geochemical data and sample information are accessible through the New England Geologic Database (NED; https://sites.google.com/umass.edu/ned/) described in Chapter 2.

Likewise, the degree of isotopic contamination presents a potentially complementary approach to trace element methods for estimating paleo-crustal thickness (DePaolo et al., 2019). The isotopic signatures of magmatic rocks are interpreted to represent mixing between a primary (mantle-derived) melt source and the contaminating (assimilated) crustal material into the melt (DePaolo et al., 2019). The degree of assimilation is highly temperature dependent and, if known, can be inverted to constrain crustal thickness. The Neodymium Crustal Index (NCI), quantifies εNd values of pluton with respect to the recharging magma and assimilated (crustal) material. The degree of contamination can be used approximate the Moho temperature and depth, with the assumption of a geothermal gradient (DePaolo et al., 2019). Results of this method have been shown to be consistent with La/Yb-derived crustal thickness estimates within error of ~10 km (DePaolo et al., 2019), although the model saturates at crustal thicknesses of >60 km. Compared to the trace element proxies, NCI is applicable to a plutons with a wider range of SiO_2 values and may provide more resolution in the range of 25 to 45 km, while also being less susceptible to later alteration.

Crustal thickness estimates were derived using the NCI model using the calibration of DePaolo et al. (2019) for convergent margin magmas. In order to use this model, measured values from plutons were assessed in context of the isotopic values for crustal contaminants and recharging magmas. The crustal component for syn-Acadian plutonic have been shown to have derived from predominantly from underlying basement of the peri-Gondwanan Gander terrane (Dorais and Paige, 2000; Dorais et al., 2012; Karabinos et al., 2017). One exception is the New Hampshire Plutonic Series, interpreted to be derived in part from crustal melting of metasedimentary rocks of the Central Maine Basin (Dorais, 2003). Potential end members have relatively restricted and similar εNd_i values (Dorais et al., 2009), supporting use of the NCI model, thus they do not significantly shift crustal thickness estimates. The isotopic composition of the recharging (mantle) component was estimated using values from mantle-derived mafic magmas and enclaves, which range between +1 and +5 εNd_i (e.g. Dorais, 2003). Samples adjacent to the contacts with country rock or isotopic signatures suggesting signficant upper crustal contamination (e.g. elevated $^{87}Sr/^{86}Sr$ or $\delta^{18}O$ relative to other samples from the same pluton) were removed. Seventy-three samples passed these filters and were used to calculate average NCI values and crustal thickness estimates for eighteen plutons. Compiled Nd isotopic values used to reconstruct crustal thickness are in Appendix B and complete sample descriptions can be found in the New England Geologic Database (NED; https://sites.google.com/umass.edu/ned/) that was described in Chapter 2.

3.5 Results and Discussion

Calculated crustal thicknesses for all plutons examined in this study are compiled in Table 1. Paleo-crustal thickness estimates are similar regardless of method (Sr/Y, La/Yb and/or NCI) and agree within systematic error. Given the consistency between these results, they are interpreted together. The similarly is generally supportive of the hypothesis that these systems are systematically influenced by, and reflective of, paleo-crustal thickness (Profeta et al., 2015; Hu et al., 2017; DePaolo et al., 2019).

TABLE 1: CRUSTAL THICKNESS ESTIMATES

Pluton	Age (Ma)	error	Sr/Y (km)	error	La/Yb (km)	error	NCI (km)
Preston	424	5	35.0	7.5			
Calais	420		34.8	7.7			
Vinalhaven	419	1	36.0	8.7	32.0	12.6	
Northport	419	1	35.0	7.7			
South Penobscot	419	2	37.7	8.1			
Sudbury	419	2	41.0	8.0			
Gouldsboro	419	2					37.2
Spruce Head	419		41.6	8.5	39.0	13.6	
Cardigan pluton	413	5					47.5
Kinsman	413	5					40.6
Andover	412	4					45.0
Meredith	410	5	32.0	7.5			45.3
Littleton	407	2	41.4	8.5	59.6	16.6	
Bethlehem	407	5	41.0	8.4	32.0	12.5	46.6
Katahdin	407	1	46.4	9.0			
Lexington	404	2					42.0
Hunt Ridge	402	4	35.0	7.8			
Coys Hill	396	2					49.0
Winnipesaukee	393	2	49.9	9.3	52.4	15.6	46.4
Mooselookmeguntic	389	2	49.8	9.3	48.6	15.0	45.9
Webhannet	383	1	38.9	8.2	49.4	15.2	
Belchertown	380	5	71.5	11.5	69.2	18.0	61.0
Eastford	378	4	66.9	11.1	48.7	15.1	
Rome	378	1	40.2	8.4	51.4	15.4	

Umbagog	377	2	47.8	9.1	58.7	16.5	
Sweepstakes	375		37.7	8.0	31.0	12.5	
Nulhegan	375				42.1	14.1	50.2
Derby	375				60.4	16.7	59.0
Knox Mountain	375	2	49.0	9.3			
Newark	375		47.8	9.1	73.0	18.5	
Victory	375		53.5	9.7	52.9	15.7	
Woodbury	375		64.0	10.8	48.2	15.0	
Echo Pond	375						44.0
West Charleston	375						53.0
Willoughby	375						44.0
Granite at Derby	375						60.0
Spider Lake	373	2	50.6	9.4	58.3	16.4	
Deer Isle	371	2	41.2	8.2			38.0
Scituate	370	7	51.7	9.5	79.6	19.4	
Waldoboro	368	4	37.8	8.1	45.2	14.6	
Averill	367	1	43.8	8.7	46.0	14.7	
Debouille	364	3	46.7	9.0	49.4	15.2	
Priestly Lake	361	3	39.0	8.2	43.6	14.3	
Stony Creek	360	4	58.0	10.2			65.0
Hardwick	360	1	61.0	16.8			
Songo	360	1	52.2	9.4			
Sunapee	355	5					62.2
Concord	355	5					54.0
Fitzwilliam	354	1	57.5	10.0			54.0
Long Mountain	350	5					61.1
Indian Head	349	6			54.0	15.9	

Table 1: Tabulation of the ages and crustal thickness estimates of plutons examined in this study. Sr/Y and La/Yb estimates are calculated using the empirical calibration of Hu et al. (2017). NCI refers to are calculated using the using the neodymium contamination index calibrated by DePaolo et al. (2019). A summary of samples are presented in Appendix A while complete geochemical data used to constrain crustal thicknesses are available at https://sites.google.com/umass.edu/ned/home/geochemistry.

Apparent crustal thickness estimates calculated from trace element ratios (Sr/Y; La/Yb) and the NCI framework are consistent within systematic error. Similar values across systems are also derived from spatially and temporally similar plutons. This consistency between different geochemical systems is supportive of the hypothesis that these systems are systematically influenced by, and reflective of, paleo-crustal thickness (Profeta et al., 2015; Hu et al., 2017; Scott et al., 2018; DePaolo et al., 2019).

The distribution of apparent crustal thicknesses shows correlations in both space and time. As most of those igneous rocks post-date terrane accretion and major faulting, palinspatic considerations are relatively minor, as reviewed by Bradley et al. (2000). Post-accretion, kilometer scale strike-slip offset has occurred along the Norumbega fault zone, however no major offsets are observed in crustal thickness across the fault zone. Only one pluton with crustal thickness data is east of faults related to the Permian Alleghanian orogeny in southeastern New England.

Crustal thickness for the time period typically defined as the Acadian orogeny (*sensu stricto*), ca. 420 to 400 Ma are all approximately 40 km (Fig. 13A). However, they show a distinct temporal trend. The oldest Acadian plutonic bodies are in coastal Maine and southeastern Connecticut with ages younger ages trending to the northwest (Fig. 13). Bradley et al. (2000) observed this pattern and suggested that the Acadian deformational front progressively migrated northwestward (present day coordinates) during the closure of the Siluro-Devonian Central Maine Basin. This basin has been interpreted to have formed on thin, extended continental crust (Ludman et al., 2017). The dataset presented suggests that this initial crustal thickening event, to ~35-40 km, followed the Acadian deformational front. Progressive crustal thickening to the northwest is supported by shifts in palæocurrent data and detrital zircons from the northwest to southeast in the mid to late Silurian, and cessation of marine depositional (Bradley and O'Sullivan, 2016). By 400 Ma, when the deformation front had generally passed through New England, the entire region may have had a generally uniform crustal thickness on the order of 35-40 km (Fig. 13).

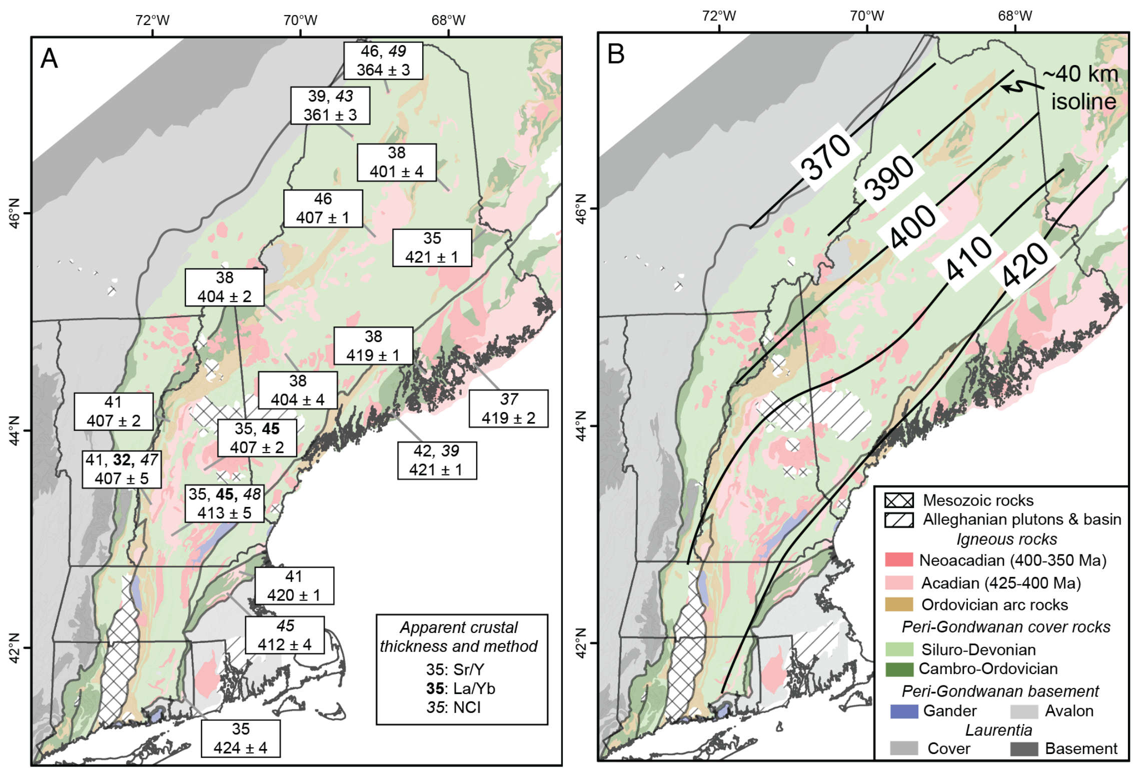

Figure 13: Crustal thickness estimates from Acadian (420-400 Ma) plutons. A: Crustal thickness estimates from individual plutons. B: Contour of 40 km crustal thickening by age in Ma. Note age progression from the southeast to northwest.

Crustal thickness patterns for 400-350 Ma plutons, correlating to the Neoacadian orogeny (van Staal et al., 2009) show a distinct spatial pattern (Fig. 14). Values are greatest in Massachusetts, Connecticut, and southern New Hampshire (55-70 km) and progressively decrease to the northeast (present day coordinates) along orogenic strike to ~50 km in northern Vermont to western Maine and further to 40-45 km in northern Maine (Fig. 14B). This implies that crustal thickness ca. 380 Ma perhaps varied by 40 km along just 400 km of orogenic strike. No distinct temporal trends are recognized in this dataset. However, the distinct crustal thickness from southern and central New

Hampshire (Massachusetts, Connecticut, and southern New Hampshire), northern New England (northern Vermont to western Maine) and coastal New England and much of Maine suggests they must have followed distinct crustal thickening and tectonic histories after 400 Ma.

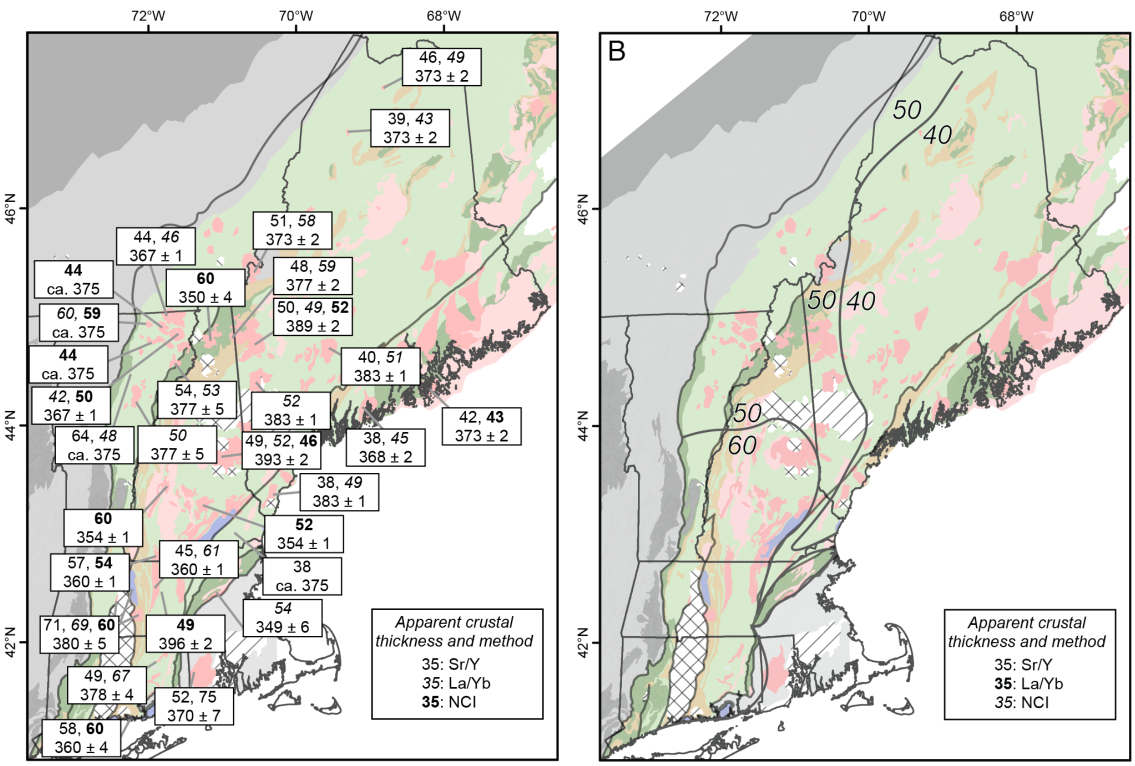

Figure 14: Crustal thickness estimates from 400-350 Ma plutons. A: Crustal thickness estimates from individual plutons. B: Contoured crustal thickness in km.

Plots of crustal thickness against time for these three regions are presented in Figure 15. Rocks from coastal and northern Maine (Fig. 15A) suggest initial thickening to ~40 km, likely from a thinned submarine crust, by 400 Ma. These crustal thicknesses seem to have persisted until ca. 360 Ma. In contrast to the two other domains, it does not appear to have undergone post 400 Ma (Neoacadian) crustal thickening.

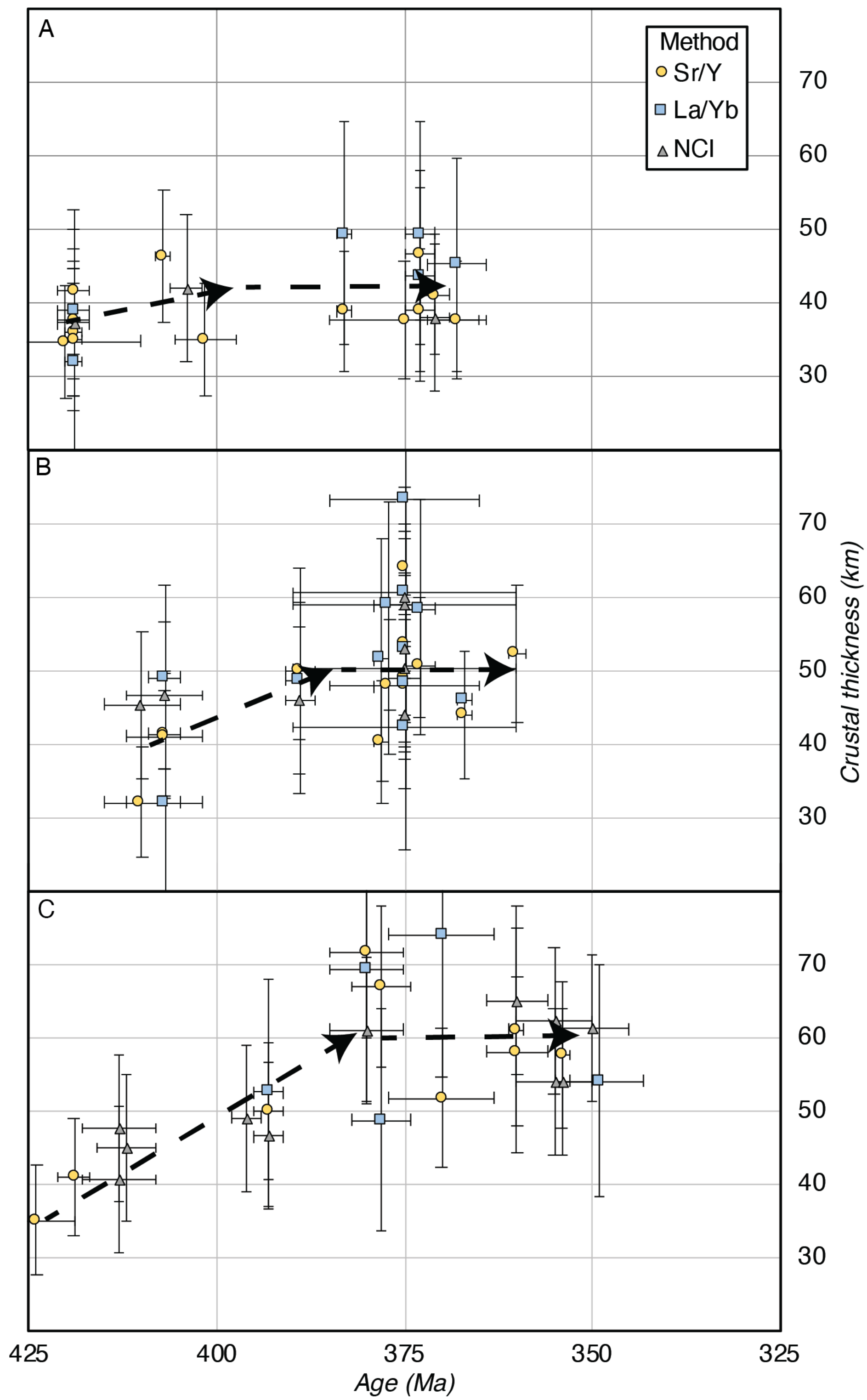

Figure 15: Time vs. crustal thickness plots for coastal and northern Maine (A), northern New England (B), and central and southern New England (C). Generalized crustal thickenness evolution for each region shown by the dashed line.

Igneous rocks from northern New Hampshire and Vermont, western Maine, and central Massachusetts suggest a two-phase crustal thickening history (Fig. 15B). The first is inferred to be similar to that 420-400 Ma Maine, involving closure of the Central Maine basin and thickening to ca. 40 Ma. Subsequently, additional crustal thickening occurred by ca. 390 Ma. belt of igneous rocks from western Maine to northern Vermont suggest a 45-55 km thick crust persisted to at least 360 Ma.

Geochemical proxies from central New England suggest continued crustal thickening between 390 and 380 Ma, providing evidence of a third Acadian crustal evolution path (Fig. 15C). Crustal thickness estimates for the ~380-370 Ma plutons suggest crustal thicknesses on the order of 60-70 km, indicating nearly a doubling of crustal thickness from ~400 Ma. Notably, this crustal thickness estimate is similar to thermobarometric estimates of Acadian lower crustal blocks (Keller and Ague, 2018). Crustal thickness estimates of ~60 km through the early Carboniferous suggest that thickened crust was maintained for at least 25 m.y. (Figs. 14; 15C). The widely distributed nature of the plutons, and existence of dikes of the Belchertown pluton throughout central New England, suggest that a large region was thickened at the same time to 60-70 km.

Today, crustal thicknesses greater than 60 km are restricted to orogenic plateaus (Laske et al., 2013). Seismologically-derived crustal thickness estimates for modern plateaus are on the order 60-75 km for the Andean Puna-Altiplano (Ryan et al., 2016) and the Tibetan plateau (Chen, 2017). In contrast, modern orogens outside of plateau regions are generally in the range of 35 to 50 km (Cassidy, 1995; Lombardi et al., 2008;

Assumpção et al., 2013; Laske et al., 2013; Robert et al., 2017). This similarity in apparent crustal thickness estimates from modern plateaus and paleo-crustal thickness estimates are suggestive of an orogenic plateau in Central New England (Fig. 14; 15C).

Further, the observation that a large region of New Engladn underwent simulatenous crustal thickening to the same amount is characteristic of the "distributed" deformation of a weak plateau crust. Geochemical data with similar systematics to those in this study have been observed in modern orogenic plateaus (Zhu et al., 2017; Scott et al., 2018, DePaolo et al., 2019; Alexander et al., 2019). Similar geochemical signatures yielding analogous crustal thickness estimates have been used to argue in support of hypothesized paleo-plateaus such as the Cretaceous Nevadaplano (55-65 km; Chapman et al., 2015) and Arizonaplano (57 ± 12; Chapman et al., 2020).

Thickened crust implies high elevation, with the assumption of isostacy. Paleoelevations, assuming Airy isostacy, were calculated for the ca. 380-350 Ma period. (Fig. 16). Estimates were calculated assuming Airy isostatic compensation with average values for the density of continental crust (2800 kg/m^3) and upper mantle (3300 kg/m^3), and thickness of the continental crust (37 km). In this model, a 60 km thick crust corresponds to a 3 to 3.5 km paleoelevation and a 70 km thick crust to ~5 km (Fig. 21A). This paleoelevation is similar to the average 3.75 km elevation of the modern Andean Altiplano and 4.5-5 km elevations of the Tibetan plateau. Paleoaltimetric analysis of the Cretaceous Nevadaplano paleo-plateau have suggested elevations between 2.2 to 3.5 km (Chapman et al., 2020). Similar paleoelevation estimates of 3 ± 1.8 km have been proposed for the Arizonaplano (Chapman et al., 2020). Bradley (1982) estimated a paleo-elevation of 4 km for the Acadian Orogeny of northern and central New England. The presence of glacial deposits in the Appalachian foreland basin in the late Devonian suggest several km of elevation (Ettensohn et al., 2019). Together, elevations from central and southern New England during ca. 380-350 Ma were likely comparable to those of modern orogenic plateaus. Paleo-elevation estimates decrease to the northeast with decreasing crustal thickness (Fig. 16B). This paleoelevation distributions is comparable to values calculated by Hooke and Winski (2014) on the basis of thermobarometric data, consideration of erosion laws, and the assumption of Airy isostacy.

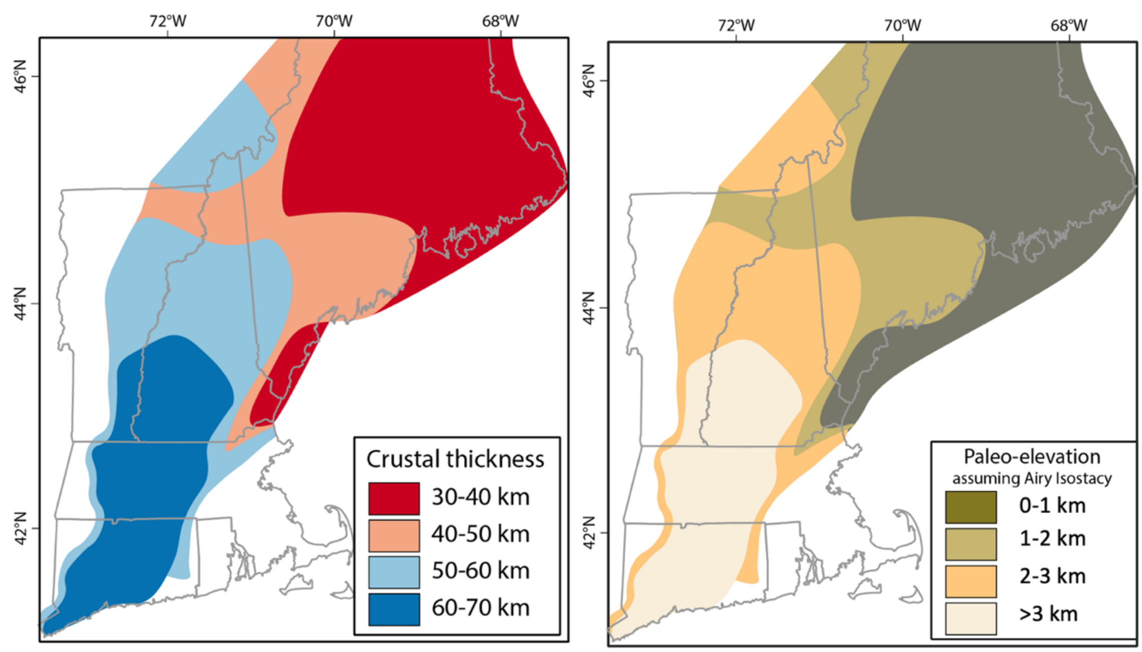

Figure 16: Interpreted crustal thickness (A) and paleoelevation (B) in the New England Appalachians ca 380-350 Ma.

The tectonic setting that produced the variations in crustal thickness is relatively poorly explained by current tectonic models. Massey et al. (2017) suggested that oblique convergence between Laurentia and the Avalone/Meguma terranes was geometrically focused in central New England by the structure of the Laurentian basement. Alternatively, Kuiper (2016) presented a model involving ridge subduction in northern

New England, which may explain why convergent tectonics was ongoing until the latest Devonian or earliest Carboniferous in central New England while coastal Maine progressively transitioned from a convergent to strike slip regime. van Staal et al. (2009) suggested the existence of a west-dipping, flat slab, Andean-style subduction regime of the Avalon terrane under composite Laurentia in Maine to explain the progressive deformation front described by Bradley et al. (2000). If this tectonic regime was active, the angle of the subducting slab may have played a factor. Slab angle varies with crustal thickness along the modern Andean margin, with flat-slab regions positioned over relatively thin crust while the 60-70 km thick Altiplano is situated over a steeply dipping portion (Assumpção et al., 2013; Garzione et al., 2017). This suggests that subduction angle may be another causative factor for along-strike variations in Acadian crustal thickness.

Crustal thickening has often been inferred from metamorphic assemblages and thermobarometry (Spear, 1993). In a classic study, Carmichael (1978) noted systematic changes in mineral assemblages in the New England Appalachians and inferred an increase in paleodepth from Maine to Connecticut (Fig 17a). Robinson et al. (1998) compiled metamorphic isograds across New England and noted a similar pattern, with higher grade assemblages in central and southern New England and lower grade assemblages in coastal and northern Maine (Fig 17B). These inferences from assemblages are consistent with quantitative thermobarometric data, which show increases in burial depth (when assuming lithostatic pressure) from <10 km in Maine to 20 to 30 km in central and southern New England (Fig. 17C). These consistent trends in metamorphic petrology are striking similar to the paleocrustal thickness map of New

England ca. 380-350 Ma, with greater crustal thickness correlating with greater paleodepth. Values from thermobarometry can be compared to the amount of exhumation suggested by crustal thickness proxies. ArcGIS 10.6 was used to subtract rasters of paleocrustal thickness from modern day values of Li et al. (2018). This model predicts the greatest exhumation, on the order of 20-30 km in central and southern New England and 5-10 km in northern Maine (Fig. 17D0. These values are broadly consistent with those of thermobarometry and the pattern of predicted exhumation closely resembles the isograd map of Robinson et al. (1998). The correlation between crustal thickness, metamorphic conditions, and exhumation suggests that differences in syn-orogenic crustal thickness strongly influenced, to a first order, orogenic collapse, exhumation, and present exposure of the metamorphic field gradient.

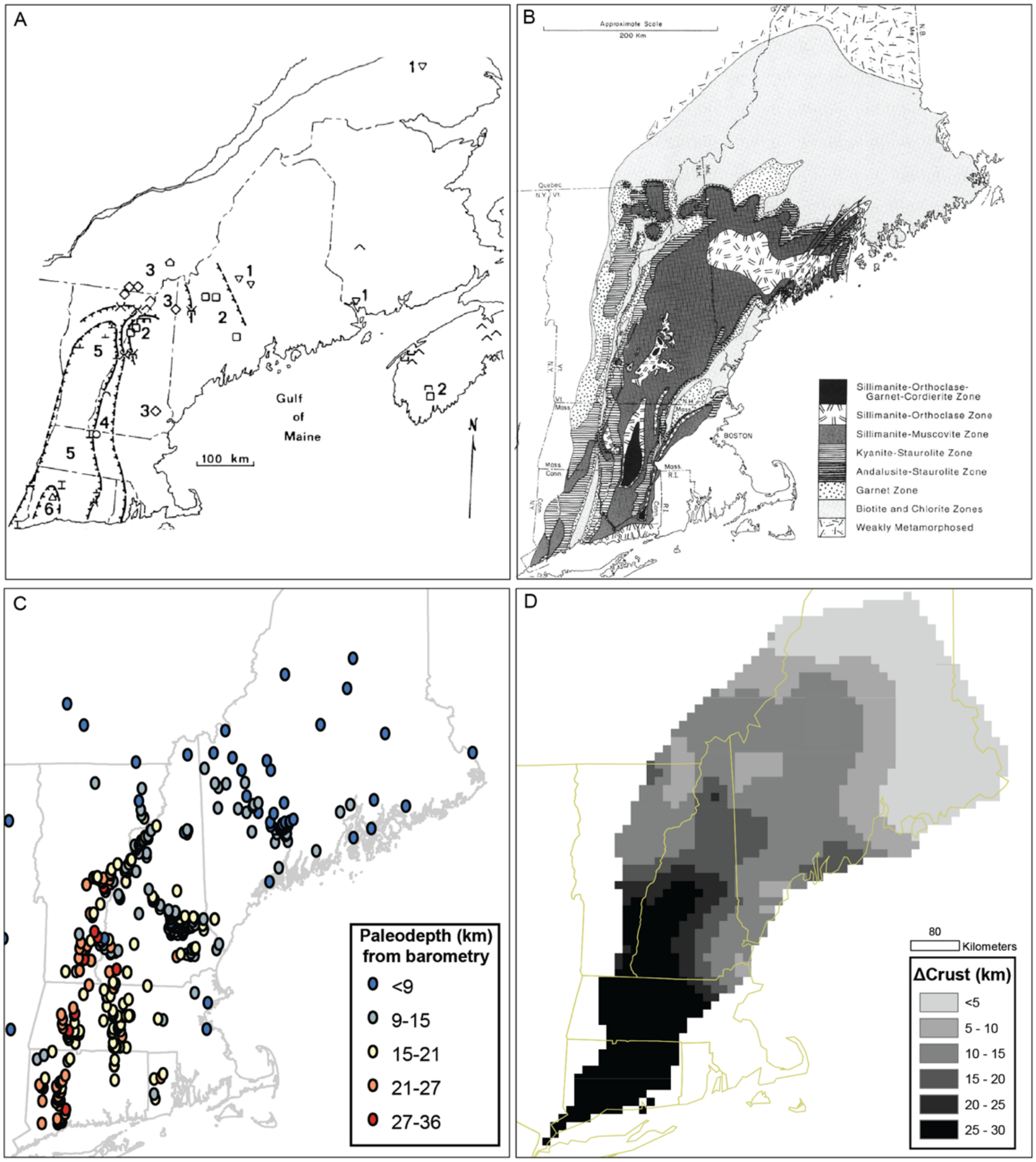

Figure 17: Petrologic constraints on metamorphism and exhumation. A: Carmicheal's (1978) bathozone map of New England. B: Acadian metamorphic isograds compiled by Robinson et al. (1998). C: Paleodepth from thermobarometry compiled in chapters 2 and 4 of this thesis, assuming lithostatic pressure. D: Amount of exhumation calculated by comparing the difference in geochemically derived crustal thickness in this study with modern values of Li et al. (2018)

Modern crustal thickness estimates for much of Maine (Li et al., 2018) are within 10 km of Acadian to Neaoacadian crustal thicknesses constrained by this study. This observation suggests that Maine a) did not experience crustal thickening significantly greater than the global average (~37 km) and b) that the crustal thickness may not have been significantly modified in at least 360 m.y and perhaps as much as 400 m.y. or more. Qualitatively, the first observation has previously been suggested on the basis of the preservation of ash flows, magma chamber and lowest greenschist facies rocks (Zen, 1991; Bradley et al., 2000; Schoonmaker et al., 2005; Fig. 17A-B). Thermobarometric estimates suggest that between 3 to 10 km have been eroded from much of Maine (Zen, 1991; Hooke and Winski, 2014; Fig. 17B). These observations compare favorably with predictions of the exhumation model in Figure 17D, which suggests 3-10 km have been denuded since the Devonian.

In constrast, significant Acadian crustal modification is required for central and northern New England where paleocrustal thickness values far exceed modern day estimes (e.g. Li et al., 2018). Several processes that could have caused this crustal thinning are now considered. Pyle et al. (2005) proposed lithopsheric delamination on the basis of high metamorphic temperatures at ca. 350 Ma obtained monazite-xenotime thermometry. While this process may also remove lower crust and contribute to crustal thinning (Garzione et al., 2017), thickened crust at 350 Ma suggests that delamination not have the primary cause. The minor degree of crustal thinning (~70 km to 55 km) possibly suggested between 380 and 350 Ma on Figure 15B could be explained by delamination, though this requires further testing and the amount of thinning, if present, cannot be precisely resolved with the current dataset and calibrations. Another possibly for crustal thinning is crustal (channelized) flow. On the basis of thermomechanical models and geophyscial observations it has been suggested that the crust of thickened regions, such as orogenic plateaus, may flow outward to regions of thinner crust or form core-complex like gneiss domes (Clark and Royden, 2000; Hacker et al., 2017, and references therein). Evidence for ductile flow in mid-crustal exposures of central Massachusetts is evident from stretching lineations and rock fabrics (Robinson et al., 1998; Massey et al., 2017). These fabrics have been dated to ca. 340-310 Ma with monazite U-Th-Pb techniques (Chapter 4 of this thesis, Hillenbrand and Williams, unpublished data). Regional $^{40}Ar/^{39}Ar$ muscovite and biotite thermochronologic data suggest widespread cooling through the closure temperatures of muscovite and biotite between 340-320 Ma, possibly suggesting exhumation from middle to upper crust (Harrison et al., 1989; chapter 4 of this thesis). Perrot et al. (2020) interpreted 10-15 km of uplift in nothern Vermont and southern Québev between ca. 345 to 335 on the basis of $^{40}Ar/^{39}Ar$ dates and thermobarometric data. ~340 Ma decompression is indicated in western New England by ~340 to 310 Ma xenotime halos formed during garnet breakdown (Gatewood et al., 2015; Hillenbrand and Williams, unpublished data).

Synchronous decompression of the large region of New England, after synchronous uplift, may also be consistent with the orogenic plateau hypothesis. Hacker et al. (2017) noted simultaneous extension in the Pamir region of the Tibetan plateau and suggested it may be charatceristic of plateaus in general. They further suggested that plateau collapse may be governed by catastrophic plateau scale events.

What then caused the significance difference in the degree exhumation across New England? Post Paleozoic events are unlikely. While New England experienced extension in the Mesozoic and steady denudation following exhumation, regional estimates of Mesozoic to present erosion are on the order of 3-5 km (Zen, 1991; West et al., 2008; Roden-Tice et al., 2009) with 1-2 km of offset along major Mesozoic extensional faults (e.g. Thompson et al., 1968). Spatially and temporally restriced periods of accelerated exhumation have been recognized (Amidon et al., 2016) however, these events cannot explain the 10s of km of denudation requried to explain the presence of high grade rocks that the present erosional surface. Hence, it must instead be related to Paleozoic Acadian-Neoacadian

Thus, exhumation on the order of 10s of km occurred during Acadian orogenic collapse in central New England but not in northern . Deformation events associated with exhumation and crustal thinning documented in northern and central New England have yet to be recognized in Maine. Higher temperatures in the thickened crust of central and southern New England may have faciliated mid and/or lower crustal flow, as suggested by the 330-310 Ma N-S stretching lineations (Robinson et al., 1998; Massey et al., 2017). These fabrics and phase of deformation are not presently recognized in Maine (Robinson et al., 1998). The process of crustal flow may perhaps to be analagous to channels hypothesized underneath the Tibetan and Altiplano-Puna plateaus (Clark and Royden, 2000; Beaumont et al., 2006; Garzione et al., 2017; Hacker et al., 2017). These process may have been also been facilitated by gravitational and isostatic instability of the overthickened plateau-like crust. In contrast, Maine, where crustal thickness estimates are on the order of global averages (~30-35 km), the crust was likely and closer to being to isostatically and gravitionally stable. Speculatively, on this basis it is suggested to have been less prone to, and less capable of, undergoing orogenic collapse.

These results and interpretations are summarized in Figure 18. Orogenesis between ca. 420 to 400 Ma closed the Central Maine Basin and crust to ca. 40 km. The crustal thickening and orogenic front progressed from the southeast to northwest between the late Silurian and early Devonian perhaps resulting in a uniform ca. 40 km thick crust across New England. Additional crustal thickening between 400 and 380 Ma varied in magnitude along strike, from 20 to 30 km in central and southern New England, to ~10 km in northern Vermont to western Maine, and minimal thickening in Maine. The uniform uplift of central and southern New England to 60-70 km by 380 Ma, the magnitude of crustal thickness, and several kilometers of elevation are suggestive of an orogenic plateau. Geochemical data suggest that ca. 380 Ma crustal thickness values were sustained in all three domains for 20-30 m.y. Slight decreases in crustal thickness estimates from the hypothesized plateau region may be reflective of uncertainity in the methods utilized here, or possibly suggestive of mid- or lower crustal flow or a delamination event. Orogenic collapse occurred ca. 340-330 Ma, on the basis of geochronologic data, and varied along strike. Collapse occurred to a much greater degree in regions of thicker crust, exhuming deeper levels of rocks and controlling, to a first order, the presently exposed metamorphic field gradient.

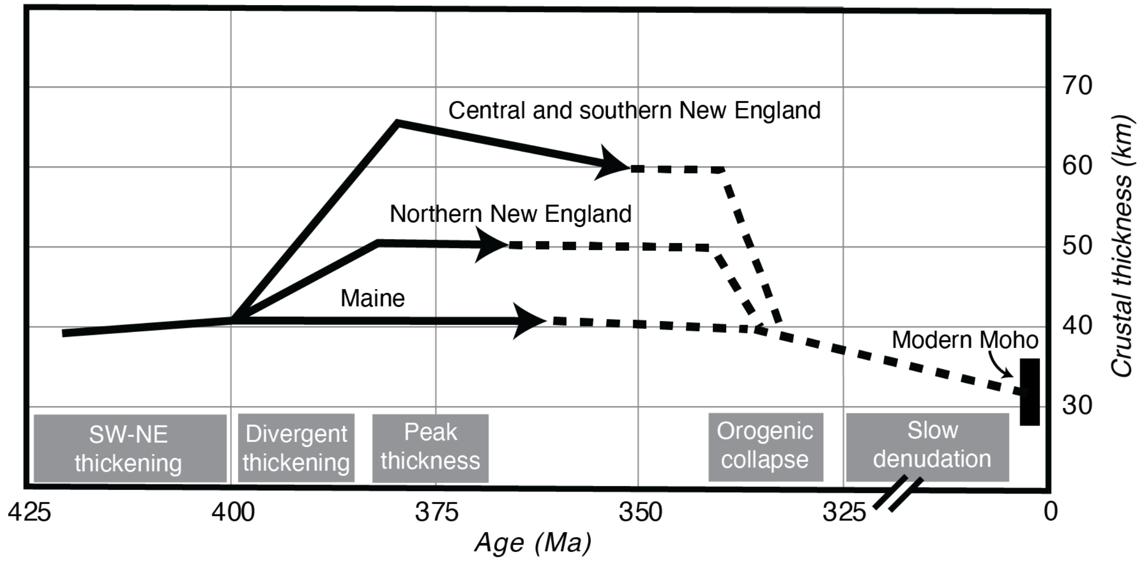

Figure 18: Interpreted crustal thickness evolution paths for New England. Distinct paths are recognized for coastal and northern Maine, northern New England (western Maine to Vermont) and central New England (Massachusetts, Connecticut, and southern Vermont and New Hampshire). Solid lines indicate periods directly constrained by geochemical proxies while dashed lines indicate crustal thicknesses inferred from other data.

4.8 Conclusions

Here, for the first time, I have quantified the crustal thickness evolution of the New England Appalachians. A newly compiled geochemical and isotopic database was used to reconstruct crustal thickness and distinguish two distinct periods of crustal thickening. Initial crustal thickening propagated northwestward from ca. 420 to 400 Ma resulting in a uniform ~40 km thick crust across New England by ~400 Ma. Subsequently, crustal thickening histories diverge, with minimal or no additional thickening in coastal and northern Maine, moderate thickening to ~50 km in western Maine to northern Vermont, and further thickening to 60-70 km in central New England by 380 Ma. Crustal thickness data from central New England suggest the uplift of an orogenic plateau which existed for at least 30 m.y. Metamorphic isograds and bathograds correlate with crustal thickness values, suggesting differing degrees of orogenic collapse along strike likely related to the crustal thickness and thermal structure. This observation suggests that exposure of the modern metamorphic field gradient is, to a first order, controlled by paleocrustal thickness.

4.9 References Cited

Amidon, W.H., Roden-Tice, M., Anderson, A.J., McKeon, R.E., and Shuster, D.L., 2016, Late cretaceous unroofing of the White Mountains, New Hampshire, USA: An episode of passive margin rejuvenation? Geology, v. 44, p. 415–418, doi:10.1130/G37429.1.

Armijo, R., Lacassin, R., Coudurier-Curveur, A., and Carrizo, D., 2015, Coupled tectonic evolution of Andean orogeny and global climate: Earth-Science Reviews, doi:10.1016/j.earscirev.2015.01.005.

Arth, J.G., and Ayuso, R.A., 1997, The Northeast Kingdom batholith, Vermont: Geochronology and Nd, O, Pb, and Sr isotopic constraints on the origin of Acadian granitic rocks: Memoir of the Geological Society of America, v. 191, p. 1–18, doi:10.1130/0-8137-1191-6.1.

Ashwal, L.D., Leo, G.W., Robinson, P., Zartman, R.E., and Hall, D.J., 1979, The Belchertown quartz monzodiorite pluton, West-central Massachusetts; a syntectonic Acadian intrusion: American Journal of Science, v. 279, p. 936–969.

Assumpção, M., Feng, M., Tassara, A., and Julià, J., 2013, Models of crustal thickness for South America from seismic refraction, receiver functions and surface wave tomography: Tectonophysics, v. 609, p. 82–96, doi:10.1016/j.tecto.2012.11.014.

Beaumont, C., Nguyen, M.H., Jamieson, R.A., and Ellis, S., 2006, Crustal flow modes in large hot orogens: Geological Society Special Publication, v. 268, p. 91–145, doi:10.1144/GSL.SP.2006.268.01.05.

Bradley, D.C., Tucker, R.D., Lux, D.R., Harris, A.G., and McGregor, D.C., 2000, Migration of the Acadian Orogen and Foreland Basin across the northern Appalachians of Maine and adjacent areas: U.S. Geological Survey Professional Paper, v. 1624, p. 1- 49.

Carmichael, D.M., 1978, Metamorphic bathozones and bathograds; a measure of the depth of post-metamorphic uplift and erosion on the regional scale: American Journal of Science, v. 278, p. 769–797.

Cassidy, J.F., 1995, Receiver function studies in the southern Canadian Cordillera: Canadian Journal of Earth Sciences, v. 32, p. 1514–1519, doi:10.1139/e95-123.

Chapman, J.B., Ducea, M.N., DeCelles, P.G., and Profeta, L., 2015, Tracking changes in crustal thickness during orogenic evolution with Sr/Y: An example from the North American Cordillera: Geology, v. 43, p. 919–922, doi:10.1130/G36996.1.

Chapman, J.B., Greig, R., and Haxel, G.B., 2020, Geochemical evidence for an orogenic plateau in the southern U.S. and northern Mexican Cordillera during the Laramide orogeny: Geology, v. 48, p. 164–168, doi:10.1130/G47117.1.

Chen, W., 2017, Determination of crustal thickness under Tibet from gravity-gradient data: Journal of Asian Earth Sciences, v. 143, p. 315–325.

Chiaradia, M., 2015, Crustal thickness control on Sr/Y signatures of recent arc magmas: an Earth scale perspective: Science Reports, v. 5, doi:10.1038/srep08115.

Clark, M.K., and Royden, L.H., 2000, Topographic ooze: Building the eastern margin of Tibet by lower crustal flow: Geology, v. 28, p. 703–706, doi:10.1130/0091-7613(2000)28<703:TOBTEM>2.0.CO;2.

DePaolo, D.J., Harrison, T.M., Wielicki, M., Zhao, Z., Zhu, D.C., Zhang, H., and Mo, X., 2019, Geochemical evidence for thin syn-collision crust and major crustal thickening between 45 and 32 Ma at the southern margin of Tibet: Gondwana Research, v. 73, p. 123–135, doi:10.1016/j.gr.2019.03.011.

Dorais, M.J., 2003, The petrogenesis and emplacement of the New Hamshire plutonic suite: American Journal of Science, v. 303, p. 447.

Dorais, M.J., and Paige, M.L., 2000, Regional geochemical and isotopic variations of Northern New England plutons: Implications for magma sources and for Grenville and Avalon basement-terrane boundaries: Bulletin of the Geological Society of America, v. 112, p. 900–914, doi:10.1130/0016-7606(2000)112<900:RGAIVO>2.0.CO;2.

Dorais, M.J., Wintsch, R.P., Kunk, M.J., Aleinikoff, J., Burton, W., Underdown, C., and Kerwin, C.M., 2012, P-T-t conditions, Nd and Pb isotopic compositions and detrital zircon geochronology of the Massabesic Gneiss Complex, New Hampshire: Isotopic and metamorphic evidence for the identification of Gander basement, central New England: American Journal of Science, v. 312, p. 1049, doi:10.2475/10.2012.01.

Dorais, M.J., Wintsch, R.P., Nelson, W.R., and Tubrett, M., 2009, Insights into the Acadian orogeny, New England Appalachians: a provenance study of the Carrabassett and Kittery formations, Maine: Atlantic Geology, v. 45, p. 50, doi:10.4138/atlgeol.2009.002.

Ettensohn, F.R., Pashin, J.C., and Gilliam, W., 2019, The Appalachian and Black Warrior Basins: Foreland Basins in the Eastern United States, *in* Miall, A.D. ed., The Sedimentary Basins of the United States and Canada, p. 129–237, doi:10.1016/b978-0-444-63895-3.00004-8.

Farner, M.J., and Lee, C.T.A., 2017, Effects of crustal thickness on magmatic differentiation in subduction zone volcanism: A global study: Earth and Planetary Science Letters, doi:10.1016/j.epsl.2017.04.025.

Fu, B., Cliff, J., and Zartman, R.E., 2014, Zircon oxygen isotopic constraints from plutonic rocks on the magmatic and crustal evolution of the northern Appalachians in southern New England, USA: Canadian Journal of Earth Sciences, v. 51, p. 485–499.

Garzione, C.N. et al., 2017, Tectonic Evolution of the Central Andean Plateau and Implications for the Growth of Plateaus: Annual Review of Earth and Planetary Sciences, v. 45, p. 529–559, doi:10.1146/annurev-earth-063016-020612.

Gatewood, M.P., Dragovic, B., Stowell, H.H., Baxter, E.F., Hirsch, D.M., and Bloom, R., 2015, Evaluating chemical equilibrium in metamorphic rocks using major element and Sm–Nd isotopic age zoning in garnet, Townshend Dam, Vermont, USA: Chemical Geology, v. 401, p. 151–168, doi:10.1016/j.chemgeo.2015.02.017.

Hacker, B.R., Ratschbacher, L., Rutte, D., Stearns, M.A., Malz, N., Stübner, K., Kylander-Clark, A.R.C., Pfänder, J.A., and Everson, A., 2017, Building the Pamir-Tibet Plateau—Crustal stacking, extensional collapse, and lateral extrusion in the Pamir: 3. Thermobarometry and petrochronology of deep Asian crust: Tectonics, v. 36, p. 1743–1766, doi:10.1002/2017TC004488.

Harrison, T.M., Spear, F.S., and Heizler, M.T., 1989, Geochronologic studies in central New England II: post-Acadian hinged and differential uplift: Geology, v. 17, p. 185–189, doi:10.1130/0091-7613(1989)017<0185:GSICNE>2.3.CO;2.

Hibbard, J.P., van Staal, C.R., Rankin, D.W., and Williams, H., 2006, Lithotectonic map of the Appalachian Orogen, Canada-United States of America:, doi:10.4095/221912.

Hillenbrand, I., Williams, M.L., Li, C., and Gao, H., 2019, Rise and Fall of the Acadian Altiplano: Geological Society of America Abstracts with Programs, v. 51, doi:10.1130/abs/2019AM-340957.

Hu, F., Ducea, M.N., Liu, S., and Chapman, J.B., 2017, Quantifying Crustal Thickness in Continental Collisional Belts : Global Perspective and a Geologic Application: Scientific Reports, v. 7, p. 1–10, doi:10.1038/s41598-017-07849-7.

Karabinos, P., Macdonald, F.A., and Crowley, J.L., 2017, Bridging the gap between the foreland and hinterland I: Geochronology and plate tectonic geometry of Ordovician magmatism and terrane accretion on the Laurentian margin of New England: American Journal of Science, v. 317, p. 515–554, doi:10.2475/05.2017.01.

Kuiper, Y.D., 2016, Development of the Norumbega fault system in mid-Paleozoic New England, USA: An integrated subducted oceanic ridge model: Geology, v. 44, p. 455–458, doi:10.1130/G37599.1.

Lombardi, D., Braunmiller, J., Kissling, E., and Giardini, D., 2008, Moho depth and Poisson's ratio in the Western-Central Alps from receiver functions: Geophysical Journal International, v. 173, p. 249–264, doi:10.1111/j.1365-246X.2007.03706.x.

Ludman, A., Hopeck, J., and Berry Iv, H.N., 2017, Provenance and paleogeography of post-Middle Ordovician, pre-Devonian sedimentary basins on the Gander composite terrane, eastern and east-central Maine: implications for Silurian tectonics in the northern Appalachians: Atlantic Geology, v. 53, p. 63.

Mantle, G.W., and Collins, W.J., 2008, Quantifying crustal thickness variations in evolving orogens: Correlation between arc basalt composition and Moho depth: Geology, v. 36, p. 87–90, doi:10.1130/G24095A.1.

Massey, M.A., Moecher, D.P., Walker, T.B., O'Brien, T.M., and Rohrer, L.P., 2017, The role and extent of dextral transpression and lateral escape on the post-Acadian tectonic evolution of South-Central New England: American Journal of Science, v. 317, p. 34–94, doi:10.2475/01.2017.02.

Molnar, P., England, P., and Martinod, J., 1993, Mantle dynamics, uplift of the Tibetan Plateau, and the Indian Monsoon: Reviews of Geophysics, v. 31, p. 357–396, doi:10.1029/93RG02030.

Perrot, M., Tremblay, A., Ruffet, G., Labrousse, L., Gervais, F., and Caroir, F., 2020, Diachronic metamorphic and structural evolution of the Connecticut Valley–Gaspé trough, Northern Appalachians: Journal of Metamorphic Geology, v. 38, p. 3–27, doi:10.1111/jmg.12510.

Profeta, L., Ducea, M.N., Chapman, J.B., Paterson, S.R., Gonzales, S.M.H., Kirsch, M., Petrescu, L., and DeCelles, P.G., 2015, Quantifying crustal thickness over time in magmatic arcs: Scientific Reports, doi:10.1038/srep17786.

Pyle, J.M., Spear, F.S., Cheney, J.T., and Layne, G., 2005, Monazite ages in the Chesham Pond Nappe, SW New Hampshire, U.S.A.: Implications for assembly of central New England thrust sheets: American Mineralogist, v. 90, p. 592–606, doi:10.2138/am.2005.1341.

Robinson, P., 2003, Tectonic–stratigraphic–metamorphic perspective of the New England Caledonides, west-central Massachusetts: Guidebook for Field Trips in the Five College Region. 95th Annual Meeting of the New England Intercollegiate Geological Conference,.

Robinson, P., Tucker, R.D., Bradley, D., Berry IV, H.N., and Osberg, P.H., 1998, Paleozoic orogens in New England, USA: GFF, v. 120, p. 119–148, doi:10.1080/11035899801202119.

Roden-Tice, M.K., West Jr, D.P., Potter, J.K., Raymond, S.M., and Winch, J.L., 2009, Presence of a Long-Term Lithospheric Thermal Anomaly: Evidence from Apatite Fission-Track Analysis in Northern New England: The Journal of Geology, v. 117, p. 627–641, doi:10.1086/605995.

Ryan, J., Beck, S., Zandt, G., Wagner, L., Minaya, E., and Tavera, H., 2016, Central Andean crustal structure from receiver function analysis: Tectonophysics, v. 682, p. 120–133, doi:10.1016/j.tecto.2016.04.048.

Schoonmaker, A., Kidd, W.S.F., and Bradley, D.C., 2005, Foreland-forearc collisional granitoid and mafic magmatism caused by lower-plate lithospheric slab breakoff: The Acadian of Maine, and other orogens: Geology, v. 33, p. 961–964, doi:10.1130/G21832.1.

Scott, E.M., Allen, M.B., Macpherson, C.G., Saville, C., Ducea, M.N., Mccaffrey, K.J.W., and Davidson, J.P., 2018, Andean surface uplift constrained by radiogenic isotopes of arc lavas: Nature Communications, p. 1–8, doi:10.1038/s41467-018-03173-4.

Spear, F.S., 1993, Metamorphic phase equilibria and pressure-temperature-time paths: Mineralogical Society of America, 799 p.

van Staal, C.R., Whalen, J.B., Valverde-Vaquero, P., Zagorevski, A., and Rogers, N., 2009, Pre-Carboniferous, episodic accretion-related, orogenesis along the Laurentian margin of the northern Appalachians: Geological Society, London, Special Publications, v. 327, p. 271–316, doi:10.1144/SP327.13.

Ver Straeten, C.A., Over, D.J., and Baird, G.C., 2020, Arc-to-craton: Devonian air-fall tephras in the eastern United States (K. L. Avary, K. O. Hasson, & R. J. Diecchio, Eds.): The Appalachian Geology of John M. Dennison: Rocks, People, and a Few

Good Restaurants along the Way, p. 0, doi:10.1130/2020.2545(03).

Thompson, J.B.J., Robinson, P., and Trask, N.J., 1968, Nappes and gneiss domes in west-central New England, *in* Zen, E.-A., White, W.S., Hadley, J., and Thompson, J.J. eds., Studies of Appalachian geology: Northern and Maritime, New York, Interscience, p. 203–218.

Tucker, R.D., Osberg, P.H., and Iv, H.N.B., 2001, The Geology of a Part of Acadia and the Nature of the Acadian Orogeny Across Central and Eastern Maine: American Journal of Science, v. 301, p. 205–260, doi:10.2475/ajs.301.3.205.

West, D.P., Roden-Tice, M.K., Potter, J.K., and Barnard, N.Q., 2008, Assessing the role of orogen-parallel faulting in post-orogenic exhumation: low-temperature thermochronology across the Norumbega Fault System, Maine: Canadian Journal of Earth Sciences, v. 45, p. 287–301, doi:10.1139/E07-073.

Zen, E.A., 1991, Phanerozoic denudation history of the southern New England Appalachians deduced from pressure data: American Journal of Science, v. 291, p. 401–424, doi:10.2475/ajs.291.4.401.

CHAPTER 4

RISE AND FALL OF THE ACADIAN ALTIPLANO: EVIDENCE FOR A PALEOZOIC OROGENIC PLATEAU IN THE NEW ENGLAND APPALACHIANS

4.1 Abstract

High elevation orogenic plateaus are formed by a complex interplay of deep and surficial processes and influence a variety of Earth systems. However, limited exposures of plateau mid-crust are presently recognized, hindering understanding of these deeper processes. We present evidence for the existence of an orogenic plateau during and after the Devonian Acadian Orogeny whose mid-crustal roots are exposed in the New England Appalachians. The four-dimensional crustal evolution of this paleo-plateau is constrained by the integration of new petrologic and geochronologic databases with geophysical imaging. Doubly thickened crust, widespread amphibolite to granulite-facies metamorphic conditions, a paleo-isobaric surface, and protracted mid-crustal anatexis indicate the development of a high elevation, low relief plateau by 380 Ma. $^{40}Ar/^{39}Ar$ thermochronology shows a distinct thermochronologic signature with very slow cooling rates of 2-4°C/m.y. following peak metamorphic conditions. Thermochronologic data, trace element and Nd isotope geochemistry, and monazite petrochronology suggest a 50 m.y. lifespan of the plateau. Orogen parallel ductile flow and extrusion of gneiss domes resulted in plateau collapse, crustal thinning, and block-like exhumation at ca. 330-310 Ma. Thinning of the plateau crust may have led to the sharp 12-15 km step in Moho depth in western New England, possibly by reactivating the suture between Laurentia and

accreted Gondwanan-derived terranes. Formation of this orogenic plateau may have influenced genesis of Li-bearing pegmatites and paleoclimate.

3.2 Introduction

Orogenic plateaus are integral to many modern collisional orogens (e.g. the Tibetan Plateau, the Andean Altiplano-Puna plateau, and the Anatolian-Zagros plateau) and the mechanism(s), rates, and timing of uplift and collapse are critical data for models of collisional tectonics (Garzione et al., 2017; Kapp and DeCelles, 2019). The creation and destruction of orogenic plateaus affect global geodynamics (Hatzfeld and Molnar, 2010), climate (Raymo and Ruddiman, 1992), atmospheric circulation (Molnar et al., 1993), and the genesis of critical resource deposits (Bradley, 2019). Current models of plateau evolution are generally informed by studies of modern orogens, which provide a field-based record of predominantly upper crustal processes. Deeper geodynamic processes are inferred from numerical models, petrogenetic studies, and geophysical imaging. The recognition of paleo-plateaus and, especially, the deeper levels of paleo-plateaus, has been hindered by overprinting events, complex deformational histories, and the limitations of geochronologic techniques. Yet, a mid-crustal perspective on the processes, kinematics, and timescales of plateau evolution may be key for placing observations made in modern orogens into a broader context, testing the predictions of numerical models, and in building four dimensional models of plateau evolution.

Here, evidence is presented for the existence of an orogenic plateau during and after the Acadian Orogeny, ca. 380-330 Ma, the exhumed mid-crustal roots of which are exposed in the New England Appalachians. The extent of the region of homogeneous uplift and exhumation are defined by thermobarometric and thermochronologic data. We constrain the timing and nature of crustal thickening, mid-crustal residence, and orogenic collapse with the integration of structural fabrics and monazite petrochronology. These results are consistent with, and may help to explain, a wide variety of geologic observations from the history of the foreland basin to modern Moho structure and paleoclimate, while providing a four-dimensional perspective on plateau evolution.

3.2 Geologic Background

The tectonic elements of the Appalachian orogen record multiple phases of Paleozoic to Mesozoic tectonism (Fig 18). The Paleozoic record is dominated by episodic collision and accretion of terranes to the margin of Laurentia followed by a Meoszoic history of continental extension and the birth of the Atlantic Ocean.

Orogenesis began with the Ordovician Taconic orogeny (475-450 Ma), interpreted to represent closure of the Iapetus ocean due to collision between the Laurentian passive margin (basement massifs and cover rocks) and Ordovician island arc(s) built on the Gondwana-derived Moretown terrane (Karabinos et al., 2017). Taconic orogenesis is marked by the emplacement of thrust sheets and ophiolites onto the Laurentian margin, foreland basin sedimentation, and amphibolite facies metamorphism in western New England. The end of the Taconic orogeny has been interpreted to have involved a reversal in subduction polarity creating a west-dipping subduction zone under Laurentia (Karabinos et al., 2017) or subsequent accretion of the Gander terrane (van Staal et al., 2009).

The subsequent Silurian Salinic orogeny (430-422 Ma), in many recent models, involved accretion of the peri-Gondwanan Gander terrane to post-Taconic margin of Laurentia. Salinic orogenesis involved dominantly sinistral oblique convergence although deformational and metamorphic effects of Salinian tectonism have not been widely recognized in New England (van Staal et al., 2009). A thick succession of clastic rocks were deposited in deep marine basins of the Central Maine and Connecticut Troughs in the Silurian through the earliest Devonian (Fig. 1A), basins which closed in the Acadian orogeny (Robinson et al., 1998; van Staal et al., 2009).

The late Silurian to Carboniferous Acadian-Neoacadian orogeny (420 to 350 Ma) was the dominant tectonic event in the northern Appalachians, producing polyphase deformation and high-grade metamorphism (Robinson et al., 1998; van Staal et al., 2009). Presently, Acadian orogenesis in central New England is understood to be marked by the emplacement of east- and west-directed thrust nappes and sheet-like intrusions (Robinson et al., 1998). The Acadian deformational front has been shown to have propogated from the southeast to northwest in the Devonian (Robinson et al., 1998; van Staal et al., 2009), and has been attributed to collision between composite Laurentia and the peri-Gondwanan Avalon terrane. Prolonged deformation, metamorphism, and magmatism between 380 and 350 Ma are interpreted to be related to accretion of the Meguma terrane to Laurentia, designated by some workers as the Neoacadian orogeny (Robinson et al., 1998; van Staal et al., 2009). Regional metamorphic conditions reached the granulite facies and were accompanied by widespread intrusions. Regional fabrics and intrusive rocks were further overprinted by transpressional fabrics.

Recently, a phase of 350 to 300 Ma tectonism characterized by dextral transpression has been recognized in central New England (Massey et al., 2017). The earlier stages of this event apparently involved dextral kinematics and sub-horizontal stretching lineations. Later deformation involved the development of isoclinal folds, localization of high strain zones, and a component of vertical extrusion. Massey et al. (2017) suggested that the transpressional event may have been related to continued collision between Meguma and Laurentia. This protacted period of late Silurian to Carboniferous tectonism is referred to here as the Acadian orogeny (*sensu lato*) because of the apparent continuity of geochronologic dates and deformation at the mid-crustal level of exposure in the central and southern New England Appalachians.

The 300-260 Ma Alleghanian orogeny is interpreted to record collision of Gondwana with Laurentia and the final assembly of the supercontinent Pangea (Robinson et al., 1998). However its effects are restricted primarily to Rhode Island and southeastern Connecticut (Robinson et al., 1998). The Mesozoic breakup of Pangea led to continental extension, magmatism, and the development of thin-skinned normal faults with associated sedimentary basins (Roden-Tice et al., 2009).

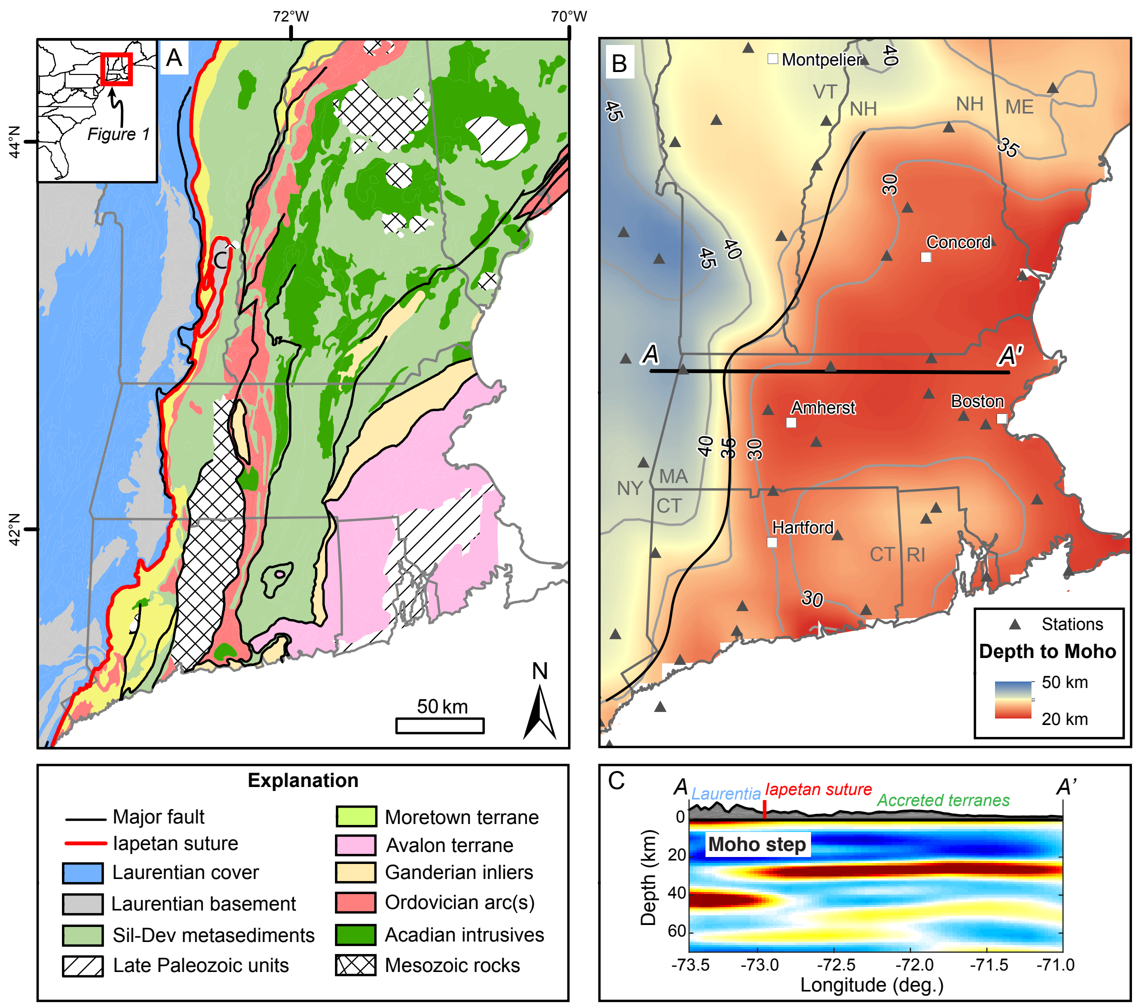

Figure 19: Tectonic map of the Appalachian Mountains (modified from Hibbard et al., 2006). Black lines indicate major faults. C: Chester Dome. Red lines mark the Iapetan Suture, interpreted to mark the boundary between tectonic elements of Laurentian and Gondwanan affinity (Karabinos et al., 2017). Inset: Location map of Figures 19A and 19B. B: Distribution of Moho depth (in kilometers) from Li et al. (2018). Triangles indicate stations used to constrain Moho depth in the teleseismic P-to-S receiver function study of Li et al. (2018). C: Cross section A-A' showing Moho depth and 12-15 km step. Note that apparent overlap in the Moho across the step is a processing artifact not suggested by receiver functions (Li et al., 2018).

4.3 Methods and Results

4.3.1 Database Compilation and Geospatial Analysis

A new geospatial database of geologic, petrologic, and thermochronologic data was compiled to investigate the 4D Paleozoic to Mesozoic crustal evolution of the New

England Appalachians (Chapter 2). Maps of petrologic and thermochronologic data were constructed by interpolating between data points using the Spline with Barriers tool (in ArcMap 10.6). Barriers were constructed to correct for offset along fault traces documented to have experienced brittle, post-orogenic displacement (Hibbard et al., 2006; Roden-Tice et al., 2009). This dataset was integrated with geophysical P-to-S receiver function results of Li et al. (2018) who recognized a sharp (12-15 km high) step in the Moho under western New England (Fig. 19B-C). Note that the geometry of the Moho step in cross section A-A' (Fig. 18C) is smoothed due to the limitation of lateral resolution in receiver function analysis.

3.3.2 Thermobarometry

Calculated metamorphic pressures (Fig. 20A) document a large region of consistent ca. 0.6 GPa (6 kbar) pressures across central New England. They are interpreted to represent amphibolite to granulite-facies Acadian conditions and the region has been referred to as the "central Massachusetts metamorphic high" (Robinson et al., 1998). The total area of ≥0.6 GPa metamorphism exceeds 20,000 km^2. The western boundary of the 0.6 GPa region roughly corresponds with the trace of the Moho step and Iapetan suture (Figs. 19, 20A), with lower grade (and older) conditions preserved farther west (Robinson et al., 1998; Zen, 1991). Locally, higher-P regions occur near the trace of the step (Fig. 19A), with pressures of 0.8 to ≥1 GPa reported from gneiss-cored domes and thrust slices (Karabinos et al., 2010; Keller and Ague, 2018).

3.3.3 Thermochronology

$^{40}Ar/^{39}Ar$ hornblende, muscovite, and biotite dates show distinct gradients near the trace of the Moho step (Figs. 19B, 20B-D). All three mineral systems yield dates that are on the order of 900 to 420 Ma west of the Moho step and can likely be attributed to cooling from the Grenvillian, Taconic, and/or Salinic orogenies. East of the step, hornblende dates are 380-340 Ma over an area corresponding to the 0.6 GPa "metamorphic high". Muscovite dates throughout the same area are 40 to 50 m.y. younger, between 340 and 300 Ma. Biotite dates show a similar spatial trend but dates are less consistent near the trend of the Moho step (Fig. 19D), probably due to a combination of excess ^{40}Ar, alteration, composition, variable diffusion radii, and/or analytical methods (e.g. Roberts et al., 2001). Within each mineral system, $^{40}Ar/^{39}Ar$ dates are consistent and show little variability across the 0.6 GPa domain.

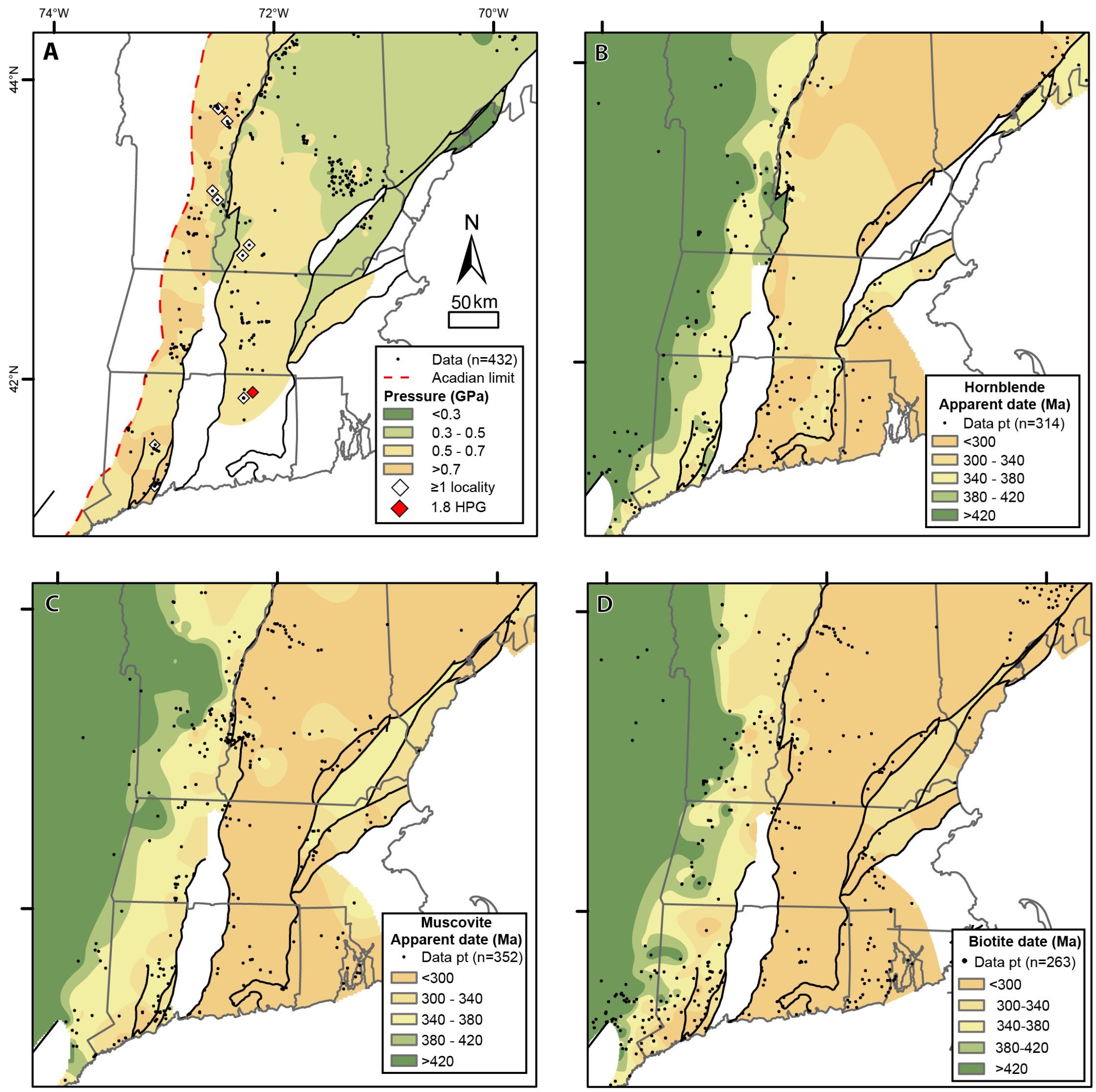

Figure 20: Maps of metamorphic pressure and high temperature thermochronologic dates. Metamorphic pressure during the Acadian orogeny (ca. 380 Ma) (A), hornblende dates (B), muscovite dates (C), and biotite dates (D). Dates are interpreted to represent regional cooling. Black circles mark individual data points. The limit of Acadian metamorphism modified from Robinson et al. (1998) and constrained to the region with hornblende dates between 420 and 310 Ma.

Low temperature thermochronometers show a different pattern of dates with little to no difference across trace of the Moho step (Fig 21). $^{40}Ar/^{39}Ar$ K-feldspar generally display upper intercept or total gas dates that are greater than 360 Ma west of the Green Mountains and 325-310 Ma across Vermont to New Hampshire (Fig. 21A). Dates are less than 250 Ma east of the New Hampshire-Vermont border along the eastern border fault of the Mesozoic Hartford Basin (Fig. 18A). Apatite fission track dates show no discernable gradient near or across the trace of the Moho step (Fig. 21B). A notable north-to-south gradient in fission track dates (80 Ma to 160 Ma) exists from central to southern New England. As in K-feldspar dates, there is an offset in apatite fission track dates along the trace of the eastern border fault. Thus, unlike higher-T thermochronometers, low-T thermochronometers are relatively unchanged across the trace of the Moho step and throughout the area of 0.6 GPa metamorphism.

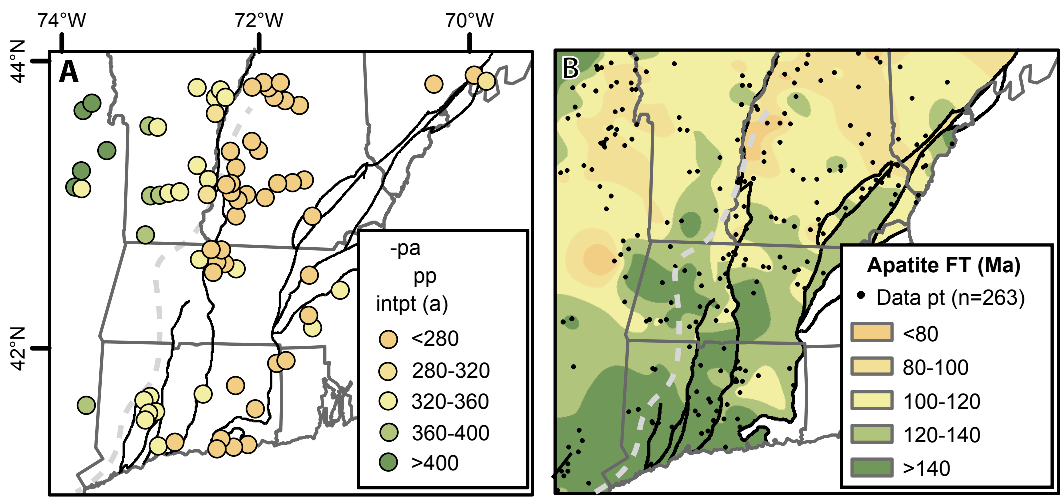

Figure 21: Distribution of low temperature thermochronologic dates. K-feldspar upper intercept and plateau dates are shown in A and apatite fission track dates in B. K-feldspar dates are represented by 40 Ma bins as data coverage is insufficient for contour mapping. Black circles mark individual data points on B. Details of individual data points are available in the supplement. Dashed gray line represents approximate location of Moho step.

3.4 Discussion

Petrologic and thermochronologic data presented here are consistent with observations from extant and ancient orogenic plateaus and also with the results of numeral modeling studies. In the following paragraphs, I integrate new and existing data and evaluate the evidence for the development of an orogenic plateau (the Acadian altiplano) and for the persistence of this plateau for at least 50 m.y. As discussed below, the recognition of this structure has important implications for Appalachian crustal evolution, foreland basin evolution, Li-bearing pegmatite genesis, and paleoclimate.

Modern orogenic plateaus are characterized by high elevation, thickened crust, and broad regions of low topographic relief (Garzione et al., 2017; Laske et al., 2013; Molnar et al., 1993). A broad zone of ~0.6 GPa metamorphic pressure characterizes much of central and western New England (Fig. 19A). This suggests that rocks at the modern erosional surface were buried by at least 20-30 km of overburden. The regionally sub-horizontal nature of the 0.6 GPa isobar combined with the consistent and homogeneous cooling ages across the same large region suggests that the region was buried by a similar amount of overburden and exhumed homogenously. A first order estimate of minimum syn-orogenic crustal thickness of 50-60 km can be derived from combining the burial depth with the ~30 km modern crustal column (Li et al., 2018). Keller and Ague (2018) suggested that Acadian crustal thickness may have been as high as 60-70 km based on thermobarometric analysis of lower crustal granulites from north-central Connecticut (Fig. 20A, 22A).

Estimates of crustal thickness are further supported by the geochemistry of syn-Acadian igneous rocks. Recent studies have shown a correlation between crustal thickness and the trace element and isotope geochemistry of Phanerozoic convergent margin magmas (e.g. Chapman et al., 2015; DePaolo et al., 2019), and that this relationship that can be applied to estimate paleo-crustal thickness. Chapter 3 of thesis applied recent trace element (Sr/Y; La/Yb) and thermoisotopic (Nd) crustal thickness calibrations to estimate the temporal and spatial evolution of crustal thickness in the northern Appalachians. Results from each of these proxies are consistent with each other and indicate crustal thicknesses of 55-70 km in the ~0.6 GPa region by 380 Ma (Fig. 22A). Further, these results suggest that crustal thicknesses of this magnitude were sustained for at least 30 m.y. (Fig. 22A). The consistency between petrologic and geochemical proxies provide compelling evidence for syn-Acadian crustal thicknesses akin to those of modern and ancient orogenic plateaus (55 to 70 km; Chapman et al., 2020; DePaolo et al., 2019; Laske et al., 2013; Rivers, 2012) and on the order of twice the modern global average of ~35 km (Laske et al., 2013). Similarly, paleo-elevation estimates derived from Airy isostacy of 2.5 to 5 km (Fig. 16; chapter 3 of this theis) are similar to estimates for modern and ancient orogenic plateaus (2.5 to 5 km; Chapman et al., 2020; Ernst, 2010; Garzione et al., 2017). While paleoelevation studies have not been carried out in the northern Appalachians due to the deep level of exposure, sedimentological evidence from the foreland basin for alpine glaciation at subtropical latitudes indicate significant (at least several km) of elevation in the Acadian hinterland (Ettensohn et al., 2019).

Numerical models suggest that rheological weakening caused by a hot, weak, low viscosity mid-crust is responsible for the signature low topographic relief of orogenic plateaus (e.g. Jamieson et al., 2004). Thermal-mechanical experiments designed to model orogenic plateaus predict mid-crustal amphibolite to granulite facies metamorphic conditions at temperatures of 600 to 800°C, accompanied by widespread partial melting (e.g. Jamieson et al., 2004). Mid-crustal exposures in New England record regional amphibolite to granulite facies conditions at temperatures of 600 to 825°C (e.g. Robinson et al., 1998; Thomson, 2001; Tracy and Dietsch, 1982; Supplementary material). These rocks also record widespread and prolonged anatexis (e.g. Massey et al., 2017; Robinson et al., 1998; Thomson, 2001). Compilation of U-Pb dates from anatectic rocks show a continuum of dates between 380 and 330 Ma, with a broad peak between 380 and 350 Ma (Fig. 22B). The wide range of these dates and lack of systematic distribution suggests that the mid-crust of central New England was hot with low viscosity. This hot, at least episodically partially molten, crust was likely too weak to support significant topographic relief favoring the existence of a low relief plateau, in accord with the consistent 0.6 GPa pressures across the large region.

Quantitative models of plateaus predict metamorphic temperatures of in excess of 900°C in the lower crust (Jamieson et al., 2004). Likewise, ultra-high temperature (>1000°C) metamorphic conditions have been observed in xenoliths from the Tibetan plateau (reviewed in Kapp and DeCelles, 2019). Rocks recording similar conditions have been reported in this region of the New England Appalachians. Disaggregated blocks and xenoliths of granulite facies gneiss locally record ultra-high temperature conditions in excess of 1000°C at pressures of 1 to 1.8 GPa (Ague et al., 2013; Keller and Ague, 2018). While precise timing of extreme metamorphic conditions and the emplacement history of these rocks remains poorly constrained, they provide evidence of a hot Acadian lower crust.

Thermochronologic data show that the central New England region of ≥0.6 GPa pressures cooled slowly and homogeneously after the peak of Acadian activity. The systematic trends of $^{40}Ar/^{39}Ar$ dates and lack of sharp differences between plutonic and metamorphic rocks indicate that they probably represent the ages of regional cooling. The lack of sharp gradients in $^{40}Ar/^{39}Ar$ hornblende, muscovite, and biotite dates, cooling rates, and thermobarometric conditions throughout central New England support the inference that the region was exhumed as a block. Slow cooling, at integrated rates of 2-4°C/m.y., is shown by the 40 to 50 m.y. lag between the time of the closure of Ar diffusion in hornblende (500 ± 50°C, Harrison, 1982) and muscovite (400 ± 50°C; Harrison et al., 2009) A maximum cooling rate of 5°C/m.y. is constrained by geospeedometry (Tracy and Dietsch, 1982). A wide range of petrologic studies have suggested a nearly isobaric P-T path for central New England including evidence from conventional thermobarometry of retrograde shear zones, fluid inclusions, and petrogenetic grid analysis (Robinson et al., 1998; Thomson, 2001; Tracy and Dietsch, 1982).

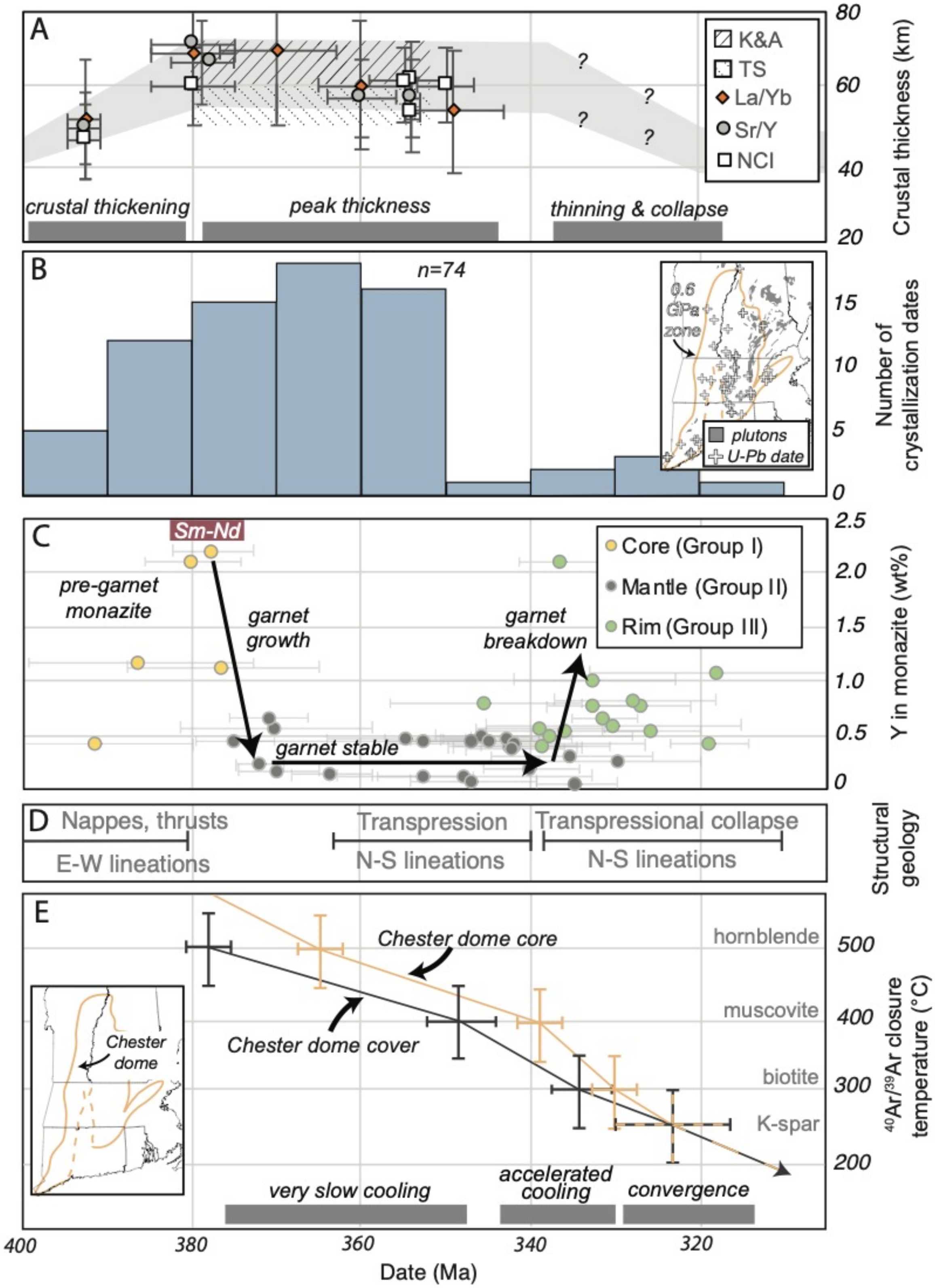

A
K&A
TS
La/Yb
Sr/Y
NCI
crustal thickening
peak thickness
thinning & collapse
Crustal thickness (km)
80
60
40
20
B
n=74
0.6 GPa zone
plutons
U-Pb date
Number of crystallization dates
15
10
5
0
C
Sm-Nd
pre-garnet monazite
garnet growth
garnet stable
garnet breakdown
Core (Group I)
Mantle (Group II)
Rim (Group III)
Y in monazite (wt%)
2.5
2.0
1.5
1.0
0.5
0
D
Nappes, thrusts
E-W lineations
Transpression
N-S lineations
Transpressional collapse
N-S lineations
Structural geology
E
Chester dome
Chester dome core
Chester dome cover
hornblende
muscovite
biotite
K-spar
very slow cooling
accelerated cooling
convergence
$^{40}Ar/^{39}Ar$ closure temperature (°C)
500
400
300
200
400
380
360
340
320
Date (Ma)

Figure 22: Synthesis of petrologic, geochemical, geochronologic, and structural data A: Crustal thickness estimates from Keller and Ague (2018) (KA; solid lines), the integration of thermobarometers with modern crustal thickness (TS; stippled lines) and geochemical crustal thickness estimates (La/Yb, Sr/Y, and NCI (Neodymium crustal index; DePaolo et al., 2019) thermoisotopic proxies) from Hillenbrand (2020). Gray region indicates the interpreted crustal thickness evolution. B) Histogram of the compiled U-Pb dates of monazite and zircon interpreted to record the time of igneous crystallization shown as 10 m.y. bins. Inset: Distribution of Middle Devonian to early Carboniferous plutonic rocks in New England (gray) modified from Hibbard et al. (2006) with localities used in compilation shown as crosses. Outline indicates region of ~0.6 GPa pressure. C: Yttrium content in monazite vs. date of core, mantle, and rims domains from representative samples from central Massachusetts. Samples used in the compilation are EB14-002, 9-1-L, 219-3-L, P14-005A-5B of McCulla (2016) and CBSZ-104-L of Massey et al. (2017b). These samples show consistent trends with a decrease in Y ca 380 Ma, low values of less than 0.5 wt% Y between 380 and 330 Ma, and an increase in Y after ~330 Ma. The decrease in Y corresponds with Sm-Nd garnet dates reported by Gatewood et al. (2015) and Sullivan (2014) and are indicated by the red box. D: Temporal evolution of regional structural geology and rock fabrics compiled from Robinson et al. (1998) and Massey et al. (2017). E: Cooling curves of $^{40}Ar/^{39}Ar$ dates from the core and cover rocks of the Chester Dome. Temperature-time paths are distinct until they converge at ca. 325 Ma and subsequently experience the same cooling history. Note increase in cooling rate ca. 340-330 Ma.

Monazite geochemistry and geochronology provide an additional record of metamorphic and structural evolution. Monazite compositional domains can be linked with silicate reactions and deformation fabrics to place constraints on the P-T history (Williams et al., 2017). In particular, the Yttrium content in monazite can be linked to reactions involving garnet, a key metamorphic index mineral, especially if other Y-bearing phases are absent. Y in monazite from central New England is systematically zoned and can be categorized into three compositional groups (Massey et al., 2017; McCulla, 2016).

Group-1 domains typically define the cores of zoned monazite grains. They are characterized by high Y content and yield 400-380 Ma dates (Fig. 22C). These domains are interpreted to predate significant garnet growth. Because Y is strongly partitioned into garnet, garnet is typically associated with low-Y monazite (Williams et al., 2017). The high Y Group-1 domains are temporally linked with fabrics related to early Acadian orogenesis involving west-directed folding, thrust faulting, and nappe emplacement (Fig. 4D; Robinson et al., 1998).

Group II domains (380-330 Ma) typically mantle group I cores. They are characterized by distinctly lower Y than Group-I domains, suggesting monazite growth in the presence of garnet. The decrease in Y in monazite is consistent with ca. 380 Ma Sm-Nd dates of garnet cores (Fig. 22C), interpreted to represent garnet growth during prograde metamorphism and crustal thickening (Gatewood et al., 2015; Sullivan, 2014). This interpretation is supported by geochemical evidence for crustal thickening between 400 and 380 Ma (Fig 22A; chapter 3 of this thesis). Low-Y monazite continued to grow until 330 Ma suggesting that garnet was stable in these rocks for as much as 50 m.y. This is also consistent with geochemical evidence of thickened crust for at least 30 m.y. (Fig 4A). Massey et al. (2017) linked Group II monazite domains to dextral transpressive fabrics and interpreted the continuous range of ages to indicate protracted deformation at mid-crustal conditions (Fig. 22D).

Group-III, Y-enriched domains form thin rims around group II mantles and yield 330-310 Ma dates (Massey et al., 2017; McCulla, 2016). We interpret this group to record the breakdown of garnet releasing Y during decompression or cooling (Fig. 22C). The microstructural setting and composition of group III monazite also constrain the timing of development of the strong, shallowly plunging N-S lineations (Massey et al., 2017). These fabrics are reflective of orogen parallel mid-crustal flow and a component of vertical thinning which characterize Acadian orogenic collapse (Fig. 4D; Massey et al., 2017).

Together, monazite geochemistry and geochronology and Sm-Nd garnet dates suggest that garnet may have been stable in these rocks for upwards of 50 m.y (ca. 380 Ma – ca. 330 Ma). This Y-monazite-garnet relationship has been observed in other terranes which have experienced prolonged residence in the mid- to deep crust of paleo-plateaus (e.g. Williams et al., 2019). The time of low-Y monazite (i.e. garnet stability at 0.6 GPa) is interpreted to correspond with thickened crust and the duration of the orogenic plateau (Fig. 22C). This interpretation is further substantiated by geochemical evidence from igneous rocks which suggest the existence of 55-70 km thick crust between at least 380 and 350 Ma (Fig. 22A; chapter 3 of this thesis). Further, as the stability of garnet is largely pressure dependent, 330-310 Ma monazite rims provide a constraint on the timing of exhumation, and thus orogenic collapse, in isobarically cooled rocks (Fig. 22C-D). These observations are in agreement with geologic and geophysical observations from both modern and ancient orogenic plateaus and accordant with the predictions of numerical models (DeCelles, 2004; Garzione et al., 2017; Jamieson et al., 2004; Kapp and DeCelles, 2019). This hypothesized paleo-plateau likely existed for 50 m.y. or more (380 to 330 Ma) based on petrologic evidence, $^{40}Ar/^{39}Ar$ thermochronology, the prolonged stability of garnet, and the dates and composition of igneous rocks.

Sustaining a thickened, partially molten crust likely requires continued compressional stress. Structural and geochronologic studies in central New England have shown protracted shortening and transpression through the Devonian and Carboniferous (Massey et al., 2017; Robinson et al., 1998). I envision that this was produced by protracted collisional orogenesis during accretion of the Avalon and/or Meguma terranes to composite Laurentia (Massey et al., 2017; Robinson et al., 1998; van Staal et al., 2009).

Orogen-parallel extension and north-south domal extrusion juxtapose high-P (0.8 to ≥1 GPa) cores of gneiss domes with 0.6 GPa cover rocks (Karabinos et al., 2010; Massey et al., 2017; Thompson et al., 1968). Thermochronologic evidence from the Chester Dome of western Vermont (C on Figure 19A) constrains the timing of juxtaposition of high-P rocks of the dome core against 0.6 GPa cover rocks. Pre-325 Ma cooling ages from the core of the dome are consistently younger than those of the cover rocks implying the core rocks were hotter and more deeply buried (Fig. 4E). However, thermochronometric dates of 325 Ma and younger are identical from core and cover rocks (Fig. 22E). This suggests that they were in thermal equilibrium and at the same structural level by ~325 Ma. Corollary evidence for exhumation of the core Chester Dome at this time comes from 340-310 Ma xenotime halos around garnet (Gatewood et al., 2015). These halos are interpreted to have formed during garnet-consuming reactions during decompression (Williams et al., 2017), i.e. during Carboniferous orogenic collapse. The structural and kinematic similarities between the Chester Dome and other New England gneiss domes (Karabinos et al., 2010) and their compatibility with 330-310 Ma fabrics in central New England (Massey et al., 2017), suggest that constraints may be broadly applicable to many of the core-complex like domal structures.

Rivers (2012) proposed that plateau collapse may produce a characteristic thermochronologic signature due to the juxtaposition of regions of colder, upper crust with hotter, deeper crust. The signature was interpreted in the Grenville province where low-grade upper crustal blocks preserving $^{40}Ar/^{39}Ar$ hornblende apparent dates that predate metamorphism in the Ottawan orogeny (ca. 1080 Ma) are juxtaposed against middle crustal blocks yielding post-Ottawan dates (Rivers, 2012). Fig. 20B shows a 200 km, N-S trending belt from northern Massachusetts to eastern Vermont of rocks with anomalously old, pre-Acadian $^{40}Ar/^{39}Ar$ hornblende apparent dates. In this belt Ordovician to Silurian dates are preserved in rocks that are commonly thought to have undergone Acadian (Devonian) metamorphism. A possible explanation is that they represent a block of Acadian upper crust that was down dropped during the phase of collapse. Ar release spectra from in this belt are complex and suggestive or one or more trapped Ar components (Spear and Harrison, 1989). Similar Ar release spectra are observed in $^{40}Ar/^{39}Ar$ hornblende dates of the Ottawan orogenic lid which also preserves anomalously old dates relative to the orogen (Rivers, 2012). Rivers (2012) attributed this to incomplete diffusion of radiogenic Ar as the cool orogenic lid came into contact with hot mid-crust during collapse of the Ottawan orogenic plateau.

Collapse of overthickened crust in New England apparently occurred with continued compressional tectonic stress (Massey et al., 2017). We suggest that collapse may have initiated as convergence rates decreased between composite Laurentia and accreting terranes or as a result of plate reorganization due to the changing stress field associated with approach of Gondwana (Robinson et al., 1998). Kuiper (2016) proposed that subduction of an oceanic ridge and associated transform fault and development of a Mendocino-style triple junction could explain concurrent patterns of collisional and strike slip tectonics in the New England Appalachians. Southwestward propagation of strike-slip motion and associated changes in plate motion in this model could have decreased stress that sustained the plateau and led to the initiation of orogenic collapse. A model in which collapse of the Acadian altiplano is related to this change in subduction style is reminiscent of hypotheses for collapse of the Nevadaplano in the western U.S.A. (Ernst, 2009).

The widespread occurrence of 0.6 GPa pressures at the present ground surface indicates that, since the mid-late Paleozoic, approximately 20 to 30 km have been stripped from the crust in central New England versus 3-7 km in eastern New York (Fig. 20A; Zen, 1991). Intriguingly, this apparent ~15 to 25 km difference in the current erosional surface is similar to the magnitude of offset of the Moho step (Fig. 19B-C; Li et al., 2019). I suggest that thinning of the overthickened crust of the orogenic plateau was associated with the development of the Moho step and the dramatic differences in Moho depth beneath these two domains. I suspect that the location and initiation of the Moho step is related to accretionary tectonics (i.e. Gondwanan terranes against Laurentia), but that it reached its present state during collapse of the Acadian altiplano.

Low temperature thermochronology place a lower bound on the timing of plateau collapse and exhumation and also on the establishment of the Moho step. The absence of an east to west gradient across the Moho step in K-feldspar and apatite fission track dates (Fig. 21) contrasts strongly with the large offset recorded by high temperature thermochronometers (Fig. 20B-D). The lack of a discontinuity suggests that rocks on either side of the Moho step were juxtaposed by the time of cooling through the closure temperature of the K-feldspar and apatite fission systems. Cooling histories compiled for rocks to the east and west of the Moho step converge between ca. 300 and 280 Ma (Fig. 23). This indicates that rocks east and west of the step were juxtaposed, and the Moho step existed, by at least this time. Thus, the Moho step is unrelated to Mesozoic continental extension or younger processes. A break in apatite fission track and K-feldspar dates is observed 40-60 km east of the step along the Hartford Basin border fault (Fig. 21B; Roden-Tice et al., 2009). This discontinuity in dates is well explained in thermal models by 1-2 km of vertical fault offset (Haugerud, 1990), an inference supported by geologic observations (Thompson et al., 1968). The relatively minimal amount of offset and listric nature of the border fault are inconsistent with the steepness and magnitude of the Moho step (Thompson et al., 1968). Further, detrital apatite (U-Th)/He dates suggest that New England has likely experienced relatively uniform Mesozoic to present exhumation and that terrane boundaries have not been significantly reactivated (McKeon, 2012).

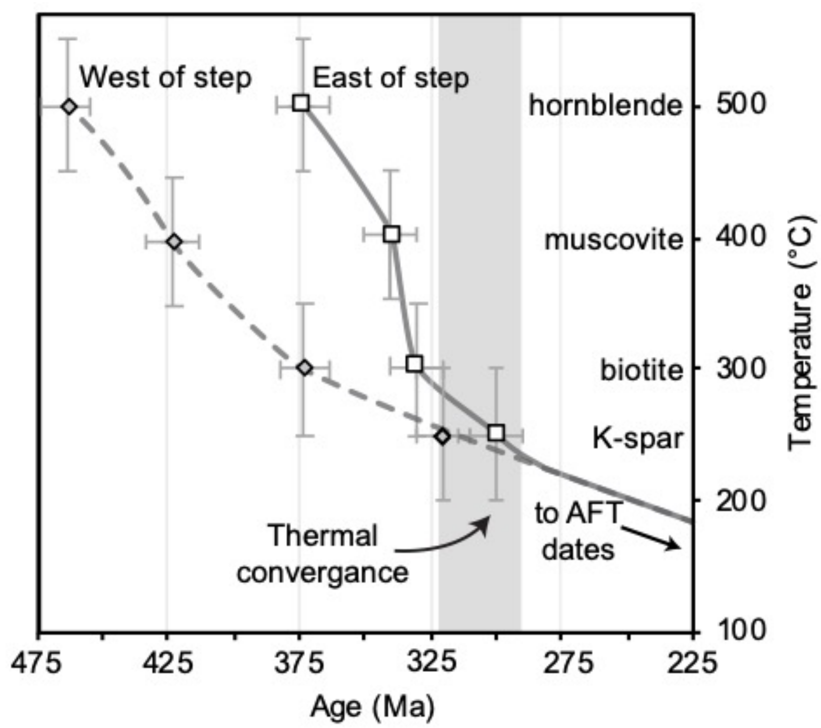

Figure 23: Compiled representative thermal histories for regions east and west of the Moho step. Note convergence between paths ca. 320-290 Ma.

One additional constraint on the crustal evolution may come from Triassic to Cretaceous magmatic rocks that are exhumed to relatively shallow levels (2-5 km) across New England and adjacent New York state (Zen, 1991). The uniform level of exposure, despite the wide spatial distribution of these rocks, may be evidence that the major crustal offset occurred prior to this magmatic episode.

Age constraints presented here indicate that the steep Moho step (Li et al., 2018) has been preserved for at least 300 m.y. Thermobarometric and thermochronologic discontinuities, and the Moho step, all follow the trend of the Iapetan suture between Laurentian- and Gondwanan-derived tectonic elements (Figs. 18, 19; Karabinos et al., 2017), suggesting that the suture may have been reactivated in forming the Moho step. The steepness of the step may reflect progressive steepening of an initially shallow tectonic boundary or the reactivation of a pre-existing steep boundary (e.g. Klepeis et al., 2019). Lithospheric differences may have played a role in development of the Moho step, as a function of the contrast between more rigid Laurentian lithosphere and the more juvenile lithosphere of the accreted terranes (Li et al., 2018). Towards the north, the dip of the Moho step decreases, but continues to correspond to the 0.6 GPa terrane boundary and gradient in Acadian cooling ages (Fig. 19). Notably the pressure gradient is also more gradual than in western New England.

These results and interpretations are summarized in Figure 24. Crustal thickening involving east-west shortening, divergent nappe emplacement, and magmatic additions occurred between ca. 400 and 380 Ma (Fig. 24A). Crustal thickening resulted in the formation of a high elevation, low relief orogenic plateau due to a hot and rheologically weak mid-crust (Fig. 24B). Continued convergence of terranes with composite Laurentia sustained the plateau for ca. 50 m.y. until collapse began ca. 330 Ma. Plateau collapse was orogen parallel, involving the formation of core complex-like gneiss domes and development of the steep Moho step (Fig. 24C).

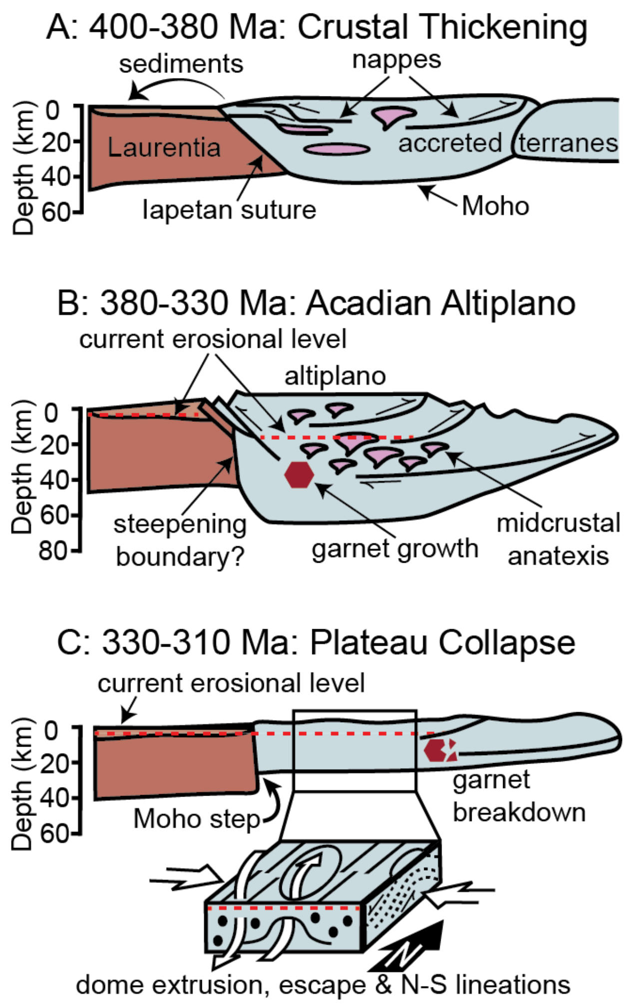

Figure 24: Simplified model for the tectonic evolution of the Acadian Orogeny and the Acadian altiplano at approximately the latitude of section A-A' in Figure 1B. Horizontal distances and garnet are not to scale. A: Early Acadian (400-380 Ma) crustal thickening involving east-west shortening, divergent nappe emplacement, and magmatic additions. B: Establishment of the Acadian altiplano ca. 380 Ma from continued thickening. Dashed red line represents the modern erosional surface. C: Collapse of the plateau, ca. 330-310 Ma. The crust of the altiplano is significantly thinned relative to Laurentian crust forming the Moho step, perhaps by reactivation of the suture between Laurentian and Gondwanan tectonic elements. Inset: Kinematic model of plateau collapse involving the northward extrusion of gneiss domes and orogen parallel escape (adapted from Karabinos et al., 2010; and Massey et al., 2017).

3.5 Implications

The Acadian altiplano in central and southern New England apparently existed for up to 50 m.y. or more (i.e. from ~380 to ~330 Ma). This duration is within the range interpreted for the Tibetan plateau (Kapp and DeCelles, 2019) and for several proposed paleo-pleateus (Chapman et al., 2020, 2015; Rivers, 2012; Williams et al., 2019). The long duration suggests a balance of forces involving tectonic convergence, ductile (gravitational) flow, and erosion. The balance was apparently disrupted at ca. 330 Ma when N-S ductile flow and erosion led to crustal thinning and exhumation. The lifespan of the plateau places constraints on tectonic models by requiring sustained plate convergence during and after the Acadian orogeny.

A suite of lithium-cesium-tantalum (LCT) pegmatites, dated to 370-325 Ma (Bradley et al., 2016), lie along the edge of the proposed plateau and the trace of the Moho step, suggesting a relationship to the altiplano. LCT pegmatites are interpreted to be the product of plate convergence and paleoclimate, commonly occurring in orogenic belts with salars perched along the orogenic axis, as deeply circulating brines interact with magma (Bradley, 2019). The uplift of orogenic plateaus have strong orographic effects (Ernst, 2010; Molnar et al., 1993) which potentially facilitate enrichment of Li in brines (Bradley, 2019). This is potentially applicable to the Acadian Altiplano hypothesis, where arid conditions are indicated by nearby concurrent deposition of climate-sensitive redbeds and paleobotanic evidence (Ettensohn et al., 2019). The current erosion level may provide insight into deeper processes ongoing today in the Li-rich districts such as the modern Andean salars and, specifically, into the primary (igneous?) source(s) of Li to the surficial brines.

Crustal thickening of the Acadian hinterland led to the development of the large Catskill foreland basin (Ettensohn et al., 2019). Black shales, including the economically significant Marcellus shale, were deposited ca. 390-380 Ma and reflect rapid subsidence in response to hinterland loading (Ettensohn et al., 2019). Isopach maps of these units, and the sedimentary wedge in general, are thickest adjacent to southern New England and to the region of thickened crust of the hypothesized plateau (Ettensohn et al., 2019; Oliver et al., 1967). The Catskill sedimentary sequence in New York preserves rocks of at least Middle Devonian age and has been suggested to have received sediment until ca. 310 Ma (Heizler and Harrison, 1998). This is consistent with basin subsidence related to Acadian loading and basin exhumation as a result of collapse. It is noted that significant Alleghanian loading in southeastern New England was likely not achieved until ca. 300 Ma or later (Robinson et al., 1998).

A currently unexplained aspect of the Catskill basin is the lack of Gondwanan-derived Neoproterozoic detrital zircon, common in the Acadian hinterland, and the dominance of Mesoproterozic, Grenville-sourced zircon (Fig. 25; Thomas et al., 2020). The orogenic plateau model may help to explain this conundrum. Orographic effects localize erosion to the edges of plateaus while simultaneously decreasing erosion from the plateau interior (Ernst, 2010). Gondwanan-derived detrital zircon is first noted in midcontinent basins at approximately the time of collapse of the plateau (Fig. 25A; Thomas et al., 2020), perhaps due to increased erosion rates and/or drainage reorganization.

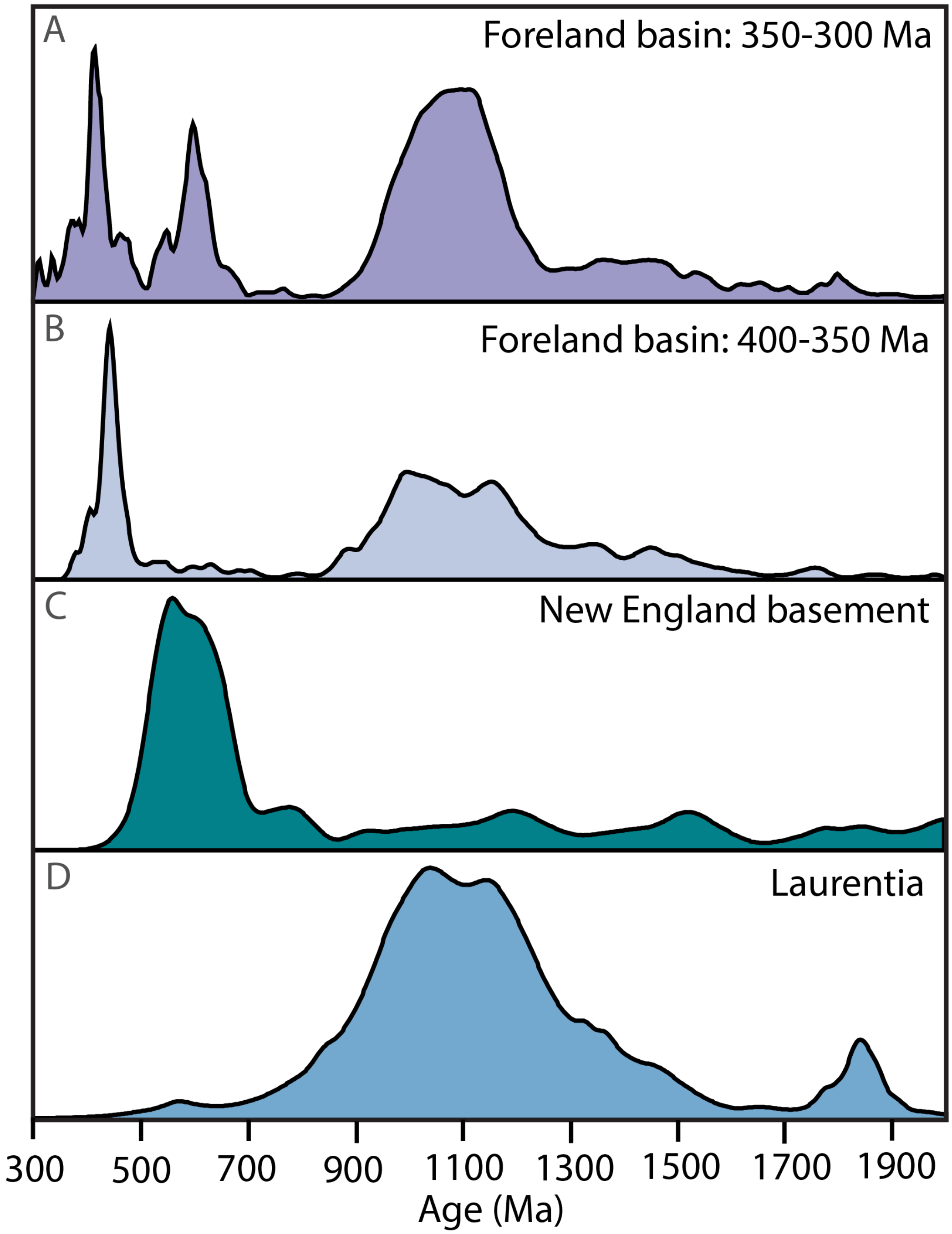

Figure 25: Detrital zircon signatures of sedimentary basins and basement terranes. Appalachian foreland basins after (A) and during (B) the hypothesized plateau, compiled from Thomas et al. (2020), compared with signatures of Gondwanan-derived New England basement and Laurentia (compiled from Karabinos et al. 2017 and references within). Note missing 500 to 700 Ma peak in 400-350 Ma foreland basins sediments.

Numerous studies have noted connections and implications of orogenesis for global carbon flux and climate on million year time scales (e.g. Macdonald et al., 2019). Orogens can serve as a source of carbon, from volcanic degassing or degassing of carbonate-bearing rocks during metamorphism, or as a sink during silicate weathering or carbon burial. Stewart and Ague (2018) calculated a total flux of $0.5*10^{18}$ to $1.7*10^{18}$ mol CO_2 Myr^{-1} for prograde metamorphism of the Acadian orogeny. These values are on the other of those which can drive global climate change and consistent with global temperature increases in the early Devonian (Stewart and Ague, 2018). However, the mid and late Devonian are characterized by a decrease in global temperature (Macdonald et al., 2019). It has been noted that the uplift of Cenozoic orogenic plateaus drove cooling through chemical weathering processes (Raymo and Ruddiman, 1992). Paleogeographic models place the Acadian orogeny in the subtropics (Bradley, 2019) where carbon sequestration via chemical weathering is relatively enhanced (Macdonald et al., 2019). Speculatively, enhanced silicate weathering of the Acadian altiplano may have contributed to late Devonian global cooling and biotic instability.

4.6 Conclusions

Petrologic, geochronologic, and geologic data from central New England are consistent with the signature of an exhumed orogenic plateau. I propose that the crust of the Acadian Altiplano was thickened to 55 to 70 km by 380 Ma and remained so through continued plate convergence for ca. 50 m.y. until it underwent orogen-parallel collapse ca. 330-310 Ma. This model is consistent with geologic observations and may help to explain enigmatic features of the foreland basin, regional Moho structure, and paleoclimate, while perhaps providing a window into the deeper processes of orogenic plateaus including partial melting, plutonism, ductile extension, and Li mineralization.

4.7 References Cited

Ague, J.J., Eckert, J.O., Chu, X., Baxter, E.F., Chamberlain, C.P., 2013. Discovery of ultrahigh-temperature metamorphism in the Acadian orogen, Connecticut, USA. Geology. https://doi.org/10.1130/G33752.1

Bradley, D., Shea, E., Buchwaldt, R., Bowring, S., Benowitz, J., O'Sullivan, P., McCauley, A., 2016. Geochronology and Tectonic Context of Lithium-cesium-tantalum Pegmatites in the Appalachians. Can. Mineral. 54, 945–969. https://doi.org/10.3749/canmin.1600035

Bradley, D.C., 2019. Tectonic and Paleoclimatic Controls of Lithium-cesium-tantalum (LCT) Pegmatite Genesis, Exhumation, and Preservation in the Appalachians. Can. Mineral. 57, 715–717. https://doi.org/10.3749/canmin.ab00002

Chapman, J.B., Ducea, M.N., DeCelles, P.G., Profeta, L., 2015. Tracking changes in crustal thickness during orogenic evolution with Sr/Y: An example from the North American Cordillera. Geology 43, 919–922. https://doi.org/10.1130/G36996.1

Chapman, J.B., Greig, R., Haxel, G.B., 2020. Geochemical evidence for an orogenic plateau in the southern U.S. and northern Mexican Cordillera during the Laramide orogeny. Geology 48, 164–168. https://doi.org/10.1130/G47117.1

DeCelles, P.G., 2004. Late Jurassic to Eocene evolution of the Cordilleran thrust belt and foreland basin system, western U.S.A. Am. J. Sci. 304, 105–168. https://doi.org/10.2475/ajs.304.2.105

DePaolo, D.J., Harrison, T.M., Wielicki, M., Zhao, Z., Zhu, D.C., Zhang, H., Mo, X., 2019. Geochemical evidence for thin syn-collision crust and major crustal thickening between 45 and 32 Ma at the southern margin of Tibet. Gondwana Res. 73, 123–135. https://doi.org/10.1016/j.gr.2019.03.011

Ernst, W.G., 2010. Young convergent-margin orogens, climate, and crustal thickness-A Late Cretaceous-Paleogene Nevadaplano in the American Southwest? Lithosphere 2, 67–75. https://doi.org/10.1130/L84.1

Ernst, W.G., 2009. Rise and fall of the Nevadaplano. Int. Geol. Rev. 51, 583–588. https://doi.org/10.1080/00206810903063315

Ettensohn, F.R., Pashin, J.C., Gilliam, W., 2019. The Appalachian and Black Warrior Basins: Foreland Basins in the Eastern United States, in: Miall, A.D. (Ed.), The Sedimentary Basins of the United States and Canada. pp. 129–237. https://doi.org/10.1016/b978-0-444-63895-3.00004-8

Garzione, C.N., McQuarrie, N., Perez, N.D., Ehlers, T.A., Beck, S.L., Kar, N., Eichelberger, N., Chapman, A.D., Ward, K.M., Ducea, M.N., Lease, R.O., Poulsen, C.J., Wagner, L.S., Saylor, J.E., Zandt, G., Horton, B.K., 2017. Tectonic Evolution of the Central Andean Plateau and Implications for the Growth of Plateaus. Annu. Rev. Earth Planet. Sci. 45, 529–559. https://doi.org/10.1146/annurev-earth-063016-020612

Gatewood, M.P., Dragovic, B., Stowell, H.H., Baxter, E.F., Hirsch, D.M., Bloom, R., 2015. Evaluating chemical equilibrium in metamorphic rocks using major element and Sm–Nd isotopic age zoning in garnet, Townshend Dam, Vermont, USA. Chem. Geol. 401, 151–168. https://doi.org/10.1016/j.chemgeo.2015.02.017

Harrison, T.M., 1982. Diffusion of 40Ar in Hornblende. Contrib. to Mineral. Petrol. 78, 324–331. https://doi.org/10.2475/ajs.303.5.410

Harrison, T.M., Célérier, J., Aikman, A.B., Hermann, J., Heizler, M.T., 2009. Diffusion of 40Ar in muscovite. Geochim. Cosmochim. Acta 73, 1039–1051. https://doi.org/10.1016/j.gca.2008.09.038

Hatzfeld, D., Molnar, P., 2010. Comparisons of the kinematics and deep structures of the Zagros and Himalaya and of the Iranian and Tibetan plateaus and geodynamic implications. Rev. Geophys. https://doi.org/10.1029/2009RG000304

Haugerud, R.A., 1990. Geochronologic studies in central New England II: Post-Acadian hinged and differential uplift. Comment Geol. 18, 183–184. https://doi.org/10.1130/0091-7613(1990)018<0183:CAROGS>2.3.CO;2

Heizler, M.T., Harrison, T.M., 1998. The thermal history of the New York basement determined from 40Ar/39Ar K-feldspar studies. J. Geophys. Res. Solid Earth 103, 29795–29814. https://doi.org/10.1029/98JB02837

Hibbard, J.P., van Staal, C.R., Rankin, D.W., Williams, H., 2006. Lithotectonic map of the Appalachian Orogen, Canada-United States of America. https://doi.org/10.4095/221912

Hillenbrand, I.W., 2020. Crustal evolution of the New England Appalachians: the rise and fall of a long-lived orogenic plateau. University of Massachusetts.

Jamieson, R.A., Beaumont, C., Medvedev, S., Nguyen, M.H., 2004. Crustal channel flows: 2. Numerical models with implications for metamorphism in the Himalayan-Tibetan orogen. J. Geophys. Res. Solid Earth 109, 1–24. https://doi.org/10.1029/2003JB002811

Kapp, P., DeCelles, P.G., 2019. Mesozoic–Cenozoic geological evolution of the Himalayan-Tibetan orogen and working tectonic hypotheses. Am. J. Sci. 319, 159–254. https://doi.org/10.2475/03.2019.01

Karabinos, P., Macdonald, F.A., Crowley, J.L., 2017. Bridging the gap between the foreland and hinterland I: Geochronology and plate tectonic geometry of Ordovician magmatism and terrane accretion on the Laurentian margin of New England. Am. J. Sci. 317, 515–554. https://doi.org/10.2475/05.2017.01

Karabinos, P., Mygatt, E.S., Cook, S.M., Student, M., 2010. Evidence for an orogen-parallel, normal-sense shear zone around the Chester dome, Vermont: a possible template for gneiss dome formation in the New England Appalachians, USA, in: Tollo, R.P., Bartholomew, M.J., Hibbard, J.P., Karabinos, P.M. (Eds.), From Rodinia to Pangea: The Lithotectonic Record of the Appalachian Region: Geological Society of America Memoir. pp. 183–203.

Keller, D., Ague, J.J., 2018. High-pressure granulite facies metamorphism (~1.8 GPa) revealed in silica-undersaturated garnet-spinel-corundum gneiss, Central Maine Terrane, Connecticut, U.S.A. Am. Mineral. 103, 1851–1868. https://doi.org/https://doi.org/10.2138/am-2018-6543

Klepeis, K., Webb, L., Blatchford, H., Schwartz, J., Jongens, R., Turnbull, R., Stowell, H., 2019. Deep Slab Collision during Miocene Subduction Causes Uplift along Crustal-Scale Reverse Faults in Fiordland, New Zealand. GSA Today 29, 4–10. https://doi.org/10.1130/gsatg399a.1

Kuiper, Y.D., 2016. Development of the Norumbega fault system in mid-Paleozoic New England, USA: An integrated subducted oceanic ridge model. Geology 44, 455–458. https://doi.org/10.1130/G37599.1

Laske, G., Masters, G., Ma, Z., Pasyanos, M., 2013. Update on CRUST1.0---A 1-degree global model of Earth’s crust, in: EGU General Assembly 2013.

Li, C., Gao, H., Williams, M.L., Levin, V., 2018. Crustal Thickness Variation in the Northern Appalachian Mountains: Implications for the Geometry of 3-D Tectonic Boundaries Within the Crust. Geophys. Res. Lett. 45, 6061–6070. https://doi.org/10.1029/2018GL078777

Macdonald, F.A., Swanson-Hysell, N. l, Park, Y., Lisiecki, L., Jagoutz, O., 2019. Arc-continent collisions in the tropics set Earth's climate state. Science (80-.). 364, 181–184.

Massey, M.A., Moecher, D.P., Walker, T.B., O'Brien, T.M., Rohrer, L.P., 2017. The role and extent of dextral transpression and lateral escape on the post-Acadian tectonic evolution of South-Central New England. Am. J. Sci. 317, 34–94. https://doi.org/10.2475/01.2017.02

McCulla, J.K., 2016. Dating Deformation in the Palmer Zone of Transpression, Central Massachusetts: Temporal Constraints on Models for Progressive Deformation in the Middle Crust [MS thesis]. University of Kentucky.

McKeon, R.E., 2012. Apatite Uranium-Thorium/Helium thermochronometry in slowly eroding landscapes: Addressing age dispersion to understand Appalachian topographic development [PhD thesis]. Lehigh University.

Molnar, P., England, P., Martinod, J., 1993. Mantle dynamics, uplift of the Tibetan Plateau, and the Indian Monsoon. Rev. Geophys. 31, 357–396. https://doi.org/10.1029/93RG02030

Oliver, W.A., Wallace, de W., Dennison, J.M., Hoskins, D.M., Huddle, J.W., 1967. Devonian of the Appalachian Basin, United States, in: Oswald, D.H. (Ed.), International Symposium on the Devonian System. Alberta Society of Petroleum Geologists, pp. 1001–1040.

Raymo, M.E., Ruddiman, W.F., 1992. Tectonic forcing of late Cenozoic climate. Nature 359, 117–122. https://doi.org/10.1038/359117a0

Rivers, T., 2012. Upper-crustal orogenic lid and mid-crustal core complexes: signature of a collapsed orogenic plateau in the hinterland of the Grenville Province. Can. J. Earth Sci. 49, 1–42. https://doi.org/10.1139/e11-014

Roberts, H.J., Kelley, S.P., Dahl, P.S., 2001. Obtaining geologically meaningful 40Ar/39Ar ages from altered biotite. Chem. Geol. 172, 277–290. https://doi.org/10.1016/S0009-2541(00)00255-2

Robinson, P., Tucker, R.D., Bradley, D., Berry IV, H.N., Osberg, P.H., 1998. Paleozoic orogens in New England, USA. GFF 120, 119–148. https://doi.org/10.1080/11035899801202119

Roden-Tice, M.K., West Jr, D.P., Potter, J.K., Raymond, S.M., Winch, J.L., 2009. Presence of a Long-Term Lithospheric Thermal Anomaly: Evidence from Apatite Fission-Track Analysis in Northern New England. J. Geol. 117, 627–641. https://doi.org/10.1086/605995

Spear, F.S., Harrison, T.M., 1989. Geochronologic studies in central New England I: evidence for pre- Acadian metamorphism in eastern Vermont. Geology. https://doi.org/10.1130/0091-7613(1989)017<0181:GSICNE>2.3.CO;2

Stewart, E.M., Ague, J.J., 2018. Infiltration-driven metamorphism, New England, USA: Regional CO2 fluxes and implications for Devonian climate and extinctions. Earth Planet. Sci. Lett. 489, 123–134. https://doi.org/10.1016/j.epsl.2018.02.028

Sullivan, N.C., 2014. Advances in Samarium-Neodymium Geochronology: Applications to Early Earth Garnet, Hydrothermal Carbonate, and High Temperature Metamorphic Systems [PhD thesis]. Boston University.

Thomas, W.A., Gehrels, G.E., Sundell, K.E., Greb, S.F., Finzel, E.S., Clark, R.J., Malone, D.H., Hampton, B.A., Romero, M.C., 2020. Detrital zircons and sediment dispersal in the eastern Midcontinent of North America 16, 1–27. https://doi.org/10.1130/GES02152.1/4974884/ges02152.pdf

Thompson, J.B.J., Robinson, P., Trask, N.J., 1968. Nappes and gneiss domes in west-central New England, in: Zen, E.-A., White, W.S., Hadley, J., Thompson, J.J. (Eds.), Studies of Appalachian Geology: Northern and Maritime. Interscience, New York, pp. 203–218.

Thomson, J.A., 2001. A counterclockwise P-T path for anatectic pelites, South-Central Massachusetts. Contrib. to Mineral. Petrol. 141, 623–641. https://doi.org/10.1007/s004100100265

Tracy, R.J., Dietsch, C.W., 1982. High-temperature retrograde reactions in pelitic gneiss, central Massachusetts. Can. Mineral. 20, 425–437.

van Staal, C.R., Whalen, J.B., Valverde-Vaquero, P., Zagorevski, A., Rogers, N., 2009. Pre-Carboniferous, episodic accretion-related, orogenesis along the Laurentian margin of the northern Appalachians. Geol. Soc. London, Spec. Publ. 327, 271–316. https://doi.org/10.1144/SP327.13

Williams, M.L., Grover, T., Jercinovic, M.J., Regan, S.P., Pless, C.R., Suarez, K.A., 2019. Constraining the timing and character of crustal melting in the Adirondack Mountains using multi-scale compositional mapping and in-situ monazite geochronology. Am. Mineral. 104, 1585–1602. https://doi.org/10.2138/am-2019-6906

Williams, M.L., Jercinovic, M.J., Mahan, K.H., Dumond, G., 2017. Electron Microprobe Petrochronology. Rev. Mineral. Geochemistry 83, 153–182. https://doi.org/10.2138/rmg.2017.83.5

Zen, E.A., 1991. Phanerozoic denudation history of the southern New England Appalachians deduced from pressure data. Am. J. Sci. 291, 401–424. https://doi.org/10.2475/ajs.291.4.401

CHAPTER 5

CONCLUSIONS

The New England Appalachians preserve evidence of a full Wilson tectonic cycle, one of the most fundamental processes to the growth, destruction, and modification of Earth's continental lithosphere. This history, occurring over a span of nearly one billion years, involves the breakup of the supercontinent Rodinia and formation of the Iapetus Ocean, the accretion of exotic terranes, the closure of Iapetus during the assembly of the supercontinent Pangea, and the creation of the modern Atlantic Ocean as Pangea rifted apart. Evidence of these tectonic events is recorded in the form of accreted terranes, poly-deformed and metamorphosed rocks, sedimentary basins, and igneous rocks. Despite intensive study the complex, multistage nature of the orogen has challenged researchers' ability to attribute particular characteristics to specific events in order to build a comprehensive model of crustal and tectonic evolution. Compilation and analysis of existing quantitative geologic data synthesized with structural fabrics and geophysical imaging in this study have provided new insights into the tectonic, structural, and lithospheric evolution.

To constrain the terrane-scale tectonic and crustal evolution a new database of geochronologic, geochemical, and geothermobarometric data was compiled. The New England Geologic Database (NED) covers the northern Appalachians and adjacent foreland basin from New Jersey to New Brunswick and comprises over 24,000 data points. This data can be applied to wide range of geologic problems, from high temperature geochemistry to detrital mineral geochronology of modern sediments. To facilitate collaboration, inspire and test new hypotheses, and serve as a repository of published data, each database is presented as an interactive web-based maps and tables at https://sites.google.com/umass.edu/ned. This database was then applied to constraining the four dimensional crustal and tectonic evolution of New England.

First, geochemical were used to constrain the timing and quantify the magnitude of crustal thickness during the Acadian-Neoacadian orogeny. Trace element and thermoisotopic geochemical proxies define two crustal thickening events. The first, 420-400 Ma, involved progressive southeast to northwest crustal thickening to ~40 km across New England. The second, 400-380 Ma, significantly thickened the crust of southern and central New England to 55-70 km. The crust of this region retained this thickness for >30 m.y., in contrast to northern New England, where minimal crustal thickening occurred in this time span. These two events correlate to the Acadian and Neoacadian orogenies and constrain the nature and significance of each. Further, the greatly thickened crust and high (3-4.5 km) paleo-elevation estimates in central and southern New England ca. 380-350 suggest the existence of an orogenic plateau. Paleo-crustal thickness estimates show a strong correlation with observations from metamorphic petrology. This suggests that first order differences in crustal thickness affected the nature of orogenic collapse, perhaps by a combination of thermal, isostatic, and gravitational forces, whereby areas with thicker crust were more deeply exhumed.

To test the hypothesis of an orogenic plateau, petrologic and geochronologic data were geospatially analyzed and integrated with published data. A large region, greater than 20,000 km^2, of consistent ≥0.6 GPa pressures was recognized. This isobaric terrane, suggestive of low topography, concides with the region of 55-70 km thick crust identified in Chapter 3. Hornblende, muscovite, and biotite $^{40}Ar/^{39}Ar$ dates show systematic patterns and suggest slow cooling at rates of 2-4°C/m.y. following Devonian Acadian Orogeny. Together, thermochronologic, thermobarometric, and geochemical data from central New England suggest crust was significantly thickened and remained so for at least 50 m.y. Metamorphic temperatures, widespread amphibolite to granulite facies metamorphism, and dates of igneous rocks indicate a rheologically weak mid-crust, favoring the development of a low relief plateau.

Additional constraints on the timing of uplift and collapse of the Acadian altiplano are provided by integrating monazite geochemistry and geochronology with structural fabrics. Pre-380 Ma high Y monazite cores are associated with W-directed shortening and predate garnet growth. 380-330 Ma monazite are depleted in Y suggesting monazite growth in the presence of stable garnet and are linked to dextral transpressive fabrics. Monazite rims younger than 330 Ma are enriched in Y and constrain the timing of garnet breakdown during decompression. Shallowly dipping N-S lineations indicate that 330-310 Ma collapse of the plateau was orogen parallel. This phase of orogenesis also led to the formation of core complex-like mantled gneiss domes.

The edge of the proposed plateau, as defined by thermochronologic and thermobarometric data, corresponds with a 12-15 km offset in Moho depth in western New England. Older and lower grade $^{40}Ar/^{39}Ar$ dates and metamorphic conditions are preserved to the west. Low temperature thermochronologic constraints suggest that a 12-15 km offset in Moho depth in western New England likely formed during orogenic collapse by 300 Ma and has not been reactivated since the Mesozoic. This suggests that crustal structures on the scale of 10 km or more can persist for hundreds of millions of years.

These results and interpretations demonstrate the power of a data-driven integration of geochronology, geochemistry, and geothermobarometry with field observations and geophysical imaging. This integrated dataset provides new constraints on the tectonic history and crustal evolution. Results of this thesis provide several lines of evidence supporting the novel hypothesis of a long-lived orogenic plateau in the New England Appalachians which has implications for tectonics, paleoclimate, genesis of critical resources, evolution of the Appalachian foreland basin, and crustal structure. Integration of top-down data-driven analysis with bottom-up field work and quantitative analysis is a promising avenue for building comprehensive models of crustal and tectonic evolution.

APPENDIX A

Selected compositional data for individual geochemical samples used to quantify crustal thickness in Chapter 3. The complete composition data and all compiled samples from northern Appalachians are available from the New England Geologic Database.

Sample	Unit	State	Reference	SiO_2	MgO	Sr/Y	La/Yb	Rb/Sr
W251788	Averill granite	VT	USGS	70.3	0.6	41.5	61.76	0.14
W251792	Averill granite	VT	USGS	68	0.85	42.73	39.38	0.22
W251793	Averill granite	VT	USGS	67.9	0.94	42	28.18	0.23
W251794	Averill granite	VT	USGS	68.6	2.15	10.91	5.63	0.16
W251791	Averill granite	VT	USGS	69	0.78	42.73	25.88	0.21
W251793	Averill granite	VT	USGS	67.9	0.94	42	28.18	0.24
W251794	Averill granite	VT	USGS	68.6	2.15	10.91	5.63	0.16
W253770	Averill granite	VT	USGS	69.1	1.22	46	16.35	0.13
W253771	Averill granite	VT	USGS	67.5	1.56	14.35	2.98	0.26
W253772	Averill granite	VT	USGS	58.5	3.1	12.26	4.34	0.20
W253773	Averill granite	VT	USGS	65.2	1.83	20.14	17.61	0.24
W253774	Averill granite	VT	USGS	59.1	2.71	11.31	16.56	0.28
W253782	Averill granite	VT	USGS	63	2.11	14.86	15.02	0.26
W253786	Averill granite	VT	USGS	67	1.16	10.21	14.15	0.28
W253792	Averill granite	VT	USGS	63.5	2.28	15.37	7.93	0.23
W253793	Averill granite	VT	USGS	69.2	0.74	9.36	11.93	0.34
W253802	Averill granite	VT	USGS	68.4	1.07	8.61	15.68	0.35
W253809	Averill granite	VT	USGS	59.9	2.78	8.96	5.49	0.34
W251769	Averill granite	VT	USGS	70.6	0.81	27.31	40.06	0.23
W251775	Averill granite	VT	USGS	68.1	0.77	35.77	39.42	0.23
W251776	Averill granite	VT	USGS	68.4	0.83	20.94	31.64	0.33
A13-A	Belchertown Complex	MA	Hollocher et al. (2019)	59.0	4.8	99.43	61.53	0.07
A13-B	Belchertown Complex	MA	Hollocher et al. (2019)	58.4	5.37	92.6	58.18	0.05
A13-C	Belchertown Complex	MA	Hollocher et al. (2019)	58.3	5.38	93.7	56.85	0.05

A21-11	Belchertown Complex	MA	Hollocher et al. (2019)	57.8	5.8	81.0	56.95	0.04
A22-2Aa	Belchertown Complex	MA	Hollocher et al. (2019)	57.4	5.98	79.6	57.26	0.04
A22-2Ab	Belchertown Complex	MA	Hollocher et al. (2019)	69.0	1.22	138.4	19.54	0.02
BT-11	Belchertown Complex	MA	van Wagener (2017)	58.1	2.9	93.5		0.05
BT-12	Belchertown Complex	MA	van Wagener (2017)	58.5	5.92	68	39.66	0.05
BT-17	Belchertown Complex	MA	van Wagener (2017)	55.5	4.44	37.9		0.01
BT-23	Belchertown Complex	MA	van Wagener (2017)	69.8	1.35	7.98		0.049
BT-3R-1	Belchertown Complex	MA	van Wagener (2017)	58.5	4.38	81.1	44.97	0.04
BT-3R-D1	Belchertown Complex	MA	van Wagener (2017)	52.4	5.17	4.37	2.66	0.21
BT-3R-D2	Belchertown Complex	MA	van Wagener (2017)	53.0	4.38	10.4		0.01
BT-4	Belchertown Complex	MA	van Wagener (2017)	59.4	5.58	72.33	38.58	0.052
BT-8	Belchertown Complex	MA	van Wagener (2017)	58.4	6	54.92	37.09	0.053
BT-9	Belchertown Complex	MA	van Wagener (2017)	58.7	5.9	55.59	38.92	0.056
BT-D10	Belchertown Complex	MA	van Wagener (2017)	50.8	5.53	2.85	2.25	0.155
BT-FH-1	Belchertown Complex	MA	van Wagener (2017)	60.2	5.42	94.66	44.55	0.043
BT-SR-1	Belchertown Complex	MA	van Wagener (2017)	59.14	5.86	59.87	33.63	0.058
W201019	Bethlehem Granodiorite	NH	USGS	69.8	1.1	19.08	8.91	0.293
SS00-131	Calais Quartz Diorite	ME	McLaughlin et al. (2003)	55.98	3.74	5.34		0.281
SS98-72	Calais Quartz Diorite	NB	McLaughlin et al. (2003)	56.33	3.61	7.56	4.47	0.182

SS00-119	Calais Quartz Diorite	ME	McLaughlin et al. (2003)	56.56	4.55	9.19		
SS00-144B	Calais Quartz Diorite	ME	McLaughlin et al. (2003)	57.83	3	7.76		
SS00-123	Calais Quartz Diorite	ME	McLaughlin et al. (2003)	58.14	4.75	8.89		0.246
SS00-144A	Calais Quartz Diorite	ME	McLaughlin et al. (2003)	59.14	2.47	13.15		0.216
MH-175B	Calais Quartz Diorite	ME	McLaughlin et al. (2003)	59.77	2.97	6.58		0.3
W225076	Deboullie	ME	USGS	68.9	1.62	37.88	40.22	0.244
W225086	Deboullie	ME	USGS	56.7	4.73	27.88	12.89	0.203
W225093	Deboullie	ME	USGS	69.1	2.22	17.17	10.2	0.154
STO-51	Deer Isle Granite	ME	Hook (2003)	67	1.65	15.82		
STO-57	Deer Isle Granite	ME	Hook (2003)	63.39	2.34	22.2		
STO-93	Deer Isle Granite	ME	Hook (2003)	69.92	0.68	6.7		
STO-34	Deer Isle Granite	ME	Hook (2003)	65.08	2.01	10.59		
STO-56	Deer Isle Granite	ME	Hook (2003)	64.38	1.61	17.26		
W227986	Deer Isle Granite	ME	USGS	58.8	2.3	19.31	7.43	0.092
DE-2	Derby pluton	VT	Arth and Aysuo (1997)	67.6	0.92		18.91	0.129
DE-4	Derby pluton	VT	Arth and Aysuo (1997)	68	1.2		33.79	0.107
DE-11	Derby pluton	VT	Arth and Aysuo (1997)	65.9	1.5		27.17	0.121
W252551	Eastford granite	CT	USGS	69	1.24	57.75	16.98	0.245
EP-9	Echo Pond pluton	VT	Arth and Aysuo (1997)	61.9	2.4		12.59	0.24
A61-3A	Fitzwilliam granite	MA	Shearer (1983)	69.3	0.75	43.55		0.319
A61-3B	Fitzwilliam granite	MA	Shearer (1983)	69.37	0.71	43.91		0.321
Rt2H2	Hardwick pluton	MA	Hollocher et al. (2019)	55.41	3.96	24.28	26.63	0.103
P-61-23	Hunt Ridge pluton	ME	Ayuso (1999)	61.3	1.75	9.67		0.11

DMA-191	Indian Head pluton	MA	Wones and Goldsmith (1991)	69.34	0.92		20.78	0.267
81208-11	Knox Mountain pluton	VT	Coish (2010)	71.9	0.64	27.23		
MJG121206(4G)	Knox Mountain pluton	VT	Coish (2010)	70.26	1.19	43.14		
MJG121206(8G)	Knox Mountain pluton	VT	Coish (2010)	70.36	1.23	27.08		
W256918	Littleton volc	NH	USGS	60.4	5.76	19.62	25.14	0.063
J98-54	Mooselookmeguntic igneous complex	ME	Tomascak et al. (2005)	63.8	2.04	21.05		0.219
W240499	Mooselookmeguntic igneous complex	ME	USGS	60.3	3.22	41.2	25.23	0.157
W240500	Mooselookmeguntic igneous complex	ME	USGS	65.7	2	30.28	17.24	0.22
W240501	Mooselookmeguntic igneous complex	ME	USGS	62.7	2.52	55.17	14.82	0.13
W240507	Mooselookmeguntic igneous complex	ME	USGS	63.4	2.98	33.25	12.62	0.186
J98-40	Mooselookmeguntic igneous complex	ME	Tomascak et al. (2005)	67	2.38	24.78		0.308
96-222	Mooselookmeguntic igneous complex	ME	Tomascak et al. (2005)	57.9	4.57	27.44		0.31
J98-43	Mooselookmeguntic igneous complex	ME	Tomascak et al. (2005)	57.7	5.2	40.3		0.222
J98-100	Mooselookmeguntic igneous complex	ME	Tomascak et al. (2005)	57.2	4.2	33.58		0.257
J98-63-2	Mooselookmeguntic igneous complex	ME	Tomascak et al. (2005)	64.6	3.09	30.18		0.235
J98-111-2	Mooselookmeguntic igneous complex	ME	Tomascak et al. (2005)	72.2	0.85	18.52		0.319
W253822	Katahdin granite	ME	USGS	71.9	0.55	27.07	75.16	0.346
MS97-6A	Newark pluton	VT	Coish (2010)	70	0.63	33.85		
MS97-3D	Newark pluton	VT	Coish (2010)	69.9	0.66	26.08		
MS97-9D§	Newark pluton	VT	Coish (2010)	70.4	0.67	29.15		
MS97-3B	Newark pluton	VT	Coish (2010)	69.8	0.77	26.36		
MS97-3A	Newark pluton	VT	Coish (2010)	70.0	0.68	28.67	58.76	0.205
MS97-6C	Newark pluton	VT	Coish (2010)	70.4	0.53	33.72	29.35	0.216
MS97-9C	Newark pluton	VT	Coish (2010)	70.1	0.61	29.24	41.98	0.218

MS97-4C	Newark pluton	VT	Coish (2010)	70.88	0.61	27.13	37.97	0.22
W223002	Northport	ME	USGS	58.7	4.1	8.94	4.02	0.273
NU-6	Nulhegan pluton	VT	Arth and Aysuo (1997)	63.4	3.69		13.39	0.36
NU-2	Nulhegan pluton	VT	Arth and Aysuo (1997)	62.1	4.2		12.63	0.323
NU-10	Nulhegan pluton	VT	Arth and Aysuo (1997)	63.6	4.29		12.73	0.28
NU-3	Nulhegan pluton	VT	Arth and Aysuo (1997)	62.3	4.48		11.66	0.223
NU-18	Nulhegan pluton	VT	Arth and Aysuo (1997)	63.4	4.48		15.58	0.393
NU-7	Nulhegan pluton	VT	Arth and Aysuo (1997)	61.9	4.65		17.16	0.245
NU-19	Nulhegan pluton	VT	Arth and Aysuo (1997)	60	4.84		12.2	0.26
NU-20	Nulhegan pluton	VT	Arth and Aysuo (1997)	62.1	4.84		16.7	0.254
NU-4	Nulhegan pluton	VT	Arth and Aysuo (1997)	61.7	4.89		14.04	0.264
NU-17	Nulhegan pluton	VT	Arth and Aysuo (1997)	61.4	4.91		11.44	0.344
NU-11	Nulhegan pluton	VT	Arth and Aysuo (1997)	60.5	5.87		11.27	0.148
B-17	Preston Gabbro	CT	Walker (1983)	62.4	1.83	4.88		
83PL-215	Priestly Lake pluton	ME	Ayuso (1999)	65.5	1.86	15.71		0.339
W225098	Priestly Lake pluton	ME	USGS	65.5	1.86	15.71	11.38	0.339
W225099	Priestly Lake pluton	ME	USGS	69.4	1.35	16.75	14.32	0.316
W225100	Priestly Lake pluton	ME	USGS	68.3	1.45	14.43	12.19	0.317
W232017	Priestly Lake pluton	ME	USGS	66.9	1.59	16.87	6.14	0.25
W232019	Priestly Lake pluton	ME	USGS	64.5	1.92	20.65	10.96	0.206
W232020	Priestly Lake pluton	ME	USGS	67.2	1.57	20.39	12.23	0.259
W225103	Priestly Lake pluton	ME	USGS	67.5	1.57	15.38	12.99	0.325

W227983	Priestly Lake pluton	ME	USGS	59	1.5	16.2	5.56	0.306
W227991	Priestly Lake pluton	ME	USGS	63	1.3	9.03	3.75	0.348
W236721	Rome granite	ME	USGS	65.9	1.38	17.88	18.68	0.325
W214867	South Penobscot	ME	USGS	56.3	5.2	26.31	5.33	0.085
W252547	Scituate granite	RI	USGS	68.2	1.32	35.08	51.69	0.304
SG-10	Songo Granodiorite	ME	Gibson and Lux (1989)	64.3	1.93	22.15		0.182
SG-18	Songo Granodiorite	ME	Gibson and Lux (1989)	64.9	1.53	32.25		0.174
SG-23	Songo Granodiorite	ME	Gibson and Lux (1989)	66.2	1.63	27.15		0.238
SG-30	Songo Granodiorite	ME	Gibson and Lux (1989)	64.7	1.9	34.28		0.186
SG-35	Songo Granodiorite	ME	Gibson and Lux (1989)	66.2	2.15	32.24		0.175
SG-38	Songo Granodiorite	ME	Gibson and Lux (1989)	62.8	2.16	30.55		0.131
SG-47	Songo Granodiorite	ME	Gibson and Lux (1989)	67.7	1.52	80.2		0.135
SG-48	Songo Granodiorite	ME	Gibson and Lux (1989)	63.2	2.3	39.19		0.152
SG-53	Songo Granodiorite	ME	Gibson and Lux (1989)	66.9	1.55	25.71		0.186
SG-59	Songo Granodiorite	ME	Gibson and Lux (1989)	66.7	1.55	32.45		0.171
SG-8*	Songo Granodiorite	ME	Gibson and Lux (1989)	70.2	1.12	23.81		0.325
SG-11*	Songo Granodiorite	ME	Gibson and Lux (1989)	69.7	1.25	39.38		0.182
SG-12*	Songo Granodiorite	ME	Gibson and Lux (1989)	64.2	2.19	28		0.172
SG-33*	Songo Granodiorite	ME	Gibson and Lux (1989)	66.4	1.2	26.5		0.264
SG-34*	Songo Granodiorite	ME	Gibson and Lux (1989)	66.3	2.08	45.93		0.123
SG-40*	Songo Granodiorite	ME	Gibson and Lux (1989)	70.9	1.43	29.69		0.204
SG-43*	Songo Granodiorite	ME	Gibson and Lux (1989)	64.7	2.33	35.95		0.161
SG-46*	Songo Granodiorite	ME	Gibson and Lux (1989)	67.1	2.03	48		0.225
SG-49*	Songo Granodiorite	ME	Gibson and Lux (1989)	64.3	1.85	40.75		0.223
SG-51*	Songo Granodiorite	ME	Gibson and Lux (1989)	64.9	1.78	51.5		0.176
SG-58*	Songo Granodiorite	ME	Gibson and Lux (1989)	66.8	1.72	26.53		0.309
S70-76	South Penobscot Intrusive Suite	ME	Stewart et al. (1995)	56.4	3.9	6.93	4.58	0.242
S70-48	South Penobscot Intrusive Suite	ME	Stewart et al. (1995)	58.8	2.3	19.31	5.79	0.092

S70-55	South Penobscot Intrusive Suite	ME	Stewart et al. (1995)	59	1.5	16.2	7.37	0.306
S70-99	South Penobscot Intrusive Suite	ME	Stewart et al. (1995)	62.6	1.3	7.45	4.95	0.3
405	South Penobscot Intrusive Suite	ME	Stewart et al. (1995)	63	1.3	9.03	3.48	0.348
W222295	Spider Lake pluton	ME	USGS	65.6	2.19	36.5	22.53	0.184
W222296	Spider Lake pluton	ME	USGS	63.2	2.8	31.35	19.37	0.169
W222297	Spider Lake pluton	ME	USGS	65.5	2.56	25.41	22.02	0.211
W222300	Spider Lake pluton	ME	USGS	65.1	2.35	35.53	18.46	0.152
W222301	Spider Lake pluton	ME	USGS	66.7	2.11	28.19	17.87	0.22
W222302	Spider Lake pluton	ME	USGS	65.6	2.05	37.14	26.79	0.171
W222298	Spider Lake pluton	ME	USGS	66.3	1.88	33.29	28.2	0.182
W222299	Spider Lake pluton	ME	USGS	66.7	1.76	39.58	46.08	0.179
THSH-102	Spruce Head composite pluton	ME	Ayuso and Arth (1997)	65	1.27	9.93	10.71	0.326
THSH-20	Spruce Head composite pluton	ME	Ayuso and Arth (1997)	66.4	1.32	22.44	12.6	0.22
ROSH-119	Spruce Head composite pluton	ME	Ayuso and Arth (1997)	65.6	1.39	8.56	11.82	0.339
THSH-4	Spruce Head composite pluton	ME	Ayuso and Arth (1997)	64	1.5	10.96	13.96	0.3
TTSH-8	Spruce Head composite pluton	ME	Ayuso and Arth (1997)	55.4	2.81	13.15	5.63	0.158
THSH-108	Spruce Head composite pluton	ME	Ayuso and Arth (1997)	56.1	2.95	10.3	5.68	0.221
D554678	Spruce Head composite pluton	ME	USGS	55.2	1.31	27.78	14.56	0.265
D554683	Spruce Head composite pluton	ME	USGS	56.3	1	26.32	9.56	0.31
D554689	Spruce Head composite pluton	ME	USGS	56.6	1.03	25.88	13.9	0.335
W240529	Spruce Head composite pluton	ME	USGS	64	1.5	10.96	13.18	0.3
W240533	Spruce Head composite pluton	ME	USGS	55.4	2.81	13.15	6.57	0.158
W240545	Spruce Head composite pluton	ME	USGS	66.4	1.32	22.44	11.12	0.22
W244897	Spruce Head composite pluton	ME	USGS	65	1.27	9.93	10.37	0.326
W244903	Spruce Head composite pluton	ME	USGS	56.1	2.95	10.3	6.31	0.221

W244914	Spruce Head composite pluton	ME	USGS	65.6	1.39	8.56	7.73	0.339
W248112	Spruce Head composite pluton	ME	USGS	61.3	1.75	9.67	5.26	0.11
W248121	Spruce Head composite pluton	ME	USGS	67.7	1.37	57.88	30.76	0.253
W248127	Spruce Head composite pluton	ME	USGS	67.4	1.78	46	19.33	0.22
W248135	Spruce Head composite pluton	ME	USGS	64	2.63	41	16.72	0.173
W248143	Spruce Head composite pluton	ME	USGS	63.4	2.67	21.39	9.67	0.24
W248146	Spruce Head composite pluton	ME	USGS	64	2.63	35.13	13.59	0.18
W253830	Spruce Head composite pluton	ME	USGS	61.3	2.32	18.94	21.51	0.248
W253832	Spruce Head composite pluton	ME	USGS	65.4	1.65	10.06	13.29	0.349
W253833	Spruce Head composite pluton	ME	USGS	63.7	1.5	22.06	26.87	0.176
W253834	Spruce Head composite pluton	ME	USGS	60	2.48	19	32.27	0.27
W253836	Spruce Head composite pluton	ME	USGS	55	2.61	8.26	8.95	0.21
SC-105	Stony Creek granite	CT	Wintsch et al. (2014)	71.8	0.19	62.41	257.2	0.526
SC-205	Stony Creek granite	CT	Wintsch et al. (2014)	69.5	0.48	26.51	158.65	0.46
Sgrtype	Sudbury Granite	MA	Dabrowski (2014)	71.9	1.28	19.30		0.292
Sgrdark	Sudbury Granite	MA	Dabrowski (2014)	63.1	2.73	16.82		0.214
S22	Sudbury Granite	MA	Dabrowski (2014)	64.2	2.74	19.53		0.099
S96	Sudbury Granite	MA	Dabrowski (2014)	63.4	2.57	20.46		0.133
S-5	Sweepstakes pluton	NH	Watts et al. (2003)	61.9	3.56	18.8		0.303
S-11	Sweepstakes pluton	NH	Watts et al. (2003)	55.9	5.35	12.06		0.211
S-12	Sweepstakes pluton	NH	Watts et al. (2003)	55.5	5.37	11.81	8.93	0.213
D309065	Umbagog pluton	NE	USGS	56.7	4.27	27.41		0.29
W210592	Umbagog pluton	NH	USGS	70.7	0.77	30.93	24.34	0.206
NEK95-120	Victory pluton	VT	Coish (2010)	70.9	0.69	43.75		
NEK95-80	Victory pluton	VT	Coish (2010)	62.7	2.02	11.34		
NEK95-98	Victory pluton	VT	Coish (2010)	62.9	3.35	31.93		
NEK95-132	Victory pluton	VT	Coish (2010)	65.7	3.63	20.13		
NEK95-101	Victory pluton	VT	Coish (2010)	56.6	3.85	37.59		

NEK95-130	Victory pluton	VT	Coish (2010)	71.9	0.57	79.88	19.16	0.171
NEK95-128	Victory pluton	VT	Coish (2010)	71.1	0.56	64	21.87	0.184
NEK95-110	Victory pluton	VT	Coish (2010)	70.6	0.72	13.33	18.41	0.223
W217941	Vinalhaven pluton	ME	USGS	57.6	4	11.79	9.1	0.107
LI-WB-1	Waldoboro pluton	ME	Ayuso (1999)	65.8	1.39	27.74		0.147
F-19-42	Waldoboro plutonic complex	ME	Sidle (1990)	58.1	3.43	14.12	5.03	0.17
LI-12-2	Waldoboro plutonic complex	ME	Sidle (1990)	61.3	1.95	8.04	13.75	0.174
WE-48-30	Waldoboro plutonic complex	ME	Sidle (1990)	58.5	3.36	20.04	7.53	0.186
WE-48-20	Waldoboro plutonic complex	ME	Sidle (1990)	60.7	3.06	21.82	12.53	0.198
F-49-7	Waldoboro plutonic complex	ME	Sidle (1990)	60.4	3.25	22.67	16.42	0.208
WE-32-6	Waldoboro plutonic complex	ME	Sidle (1990)	62.6	2.72	16.68	20.46	0.218
WE-40-9	Waldoboro plutonic complex	ME	Sidle (1990)	62.9	2.5	16.13	14.34	0.251
LI-35-2	Waldoboro plutonic complex	ME	Sidle (1990)	62.8	3.19	7.88	8.46	0.254
WE-18-15	Waldoboro plutonic complex	ME	Sidle (1990)	62.9	2.05	13.55	19.07	0.265
LI-26-3	Waldoboro plutonic complex	ME	Sidle (1990)	64.5	2.38	11.33	6.26	0.265
LI-2-1	Waldoboro plutonic complex	ME	Sidle (1990)	64.6	2.61		13.19	0.287
WE-25-12	Waldoboro plutonic complex	ME	Sidle (1990)	0.75	5.3	16.13	0.29	38.93
WW-48-4	Waldoboro plutonic complex	ME	Sidle (1990)	66.8	1.92	8.31	8.68	0.296
LI-14-20	Waldoboro plutonic complex	ME	Sidle (1990)	64.5	2.02	7.82	49.59	0.305
WE-25-8	Waldoboro plutonic complex	ME	Sidle (1990)	0.7	4.33	16.01	0.318	35.84
LI-3-16	Waldoboro plutonic complex	ME	Sidle (1990)		0.05	8.75	4.58	
WE-15-18	Waldoboro plutonic complex	ME	Sidle (1990)	0.7	4.02	15.36	0.337	35.22
LI-25-1	Waldoboro plutonic complex	ME	Sidle (1990)	64.5	2.3	14.08	35.66	0.343
W-3	Webhannet pluton	ME	Watts et al. (2003)	63.86	2.57	16	17.4	0.245
WC-1	West Charleston pluton	VT	Arth and Aysuo (1997)	69.3	1.2		9.86	0.338
WQD-11	Winnepesaukee pluton	NH	Dorais (2003)	67.79	1.62	38.15	25.04	0.155
WQD-15	Winnepesaukee pluton	NH	Dorais (2003)	64.21	1.81	33.4	17.79	0.335

WQD-16	Winnepesaukee pluton	NH	Dorais (2003)	59.97	2.05	19.6	10.98	0.304
WQD-17	Winnepesaukee pluton	NH	Dorais (2003)	58.81	2.25	45.5	10.86	0.22
WQD-2	Winnepesaukee pluton	NH	Dorais (2003)	58.52	2.89	24.9	2.51	0.175
WQD-3	Winnepesaukee pluton	NH	Dorais (2003)	67.16	1.01	30.28	22.12	0.222
WQD-4	Winnepesaukee pluton	NH	Dorais (2003)	70.39	1.07	47.18	57.19	0.241
WQD-78	Winnepesaukee pluton	NH	Dorais (2003)	68.54	1.01	20.05	15.47	0.247
RM07-03	Woodbury pluton	VT	Coish (2010)	71.6	0.7	28.11		
RM07-20	Woodbury pluton	VT	Coish (2010)	71.29	0.8	45.63		
RM07 26	Woodbury pluton	VT	Coish (2010)	70	0.85	50.63		
RM07 34	Woodbury pluton	VT	Coish (2010)	70.59	0.86	64		
RM07 35	Woodbury pluton	VT	Coish (2010)	70.2	1.03	44.67		
RM07 28	Woodbury pluton	VT	Coish (2010)	70.64	1.06	49.75		
RM07-05	Woodbury pluton	VT	Coish (2010)	71.58	1.14	58.33		
RM07-11	Woodbury pluton	VT	Coish (2010)	66.6	1.5	48.09		
RM07-12	Woodbury pluton	VT	Coish (2010)	65.6	1.57	49.7		
RM07-02	Woodbury pluton	VT	Coish (2010)	70.3	0.83	83.43	17.12	0.211
RM07-22	Woodbury pluton	VT	Coish (2010)	70.6	0.75	43.33	12.91	0.242
RM07-14	Woodbury pluton	VT	Coish (2010)	67.1	1.55	62	23.23	0.276
RM07-21	Woodbury pluton	VT	Coish (2010)	71.3	0.9	66.71	15.01	0.345

Appendix A References

Arth, J.G., and Ayuso, R.A., 1997, The Northeast Kingdom batholith, Vermont: Geochronology and Nd, O, Pb, and Sr isotopic constraints on the origin of Acadian granitic rocks: Memoir of the Geological Society of America, v. 191, p. 1–18, doi:10.1130/0-8137-1191-6.1.

Ayuso, R.A., and Arth, J.G., 1997, The Spruce Head composite pluton: An example of mafic to silk Salinian magmatism in coastal Maine, northern Appalachians: The Nature of Magmatism in the Appalachian Orogen, v. 191, p. 19.

Coish, R.A., 2010, Magmatism in the Vermont Appalachians: From Rodinia to Pangea: the lithotectonic record of the Appalachian Region. Edited by R. Tollo, J. Bartholomew, J. Hibbard, and P. Karabinos. Geological Society of America Memoir, v. 206, p. 91–110.

Gibson, D., and Lux, D.R., 1989, Petrographic and geochemical variations within the Songo pluton, western Maine: in Tucker, R.D., and Marvinney, R.G. (eds.), Studies in Maine geology: Volume 4 -igneous and metamorphic geology: Maine Geological Survey.

Hook, B.P., 2003, Petrology of the Deer Isle Pluton, Coastal Maine: A Complex Mixed Magma System: [MS Thesis]: University of Maine, 185 p.

Hollocher, K., Robinson, P., Lucas, B., and Mabee, S., 2019, Geochemistry of intrusive rocks on the Prescott Peninsula, central Massachusetts, USA: Implications for late detachment faulting within the Ordovician Taconian volcanic arc: American Journal of Science, v. 319, p. 658–693, doi:10.2475/08.2019.02.

McLaughlin, K.J., Barr, S.M., Hill, M.D., Thompson, M.D., Ramezani, J., and Reynolds, P.H., 2003, The Moosehorn Plutonic Suite, southeastern Maine and southwestern New Brunswick: Age, petrochemistry, and tectonic setting: Atlantic Geology, v. 39, p. 123–146.

Shearer, C., 1983, Petrography, Mineral Chemistry, and Geochemistry of the Hardwick Tonalite and Associated Igneous Rocks, Central Massachusetts.: University of Massachusetts Amherst, 210 p.

Sidle, W.C., 1990, Structure, petrology, and geochemistry of the Waldoboro Pluton Complex, Maine: Ohio State, 369 p.

Stewart, D.B., Unger, J.D., and Hutchinson, D.R., 1995, Silurian tectonic history of Penobscot Bay region, Maine: Atlantic Geology, v. 31, p. 67–79.

Tomascak, P.B., Brown, M., Solar, G.S., Becker, H.J., Centorbi, T.L., and Tian, J., 2005, Source contributions to Devonian granite magmatism near the Laurentian border, New Hampshire and western Maine, USA: LITHOS, v. 80, p. 75–99.

Van Wagner, K.J., 2017, Petrogenesis and Concentric Zonation of the Belchertown Intrusive Complex, West-Central Massachusetts: [MS thesis]: University of Massachusetts Amherst, 90 p.

Walker III, A.T., 1983, The Preston Gabbro of southeastern Connecticut; Geochemistry and History of Formation: Lehigh University, 199 p.

Watts B. G., Dorais, M. J., and Wintsch, R. P., 2000, Geochemistry of Early Devonian calc- alkaline plutons in the Merrimack belt: Implications for Mid-Paleozoic terrane relationships in the New England Appalachians: Atlantic Geology, v. 36, p. 79102.

Wintsch, R.P., Yi, K., and Dorais, M.J., 2014, Crustal thickening by tectonic wedging of the Ganderian rocks, southern New England, USA: Evidence from cataclastic zircon microstructures and U–Pb ages: Journal of Structural Geology, v. 69, p. 428–448, doi:https://doi.org/10.1016/j.jsg.2014.07.019.

Wones, D.R., and Goldsmith, R., 1991, Intrusive rocks of eastern Massachusetts, in Hatch, N.L., Jr., ed., The Bedrock Geology of Massachusetts: U.S. Geological Survey Professional Paper 1366-I, p. 1-61.

APPENDIX B

Nd isotopic data for individual geochemical samples used to quantify crustal thickness in Chapter 3. The complete dataset is available from the New England Geologic Database.

Sample	Unit	State	Reference	$^{147}Sm/^{144}Nd$	$^{143/144}Nd_t$	$^{143/144}Nd_i$	εNd_t	εNd_i
-	Andover	MA	Hill et al. (1984)	-	-	0.5120	-1.24	-5.49
-	Andover	MA	Hill et al. (1984)	-	-	0.5123	-0.66	0.36
BT-3	Belchertown pluton	MA	Van Wagner (2017)	0.097	0.5123	0.5121	-6.09	-1.29
BT-QB-5	Belchertown pluton	MA	Van Wagner (2017)	0.196	0.5127	0.5122	1.56	1.55
BT-SR-4	Belchertown pluton	MA	Van Wagner (2017)	0.114	0.5123	0.5121	-5.74	-1.75
92ASL59 (59)	Bethlehem Gneiss	NH	Lathrop (1994)	0.123	0.5122	0.5119	-7.67	-3.86
92ASL60 (60)	Bethlehem Gneiss	NH	Lathrop (1994)	0.119	0.5122	0.5119	-8.97	-4.96
92ASL61	Bethlehem Gneiss	NH	Lathrop (1994)	0.127	0.5122	0.5119	-8.56	-4.96
92ASL74	Bethlehem Gneiss	NH	Lathrop (1994)	0.123	0.5121	0.5118	-9.73	-5.95
92ASL77 (77)	Bethlehem Gneiss	NH	Lathrop (1994)	0.127	0.5122	0.5119	-8.74	-5.16
92ASL79 (79)	Bethlehem Gneiss	NH	Lathrop (1994)	0.124	0.5123	0.5119	-7.37	-3.65
M15-73(15L)	Bethlehem Gneiss	NH	Lathrop (1994)	0.241	0.5123	0.5116	-6.92	-9.27
M16-73(16L)	Bethlehem Gneiss	NH	Lathrop (1994)	0.123	0.5125	0.5121	-3.26	0.55
CP-4G-A	Cardigan pluton	NH	Dorais (2009)	0.248	0.5122	0.5116	-7.72	-10.48
CP-23G	Cardigan pluton	NH	Dorais (2009)	0.122	0.5122	0.5119	-8.90	-4.97
CP-32G	Cardigan pluton	NH	Dorais (2009)	0.141	0.5123	0.5120	-5.72	-2.83
CP-34G	Cardigan pluton	NH	Dorais (2009)	0.133	0.5122	0.5119	-8.31	-4.96
CP-5P	Cardigan pluton	NH	Dorais (2009)	0.130	0.5122	0.5118	-8.82	-5.36
CP-2P	Cardigan pluton	NH	Dorais (2009)	0.169	0.5123	0.5118	-6.55	-5.11
QNH61-13	Concord granite	NH	Foland and Allen (1991)	0.108	0.5122	0.5120	-8.15	-4.16
92ASL37 (37)	Coys Hill pluton	NH	Lathrop (1994)	0.116	0.5123	0.5120	-7.51	-3.47

STO-30	Deer Isle Granite	ME	Hook (2003)	0.117	0.5125	0.5122	-3.67	0.08
STO-37	Deer Isle Granite	ME	Hook (2003)	0.092	0.5125	0.5122	-3.53	1.42
STO-76B	Deer Isle Granite	ME	Hook (2003)	0.102	0.5125	0.5122	-2.89	1.55
STO-50	Deer Isle Granite	ME	Hook (2003)	0.104	0.5125	0.5122	-3.20	1.17
STO-57	Deer Isle Granite	ME	Hook (2003)	0.106	0.5125	0.5123	-2.20	2.07
STO-51	Deer Isle Granite	ME	Hook (2003)	0.106	0.5125	0.5123	-2.11	2.17
STO-78	Deer Isle Granite	ME	Hook (2003)	0.116	0.5124	0.5121	-4.47	-0.65
STO-92	Deer Isle Granite	ME	Hook (2003)	0.102	0.5125	0.5122	-3.18	1.28
STO-42	Deer Isle Granite	ME	Hook (2003)	0.090	0.5125	0.5123	-3.30	1.75
STO-49	Deer Isle Granite	ME	Hook (2003)	0.106	0.5125	0.5123	-2.28	1.99
STO-66	Deer Isle Granite	ME	Hook (2003)	0.100	0.5125	0.5123	-2.89	1.64
STO-35	Deer Isle Granite	ME	Hook (2003)	0.098	0.5125	0.5123	-2.81	1.86
MED17	Derby pluton	VT	Arth and Ayuso (1997)	0.132	0.5122	0.5119	-8.74	-5.69
IPEP14	Echo Pond Pluton	VT	Arth and Ayuso (1997)	0.098	0.5123	0.5121	-5.81	-1.19
IPEP19	Echo Pond Pluton	VT	Arth and Ayuso (1997)	0.093	0.5122	0.5120	-7.96	-3.09
IPEP03	Echo Pond Pluton	VT	Arth and Ayuso (1997)	0.124	0.5123	0.5120	-6.59	-3.17
QNH61-15	Fitzwilliam granite	NH	Foland and Allen (1991)	0.122	0.5122	0.5120	-7.96	-4.63
CKGP-07b	Gouldsboro Complex	ME	Koteas (2010)	0.149	0.5127	0.5122	0.25	2.75
CKGP-93	Gouldsboro Complex	ME	Koteas (2010)	0.132	0.5126	0.5122	-0.94	2.49
CKGP-196	Gouldsboro Complex	ME	Koteas (2010)	0.171	0.5127	0.5122	1.19	2.54
CKGP-198	Gouldsboro Complex	ME	Koteas (2010)	0.139	0.5126	0.5122	-0.64	2.42
09CKGD-b018	Gouldsboro Complex	ME	Koteas (2010)	0.235	0.5131	0.5125	9.91	7.86
CKGP-60(1)	Gouldsboro Complex	ME	Koteas (2010)	0.141	0.5123	0.5119	-6.03	-3.08
CKGP-188B	Gouldsboro Complex	ME	Koteas (2010)	0.130	0.5127	0.5123	0.29	3.79
CKGP-201	Gouldsboro Complex	ME	Koteas (2010)	0.153	0.5126	0.5122	-0.29	1.98

CKGP-30	Gouldsboro Complex	ME	Koteas (2010)	0.155	0.5123	0.5119	-6.53	-4.36
CKGP-114	Gouldsboro Complex	ME	Koteas (2010)	0.146	0.5124	0.5120	-5.52	-2.86
CKGP-153	Gouldsboro Complex	ME	Koteas (2010)	0.139	0.5126	0.5122	-0.29	2.76
CKGP-172	Gouldsboro Complex	ME	Koteas (2010)	0.146	0.5126	0.5122	-0.08	2.61
MED05	Granite at Derby Quarry	VT	Arth and Ayuso (1997)	0.120	0.5121	0.5118	-11.30	-7.65
91JDB14 (14)	Kinsman Quartz Monzonite	NH	Lathrop (1994)	0.122	0.5121	0.5118	-10.30	-6.40
92ASL20 (20)	Kinsman Quartz Monzonite	NH	Lathrop (1994)	0.128	0.5122	0.5118	-8.90	-5.30
92ASL63 (63)	Kinsman Quartz Monzonite	NH	Lathrop (1994)	0.113	0.5121	0.5118	-10.10	-5.80
92ASL67 (67)	Kinsman Quartz Monzonite	NH	Lathrop (1994)	0.118	0.5126	0.5123	-1.33	2.80
28	Lexington pluton	ME	Williamson (1999)	0.134	0.5125	0.5121	-2.83	0.40
28	Lexington pluton	ME	Williamson (1999)	0.101	0.5124	0.5121	-4.58	0.31
14A	Lexington pluton	ME	Williamson (1999)	0.128	0.5123	0.5120	-6.36	-2.86
26	Lexington pluton	ME	Williamson (1999)	0.125	0.5126	0.5122	-1.64	2.01
96-296-2	Lexington pluton central	ME	Tomascak et al. (2005)	0.120	0.5122	0.5119	-8.29	-4.37
98-10-1	Lexington pluton central	ME	Tomascak et al. (2005)	0.120	0.5122	0.5119	-7.63	-3.72
98-1	Lexington pluton north	ME	Tomascak et al. (2005)	0.110	0.5123	0.5120	-6.87	-2.43
98-2	Lexington pluton south	ME	Tomascak et al. (2005)	0.132	0.5122	0.5119	-8.06	-4.76
NH/Di 5-82	Long Mountain pluton	NH	Harrison et al. (1987)	0.512	37.0000	-10.3800	-6.34	0.90
MPG-10	Meredith Porphyritic Granite	NH	Dorais (2003)	0.150	0.5124	0.5120	-5.36	-3.07
MPG-14	Meredith Porphyritic Granite	NH	Dorais (2003)	0.129	0.5124	0.5121	-4.84	-1.47
NH-76-38	Meredith porphyritic granite	NH	Foland and Allen (1991)	0.133	0.5123	0.5120	-6.61	-3.46
96-216	Mooselookmeguntic complex	ME	Tomascak et al. (2005)	0.127	0.5123	0.5120	-6.03	-2.62
J98-32-2	Mooselookmeguntic complex	ME	Tomascak et al. (2005)	0.108	0.5119	0.5116	-14.20	-9.85

J98-54	Mooselookmeguntic complex	ME	Tomascak et al. (2005)	0.103	0.5123	0.5120	-7.16	-2.55
J98-93	Mooselookmeguntic complex	ME	Tomascak et al. (2005)	0.102	0.5124	0.5122	-4.41	0.29
J98-111-3	Mooselookmeguntic complex	ME	Tomascak et al. (2005)	0.101	0.5123	0.5121	-5.79	-1.07
J98-40	Mooselookmeguntic complex	ME	Tomascak et al. (2005)	0.125	0.5124	0.5120	-5.36	-1.86
96-60	Mooselookmeguntic complex	ME	Tomascak et al. (2005)	0.101	0.5122	0.5120	-8.41	-3.68
96-91	Mooselookmeguntic complex	ME	Tomascak et al. (2005)	0.107	0.5123	0.5120	-7.57	-3.17
J98-63-1	Mooselookmeguntic complex	ME	Tomascak et al. (2005)	0.132	0.5122	0.5119	-8.70	-5.50
J98-88	Mooselookmeguntic complex complex granite	ME	Tomascak et al. (2005)	0.153	0.5124	0.5120	-5.07	-2.94
J98-92-2	Mooselookmeguntic igneous complex granite	ME	Tomascak et al. (2005)	0.109	0.5121	0.5119	-9.69	-5.38
J98-94	Mooselookmeguntic igneous complex granite	ME	Tomascak et al. (2005)	0.113	0.5124	0.5121	-4.55	-0.42
J98-111-2	Mooselookmeguntic igneous complex granite	ME	Tomascak et al. (2005)	0.091	0.5123	0.5120	-7.41	-2.17
96-100	Mooselookmeguntic igneous complex granite	ME	Tomascak et al. (2005)	0.104	0.5123	0.5121	-6.36	-1.79
96-210	Mooselookmeguntic igneous complex granite	ME	Tomascak et al. (2005)	0.112	0.5122	0.5119	-8.31	-4.16
J98-03	Mooselookmeguntic igneous complex granite	ME	Tomascak et al. (2005)	0.109	0.5123	0.5120	-6.87	-2.53
J98-04	Mooselookmeguntic igneous complex granite	ME	Tomascak et al. (2005)	0.108	0.5123	0.5120	-6.59	-2.22
J98-24	Mooselookmeguntic igneous complex granite	ME	Tomascak et al. (2005)	0.139	0.5121	0.5118	-9.69	-6.88
J98-32	Mooselookmeguntic igneous complex granite	ME	Tomascak et al. (2005)	0.132	0.5122	0.5119	-7.69	-4.49
J98-99	Mooselookmeguntic igneous complex granite	ME	Tomascak et al. (2005)	0.162	0.5123	0.5119	-6.96	-5.27

J98-108	Mooselookmeguntic igneous complex granite	ME	Tomascak et al. (2005)	0.111	0.5122	0.5119	-9.07	-4.85
J98-114	Mooselookmeguntic igneous complex granite	ME	Tomascak et al. (2005)	0.151	0.5123	0.5119	-7.18	-4.95
96-222	Mooselookmeguntic igneous complex monzodiorite	ME	Tomascak et al. (2005)	0.109	0.5124	0.5121	-4.95	-0.62
J98-43	Mooselookmeguntic igneous complex monzodiorite	ME	Tomascak et al. (2005)	0.114	0.5123	0.5120	-6.11	-2.01
J98-100	Mooselookmeguntic igneous complex monzodiorite	ME	Tomascak et al. (2005)	0.100	0.5123	0.5120	-7.33	-2.58
J98-63-2	Mooselookmeguntic igneous complex monzodiorite	ME	Tomascak et al. (2005)	0.115	0.5123	0.5121	-5.72	-1.69
AVNU17	Nulhegan Pluton	VT	Arth and Ayuso (1997)	0.124	0.5123	0.5120	-6.59	-3.02
IPNU05	Nulhegan Pluton	VT	Arth and Ayuso (1997)	0.110	0.5122	0.5119	-8.74	-4.46
SC-105	Stony Creek granite	CT	Wintsch et al. (2014)	0.094	0.5120	0.5118	-12.07	-7.41
SC-205	Stony Creek granite	CT	Wintsch et al. (2014)	0.088	0.5120	0.5118	-12.39	-7.40
SC-505	Stony Creek granite	CT	Wintsch et al. (2014)	0.102	0.5121	0.5118	-10.94	-6.60
NH/S 1-82	Sunapee pluton	NH	Harrison et al. (1987)	0.512	20.0000	-9.0100	-6.56	1.30
MEWC01	West Charleton pluton	VT	Arth and Ayuso (1997)	0.146	0.5123	0.5119	-6.79	-4.42
MEWC02	West Charleton pluton	VT	Arth and Ayuso (1997)	0.150	0.5125	0.5121	-2.69	-0.48
MEWC04	West Charleton pluton	VT	Arth and Ayuso (1997)	0.172	0.5126	0.5121	-1.72	-0.57
MEWI01	Willoughby pluton	VT	Arth and Ayuso (1997)	0.140	0.5123	0.5119	-7.18	-4.50
LYWI08	Willoughby pluton	VT	Arth and Ayuso (1997)	0.096	0.5123	0.5120	-7.37	-2.57
WQD-1	Winnepesaukee pluton	NH	Dorais (2003)	0.110	0.5124	0.5121	-4.37	-0.03
WQD-10	Winnepesaukee pluton	NH	Dorais (2003)	0.150	0.5122	0.5119	-7.74	-5.46
WQD-13	Winnepesaukee pluton	NH	Dorais (2003)	0.095	0.5123	0.5121	-6.75	-1.70

WQD-14	Winnepesaukee pluton	NH	Dorais (2003)	0.129	0.5122	0.5119	-7.61	-4.24
WQD-2	Winnepesaukee pluton	NH	Dorais (2003)	0.129	0.5123	0.5120	-5.81	-2.45
WQD-9	Winnepesaukee pluton	NH	Dorais (2003)	0.138	0.5122	0.5119	-8.33	-5.43
QNH61-23	Winnipesaukee quartz diorite	NH	Foland and Allen (1991)	0.134	0.5124	0.5121	-4.25	-1.14

Appendix B References

Arth, J.G., and Ayuso, R.A., 1997, The Northeast Kingdom batholith, Vermont: Geochronology and Nd, O, Pb, and Sr isotopic constraints on the origin of Acadian granitic rocks: Memoir of the Geological Society of America, v. 191, p. 1–18, doi:10.1130/0-8137-1191-6.1.

Dorais, M.J., 2003, The petrogenesis and emplacement of the New Hamshire plutonic suite: American Journal of Science, v. 303, p. 447.

Dorais, M.J., Pett, T.K., and Tubrett, M., 2009, Garnetites of the Cardigan Pluton, New Hampshire: Evidence for peritectic garnet entrainment and implications for source rock compositions: Journal of Petrology, v. 50, p. 1993–2016, doi:10.1093/petrology/egp058.

Foland, K.A., and Allen, J.C., 1991, Magma sources for Mesozoic anorogenic granites of the White Mountain magma series, New England, USA: Contributions to Mineralogy and Petrology, doi:10.1007/BF00306479.

Harrison, T.M., Aleinikoff, J.N., and Compston, W., 1987, Observations and controls on the occurrence of inherited zircon in Concord-type granitoids, New Hampshire: Geochimica et Cosmochimica Acta, v. 51, p. 2549–2558, doi:10.1016/0016-7037(87)90305-X.

Hill, M.D., Hepburn, J.C., Collins, R.D., Hon, R., and Hanson, L.S., 1984, Igneous rocks of the Nashoba block, eastern Massachusett: New England Intercollegiate Geological Conference,.

Hook, B.P., 2003, Petrology of the Deer Isle Pluton, Coastal Maine: A Complex Mixed Magma System: [MS Thesis]: University of Maine, 185 p.

Koteas, C.G., 2010, Analysis of the Gouldsboro Pluton and the Fehr Granite: Understanding the Scales of Magmatic Processes and Partial Melt Generation from the Deep to Shallow Crust: [PhD Thesis]: University of Massachusetts Amherst, 203 p.

Lathrop, A.S., Blum, J.D., and Chamberlain, C.P., 1994, Isotopic evidence for closed-system anatexis at midcrustal levels: an example from the Acadian Appalachians of New England: Journal of Geophysical Research, v. 99, p. 9453–9468, doi:10.1029/93JB03598.

Tomascak, P.B., Brown, M., Solar, G.S., Becker, H.J., Centorbi, T.L., and Tian, J., 2005, Source contributions to Devonian granite magmatism near the Laurentian border, New Hampshire and western Maine, USA: LITHOS, v. 80, p. 75–99.

Van Wagner, K.J., 2017, Petrogenesis and Concentric Zonation of the Belchertown Intrusive Complex, West-Central Massachusetts: [MS thesis]: University of Massachusetts Amherst, 90 p.

Williamson, K., 1999, K-feldspar Megacrysts, Magma Mingling, and Granitic Magma Evolution in the Lexington Batholith, West-Central Maine: [MS thesis]: University of Massachusetts Amherst, 80 p.

Wintsch, R.P., Yi, K., and Dorais, M.J., 2014, Crustal thickening by tectonic wedging of the Ganderian rocks, southern New England, USA: Evidence from cataclastic zircon microstructures and U–Pb ages: Journal of Structural Geology, v. 69, p. 428–448, doi:https://doi.org/10.1016/j.jsg.2014.07.019.

REFERENCES

Amidon, W.H., Roden-Tice, M., Anderson, A.J., McKeon, R.E., and Shuster, D.L., 2016, Late cretaceous unroofing of the White Mountains, New Hampshire, USA: An episode of passive margin rejuvenation? Geology, v. 44, p. 415–418, doi:10.1130/G37429.1.

Armijo, R., Lacassin, R., Coudurier-Curveur, A., and Carrizo, D., 2015, Coupled tectonic evolution of Andean orogeny and global climate: Earth-Science Reviews, doi:10.1016/j.earscirev.2015.01.005.

Ashwal, L.D., Leo, G.W., Robinson, P., Zartman, R.E., and Hall, D.J., 1979, The Belchertown quartz monzodiorite pluton, West-central Massachusetts; a syntectonic Acadian intrusion: American Journal of Science, v. 279, p. 936–969.

Bird, J.M., and Dewey, J.F., 1970, Lithosphere plate-continental margin tectonics and the evolution of the appalachian orogen: Geological Society of America Bulletin, v. 81, p. 1031–1060, doi:10.1130/0016-7606(1970)81[1031:LPMTAT]2.0.CO;2.

Bosse, V., and Villa, I.M., 2019, Petrochronology and hygrochronology of tectonometamorphic events: Gondwana Research, v. 71, p. 76–90, doi:10.1016/j.gr.2018.12.014.

Bradley, D.C., 1983, Tectonics of the Acadian Orogeny in New England and adjacent Canada (USA): Journal of Geology, v. 91, p. 381–400, doi:10.1086/628785.

Bradley, D.C., McCauley, A.D., and Stillings, L.L., 2017, Mineral-deposit model for lithium-cesium-tantalum pegmatites: Scientific Investigations Report, doi:10.3133/sir20105070O.

Bradley, D.C., and O'Sullivan, P., 2017, Detrital zircon geochronology of pre- and syncollisional strata, Acadian orogen, Maine Appalachians: Basin Research, v. 29, p. 571–590, doi:10.1111/bre.12188.

Campbell, I.H., and Squire, R.J., 2010, The mountains that triggered the Late Neoproterozoic increase in oxygen: The Second Great Oxidation Event: Geochimica et Cosmochimica Acta, v. 74, p. 4187–4206, doi:10.1016/j.gca.2010.04.064.

Clark, G.S., and Kulp, J.L., 1968, Isotopic age study of metamorphism and intrusion in western Connecticut and southeastern New York: American Journal of Science, v. 266, p. 865–894.

Dalziel, I.W.D., and Dewey, J.F., 2019, The classic wilson cycle revisited: Geological Society Special Publication, v. 470, p. 19–38, doi:10.1144/SP470.1.

DeCelles, P.G., 2004, Late Jurassic to Eocene evolution of the Cordilleran thrust belt and foreland basin system, western U.S.A: American Journal of Science, v. 304, p. 105–168, doi:10.2475/ajs.304.2.105.

Farner, M.J., and Lee, C.T.A., 2017, Effects of crustal thickness on magmatic differentiation in subduction zone volcanism: A global study: Earth and Planetary Science Letters, doi:10.1016/j.epsl.2017.04.025.

Faul, H., Stern, T.W., Thomas, H.H., and Elmore, P.L.D., 1963, Ages of intrusion and metamorphism in the northern Appalachians: American Journal of Science, v. 261, p. 1–19.

France-Lanord, C., and Derry, L.A., 1997, Organic carbon burial forcing of the carbon cycle from himalayan erosion: Nature, doi:10.1038/36324.

Gehrels, G., 2014, Detrital Zircon U-Pb Geochronology Applied to Tectonics: Annual Review of Earth and Planetary Sciences, v. 42, p. 127–149, doi:10.1146/annurevearth-050212-124012.
Harper, C.T., 1968, Isotopic ages from the Appalachians and their tectonic significance: Canadian Journal of Earth Sciences, v. 5, p. 49–59.
Harrison, T.M., Célérier, J., Aikman, A.B., Hermann, J., and Heizler, M.T., 2009, Diffusion of 40Ar in muscovite: Geochimica et Cosmochimica Acta, v. 73, p. 1039–1051, doi:10.1016/j.gca.2008.09.038.
Harrison, T.M., Copeland, P., Kidd, W.S.F., and Yin, A., 1992, Raising Tibet: Science, v. 255, p. 1663–1670, doi:10.1126/science.255.5052.1663.
Hollocher, K., Robinson, P., Lucas, B., and Mabee, S., 2019, Geochemistry of intrusive rocks on the Prescott Peninsula, central Massachusetts, USA: Implications for late detachment faulting within the Ordovician Taconian volcanic arc: American Journal of Science, v. 319, p. 658–693, doi:10.2475/08.2019.02.
Hurley, P.M., Boucot, A.J., Albee, A.L., Faul, H., Pinson, W.H., and Fairbairn, H.W., 1959, Minimum age of the Lower Devonian slate near Jackman, Maine: Geological Society of America Bulletin, v. 70, p. 947–950.
Hurley, P.M., Fairbairn, H.W., Pinson, W.H., and Faure, G., 1960, KA and Rb-Sr minimum ages for the Pennsylvanian section in the Narragansett Basin: Geochimica et Cosmochimica Acta, v. 18, p. 247–258.
Iaffaldano, G., Bunge, H.P., and Dixon, T.H., 2006, Feedback between mountain belt growth and plate convergence: Geology, v. 34, p. 893–896, doi:10.1130/G22661.1.
Kapp, P., and DeCelles, P.G., 2019, Mesozoic–Cenozoic geological evolution of the Himalayan-Tibetan orogen and working tectonic hypotheses: American Journal of Science, v. 319, p. 159–254, doi:10.2475/03.2019.01.
Karabinos, P., Macdonald, F.A., and Crowley, J.L., 2017, Bridging the gap between the foreland and hinterland I: Geochronology and plate tectonic geometry of Ordovician magmatism and terrane accretion on the Laurentian margin of New England: American Journal of Science, v. 317, p. 515–554, doi:10.2475/05.2017.01.
Keller, B., and Schoene, B., 2018, Plate tectonics and continental basaltic geochemistry throughout Earth history: Earth and Planetary Science Letters, v. 481, p. 290–304, doi:10.1016/j.epsl.2017.10.031.
Keller, C.B., and Schoene, B., 2012, Statistical geochemistry reveals disruption in secular lithospheric evolution about 2.5 Gyr ago: Nature, v. 485, p. 490–493, doi:10.1038/nature11024.
Kellett, D.A., Pehrsson, S., Skipton, D.R., Regis, D., Camacho, A., Schneider, D.A., and Berman, R., 2020, Thermochronological history of the Northern Canadian Shield: Precambrian Research, v. 342, p. 105703, doi:10.1016/j.precamres.2020.105703.
Kim, J., Klepeis, K., Webb, L., and Amidon, W., 2019, New Insights on the Ordovician-Neogene Tectonic History of the Champlain Valley Belt from Drone Surveys, Photogammetry, and Geochronology, West-Central Vermont: New England Intercollegiate Geological Conference, v. B1, p. 90.
Levin, V., Long, M.D., Skryzalin, P., Li, Y., and López, I., 2018, Seismic evidence for a recently formed mantle upwelling beneath New England: Geology, v. 46, p. 87–90, doi:10.1130/G39641.1.
Li, C., Gao, H., and Williams, M.L., 2020, Seismic characteristics of the eastern North American crust with Ps converted waves: terrane accretion and modification of continental crust: Journal of Geophysical Research: Solid Earth, doi:10.1029/2019jb018727.

Li, C., Gao, H., Williams, M.L., and Levin, V., 2018, Crustal Thickness Variation in the Northern Appalachian Mountains: Implications for the Geometry of 3-D Tectonic Boundaries Within the Crust: Geophysical Research Letters, v. 45, p. 6061–6070, doi:10.1029/2018GL078777.
Long, M.D., Aragon, J.C., Yang, X., Gao, H., Goldhagen, G., Ford, H., and Kuiper, Y.D., 2019, Modification of Lithospheric Structure beneath Connecticut via Subduction, Terrane Accretion, and Rifting: Insights from the SEISCONN Experiment, in Geological Society of America Abstracts with Programs, doi:10.1130/abs/2019NE-327980.
Long, L.E., and Kulp, J.L., 1962, Isotopic age study of the metamorphic history of the Manhattan and Reading Prongs: Geological Society of America Bulletin, v. 73, p. 969–996.
Macdonald, F.A., Karabinos, P.M., Crowley, J.L., Hodgin, E.B., Crockford, P.W., and Delano, J.W., 2017, Bridging the gap between the foreland and hinterland II: Geochronology and tectonic setting of Ordovician magmatism and basin formation on the Laurentian margin of New England and Newfoundland: American Journal of Science, v. 317, p. 555.
Macdonald, F.A., Ryan-Davis, J., Coish, R.A., Crowley, J.L., and Karabinos, P.M., 2014, A newly identified Gondwanan terrane in the northern Appalachian Mountains: Implications for the Taconic orogeny and closure of the Iapetus Ocean: Geology, v. 43, p. 539–542, doi:10.1130/G36575Y.1.
Macdonald, F.A., Swanson-Hysell, N. l, Park, Y., Lisiecki, L., and Jagoutz, O., 2019, Arc-continent collisions in the tropics set Earth’s climate state: Science, v. 364, p. 181–184.
McKerrow, W.S., and Ziegler, A.M., 1972, Palaeozoic Oceans: Nature Physical Science, doi:10.1038/physci240092b0.
Meert, J.G., and Lieberman, B.S., 2008, The Neoproterozoic assembly of Gondwana and its relationship to the Ediacaran-Cambrian radiation: Gondwana Research, v. 14, p. 5–21, doi:10.1016/j.gr.2007.06.007.
Miao, Y., Herrmann, M., Wu, F., Yan, X., and Yang, S., 2012, What controlled Mid-Late Miocene long-term aridification in Central Asia? - Global cooling or Tibetan Plateau uplift: A review: Earth-Science Reviews, v. 112, p. 155–172, doi:10.1016/j.earscirev.2012.02.003.
Molnar, P., England, P.C., and Jones, C.H., 2015, Mantle dynamics, isostasy, and the support of high terrain: Journal of Geophysical Research: Solid Earth, v. 120, p. 1932–1957, doi:10.1002/2014JB011724.
Molnar, P., England, P., and Martinod, J., 1993, Mantle dynamics, uplift of the Tibetan Plateau, and the Indian Monsoon: Reviews of Geophysics, v. 31, p. 357–396, doi:10.1029/93RG02030.
Naylor, R.S., 1971, Acadian orogeny: An abrupt and brief event: Science, v. 172, p. 558–560, doi:10.1126/science.172.3983.558.
Perrot, M., Tremblay, A., Ruffet, G., Labrousse, L., Gervais, F., and Caroir, F., 2020, Diachronic metamorphic and structural evolution of the Connecticut Valley–Gaspé trough, Northern Appalachians: Journal of Metamorphic Geology, v. 38, p. 3–27, doi:10.1111/jmg.12510.

Porder, S., Vitousek, P.M., Chadwick, O.A., Chamberlain, C.P., and Hilley, G.E., 2007, Uplift, erosion, and phosphorus limitation in terrestrial ecosystems: Ecosystems, v. 10, p. 159–171, doi:10.1007/s10021-006-9011-x.
Profeta, L., Ducea, M.N., Chapman, J.B., Paterson, S.R., Gonzales, S.M.H., Kirsch, M., Petrescu, L., and DeCelles, P.G., 2015, Quantifying crustal thickness over time in magmatic arcs: Scientific Reports, doi:10.1038/srep17786.
Raymo, M.E., and Ruddiman, W.F., 1992, Tectonic forcing of late Cenozoic climate: Nature, v. 359, p. 117–122, doi:10.1038/359117a0.
Richards, J.P., 2015, Tectonic, magmatic, and metallogenic evolution of the Tethyan orogen: From subduction to collision: Ore Geology Reviews, v. 70, p. 323–345, doi:10.1016/j.oregeorev.2014.11.009.
Roberts, N.M.W., and Spencer, C.J., 2015, The zircon archive of continent formation through time: Geological Society Special Publication, doi:10.1144/SP389.14.
Robinson, P., and Hall, L.M., 1980, Tectonic synthesis of southern New England, in International Geological Correlation Project, Proceedings, Project, v. 27, p. 73–82.
Robinson, P., Tucker, R.D., Bradley, D., Berry IV, H.N., and Osberg, P.H., 1998, Paleozoic orogens in New England, USA: GFF, v. 120, p. 119–148, doi:10.1080/11035899801202119.
Ryan, P.D., and Dewey, J.F., 2019, The sources of metamorphic heat during collisional orogeny: The Barrovian Enigma: Canadian Journal of Earth Sciences, v. 56, p. 1309–1317, doi:10.1139/cjes-2018-0182.
Schmandt, B., and Lin, F.C., 2014, P and S wave tomography of the mantle beneath the United States: Geophysical Research Letters, doi:10.1002/2014GL061231.
Schmittner, A., Silva, T.A.M., Fraedrich, K., Kirk, E., and Lunkeit, F., 2011, Effects of mountains and ice sheets on global ocean circulation: Journal of Climate, v. 24, p. 2814–2829, doi:10.1175/2010JCLI3982.1.
van Staal, C.R., Dewey, J.F., Niocaill, C. Mac, and Mckerrow, W.S., 1998, The Cambrian-Silurian tectonic evolution of the northern Appalachians and British Caledonides: history of a complex, west and southwest Pacific- type segment of Iapetus: Geological Society Special Publication, v. 143, p. 197–242, doi:10.1144/GSL.SP.1998.143.01.17.
van Staal, C.R., Whalen, J.B., Valverde-Vaquero, P., Zagorevski, A., and Rogers, N., 2009, Pre-Carboniferous, episodic accretion-related, orogenesis along the Laurentian margin of the northern Appalachians: Geological Society, London, Special Publications, v. 327, p. 271–316, doi:10.1144/SP327.13.
Sun, W., Zhang, H., Ling, M.X., Ding, X., Chung, S.L., Zhou, J., Yang, X.Y., and Fan, W., 2011, The genetic association of adakites and Cu-Au ore deposits: International Geology Review, v. 53, p. 691–703, doi:10.1080/00206814.2010.507362.
Thompson, J.B.J., Robinson, P., and Trask, N.J., 1968, Nappes and gneiss domes in westcentral New England, in Zen, E.-A., White, W.S., Hadley, J., and Thompson, J.J. eds., Studies of Appalachian geology: Northern and Maritime, New York, Interscience, p. 203–218.

Tracy, R.J., Robinson, P., and Thompson, A.B., 1976, Garnet composition and zoning in the determination of temperature and pressure of metamorphism, central Massachusetts: American Mineralogist, v. 61, p. 762–775.
Turner, S.J., and Langmuir, C.H., 2015, The global chemical systematics of arc front stratovolcanoes: Evaluating the role of crustal processes: Earth and Planetary Science Letters, doi:10.1016/j.epsl.2015.03.056.
Valley, P.M., Walsh, G.J., Merschat, A.J., and McAleer, R.J., 2019, Geochronology of the Oliverian Plutonic Suite and the Ammonoosuc Volcanics in the Bronson Hill arc: Western New Hampshire, USA: Geosphere, v. 16, doi:10.1130 /GES02170.1.
Waldron, J.W.F., Schofield, D.I., and Murphy, J.B., 2017, Diachronous Palaeozoic accretion of peri-Gondwanan terranes at the Laurentianmargin: Geological Society of London Special Publication,.
Williams, M.L., Jercinovic, M.J., Mahan, K.H., and Dumond, G., 2017, Electron Microprobe Petrochronology: Reviews in Mineralogy and Geochemistry, v. 83, p. 153–182, doi:10.2138/rmg.2017.83.5.
Wilson, J.T., 1966, Did the Atlantic Close and then Re-Open? Nature, doi:10.1038/211676a0.
Wise, D.U., 1992, Dip domain method applied to the Mesozoic Connecticut Valley Rift Basins: Tectonics, v. 11, p. 1357–1368, doi:10.1029/92TC01103.
Wolfe, O.M., and Spear, F.S., 2018, Determining the amount of overstepping required to nucleate garnet during Barrovian regional metamorphism, Connecticut Valley Synclinorium: Journal of Metamorphic Geology, v. 36, p. 79–94, doi:10.1111/jmg.12284.
Yakymchuk, C., Clark, C., and White, R.W., 2017, Phase Relations, Reaction Sequences and Petrochronology: Reviews in Mineralogy and Geochemistry, v. 83, p. 13–53, doi:10.2138/rmg.2017.83.2.
Yang, X., and Gao, H., 2018, Full-Wave Seismic Tomography in the Northeastern United States: New Insights Into the Uplift Mechanism of the Adirondack Mountains: Geophysical Research Letters, v. 45, p. 5992–6000, doi:10.1029/2018GL078438.
Yasunari, T., 2020, The Uplift of the Himalaya-Tibetan Plateau and Human Evolution: An Overview on the Connection Among the Tectonics, Eco-Climate System and Human Evolution During the Neogene Through the Quaternary Period, in Himalayan Weather and Climate and their Impact on the Environment, p. 281–305, doi:10.1007/978-3-030-29684-1_15.
Zandt, G., Gilbert, H., Owens, T.J., Ducea, M., Saleeby, J., and Jones, C.H., 2004, Active foundering of a continental arc root beneath the southern Sierra Nevada in California: Nature, doi:10.1038/nature02847.
Zartman, R.E., 1977, Geochronology of some alkalic rock provinces in eastern and central United States: Annual Review of Earth and Planetary Sciences, v. 5, p. 257–286.
Zartman, R.E., 1988, Three decades of geochronologic studies in the New England Appalachians: Geological Society of America Bulletin, v. 100, p. 1168–1180, doi:10.1130/0016-7606(1988)100<1168:TDOGSI>2.3.CO;2.
Zartman, R.E., Hurley, P.M., Krueger, H.W., and Giletti, B.J., 1970, A Permian disturbance of K-Ar radiometric ages in New England: Its occurrence and cause: Geological Society of America Bulletin, v. 81, p. 3359–3374.
Zhisheng, A., Kutzbach, J.E., Prell, W.L., and Porter, S.C., 2001, Evolution of Asian monsoons and phased uplift of the Himalaya - Tibetan plateau since Late Miocene times: Nature, doi:10.1038/35075035.

Alexander, E., Wielicki, M.M., Harrison, T.M., DePaolo, D.J., Zhao, Z.D., and Zhu, D.C., 2019, Hf and Nd Isotopic Constraints on Pre - and Syn - collisional Crustal Thickness of Southern Tibet Journal of Geophysical Research : Solid Earth: Journal of Geophysical Research: Solid Earth, v. 124, p. 1–17, doi:10.1029/2019JB017696.
Amidon, W.H., Roden-Tice, M., Anderson, A.J., McKeon, R.E., and Shuster, D.L., 2016, Late cretaceous unroofing of the White Mountains, New Hampshire, USA: An episode of passive margin rejuvenation? Geology, v. 44, p. 415–418, doi:10.1130/G37429.1.
Attenoukon, M.B., 2009, Age and Origins of Metamorphic Fabrics and the Tectonics of Southeastern New England: [PhD thesis] Indiana University, 295 p.
Bird, J.M., and Dewey, J.F., 1970, Lithosphere plate-continental margin tectonics and the evolution of the appalachian orogen: Geological Society of America Bulletin, v. 81, p. 1031–1060, doi:10.1130/0016-7606(1970)81[1031:LPMTAT]2.0.CO;2.
Blackburn, T., Bowring, S.A., Schoene, B., Mahan, K., and Dudas, F., 2011, U-Pb thermochronology: Creating a temporal record of lithosphere thermal evolution: Contributions to Mineralogy and Petrology, doi:10.1007/s00410-011-0607-6.
Blackburn, T.J., Olsen, P.E., Bowring, S.A., McLean, N.M., Kent, D. V., Puffer, J., McHone, G., Rasbury, E.T., and Et-Touhami, M., 2013, Zircon U-Pb geochronology links the end-triassic extinction with the central Atlantic magmatic province: Science, doi:10.1126/science.1234204.
Bradley, D.C., 2011, Secular trends in the geologic record and the supercontinent cycle: Earth-Science Reviews, v. 108, p. 16–33, doi:10.1016/j.earscirev.2011.05.003.
Bradley, D.C., O'Sullivan, P., and Bradley, L.M., 2015, Detrital zircons from modern sands in New England and the timing of Neoproterozoic to Mesozoic Magmatism: American Journal of Science, v. 315, p. 460.
Bradley, D.C., Tucker, R.D., Lux, D.R., Harris, A.G., and McGregor, D.C., 2000, Migration of the Acadian Orogen and Foreland Basin across the northern Appalachians of Maine and adjacent areas: U.S. Geological Survey Professional Paper, v. 1624, p. 1- 49.
Cartwright, S.F.A., West, Jr., D.P., and Amidon, W.H., 2019, Depositional constraints from detrital zircon geochronology of strata from multiple lithotectonic belts in south-central Maine, USA: Atlantic Geology, v. 136, p. 093–136, doi:10.4138/atlgeol.2019.003.
Chapman, J.B., Ducea, M.N., DeCelles, P.G., and Profeta, L., 2015, Tracking changes in crustal thickness during orogenic evolution with Sr/Y: An example from the North American Cordillera: Geology, v. 43, p. 919–922, doi:10.1130/G36996.1.
Chapman, J.B., Ducea, M.N., Kapp, P., Gehrels, G.E., and DeCelles, P.G., 2017, Spatial and temporal radiogenic isotopic trends of magmatism in Cordilleran orogens: Gondwana Research, v. 48, p. 189–204, doi:10.1016/j.gr.2017.04.019.
Chapman, J.B., and Kapp, P., 2017, Tibetan Magmatism Database: Geochemistry, Geophysics, Geosystems, v. 18, p. 4229–4234, doi:10.1002/2017GC007217.
Chiaradia, M., 2015, Crustal thickness control on Sr/Y signatures of recent arc magmas: an Earth scale perspective: Science Reports, v. 5, doi:10.1038/srep08115.
Condie, K.C., and Kröner, A., 2008, When did plate tectonics begin? Evidence from the geologic record: Special Paper of the Geological Society of America, v. 440, p. 281–294, doi:10.1130/2008.2440(14).
Crough, S.T., 1981, Mesozoic hotspot epeirogeny in eastern North America: Geology, v. 9, p. 2–6, doi:10.1130/0091-7613(1981)9<2:MHEIEN>2.0.CO;2.

DePaolo, D.J., 1981, Neodymium isotopes in the Colorado Front Range and crust-mantle evolution in the Proterozoic: Nature, v. 291, p. 193–196, doi:10.1038/291193a0.
DePaolo, D.J., Harrison, T.M., Wielicki, M., Zhao, Z., Zhu, D.C., Zhang, H., and Mo, X., 2019, Geochemical evidence for thin syn-collision crust and major crustal thickening between 45 and 32 Ma at the southern margin of Tibet: Gondwana Research, v. 73, p. 123–135, doi:10.1016/j.gr.2019.03.011.
DePaolo, D.J., Perry, F., and Baldrige, W., 1992, Crustal versus mantle sources of granitic magmas: a two-parameter model based on Nd isotopic studies: Earth Science Transactions of the Royal Society of Edinburgh, v. 83, p. 439–446.
Doherty, J.T., and Lyons, J.B., 1980, Mesozoic erosion rates in northern New England.: Geological Society of America Bulletin, v. 91, p. 16–20, doi:10.1130/0016-7606(1980)91<16:MERINN>2.0.CO;2.
Dorais, M.J., 2003, The petrogenesis and emplacement of the New Hamshire plutonic suite: American Journal of Science, v. 303, p. 447.
Dorais, M.J., and Paige, M.L., 2000, Regional geochemical and isotopic variations of Northern New England plutons: Implications for magma sources and for Grenville and Avalon basement-terrane boundaries: Bulletin of the Geological Society of America, v. 112, p. 900–914, doi:10.1130/0016-7606(2000)112<900:RGAIVO>2.0.CO;2.
Dorais, M.J., Wintsch, R.P., Kunk, M.J., Aleinikoff, J., Burton, W., Underdown, C., and Kerwin, C.M., 2012, P-T-t conditions, Nd and Pb isotopic compositions and detrital zircon geochronology of the Massabesic Gneiss Complex, New Hampshire: Isotopic and metamorphic evidence for the identification of Gander basement, central New England: American Journal of Science, v. 312, p. 1049, doi:10.2475/10.2012.01.
Eby, N., 1989, Petrology and geochemistry of Mount Yamaska, Quebec, Canada: a mafic representative of the Monteregian Hills igneous province, in p. 63–82, doi:10.13140/RG.2.1.2270.3760.
Eby, G.N., Krueger, H.W., and Creasy, J.W., 1992, Geology, geochronology, and geochemistry of the White Mountain batholith, New Hampshire: Special Paper of the Geological Society of America, doi:10.1130/SPE268-p379.
England, P.C., and Thompson, A.B., 1984, Pressure - temperature - time paths of regional metamorphism I. heat transfer during the evolution of regions of thickened continental crust: Journal of Petrology, doi:10.1093/petrology/25.4.894.
Ettensohn, F.R., 1994, Tectonic Control on Formation and Cyclicity of Major Appalachian Unconformities and Associated Stratigraphic Sequences, in Tectonic And Eustatic Controls on Sedimentary Cycles, doi:10.2110/csp.94.04.0217.
Ettensohn, F.R., Pashin, J.C., and Gilliam, W., 2019, The Appalachian and Black Warrior Basins: Foreland Basins in the Eastern United States, in Miall, A.D. ed., The Sedimentary Basins of the United States and Canada, p. 129–237, doi:10.1016/b978-0-444-63895-3.00004-8.
Eusden, J.D., Baker, S., Cargill, J., Divan, E., Hillenbrand, I., O'Sullivan, P., and Wheatcroft, A., 2017, C3: Transect From the Migmatized Central Maine Belt to the Bronson Hill Anticlinorium:
Eusden, J.D., and Barreiro, B., 1988, The timing of peak high-grade metamorphism in central-eastern New England: Atlantic Geology, v. 24, p. 241–255.

Eusden, J.D., Guzofski, C.A., Robinson, A.C., and Tucker, R.D., 2000, Timing of the Acadian Orogeny in Northern New Hampshire: The Journal of Geology, v. 108, p. 219–232, doi:10.1086/314396.

Farner, M.J., and Lee, C.T.A., 2017, Effects of crustal thickness on magmatic differentiation in subduction zone volcanism: A global study: Earth and Planetary Science Letters, doi:10.1016/j.epsl.2017.04.025.

Foland, K.A., Henderston, C.M.B., and Gleason, J., 1985, Petrogenesis of the magmatic complex at Mount Ascutney, Vermont, USA I: Assimilation of crust by mafic magmas based on Sr and O isotopic and major element relationships: Contributions to Mineralogy and Petrology, v. 90, p. 331–345.

Fu, B., Cliff, J., and Zartman, R.E., 2014, Zircon oxygen isotopic constraints from plutonic rocks on the magmatic and crustal evolution of the northern Appalachians in southern New England, USA: Canadian Journal of Earth Sciences, v. 51, p. 485–499.

Gale, A., Dalton, C.A., Langmuir, C.H., Su, Y., and Schilling, J.G., 2013, The mean composition of ocean ridge basalts: v. 14, 489–518 p., doi:10.1029/2012GC004334.

Gaschnig, R.M., 2019, Benefits of a Multiproxy Approach to Detrital Mineral Provenance Analysis: An Example from the Merrimack River, New England, USA: Geochemistry, Geophysics, Geosystems, v. 20, p. 1557–1573, doi:10.1029/2018GC008005.

Gehrels, G., 2014, Detrital Zircon U-Pb Geochronology Applied to Tectonics: Annual Review of Earth and Planetary Sciences, v. 42, p. 127–149, doi:10.1146/annurevearth-050212-124012.

Guo, P., Niu, Y., Sun, P., Gong, H., and Wang, X., 2020, Lithosphere thickness controls continental basalt compositions: An illustration using Cenozoic basalts from eastern China: Geology, v. 48, p. 128–133, doi:10.1130/G46710.1.

Harrison, T.M., 1982, Diffusion of 40Ar in Hornblende: Contributions to Mineralogy and Petrology, v. 78, p. 324–331, doi:10.2475/ajs.303.5.410.

Harrison, T.M., Aleinikoff, J.N., and Compston, W., 1987, Observations and controls on the occurrence of inherited zircon in Concord-type granitoids, New Hampshire: Geochimica et Cosmochimica Acta, v. 51, p. 2549–2558, doi:10.1016/0016-7037(87)90305-X.

Harrison, T.M., Spear, F.S., and Heizler, M.T., 1989, Geochronologic studies in central New England II: post-Acadian hinged and differential uplift: Geology, v. 17, p. 185–189, doi:10.1130/0091-7613(1989)017<0185:GSICNE>2.3.CO;2.

Hatcher, R.D., 2010, The Appalachian orogen: A brief summary: From Rodinia to Pangea: The Lithotectonic Record of the Appalachian Region: Geological Society of America Memoir, v. 206, p. 1–19, doi:10.1130/2010.1206(01).

Hibbard, J.P., van Staal, C.R., Rankin, D.W., and Williams, H., 2006, Lithotectonic map of the Appalachian Orogen, Canada-United States of America:, doi:10.4095/221912.

Hillenbrand, I.W., 2020, Crustal evolution of the New England Appalachians: the rise and fall of a long-lived orogenic plateau: University of Massachusetts, 159 p.

Hillenbrand, I., Williams, M.L., Li, C., and Gao, H., 2019, Rise and Fall of the Acadian Altiplano: Geological Society of America Abstracts with Programs, v. 51, doi:10.1130/abs/2019AM-340957.

Hu, F., Ducea, M.N., Liu, S., and Chapman, J.B., 2017, Quantifying Crustal Thickness in Continental Collisional Belts : Global Perspective and a Geologic Application: Scientific Reports, v. 7, p. 1–10, doi:10.1038/s41598-017-07849-7.

Hubbard, M.S., 1999, Norumbega fault zone: Part of an orogen-parallel strike-slip system, northern Appalachians: Special Paper of the Geological Society of America, p. 155–166, doi:10.1130/0-8137-2331-0.155.
Jamieson, R.A., Beaumont, C., Medvedev, S., and Nguyen, M.H., 2004, Crustal channel flows: 2. Numerical models with implications for metamorphism in the Himalayan-
Tibetan orogen: Journal of Geophysical Research: Solid Earth, v. 109, p. 1–24, doi:10.1029/2003JB002811.
Jourdan, F., Marzoli, A., Bertrand, H., Cirilli, S., Tanner, L.H., Kontak, D.J., McHone,
G., Renne, P.R., and Bellieni, G., 2009, 40Ar/39Ar ages of CAMP in North America: implications for the Triassic–Jurassic boundary and the 40K decay constant bias: LITHOS, v. 110, p. 167–180.
Karabinos, P., Macdonald, F.A., and Crowley, J.L., 2017, Bridging the gap between the foreland and hinterland I: Geochronology and plate tectonic geometry of Ordovician
magmatism and terrane accretion on the Laurentian margin of New England: American Journal of Science, v. 317, p. 515–554, doi:10.2475/05.2017.01.
Karabinos, P., Morris, D., Hamilton, M., and Rayner, N., 2008, Age, origin, and tectonic significance of Mesoproterozoic and Silurian felsic sills in the Berkshire massif,
Massachusetts: American Journal of Science, v. 308, p. 787–812, doi:10.2475/06.2008.03.
Karabinos, P., Samson, S.D., Hepburn, J.C., and Stoll, H.M., 1998, Taconian orogeny in
the New England Appalachians: Collision between Laurentia and the Shelburne Falls arc: Geology, v. 26, p. 215–218, doi:10.1130/0091-7613(1998)026<0215:TOITNE>2.3.CO;2.
Karabinos, P., Westerman, D.S., Crowley, J.L., and Macdonald, F.A., 2019, Stratigraphic and Structural Evidence for a Fault Contact Between Ordovician Arc Rocks and the Connecticut Valley-Gaspé Sequence in Vermont, in New England Intercollegiate Geological Conference, v. C1, p. 145–176.
Keller, C.B., Husson, J.M., Mitchell, R.N., Bottke, W.F., Gernon, T.M., Boehnke, P., Bell, E.A., Swanson-Hysell, N.L., and Peters, S.E., 2019, Neoproterozoic glacial origin of the Great Unconformity: Proceedings of the National Academy of Sciences, v. 116, p. 1136–1145, doi:10.1073/pnas.1804350116.
Keller, B., and Schoene, B., 2018, Plate tectonics and continental basaltic geochemistry
throughout Earth history: Earth and Planetary Science Letters, v. 481, p. 290–304, doi:10.1016/j.epsl.2017.10.031.
Keller, C.B., and Schoene, B., 2012, Statistical geochemistry reveals disruption in secular
lithospheric evolution about 2.5 Gyr ago: Nature, v. 485, p. 490–493, doi:10.1038/nature11024.
Kellett, D.A., Pehrsson, S., Skipton, D.R., Regis, D., Camacho, A., Schneider, D.A., and
Berman, R., 2020, Thermochronological history of the Northern Canadian Shield: Precambrian Research, v. 342, p. 105703, doi:10.1016/j.precamres.2020.105703.

Kellett, D.A., van Staal, C., Wilson, R.A., and Rogers, N., 2017, The age of salinic deformation constrained by 40Ar/39Ar dating of multiple cleavage domains: Bathurst Supergroup, New Brunswick Appalachians: American Journal of Science,
v. 317, p. 338–368.
Kim, J., Klepeis, K., Webb, L., and Amidon, W., 2019, New Insights on the Ordovician-Neogene Tectonic History of the Champlain Valley Belt from Drone Surveys, Photogammetry, and Geochronology, West-Central Vermont: New England Intercollegiate Geological Conference, v. B1, p. 90.
Kinney, S.T., Maclennan, S.A., Setera, J., Schoene, B., Vantongeren, J., Oksen, P.E., Strauss, J. V, Town, C.F., and Bradley, D., 2019, Causal Implications of a new zircon U-Pb frameowrk for Mesozoic magmatism in northern New England and
Quebec: What are the Rift/Post-rift igneous rocks of the White Mountains? Geological Society of America Abstracts with Programs, v. 51,
doi:10.1130/abs/2019NE-328495.
Kuiper, Y.D., 2016, Development of the Norumbega fault system in mid-Paleozoic New England, USA: An integrated subducted oceanic ridge model: Geology, v. 44, p.
455–458, doi:10.1130/G37599.1.
Kuiper, Y.D., Thompson, M.D., Barr, S.M., White, C.E., Hepburn, J.C., and Crowley, J.L., 2017, Detrital zircon evidence for Paleoproterozoic West African crust along the eastern North American continental margin, Georges Bank, offshore Massachusetts, USA: Geology, v. 45, p. 811–814.
Kumarapeli, P.S., Dunning, G.R., Pintson, H., and Shaver, J., 1989, Geochemistry and U–Pb zircon age of comenditic metafelsites of the Tibbit Hill Formation, Quebec Appalachians: Canadian Journal of Earth Sciences, v. 26, p. 1374–1383.
Levin, V., Long, M.D., Skryzalin, P., Li, Y., and López, I., 2018, Seismic evidence for a recently formed mantle upwelling beneath New England: Geology, v. 46, p. 87–90,
doi:10.1130/G39641.1.
Li, C., Gao, H., and Williams, M.L., 2020, Seismic characteristics of the eastern North American crust with Ps converted waves: terrane accretion and modification of continental crust: Journal of Geophysical Research: Solid Earth,
doi:10.1029/2019jb018727.
Li, C., Gao, H., Williams, M.L., and Levin, V., 2018, Crustal Thickness Variation in the Northern Appalachian Mountains: Implications for the Geometry of 3-D Tectonic Boundaries Within the Crust: Geophysical Research Letters, v. 45, p. 6061–6070,
doi:10.1029/2018GL078777.
Long, M.D., Benoit, M.H., Aragon, J.C., and King, S.D., 2019, Seismic imaging of midcrustal structure beneath central and eastern North America: Possibly the elusive Grenville deformation? Geology, v. 47, p. 371–374, doi:10.1130/G46077.1.
Macdonald, F.A., Karabinos, P.M., Crowley, J.L., Hodgin, E.B., Crockford, P.W., and Delano, J.W., 2017, Bridging the gap between the foreland and hinterland II: Geochronology and tectonic setting of Ordovician magmatism and basin formation
on the Laurentian margin of New England and Newfoundland: American Journal of Science, v. 317, p. 555.
Macdonald, F.A., Ryan-Davis, J., Coish, R.A., Crowley, J.L., and Karabinos, P.M., 2014,
A newly identified Gondwanan terrane in the northern Appalachian Mountains: Implications for the Taconic orogeny and closure of the Iapetus Ocean: Geology, v.
43, p. 539–542, doi:10.1130/G36575Y.1.

Massey, M.A., Berg, C.A., and Moecher, D.P., 2017a, Pre- and Syn-Kinematic P-T Constraints Acoss a Zone of Transpession, Vertical Extrusion, and Lateral Escape in the Southern New England Appalachians: Geological Society of America Abstracts with Programs, v. 49, doi:10.1130/abs/2017NE-291167.
Massey, M.A., Moecher, D.P., Walker, T.B., O'Brien, T.M., and Rohrer, L.P., 2017b, The role and extent of dextral transpression and lateral escape on the post-Acadian tectonic evolution of South-Central New England: American Journal of Science, v. 317, p. 34–94, doi:10.2475/01.2017.02.
McCulla, J.K., 2016, Dating Deformation in the Palmer Zone of Transpression, Central Massachusetts: Temporal Constraints on Models for Progressive Deformation in the Middle Crust [MS thesis]: University of Kentucky, 166 p.
McHone, J.G., Hussey II, A.M., West Jr., D.P., and Bailey, D.G., 2014, The Christmas Cove Dyke of coastal Maine, USA, and regional sources for Early Mesozoic flood basalts in northeastern North America: Atlantic Geology, v. 50, p. 66–90, doi:10.4138/atlgeol.2014.004.
McKerrow, W.S., and Ziegler, A.M., 1972, Palaeozoic Oceans: Nature Physical Science, doi:10.1038/physci240092b0.
McWilliams, C.K., Walsh, G.J., and Wintsch, R.P., 2010, Silurian-Devonian age and tectonic setting of the Connecticut Valley-Gaspé trough in Vermont based on U-Pb SHRIMP analyses of detrital zircons: American Journal of Science, v. 310, p. 325–363, doi:10.2475/05.2010.01.
Menke, W., Lamoureux, J., Abbott, D., Hopper, E., Hutson, D., and Marrero, A., 2018, Crustal Heating and Lithospheric Alteration and Erosion Associated With Asthenospheric Upwelling Beneath Southern New England (USA): Journal of Geophysical Research: Solid Earth, v. 123, p. 8995–9008, doi:10.1029/2018JB015921.
Mercer, C.M., and Hodges, K. V, 2016, ArAR — A software tool to promote the robust comparison of K–Ar and 40Ar/39Ar dates published using different decay, isotopic, and monitor-age parameters: Chemical Geology, v. 440, p. 148–163, doi:https://doi.org/10.1016/j.chemgeo.2016.06.020.
Miller, B. V, Barr, S.M., Tesfai, F., and White, C.E., 2018, Tonian Fe-Ti-P ferronorite and alkali anorthosite in the northern Appalachian orogen, southern New Brunswick, Canada: Amazonian basement in Ganderia? Precambrian Research, v. 317, p. 77–88.
Moench, R.H., and Aleinikoff, J.N., 2002, Stratigraphy, geochronology, and accretionary terrane settings of two Bronson Hill arc sequences, northern New England: Physics and Chemistry of the Earth, v. 27, p. 47–95, doi:10.1016/S1474-7065(01)00003-1.
Nelson, K.D. et al., 1996, Partially molten middle crust beneath southern Tibet: Synthesis of project INDEPTH results: Science, v. 274, p. 1684–1688, doi:10.1126/science.274.5293.1684.
Olsen, P.E., 1997, Stratigraphic Record of the Early Mesozoic Breakup of Pangea in the Laurasia-Gondwana Rift System: Annual Review of Earth and Planetary Sciences, v. 25, p. 337–401, doi:10.1146/annurev.earth.25.1.337.
Perrot, M., Tremblay, A., Ruffet, G., and David, J., 2018, Detrital U-Pb and 40Ar/39Ar geochronology of the Connecticut Valley-Gaspé trough, southern Quebec and northern Vermont – Transitional tectonism from Salinic to Acadian orogenic cycles: Tectonophysics, v. 745, p. 430–452, doi:10.1016/j.tecto.2018.08.006.

Perrot, M., Tremblay, A., Ruffet, G., Labrousse, L., Gervais, F., and Caroir, F., 2020, Diachronic metamorphic and structural evolution of the Connecticut Valley–Gaspé trough, Northern Appalachians: Journal of Metamorphic Geology, v. 38, p. 3–27, doi:10.1111/jmg.12510.
Profeta, L., Ducea, M.N., Chapman, J.B., Paterson, S.R., Gonzales, S.M.H., Kirsch, M., Petrescu, L., and DeCelles, P.G., 2015, Quantifying crustal thickness over time in magmatic arcs: Scientific Reports, doi:10.1038/srep17786.
Pyle, J.M., Spear, F.S., Cheney, J.T., and Layne, G., 2005, Monazite ages in the Chesham Pond Nappe, SW New Hampshire, U.S.A.: Implications for assembly of central New England thrust sheets: American Mineralogist, v. 90, p. 592–606, doi:10.2138/am.2005.1341.
Rankin, D.W., Coish, R.A., Tucker, R.D., Peng, Z.X., Wilson, S.A., and Rouff, A.A., 2007, Silurian extension in the Upper Connecticut Valley, United States and the origin of middle Paleozoic basins in the Quebec embayment: American Journal of Science, v. 307, p. 216–264.
Robinson, P., Tucker, R.D., Bradley, D., Berry IV, H.N., and Osberg, P.H., 1998, Paleozoic orogens in New England, USA: GFF, v. 120, p. 119–148, doi:10.1080/11035899801202119.
Roden-Tice, M.K., and Wintsch, R.P., 2002, Early Cretaceous normal faulting in southern New England: Evidence from apatite and zircon fission-track ages: The Journal of Geology, v. 110, p. 159–178, doi:10.1086/338281.
Roden-Tice, M.K., West Jr, D.P., Potter, J.K., Raymond, S.M., and Winch, J.L., 2009, Presence of a Long-Term Lithospheric Thermal Anomaly: Evidence from Apatite Fission-Track Analysis in Northern New England: The Journal of Geology, v. 117, p. 627–641, doi:10.1086/605995.
Spear, F.S., and Harrison, T.M., 1989, Geochronologic studies in central New England I: evidence for pre-Acadian metamorphism in eastern Vermont: Geology, v. 17, p. 181–184, doi:10.1130/0091-7613(1989)017<0181:GSICNE>2.3.CO;2.
van Staal, C.R., Currie, K.L., Rowbotham, G., Goodfellow, W., and Rogers, N., 2008, Pressure-temperature paths and exhumation of Late Ordovician-Early Silurian blueschists and associated metamorphic nappes of the Salinic Brunswick subduction complex, northern Appalachians: Bulletin of the Geological Society of America, doi:10.1130/B26324.1.
van Staal, C.R., Whalen, J.B., Valverde-Vaquero, P., Zagorevski, A., and Rogers, N., 2009, Pre-Carboniferous, episodic accretion-related, orogenesis along the Laurentian margin of the northern Appalachians: Geological Society, London, Special Publications, v. 327, p. 271–316, doi:10.1144/SP327.13.
Stanley, R.S., and Ratcliffe, N.M., 1985, Tectonic synthesis of the Taconian orogeny in western New England (USA).: Geological Society of America Bulletin, doi:10.1130/0016-7606(1985)96<1227:TSOTTO>2.0.CO;2.
Steiger, R.H., and Jäger, E., 1977, Subcommission on geochronology: Convention on the use of decay constants in geo- and cosmochronology: Earth and Planetary Science Letters, doi:10.1016/0012-821X(77)90060-7.

Swanson, M.T., 1999, Kinematic indicators for regional dextral shear along the Norumbega fault system in the Casco Bay area, coastal Maine: Geological Society
of America Special Papers, v. 331, p. 1–23, doi:10.1130/0-8137-2331-0.1.
Thigpen, J.R., and Hatcher Jr., R.D., 2017, Paleozoic tectonic evolution of the western
Blue Ridge, southern Appalachians: A critical examination of long-standing
conflicts in a polydeformed system (R. D. Law, J. R. Thigpen, A. J. Merschat, & H.
H. Stowell, Eds.): Linkages and Feedbacks in Orogenic Systems, v. 213, p. 0,
doi:10.1130/2017.1213(04).
Thompson, M.D., Barr, S.M., and Grunow, A.M., 2012, Avalonian perspectives on
Neoproterozoic paleogeography: Evidence from Sm-Nd isotope geochemistry and
detrital zircon geochronology in SE New England, USA: Bulletin, v. 124, p. 517–
531.
Thompson, M.D., Grunow, A.M., and Ramezani, J., 2007, Late Neoproterozoic paleogeography of the southeastern New England Avalon zone: Insights from U-Pb
geochronology and paleomagnetism: Geological Society of America Bulletin, v.
119, p. 681–696.
Thompson, J.B.J., Robinson, P., and Trask, N.J., 1968, Nappes and gneiss domes in westcentral New England, in Zen, E.-A., White, W.S., Hadley, J., and Thompson, J.J.
eds., Studies of Appalachian geology: Northern and Maritime, New York,
Interscience, p. 203–218.
Tollo, R.P., Aleinikoff, J.N., Bartholomew, M.J., and Rankin, D.W., 2004,
Neoproterozoic A-type granitoids of the central and southern Appalachians: intraplate magmatism associated with episodic rifting of the Rodinian
supercontinent: Precambrian Research, v. 128, p. 3–38.
Tomascak, P.B., Krogstad, E.J., and Walker, R.J., 1996, U-Pb Monazite Geochronology
of Granitic Rocks from Maine : Implications for Late Paleozoic Tectonics in the Northern Appalachians Author (s): Paul B . Tomascak , Eirik J . Krogstad and
Richard J . Walker Published by : The University of Chicago Press St: The Journal of Geology, v. 104, p. 185–195.
Tracy, R.J., and Dietsch, C.W., 1982, High-temperature retrograde reactions in pelitic gneiss, central Massachusetts.: Canadian Mineralogist, v. 20, p. 425–437.
Tucker, R.D., Osberg, P.H., and Iv, H.N.B., 2001, The Geology of a Part of Acadia and
the Nature of the Acadian Orogeny Across Central and Eastern Maine: American
Journal of Science, v. 301, p. 205–260, doi:10.2475/ajs.301.3.205.
Tucker, R.D., and Robinson, P., 1990, Geological Society of America Bulletin Age and
setting of the Bronson Hill magmatic arc : A re-evaluation based on U-Pb zircon
ages in southern New England: Geological Society of America Bulletin, v. 102, p.
1404–1419, doi:10.1130/0016-7606(1990)102<1404.
Turner, S.J., and Langmuir, C.H., 2015a, The global chemical systematics of arc front stratovolcanoes: Evaluating the role of crustal processes: Earth and Planetary
Science Letters, doi:10.1016/j.epsl.2015.03.056.
Turner, S.J., and Langmuir, C.H., 2015b, What processes control the chemical compositions of arc front stratovolcanoes? Geochemistry, Geophysics, Geosystems,
doi:10.1002/2014GC005633.
Turner, S.J., Langmuir, C.H., Dungan, M.A., and Escrig, S., 2017, The importance of
mantle wedge heterogeneity to subduction zone magmatism and the origin of EM1: Earth and Planetary Science Letters, v. 472, p. 216–228,
doi:10.1016/j.epsl.2017.04.051.

Valley, P.M., Walsh, G.J., Merschat, A.J., and McAleer, R.J., 2019, Geochronology of the Oliverian Plutonic Suite and the Ammonoosuc Volcanics in the Bronson Hill arc: Western New Hampshire, USA: Geosphere, v. 16, doi:10.1130 /GES02170.1.
Vermeesch, P., 2013, Multi-sample comparison of detrital age distributions: Chemical Geology, v. 341, p. 140–146, doi:10.1016/j.chemgeo.2013.01.010.
Vermeesch, P., 2012, On the visualisation of detrital age distributions: Chemical Geology, v. 312–313, p. 190–194, doi:10.1016/j.chemgeo.2012.04.021.
Vry, J.K., and Baker, J.A., 2006, LA-MC-ICPMS Pb-Pb dating of rutile from slowly cooled granulites: Confirmation of the high closure temperature for Pb diffusion in rutile: Geochimica et Cosmochimica Acta, v. 70, p. 1807–1820, doi:10.1016/j.gca.2005.12.006.
Waldron, J.W.F., Schofield, D.I., Murphy, J.B., and Thomas, C.W., 2014, How was the Iapetus Ocean infected with subduction? Geology, v. 42, p. 1095–1098, doi:10.1130/G36194.1.
Walsh, G.J., and Aleinikoff, J.N., 1999, U-Pb zircon age of metafelsite from the Pinney Hollow Formation; implications for the development of the Vermont Appalachians: American Journal of Science, v. 299, p. 157–170.
Walsh, G.J., Aleinikoff, J.N., and Dorais, M.J., 2011, Bedrock geologic map of the Grafton quadrangle, Worcester County, Massachusetts: US Department of the Interior, US Geological Survey.
Walsh, G.J., Aleinikoff, J.N., and Fanning, C., 2004, U-Pb geochronology and evolution of Mesoproterozoic basement rocks, western Connecticut, in Proterozoic tectonic evolution of the Grenville orogen in North America, Geological Society of America Inc.
Walsh, G.J., Aleinikoff, J.N., and Wintsch, R.P., 2007, Origin of the Lyme Dome and implications for the timing of multiple Alleghanian deformational and intrusive events in southern Connecticut: American Journal of Science, v. 307, p. 168–215, doi:10.2475/06.2007.06.
Wathen, B., Helou, C., Wintsch, R.P., Deasy, R.T., Yi, K., and McAleer, R., 2015, Deformation spanning 200 Million Years Along the peri-Laurentian (Pumpkin Ground Orthogneiss) Buttress and the East Derby Shear Zone, South-Central Connecticut, in Gilmore, M.S. and Resor, P.G. eds., Guidebook to field trips in Connecticut and Massachusetts: Middletown, Connecticut, Middletown, Connecticut, Wesleyan University, p. 153–173.
West Jr., D.P., Lux, D.R., and Hussey II, A.M., 1988, 40 Ar/ 39 Ar hornblende ages from southwestern Maine: evidence for Late Paleozoic metamorphism: 1988, doi:10.4138/1653.
West Jr, D.P., and Lux, D.R., 1993, Dating mylonitic deformation by the 40Ar-39Ar method: An example from the Norumbega fault zone, Maine: Earth and Planetary Science Letters, v. 120, p. 221–237.
West Jr, D.P., and Roden-Tice, M.K., 2003, Late Cretaceous reactivation of the Norumbega fault zone, Maine: Evidence from apatite fission-track ages: Geology, v. 31, p. 649–652.
Whalen, J.B., and Hildebrand, R.S., 2019, Trace element discrimination of arc, slab failure, and A-type granitic rocks: Lithos, v. 348, doi:10.1016/j.lithos.2019.105179.
Wilson, J.T., 1966, Did the Atlantic Close and then Re-Open? Nature, doi:10.1038/211676a0.

Wintsch, R.P., Sutter, J.F., Kunk, M.J., Aleinikoff, J.N., and Dorais, M.J., 1992, Contrasting P-T-t paths: Thermochronologic evidence for a Late Paleozoic final assembly of the Avalon Composite Terrane in the New England Appalachians: Tectonics, v. 11, p. 672–689.
Wintsch, R.P., Yi, K., and Dorais, M.J., 2014, Crustal thickening by tectonic wedging of the Ganderian rocks, southern New England, USA: Evidence from cataclastic zircon microstructures and U–Pb ages: Journal of Structural Geology, v. 69, p. 428–448, doi:https://doi.org/10.1016/j.jsg.2014.07.019.
Wise, D.U., 1992, Dip domain method applied to the Mesozoic Connecticut Valley Rift Basins: Tectonics, v. 11, p. 1357–1368, doi:10.1029/92TC01103.
Yang, X., and Gao, H., 2018, Full-Wave Seismic Tomography in the Northeastern United States: New Insights Into the Uplift Mechanism of the Adirondack Mountains: Geophysical Research Letters, v. 45, p. 5992–6000, doi:10.1029/2018GL078438.
Zartman, R.E., and Hermes, O.D., 1987, Archean inheritance in zircon from late Paleozoic granites from the Avalon zone of southeastern New England: an African connection: Earth and Planetary Science Letters, v. 82, p. 305–315.
Amidon, W.H., Roden-Tice, M., Anderson, A.J., McKeon, R.E., and Shuster, D.L., 2016, Late cretaceous unroofing of the White Mountains, New Hampshire, USA: An episode of passive margin rejuvenation? Geology, v. 44, p. 415–418, doi:10.1130/G37429.1.
Armijo, R., Lacassin, R., Coudurier-Curveur, A., and Carrizo, D., 2015, Coupled tectonic evolution of Andean orogeny and global climate: Earth-Science Reviews, doi:10.1016/j.earscirev.2015.01.005.
Arth, J.G., and Ayuso, R.A., 1997, The Northeast Kingdom batholith, Vermont: Geochronology and Nd, O, Pb, and Sr isotopic constraints on the origin of Acadian granitic rocks: Memoir of the Geological Society of America, v. 191, p. 1–18, doi:10.1130/0-8137-1191-6.1.
Ashwal, L.D., Leo, G.W., Robinson, P., Zartman, R.E., and Hall, D.J., 1979, The Belchertown quartz monzodiorite pluton, West-central Massachusetts; a syntectonic Acadian intrusion: American Journal of Science, v. 279, p. 936–969.
Assumpção, M., Feng, M., Tassara, A., and Julià, J., 2013, Models of crustal thickness for South America from seismic refraction, receiver functions and surface wave tomography: Tectonophysics, v. 609, p. 82–96, doi:10.1016/j.tecto.2012.11.014.
Beaumont, C., Nguyen, M.H., Jamieson, R.A., and Ellis, S., 2006, Crustal flow modes in large hot orogens: Geological Society Special Publication, v. 268, p. 91–145, doi:10.1144/GSL.SP.2006.268.01.05.
Bradley, D.C., Tucker, R.D., Lux, D.R., Harris, A.G., and McGregor, D.C., 2000, Migration of the Acadian Orogen and Foreland Basin across the northern Appalachians of Maine and adjacent areas: U.S. Geological Survey Professional Paper, v. 1624, p. 1- 49.
Carmichael, D.M., 1978, Metamorphic bathozones and bathograds; a measure of the depth of post-metamorphic uplift and erosion on the regional scale: American Journal of Science, v. 278, p. 769–797.
Cassidy, J.F., 1995, Receiver function studies in the southern Canadian Cordillera: Canadian Journal of Earth Sciences, v. 32, p. 1514–1519, doi:10.1139/e95-123.
Chapman, J.B., Ducea, M.N., DeCelles, P.G., and Profeta, L., 2015, Tracking changes in crustal thickness during orogenic evolution with Sr/Y: An example from the North American Cordillera: Geology, v. 43, p. 919–922, doi:10.1130/G36996.1.

Chapman, J.B., Greig, R., and Haxel, G.B., 2020, Geochemical evidence for an orogenic plateau in the southern U.S. and northern Mexican Cordillera during the Laramide orogeny: Geology, v. 48, p. 164–168, doi:10.1130/G47117.1.
Chen, W., 2017, Determination of crustal thickness under Tibet from gravity-gradient data: Journal of Asian Earth Sciences, v. 143, p. 315–325.
Chiaradia, M., 2015, Crustal thickness control on Sr/Y signatures of recent arc magmas: an Earth scale perspective: Science Reports, v. 5, doi:10.1038/srep08115.
Clark, M.K., and Royden, L.H., 2000, Topographic ooze: Building the eastern margin of Tibet by lower crustal flow: Geology, v. 28, p. 703–706, doi:10.1130/0091-7613(2000)28<703:TOBTEM>2.0.CO;2.
DePaolo, D.J., Harrison, T.M., Wielicki, M., Zhao, Z., Zhu, D.C., Zhang, H., and Mo, X., 2019, Geochemical evidence for thin syn-collision crust and major crustal thickening between 45 and 32 Ma at the southern margin of Tibet: Gondwana Research, v. 73, p. 123–135, doi:10.1016/j.gr.2019.03.011.
Dorais, M.J., 2003, The petrogenesis and emplacement of the New Hamshire plutonic suite: American Journal of Science, v. 303, p. 447.
Dorais, M.J., and Paige, M.L., 2000, Regional geochemical and isotopic variations of Northern New England plutons: Implications for magma sources and for Grenville and Avalon basement-terrane boundaries: Bulletin of the Geological Society of America, v. 112, p. 900–914, doi:10.1130/0016-7606(2000)112<900:RGAIVO>2.0.CO;2.
Dorais, M.J., Wintsch, R.P., Kunk, M.J., Aleinikoff, J., Burton, W., Underdown, C., and Kerwin, C.M., 2012, P-T-t conditions, Nd and Pb isotopic compositions and detrital zircon geochronology of the Massabesic Gneiss Complex, New Hampshire: Isotopic and metamorphic evidence for the identification of Gander basement, central New England: American Journal of Science, v. 312, p. 1049, doi:10.2475/10.2012.01.
Dorais, M.J., Wintsch, R.P., Nelson, W.R., and Tubrett, M., 2009, Insights into the Acadian orogeny, New England Appalachians: a provenance study of the Carrabassett and Kittery formations, Maine: Atlantic Geology, v. 45, p. 50, doi:10.4138/atlgeol.2009.002.
Ettensohn, F.R., Pashin, J.C., and Gilliam, W., 2019, The Appalachian and Black Warrior Basins: Foreland Basins in the Eastern United States, in Miall, A.D. ed., The Sedimentary Basins of the United States and Canada, p. 129–237, doi:10.1016/b978-0-444-63895-3.00004-8.
Farner, M.J., and Lee, C.T.A., 2017, Effects of crustal thickness on magmatic differentiation in subduction zone volcanism: A global study: Earth and Planetary Science Letters, doi:10.1016/j.epsl.2017.04.025.
Fu, B., Cliff, J., and Zartman, R.E., 2014, Zircon oxygen isotopic constraints from plutonic rocks on the magmatic and crustal evolution of the northern Appalachians in southern New England, USA: Canadian Journal of Earth Sciences, v. 51, p. 485–499.
Garzione, C.N. et al., 2017, Tectonic Evolution of the Central Andean Plateau and Implications for the Growth of Plateaus: Annual Review of Earth and Planetary Sciences, v. 45, p. 529–559, doi:10.1146/annurev-earth-063016-020612.

Gatewood, M.P., Dragovic, B., Stowell, H.H., Baxter, E.F., Hirsch, D.M., and Bloom, R., 2015, Evaluating chemical equilibrium in metamorphic rocks using major element and Sm–Nd isotopic age zoning in garnet, Townshend Dam, Vermont, USA: Chemical Geology, v. 401, p. 151–168, doi:10.1016/j.chemgeo.2015.02.017.
Hacker, B.R., Ratschbacher, L., Rutte, D., Stearns, M.A., Malz, N., Stübner, K., Kylander-Clark, A.R.C., Pfänder, J.A., and Everson, A., 2017, Building the Pamir-Tibet Plateau—Crustal stacking, extensional collapse, and lateral extrusion in the Pamir: 3. Thermobarometry and petrochronology of deep Asian crust: Tectonics, v. 36, p. 1743–1766, doi:10.1002/2017TC004488.
Harrison, T.M., Spear, F.S., and Heizler, M.T., 1989, Geochronologic studies in central New England II: post-Acadian hinged and differential uplift: Geology, v. 17, p. 185–189, doi:10.1130/0091-7613(1989)017<0185:GSICNE>2.3.CO;2.
Hibbard, J.P., van Staal, C.R., Rankin, D.W., and Williams, H., 2006, Lithotectonic map of the Appalachian Orogen, Canada-United States of America:, doi:10.4095/221912.
Hillenbrand, I., Williams, M.L., Li, C., and Gao, H., 2019, Rise and Fall of the Acadian Altiplano: Geological Society of America Abstracts with Programs, v. 51, doi:10.1130/abs/2019AM-340957.
Hu, F., Ducea, M.N., Liu, S., and Chapman, J.B., 2017, Quantifying Crustal Thickness in Continental Collisional Belts : Global Perspective and a Geologic Application: Scientific Reports, v. 7, p. 1–10, doi:10.1038/s41598-017-07849-7.
Karabinos, P., Macdonald, F.A., and Crowley, J.L., 2017, Bridging the gap between the foreland and hinterland I: Geochronology and plate tectonic geometry of Ordovician magmatism and terrane accretion on the Laurentian margin of New England: American Journal of Science, v. 317, p. 515–554, doi:10.2475/05.2017.01.
Kuiper, Y.D., 2016, Development of the Norumbega fault system in mid-Paleozoic New England, USA: An integrated subducted oceanic ridge model: Geology, v. 44, p. 455–458, doi:10.1130/G37599.1.
Lombardi, D., Braunmiller, J., Kissling, E., and Giardini, D., 2008, Moho depth and Poisson's ratio in the Western-Central Alps from receiver functions: Geophysical Journal International, v. 173, p. 249–264, doi:10.1111/j.1365-246X.2007.03706.x.
Ludman, A., Hopeck, J., and Berry Iv, H.N., 2017, Provenance and paleogeography of post-Middle Ordovician, pre-Devonian sedimentary basins on the Gander composite terrane, eastern and east-central Maine: implications for Silurian tectonics in the northern Appalachians: Atlantic Geology, v. 53, p. 63.
Mantle, G.W., and Collins, W.J., 2008, Quantifying crustal thickness variations in evolving orogens: Correlation between arc basalt composition and Moho depth: Geology, v. 36, p. 87–90, doi:10.1130/G24095A.1.
Massey, M.A., Moecher, D.P., Walker, T.B., O'Brien, T.M., and Rohrer, L.P., 2017, The role and extent of dextral transpression and lateral escape on the post-Acadian tectonic evolution of South-Central New England: American Journal of Science, v. 317, p. 34–94, doi:10.2475/01.2017.02.
Molnar, P., England, P., and Martinod, J., 1993, Mantle dynamics, uplift of the Tibetan Plateau, and the Indian Monsoon: Reviews of Geophysics, v. 31, p. 357–396, doi:10.1029/93RG02030.

Perrot, M., Tremblay, A., Ruffet, G., Labrousse, L., Gervais, F., and Caroir, F., 2020, Diachronic metamorphic and structural evolution of the Connecticut Valley–Gaspé trough, Northern Appalachians: Journal of Metamorphic Geology, v. 38, p. 3–27, doi:10.1111/jmg.12510.
Profeta, L., Ducea, M.N., Chapman, J.B., Paterson, S.R., Gonzales, S.M.H., Kirsch, M., Petrescu, L., and DeCelles, P.G., 2015, Quantifying crustal thickness over time in magmatic arcs: Scientific Reports, doi:10.1038/srep17786.
Pyle, J.M., Spear, F.S., Cheney, J.T., and Layne, G., 2005, Monazite ages in the Chesham Pond Nappe, SW New Hampshire, U.S.A.: Implications for assembly of central New England thrust sheets: American Mineralogist, v. 90, p. 592–606, doi:10.2138/am.2005.1341.
Robinson, P., 2003, Tectonic–stratigraphic–metamorphic perspective of the New England Caledonides, west-central Massachusetts: Guidebook for Field Trips in the Five College Region. 95th Annual Meeting of the New England Intercollegiate Geological Conference,.
Robinson, P., Tucker, R.D., Bradley, D., Berry IV, H.N., and Osberg, P.H., 1998, Paleozoic orogens in New England, USA: GFF, v. 120, p. 119–148, doi:10.1080/11035899801202119.
Roden-Tice, M.K., West Jr, D.P., Potter, J.K., Raymond, S.M., and Winch, J.L., 2009, Presence of a Long-Term Lithospheric Thermal Anomaly: Evidence from Apatite Fission-Track Analysis in Northern New England: The Journal of Geology, v. 117, p. 627–641, doi:10.1086/605995.
Ryan, J., Beck, S., Zandt, G., Wagner, L., Minaya, E., and Tavera, H., 2016, Central Andean crustal structure from receiver function analysis: Tectonophysics, v. 682, p. 120–133, doi:10.1016/j.tecto.2016.04.048.
Schoonmaker, A., Kidd, W.S.F., and Bradley, D.C., 2005, Foreland-forearc collisional granitoid and mafic magmatism caused by lower-plate lithospheric slab breakoff: The Acadian of Maine, and other orogens: Geology, v. 33, p. 961–964, doi:10.1130/G21832.1.
Scott, E.M., Allen, M.B., Macpherson, C.G., Saville, C., Ducea, M.N., Mccaffrey, K.J.W., and Davidson, J.P., 2018, Andean surface uplift constrained by radiogenic isotopes of arc lavas: Nature Communications, p. 1–8, doi:10.1038/s41467-018-03173-4.
Spear, F.S., 1993, Metamorphic phase equilibria and pressure-temperature-time paths: Mineralogical Society of America, 799 p.
van Staal, C.R., Whalen, J.B., Valverde-Vaquero, P., Zagorevski, A., and Rogers, N., 2009, Pre-Carboniferous, episodic accretion-related, orogenesis along the Laurentian margin of the northern Appalachians: Geological Society, London, Special Publications, v. 327, p. 271–316, doi:10.1144/SP327.13.
Ver Straeten, C.A., Over, D.J., and Baird, G.C., 2020, Arc-to-craton: Devonian air-fall tephras in the eastern United States (K. L. Avary, K. O. Hasson, & R. J. Diecchio, Eds.): The Appalachian Geology of John M. Dennison: Rocks, People, and a Few Good Restaurants along the Way, p. 0, doi:10.1130/2020.2545(03).

Thompson, J.B.J., Robinson, P., and Trask, N.J., 1968, Nappes and gneiss domes in westcentral New England, in Zen, E.-A., White, W.S., Hadley, J., and Thompson, J.J.
eds., Studies of Appalachian geology: Northern and Maritime, New York,
Interscience, p. 203–218.
Tucker, R.D., Osberg, P.H., and Iv, H.N.B., 2001, The Geology of a Part of Acadia and
the Nature of the Acadian Orogeny Across Central and Eastern Maine: American
Journal of Science, v. 301, p. 205–260, doi:10.2475/ajs.301.3.205.
West, D.P., Roden-Tice, M.K., Potter, J.K., and Barnard, N.Q., 2008, Assessing the role of orogen-parallel faulting in post-orogenic exhumation: low-temperature thermochronology across the Norumbega Fault System, Maine: Canadian Journal of
Earth Sciences, v. 45, p. 287–301, doi:10.1139/E07-073.
Zen, E.A., 1991, Phanerozoic denudation history of the southern New England
Appalachians deduced from pressure data: American Journal of Science, v. 291, p.
401–424, doi:10.2475/ajs.291.4.401.
Ague, J.J., Eckert, J.O., Chu, X., Baxter, E.F., Chamberlain, C.P., 2013. Discovery of
ultrahigh-temperature metamorphism in the Acadian orogen, Connecticut, USA.
Geology. https://doi.org/10.1130/G33752.1
Bradley, D., Shea, E., Buchwaldt, R., Bowring, S., Benowitz, J., O'Sullivan, P.,
McCauley, A., 2016. Geochronology and Tectonic Context of Lithium-cesiumtantalum Pegmatites in the Appalachians. Can. Mineral. 54, 945–969.
https://doi.org/10.3749/canmin.1600035
Bradley, D.C., 2019. Tectonic and Paleoclimatic Controls of Lithium-cesium-tantalum (LCT) Pegmatite Genesis, Exhumation, and Preservation in the Appalachians. Can.
Mineral. 57, 715–717. https://doi.org/10.3749/canmin.ab00002
Chapman, J.B., Ducea, M.N., DeCelles, P.G., Profeta, L., 2015. Tracking changes in
crustal thickness during orogenic evolution with Sr/Y: An example from the North
American Cordillera. Geology 43, 919–922. https://doi.org/10.1130/G36996.1
Chapman, J.B., Greig, R., Haxel, G.B., 2020. Geochemical evidence for an orogenic plateau in the southern U.S. and northern Mexican Cordillera during the Laramide orogeny. Geology 48, 164–168.
https://doi.org/10.1130/G47117.1
DeCelles, P.G., 2004. Late Jurassic to Eocene evolution of the Cordilleran thrust belt and
foreland basin system, western U.S.A. Am. J. Sci. 304, 105–168.
https://doi.org/10.2475/ajs.304.2.105
DePaolo, D.J., Harrison, T.M., Wielicki, M., Zhao, Z., Zhu, D.C., Zhang, H., Mo, X.,
2019. Geochemical evidence for thin syn-collision crust and major crustal thickening between 45 and 32 Ma at the southern margin of Tibet. Gondwana Res.
73, 123–135. https://doi.org/10.1016/j.gr.2019.03.011
Ernst, W.G., 2010. Young convergent-margin orogens, climate, and crustal thickness-A
Late Cretaceous-Paleogene Nevadaplano in the American Southwest? Lithosphere 2, 67–75. https://doi.org/10.1130/L84.1
Ernst, W.G., 2009. Rise and fall of the Nevadaplano. Int. Geol. Rev. 51, 583–588.
https://doi.org/10.1080/00206810903063315

Ettensohn, F.R., Pashin, J.C., Gilliam, W., 2019. The Appalachian and Black Warrior Basins: Foreland Basins in the Eastern United States, in: Miall, A.D. (Ed.), The Sedimentary Basins of the United States and Canada. pp. 129–237. https://doi.org/10.1016/b978-0-444-63895-3.00004-8
Garzione, C.N., McQuarrie, N., Perez, N.D., Ehlers, T.A., Beck, S.L., Kar, N., Eichelberger, N., Chapman, A.D., Ward, K.M., Ducea, M.N., Lease, R.O., Poulsen, C.J., Wagner, L.S., Saylor, J.E., Zandt, G., Horton, B.K., 2017. Tectonic Evolution of the Central Andean Plateau and Implications for the Growth of Plateaus. Annu. Rev. Earth Planet. Sci. 45, 529–559. https://doi.org/10.1146/annurev-earth-063016-020612
Gatewood, M.P., Dragovic, B., Stowell, H.H., Baxter, E.F., Hirsch, D.M., Bloom, R., 2015. Evaluating chemical equilibrium in metamorphic rocks using major element and Sm–Nd isotopic age zoning in garnet, Townshend Dam, Vermont, USA. Chem. Geol. 401, 151–168. https://doi.org/10.1016/j.chemgeo.2015.02.017
Harrison, T.M., 1982. Diffusion of 40Ar in Hornblende. Contrib. to Mineral. Petrol. 78, 324–331. https://doi.org/10.2475/ajs.303.5.410
Harrison, T.M., Célérier, J., Aikman, A.B., Hermann, J., Heizler, M.T., 2009. Diffusion of 40Ar in muscovite. Geochim. Cosmochim. Acta 73, 1039–1051. https://doi.org/10.1016/j.gca.2008.09.038
Hatzfeld, D., Molnar, P., 2010. Comparisons of the kinematics and deep structures of the Zagros and Himalaya and of the Iranian and Tibetan plateaus and geodynamic implications. Rev. Geophys. https://doi.org/10.1029/2009RG000304
Haugerud, R.A., 1990. Geochronologic studies in central New England II: Post-Acadian hinged and differential uplift. Comment Geol. 18, 183–184. https://doi.org/10.1130/0091-7613(1990)018<0183:CAROGS>2.3.CO;2
Heizler, M.T., Harrison, T.M., 1998. The thermal history of the New York basement determined from 40Ar/39Ar K-feldspar studies. J. Geophys. Res. Solid Earth 103, 29795–29814. https://doi.org/10.1029/98JB02837
Hibbard, J.P., van Staal, C.R., Rankin, D.W., Williams, H., 2006. Lithotectonic map of the Appalachian Orogen, Canada-United States of America. https://doi.org/10.4095/221912
Hillenbrand, I.W., 2020. Crustal evolution of the New England Appalachians: the rise and fall of a long-lived orogenic plateau. University of Massachusetts.
Jamieson, R.A., Beaumont, C., Medvedev, S., Nguyen, M.H., 2004. Crustal channel flows: 2. Numerical models with implications for metamorphism in the Himalayan-Tibetan orogen. J. Geophys. Res. Solid Earth 109, 1–24. https://doi.org/10.1029/2003JB002811
Kapp, P., DeCelles, P.G., 2019. Mesozoic–Cenozoic geological evolution of the Himalayan-Tibetan orogen and working tectonic hypotheses. Am. J. Sci. 319, 159–254. https://doi.org/10.2475/03.2019.01
Karabinos, P., Macdonald, F.A., Crowley, J.L., 2017. Bridging the gap between the foreland and hinterland I: Geochronology and plate tectonic geometry of Ordovician magmatism and terrane accretion on the Laurentian margin of New England. Am. J. Sci. 317, 515–554. https://doi.org/10.2475/05.2017.01

Karabinos, P., Mygatt, E.S., Cook, S.M., Student, M., 2010. Evidence for an orogenparallel, normal-sense shear zone around the Chester dome, Vermont: a possible template for gneiss dome formation in the New England Appalachians, USA, in: Tollo, R.P., Bartholomew, M.J., Hibbard, J.P., Karabinos, P.M. (Eds.), From Rodinia to Pangea: The Lithotectonic Record of the Appalachian Region: Geological Society of America Memoir. pp. 183–203.
Keller, D., Ague, J.J., 2018. High-pressure granulite facies metamorphism (~1.8 GPa) revealed in silica-undersaturated garnet-spinel-corundum gneiss, Central Maine Terrane, Connecticut, U.S.A. Am. Mineral. 103, 1851–1868.
https://doi.org/https://doi.org/10.2138/am-2018-6543
Klepeis, K., Webb, L., Blatchford, H., Schwartz, J., Jongens, R., Turnbull, R., Stowell, H., 2019. Deep Slab Collision during Miocene Subduction Causes Uplift along Crustal-Scale Reverse Faults in Fiordland, New Zealand. GSA Today 29, 4–10.
https://doi.org/10.1130/gsatg399a.1
Kuiper, Y.D., 2016. Development of the Norumbega fault system in mid-Paleozoic New England, USA: An integrated subducted oceanic ridge model. Geology 44, 455–458.
https://doi.org/10.1130/G37599.1
Laske, G., Masters, G., Ma, Z., Pasyanos, M., 2013. Update on CRUST1.0---A 1-degree global model of Earth's crust, in: EGU General Assembly 2013.
Li, C., Gao, H., Williams, M.L., Levin, V., 2018. Crustal Thickness Variation in the Northern Appalachian Mountains: Implications for the Geometry of 3-D Tectonic Boundaries Within the Crust. Geophys. Res. Lett. 45, 6061–6070.
https://doi.org/10.1029/2018GL078777
Macdonald, F.A., Swanson-Hysell, N. l, Park, Y., Lisiecki, L., Jagoutz, O., 2019. Arccontinent collisions in the tropics set Earth's climate state. Science (80-.). 364, 181–184.
Massey, M.A., Moecher, D.P., Walker, T.B., O'Brien, T.M., Rohrer, L.P., 2017. The role and extent of dextral transpression and lateral escape on the post-Acadian tectonic evolution of South-Central New England. Am. J. Sci. 317, 34–94.
https://doi.org/10.2475/01.2017.02
McCulla, J.K., 2016. Dating Deformation in the Palmer Zone of Transpression, Central Massachusetts: Temporal Constraints on Models for Progressive Deformation in the Middle Crust [MS thesis]. University of Kentucky.
McKeon, R.E., 2012. Apatite Uranium-Thorium/Helium thermochronometry in slowly eroding landscapes: Addressing age dispersion to understand Appalachian topographic development [PhD thesis]. Lehigh University.
Molnar, P., England, P., Martinod, J., 1993. Mantle dynamics, uplift of the Tibetan Plateau, and the Indian Monsoon. Rev. Geophys. 31, 357–396.
https://doi.org/10.1029/93RG02030
Oliver, W.A., Wallace, de W., Dennison, J.M., Hoskins, D.M., Huddle, J.W., 1967. Devonian of the Appalachian Basin, United States, in: Oswald, D.H. (Ed.), International Symposium on the Devonian System. Alberta Society of Petroleum Geologists, pp. 1001–1040.
Raymo, M.E., Ruddiman, W.F., 1992. Tectonic forcing of late Cenozoic climate. Nature 359, 117–122. https://doi.org/10.1038/359117a0

Rivers, T., 2012. Upper-crustal orogenic lid and mid-crustal core complexes: signature of a collapsed orogenic plateau in the hinterland of the Grenville Province. Can. J. Earth Sci. 49, 1–42. https://doi.org/10.1139/e11-014
Roberts, H.J., Kelley, S.P., Dahl, P.S., 2001. Obtaining geologically meaningful 40Ar/39Ar ages from altered biotite. Chem. Geol. 172, 277–290. https://doi.org/10.1016/S0009-2541(00)00255-2
Robinson, P., Tucker, R.D., Bradley, D., Berry IV, H.N., Osberg, P.H., 1998. Paleozoic orogens in New England, USA. GFF 120, 119–148. https://doi.org/10.1080/11035899801202119
Roden-Tice, M.K., West Jr, D.P., Potter, J.K., Raymond, S.M., Winch, J.L., 2009. Presence of a Long-Term Lithospheric Thermal Anomaly: Evidence from Apatite Fission-Track Analysis in Northern New England. J. Geol. 117, 627–641. https://doi.org/10.1086/605995
Spear, F.S., Harrison, T.M., 1989. Geochronologic studies in central New England I: evidence for pre-Acadian metamorphism in eastern Vermont. Geology. https://doi.org/10.1130/0091-7613(1989)017<0181:GSICNE>2.3.CO;2
Stewart, E.M., Ague, J.J., 2018. Infiltration-driven metamorphism, New England, USA: Regional CO2 fluxes and implications for Devonian climate and extinctions. Earth Planet. Sci. Lett. 489, 123–134. https://doi.org/10.1016/j.epsl.2018.02.028
Sullivan, N.C., 2014. Advances in Samarium-Neodymium Geochronology: Applications to Early Earth Garnet, Hydrothermal Carbonate, and High Temperature Metamorphic Systems [PhD thesis]. Boston University.
Thomas, W.A., Gehrels, G.E., Sundell, K.E., Greb, S.F., Finzel, E.S., Clark, R.J., Malone, D.H., Hampton, B.A., Romero, M.C., 2020. Detrital zircons and sediment dispersal in the eastern Midcontinent of North America 16, 1–27. https://doi.org/10.1130/GES02152.1/4974884/ges02152.pdf
Thompson, J.B.J., Robinson, P., Trask, N.J., 1968. Nappes and gneiss domes in westcentral New England, in: Zen, E.-A., White, W.S., Hadley, J., Thompson, J.J. (Eds.), Studies of Appalachian Geology: Northern and Maritime. Interscience, New York, pp. 203–218.
Thomson, J.A., 2001. A counterclockwise P-T path for anatectic pelites, South-Central Massachusetts. Contrib. to Mineral. Petrol. 141, 623–641. https://doi.org/10.1007/s004100100265
Tracy, R.J., Dietsch, C.W., 1982. High-temperature retrograde reactions in pelitic gneiss, central Massachusetts. Can. Mineral. 20, 425–437.
van Staal, C.R., Whalen, J.B., Valverde-Vaquero, P., Zagorevski, A., Rogers, N., 2009. Pre-Carboniferous, episodic accretion-related, orogenesis along the Laurentian margin of the northern Appalachians. Geol. Soc. London, Spec. Publ. 327, 271–316. https://doi.org/10.1144/SP327.13
Williams, M.L., Grover, T., Jercinovic, M.J., Regan, S.P., Pless, C.R., Suarez, K.A., 2019. Constraining the timing and character of crustal melting in the Adirondack Mountains using multi-scale compositional mapping and in-situ monazite geochronology. Am. Mineral. 104, 1585–1602. https://doi.org/10.2138/am-2019-6906
Williams, M.L., Jercinovic, M.J., Mahan, K.H., Dumond, G., 2017. Electron Microprobe Petrochronology. Rev. Mineral. Geochemistry 83, 153–182. https://doi.org/10.2138/rmg.2017.83.5

Zen, E.A., 1991. Phanerozoic denudation history of the southern New England Appalachians deduced from pressure data. Am. J. Sci. 291, 401–424. https://doi.org/10.2475/ajs.291.4.401